CHARACTERISATION OF ACC OXIDASE DURING LEAF MATURATION AND SENESCENCE IN WHITE CLOVER (*TRIFOLIUM REPENS* L.)

A thesis presented in partial fulfilment of the requirements
for the degree of

Doctor of Philosophy

at

Massey University

DONALD ALEXANDER HUNTER

1998

Dedication

This thesis is
dedicated to my parents

John & Marie

and to

Stephanie

Abstract

ACC oxidase, the enzyme which converts 1-aminocyclopropane-1-carboxylic acid (ACC) to ethylene, has been studied in leaves of a single genotype of white clover (*Trifolium repens* L., Genotype 10F) during leaf maturation and senescence.

Leaf senescence in genotype 10F is associated with an increase in both ACC content and ethylene evolution of the leaves. The increase in levels of ACC slightly precedes that of ethylene production, but occurs concomitantly with the onset of senescence (as judged by chlorophyll loss).

The coding regions of two distinct ACC oxidases were generated from leaf tissue of genotype 10F using RT-PCR with degenerate oligonucleotide primers. The coding regions were designated TR-ACO1 and TR-ACO2. TR-ACO1 and 2 are 84 % and 87 % similar in nucleotide and amino acid sequence respectively. Genomic Southern analysis using these regions as probes confirmed that both sequences are encoded by distinct genes, but also suggested that there may be additional genes closely related to both TR-ACO1 and TR-ACO2.

Gene expression studies during leaf maturation and senescence were undertaken using these regions as probes. TR-ACO1 hybridised to a single RNA transcript of *ca.* 1.35 Kb on the northern blot. Expression of this transcript was high in mature green leaves but declined as the leaves senesced. By contrast, TR-ACO2 hybridised equally to two RNA transcripts of *ca.* 1.17 Kb and 1.35 Kb on the northern blot, and unlike expression of TR-ACO1, the levels of these transcripts were low in mature green leaves and increased as the leaves senesced.

The 3'-UTRs of TR-ACO1 and TR-ACO2 were generated using 3'-RACE (Randomly Amplified cDNA Ends). Repeating the genomic Southern analysis with these regions as probes indicated that the gene for TR-ACO1 may be polymorphic, and that there may be an additional ACC oxidase gene in the genome that encodes a transcript with a similar coding region, but divergent 3'-UTR to TR-ACO2.

The 3'-UTRs of TR-ACO1 and 2 confirmed the expression patterns of their cognate coding regions in northern analysis, except that the 3'-UTR of TR-ACO2 hybridised only to the 1.35 Kb and not the 1.17 Kb transcript.

ACC oxidase activity assayed *in vitro* correlated with the levels of gene expression of TR-ACO1 but not the senescence-associated TR-ACO2, with the activity being highest in mature green leaves and declining as the leaves senesced. The decrease in activity was greatest when expressed on a per unit fresh weight basis (*ca.* 8-fold) than per unit protein basis (*ca.* 3-fold). The extraction and assay conditions altered in this study were not able to prevent the decline in ACC oxidase activity *in vitro* that occurred during leaf senescence.

Polyclonal antibodies raised against the translation products of TR-ACO1 and 2 expressed in *E. coli* recognised a protein of the expected size (*ca.* 36.4 kDa) for ACC oxidase using western analysis. The pattern of protein accumulation recognised by the antibodies raised against TR-ACO1 (in rabbits) broadly matched gene expression of TR-ACO1 and activity of ACC oxidase. That is, antibody recognition was highest in mature green leaves and declined as the leaves senesced. By comparison, the antibodies raised against TR-ACO2 (in rats) recognised a protein of the same size with weak avidity. The pattern of accumulation was similar to that observed with the TR-ACO1-raised-antibodies, and therefore not consistent with the gene expression pattern of TR-ACO2. It was concluded that these antibodies were cross-reacting with the same protein as that recognised by the TR-ACO1-raised-antibodies and that the lower enzyme activity was due to lower TR-ACO1 ACC oxidase protein.

Wounding mature green leaves increased TR-ACO2 gene expression, but as observed for the senescing leaves, increased gene expression of TR-ACO2 was not correlated with increased protein accumulation or ACC oxidase enzyme activity.

Potential explanations as to why the increased gene expression of TR-ACO2 during leaf senescence (or wounding) is not accompanied by increased protein accumulation and ACC oxidase activity are discussed.

Acknowledgments

I wish to thank my supervisors, Dr Michael T. McManus and Professor Paula E. Jameson for their encouragement and guidance throughout the course of this project. As my chief supervisor, Michael has been everything people said he would be, extremely competent, enthusiastic, supportive, and a perfect role model. I feel I cannot say enough, thank you again Michael. Paula has been brilliant in a supportive role throughout. I am especially grateful for the time she has spent towards the end of my writing, offering a fresh and valuable perspective on organisation of the thesis, as well as assisting in proofing. Thank you again Paula.

I can't go much further without mentioning Lyn, Michael's research assistant, and the person responsible for keeping the lab running smoothly. "Lyn - look I've finished!!!!!". Always willing to help, I don't know how many thousands of chocolate fish I must owe you, thanks again. To Sang Dong (Sangie !), my partner in oxidase, thank you for your very generous help throughout.

Thanks to rest of the crew of lab C 5:19, Trish, Simone, Celia, Deming, Marian, Michelle, Huaibi, and Nigel who have made it such a great place to work.

There are various people who have helped with specific aspects of the project. I would like to thank Steve Butcher for initial help in getting this project underway, Jocelyn Tilbrook, Sang Dong and Trish for helping with harvesting tissue, Marty Hunt for helping me get up to speed with the GC and for loan of a chart recorder, Dr Peter Lockhart and Richard Winkworth for phylogenetic analysis, and Steven Northover for help with the bibliography.

To the many staff and students of the Department of Plant Biology and Biotechnology who I have for one reason or another asked for assistance, thank you.

My appreciation also goes out to the staff of the Plant Molecular Genetics Lab at AgResearch, Grasslands. All of whom have been friendly, and generous to the (what do you want this time!) guy who kept popping up at their doorstep. In particular, I would like to thank, Andrew, Tina, Ferenc, Briggida, Nick, Margaret, Mush and Anne (CRI Campus Library).

I'm also grateful to the New Zealand Pastoral and Agricultural Research Institute Limited for providing financial assistance in the form of a three year stipend, and to the New

Zealand Society of Plant Physiologists for providing generous travel assistance grants. In addition, I would like to thank the Department of Plant Biology and Biotechnology for providing me with a J. P. Skipworth Scholarship in 1998

My final and very special thanks must go to both my parents, John and Marie, and to my partner, Stephanie. I cannot thank them enough for all the support and encouragement they have given to me.

Table of Contents

List of Figures

List of Tables

Abbreviations

$A_{260\ nm}$	absorbance [$\log(I_0/I)$] in a 1 cm light path at 260nm
ACC	1-aminocyclopropane-1-carboxylic acid
AdoMet	S-adenosyl-L-methionine
Amp^{100}	ampicillin (100 mg / mL)
AOA	aminoethoxyacetic acid
APS	ammonium persulphate
ATP	adenosine 5'- triphosphate
AVG	aminoethoxyvinylglycine
BCIP	5-bromo-4-chloro-3-indoyl phosphate
BSA	bovine serum albumin
°C	degrees celsius
ca.	approximately
CAMV	cauliflower mosaic virus
CBB	coomassie brilliant blue
dATP	2'-deoxyadenosine 5'-triphosphate
dCTP	2'-deoxycytidine 5'-triphosphate
dGTP	2'-deoxyguanosine 5'-triphosphate
DMF	N, N-dimethyl formamide
DMSO	dimethyl sulphoxide
DNA	deoxyribonucleic acid
DNase	deoxyribonuclease
DTT	dithiothreitol
dTTP	2'-deoxythymidine 5'-triphosphate
EDTA	ethylenediaminetetraacetic acid
EDTA(Na_2)	ethylenediaminetetraacetic acid, disodium salt
EFE	ethylene forming enzyme
EFS	ethylene forming system

EGTA	1,2,di(2-aminoethoxy)ethane- N, N,N',N',-tetraacetic acid
FW	fresh weight
g	gram
g	acceleration due to gravity (9.81 m s^{-2})
GARAP	goat anti-rabbit alkaline phosphatase
GACC	1-(gamma-L-glutamylamino)cyclopropane-1-carboxylic acid
GC	gas chromatography
GSP	gene-specific primer
GUS	β-glucuronidase
h	hour
HPLC	high perfomance liquid chromatography
HEPES	4-(2-hydroxyethyl)-1-piperazineethanesulphonic acid
IAA	indole-3-acetic acid
IPTG	isopropyl-β-D-thiogalactopyranoside
Kb	kilobase-pairs
kDa	kilodaltons
LB	Luria-Bertani (media or broth)
L	litre
M	molar, moles per litre
MACC	1-(malonylamino)cyclopropane-1-carboxylic acid
1-MCP	1-methylcyclopropene
mcs	multiple cloning site
MES	2-[N-morpholino]ethanesulphonic acid
mg	milligram
mL	millilitre
µg	microgram

min	minute
MilliQ water	water that has been purified by passing through a MilliQ ion exchange column
Mr	relative molecular mass (g mol^{-1})
MTA	5'-methylthioadenosine
MTR	5'-methylthioribose
MOPS	Na(3-[N-Morpholino]propanesulphonic acid)
NaOAc	sodium acetate
ng	nanogram
NBD	norbornadiene
NBT	*p*-nitro blue tetrazolium chloride
2-ODD	2-oxoacid dependent dioxygenase
OD^x	optical density at x nm in a 1 cm light path
PAGE	polyacrylamide gel electrophoresis
PAG	photosynthetic associated gene
PBSalt	50 mM sodium phosphate pH 7.4 in 250 mM NaCl
PCR	polymerase chain reaction
pH	-log [H+]
PVDF	polyvinylidene difluoride
PVPP	polyvinyl polypyrrolidone
RNase	ribonuclease
RO	reverse osmosis
RT-PCR	reverse transcriptase-polymerase chain reaction
RUBISCO	ribulose bisphosphate carboxylase
s	second
sem	standard error of the mean
SAGs	senescence associated genes
SDS	sodium dodecyl sulphate

SSPE	saline, sodium phosphate, and EDTA buffer
SA-PMPs	Streptavidin MagneSphere® Particles
TE	10 mM Tris/ 1 mM EDTA, pH 8.0
TEMED	*N,N,N',N'*-tetramethylethylenediamine
Temp.	temperature
TES	10 mM Tris/ 100 mM sodium chloride/ 1mM EDTA, pH 8.0
Tris	tris (hydroxymethyl)aminomethane
Triton X-100	octylphenoxy polyethoxyethanol
Tween 20	polyoxyethylenesorbitan monolaurate
U	units
UTR	untranslated region
UV	ultra violet light
V	volt (m^2 kg s^{-3} A^{-1})
v/v	volume per volume
W	watt (m^2 kg s^{-3}) or (V A)
w/v	weight per volume

1. INTRODUCTION

Overview

The plant hormone ethylene has been shown to regulate a diverse array of physiological processes in plants. An important aspect of how the hormone mediates these processes is the regulation of ethylene biosynthesis. The 1-aminocyclopropane-1-carboxylic acid (ACC)-mediated biosynthetic pathway in higher plants comprises three enzyme steps which together convert methionine to ethylene. Traditionally, the conversion of *S*-adenosylmethionine to ACC, catalyses by ACC synthase, has been considered to be the rate determining step in the pathway. More recently, there is an emerging view that regulation of ACC oxidase, which catalyses the terminal step in the pathway (the conversion of ACC to ethylene), also represents a further tier of control of the pathway. In the few plants that have been examined thus far, ACC oxidase has been shown to comprise a small multigene-family with each member under different temporal, environmental and/or developmental control.

This thesis examines the transcription and translation of ACC oxidase genes during leaf maturation and senescence in the pasture legume white clover. The aim is to seek evidence for differential transcription and translation of the white clover ACC oxidase gene family during this physiological process.

1.1 Ethylene in plant development

Human civilisation has unknowingly used the plant hormone ethylene to manipulate plant development for hundreds, perhaps thousands of years. The Chinese, for instance, used burning incense to ripen their fruits (Yang and Dong, 1993), and Puerto Rican pineapple growers and Philippine mango growers used bonfires around their crops to help initiate and synchronise flowering (Salisbury and Ross, 1985). Both affects are now attributed to ethylene. However, it was not until early this century that ethylene was identified directly as being able to modify plant responses (Neljubov, 1901, cited in Abeles *et al.*, 1992). Neljubov reported that treatment of etiolated pea seedlings with ethylene caused:

- thickening of the stem and inhibition of root and hypocotyl elongation
- more pronounced curvature of the apical hook

- a horizontal growth habit

Collectively these morphological adaptations have been termed the triple response, the physiological purpose of which may be to facilitate soil penetration by germinating seeds (see below).

The importance of ethylene for survival of plants is suggested by its omniscient presence in plants. There is, for instance, only one documented example of a higher plant (*Potamogeton pectinatus*) that is unable to produce ethylene and survive successfully in the environment (Summers *et al.,* 1996).

Ethylene influences a diverse array of plant growth and developmental processes. Some of these are listed below along with, in most cases, some recent evidence which demonstrates unequivocally the involvement of ethylene in these processes.

- Seed germination: Application of ethylene breaks the dormancy of many seeds including, lettuce (Lieberman, 1979), *Amaranthus* (Kepczynski *et al.,* 1997), and cocklebur (Yoshiyama *et al.,* 1996).
- Emergence of seedlings from soil: Ethylene action has been shown to be important for enabling newly germinated seedlings to emerge through soil. For example, *Arabidopsis thaliana* seedlings selected by their ability to elongate in the presence of 10 $\mu L\ L^{-1}$ ethylene (i.e. absence of the triple response phenotype) were less able to emerge through sand than wild type seedlings (Harpham *et al.,* 1991), with the ability to emerge being directly proportional to their sensitivity to ethylene.
- Root production and growth: The rate of root elongation of sunflower seedlings treated with 10 µM ACC was 40 % that of the control plants 12 hours after application (Finlayson *et al.,* 1996). This inhibition of elongation could be prevented by treatment of the seedlings with silver thiosulphate (STS; an inhibitor of ethylene action). The number of root primordia formed on cut hypocotyls of sunflower could be lowered by application of aminoethoxyvinyl glycine (AVG), an inhibitor of ethylene biosynthesis (Liu *et al.,* 1990). This effect could be reversed by application of ethephon (a compound that readily degrades to ethylene).
- Aerenchyma formation in roots: Aerenchyma is stimulated by anoxic conditions, for example those experienced by roots during flooding, and it involves cell death and lysis of cell walls of specific cortical cells. It is thought to enable acceleration of O_2 diffusion

from aerial parts to O_2-deficient tissues of the root. Aerenchyma formation can be promoted by exogenous ethylene in stems of sunflower under fully aerobic conditions (Kawase, 1981). More recently, the formation of aerenchyma in maize roots by treatment with ethylene has been reported to be blocked by EGTA a chelator of calcium (He *et al.,* 1996). Calcium has previously been shown to be an important secondary messenger in the ethylene signal transduction pathway (Raz and Fluhr, 1992).

- Shoot elongation: Induction of ethylene can either inhibit shoot elongation (for example, as part of the triple response) or promote it, as in rice (Sanders *et al.,* 1990). Norbornadiene (NBD; an inhibitor of ethylene action) was able to inhibit the promotion of shoot elongation of rice coleoptiles (Sanders *et al.,* 1990).

- Flower initiation, development and senescence: Application of ethylene can replace drought or chilling as an inducer of flowering (Reid, 1995). Senescence of certain flowers is considered to be an ethylene-mediated event. For example, increased levels of ethylene are associated with senescence of carnation flowers (Sisler *et al.,* 1996), and both the increase in ethylene and flower senescence can be inhibited by treatment of the flowers with 1-methylcyclopropene (1-MCP; an inhibitor of ethylene action). Treatment of roses with 1-MCP has also been shown to delay flower senescence and abscission of buds (Sisler and Serek, 1997).

- Ratio of male to female flowers: Application of ethylene enhances the formation of female flowers in cucumber (Reid, 1995). A study of monoecious (separate male and female flowers on the same plant) and gynoecious (female flowers only) cucumber plants has revealed the presence of an additional copy of ACC synthase (an enzyme in the ethylene biosynthetic pathway) in the gynoecious plants that is closely linked (as determined by segregation analysis) to the locus F that determines female sex expression (Trebitsh *et al.,* 1997).

- Fruit ripening: Ethylene is considered to control the initiation of changes in colour, aromas, texture, flavour and other biochemical and physiological attributes in climacteric fruit (Lelievre *et al.,* 1997). When ethylene biosynthesis in tomato fruit is downregulated (by the introduction of a gene for ACC synthase in antisense orientation and under the control of the CaMV 35S promoter) the fruit fail to ripen fully (Oeller *et al.,* 1991).

- Nodulation of legumes: Ethylene may have a role in limiting rhizobium infections as an ethylene insensitive mutant of *Medicargo trunculata* was found to exhibit an increase in the number of persistent rhizobium infections compared with wild-type plants (Penmetsa and Cook, 1997).

- Response to pathogen: Sequences in the promoter regions of pathogenesis related proteins have been shown to confer ethylene responsiveness (Shinshi *et al.,* 1995). Further evidence includes the increase in accumulation of two gene transcripts of ACC oxidase (an enzyme in the ethylene biosynthetic pathway) in tobacco leaves infected with the tobacco mosaic virus (Kim *et al.,* 1998).

- Abscission: Ethylene has a crucial role in regulating the timing of abscission (Roberts *et al.,* 1988; Osborne *et al.,* 1989). Using a ß-glucuronidase (GUS) reporter gene fused to the promoter of ACC oxidase, Blume *et al.,* (1997) were able to show an increase in GUS expression in cell layers of the green leaf petiole next to the future abscission zone (before any visible tissue separation), which is consistent with a role for ethylene in promoting the formation of the abscission zone.

- Leaf senescence: (see section 1.4.7)

1.2 Mode of ethylene action

The ability of ethylene to influence such a diverse array of plant responses, from seed germination to senescence, begs the question as to how a single hormone is able to achieve this. Currently, the weight of evidence suggests that ethylene reception and transduction rather than ethylene metabolism is the mediator of ethylene action as (i) the products of ethylene metabolism do not elicit ethylene-like responses, and (ii) ethylene effects can be mimicked by some hydrocarbons (McKeon *et al.,* 1995).

The ethylene receptor and some of the components of its associated transduction pathway that lead to ethylene response have now been identified in *A. thaliana* (see reviews by Chang and Meyerowitz, 1995; Chang, 1996). The ethylene receptor was initially found by screening *A. thaliana* plants for absence of the triple response after treatment with ethylene (Bleecker *et al.,* 1988). One mutant, designated ETR1, was shown to lack a number of responses to ethylene that are present in the wild type plant. These responses included inhibition of cell elongation, promotion of seed germination, enhancement of peroxidase activity, feedback suppression of ethylene synthesis and acceleration of leaf senescence. As

it was also shown to have a reduced capacity to bind ethylene (20 % of wild type), it was suggested that the ETR1 gene may encode the ethylene receptor (Bleecker *et al.,* 1988). The ETR1 gene has now been cloned (Chang *et al.,* 1993), found to display sequence homology to a family of prokaryotic environmental signal transducers known as two-component regulators, and when expressed in yeast demonstrated to bind ethylene (Schaller and Bleecker, 1995). The ability to affect many developmental processes, and to bind ethylene, coupled with its homology to other known prokaryotic environmental signal transducers suggest that the ETR1 protein is not just an ethylene binding protein, but an ethylene receptor.

The ethylene receptor in *A. thaliana* and tomato is encoded by a multigene family with four members in *A. thaliana* (ERS, Hua *et al.,* 1995; ein 4, Roman *et al.,* 1995; ETR2, Sakai, *et al.,* 1998) and two in tomato (tETR, Paynton *et al.,* 1996; eTAE1, Zhou *et al.,* 1996).

The presence of different forms of the receptor may, in part, explain changes in ethylene sensitivity of tissue (Barendse and Peeters, 1995). For instance, the ETR1 homologue in tomato (tETR), is expressed differentially during ripening, flowering, senescence and abscission (Payton *et al.,* 1996). Levels of tETR were undetectable in unripe fruit and presenescent flowers, but accumulated during the early stages of ripening and flower senescence. Similarly in floral abscission zones, levels of tETR increased after anthesis.

A consequence of ethylene binding to its receptor is the induction of mRNAs and proteins which carry out the ethylene response. There are now examples of mRNAs that are induced by ethylene. These include the mRNAs encoding chitinase (Ishige *et al.,* 1991), cellulase (Ferrarese *et al.,* 1995) and a cysteine protease (Jones *et al.,* 1995). Progress has now been made in identifying the promoter elements in the sequences of these genes that confer ethylene responsiveness (Ohme-Takagi and Shinshi, 1995). These sequences (ethylene response elements, EREs) have been shown to be conserved in the promoter regions of a number of pathogenesis-related proteins and found to consist of an 11 base pair sequence (TAAGAGCCGCC) named the GCC box. This sequence has been shown to be important for ethylene responsiveness because deletion of the GCC box eliminates ethylene responsiveness of promoters (for example, the chitinase promoter of tobacco; Shinshi *et al.,* 1995), and because it is able to confer ethylene responsiveness to a minimal CaMV promoter (Ohme-Takagi and Shinshi, 1995). Recently, an AT rich enhancer sequence (distinct from the GCC box) has been shown to confer ethylene responsiveness to

a carnation glutathione *S*-transferase gene by GUS-promoter deletion studies (Maxson and Woodson, 1997).

Changes in sensitivity (or competence to respond) to ethylene are important in determining the ability of the plant to respond to the hormone. Tomato fruits, for example, need to have reached a certain developmental stage in order to be responsive to the ripening effects of ethylene (Grierson and Kader, 1986). However, of equal importance, is the concentration of ethylene that the fruit tissue is exposed to. For example, the fruit of transgenic tomato plants that have been genetically engineered to produce low levels of ethylene (as compared with wild type) ripen more slowly (Klee, 1993) and in some instances fail to completely ripen (Oeller *et al.*, 1991). Furthermore, transgenic tomato plants that are unable to produce high levels of ethylene in response to flooding stress (through the introduction of an ACC oxidase gene in the antisense orientation) display lesser epinastic curvatures of the petioles (an ethylene-mediated response) than wild type (English *et al.*, 1995). It would appear then, that control of ethylene production is an important aspect of how the hormone regulates a diverse array of responses in plants.

1.3 Ethylene biosynthesis

In higher plants (cycads, gnetales, gymnosperms, and angiosperms; Osborne *et al.*, 1996), production of ethylene is regulated both in a developmental manner and by external factors (biotic and abiotic). Typically, production is high in young fruit, vegetative and floral tissue during the period of rapid cell division, but declines during cell expansion before increasing again during ripening and senescence (Abeles *et al.*, 1992). An increase in ethylene production due to the presence of external factors is termed stress ethylene (Abeles *et al.*, 1973). Stresses of abiotic nature that increase ethylene production by tissue include mechanical wounding, bending, rubbing, physical restraint, radiation, elevated temperatures, chilling, dehydration, and various chemical stimuli such as heavy metal ions, herbicides, and defoliants and gases such as sulphur dioxide and ozone (Hyodo, 1991; Abeles *et al.*, 1992). In contrast, biotic stresses are caused by invasion of tissues by viruses, bacteria, fungi, or attack by insects and nematodes.

The pathway by which ethylene is formed in higher plants differs from that of lower plants (liverworts, mosses and ferns). Treatments that influence the rate of ethylene production in higher plants (wounding, hormone treatment, ACC application) have little or no effect in lower plants (Osborne *et al.*, 1996). While it remains unclear how ethylene is produced in

lower plants (Osborne *et al.*, 1996), significant progress has been achieved in determining the pathway of ethylene formation in higher plants (Yang and Hoffman 1984).

Ethylene may be produced from three sources in higher plants; the methionine cycle (Yang cycle), from non-enzymatic oxidative processes resulting from the interaction of free radicals with ACC (Lesham, 1992), and from conversion of short linear aldehydes (pentanal) to ethylene (Knudsen *et al.*, 1994). The physiological significance of the latter two sources remains unclear. In contrast, it is well established that in higher plants ethylene is formed predominantly *via* the ACC-mediated biosynthetic pathway (an offshoot of the methionine cycle) (Yang and Hoffman 1984).

1.3.1 ACC-mediated ethylene production

Elucidation of the ACC-mediated pathway was mainly achieved by S.F. Yang and associates (see Yang and Hoffman, 1984). Initially, model (non-enzymatic) systems were used to unravel the biosynthetic pathway (Lieberman, 1979) since no ethylene could be produced from tissue in the cell-free state.

One of the first systems investigated was the peroxidised linolenate system (Lieberman and Mapson, 1964). This system was considered originally as analogous to the natural (*in vivo*) ethylene forming system (EFS), which acted upon linolenate released from membranes during senescent-associated disintegration. However, although ethylene could be produced by this model system, it did not represent the EFS *in vivo* as ^{14}C-linolenate was not converted by apple, tomato, or cauliflower tissue into ^{14}C-ethylene (Mapson *et al.*, 1970).

The discovery of methionine (a known free radical scavenger) as an intermediate of the pathway occurred fortuitously. When methionine was added to the linolenate system in an attempt to reduce ethylene production (by quenching free radical production), ethylene production increased. It was then discovered that methionine itself could act as a substrate for ethylene in the model system in the absence of peroxidised linolenate (Lieberman *et al.*, 1965). Further proof that methionine may be part of the EFS came from studies which showed that ^{14}C-methionine, labelled at carbons 3 and 4, was incorporated into ethylene in apple tissue (Lieberman *et al.*, 1966).

Tissue systems *in vivo* using ^{14}C-methionine, together with inhibitors of ethylene biosynthesis, were then used to identify further components of the pathway. *S*-adenosyl-L-methionine (AdoMet) was proposed by Adams and Yang (1977) to be an intermediate of

the pathway, because ^{14}C methionine fed to apple tissue was incorporated into both 5'-methyl thioadenosine (MTA) and 5'-methyl thioribose (MTR), which were known products of the reaction catalysed by ATP: methionine *S*-adenosyltransferase (AdoMet synthetase).

The immediate precursor of ethylene was then found using another characteristic of the *in vivo* ethylene forming system, the requirement for oxygen. The substrate for the ethylene forming enzyme (EFE) was identified in 1979 by feeding radiolabelled ^{14}C methionine to plugs of apple fruit tissue (Adams and Yang, 1979). Apple tissue efficiently converted ^{14}C-methionine to ethylene when the tissue was held in air, but if the tissue was made anaerobic (held in N_2), ^{14}C-methionine was not metabolised to ethylene, but to a compound "X" which accumulated. Upon placing the tissue back in air, the level of compound "X" decreased with a concomitant surge in ethylene production. This compound was identified by Adams and Yang (1979) as the cyclic non protein amino acid, ACC.

The complete pathway for ethylene synthesis is now well established (Kende, 1993). The pathway starts by the diversion of methionine into the Yang (or methionine) cycle (Figure 1). The adenosyl group of ATP is then attached to methionine by AdoMet synthetase to produce *S*-adenosyl-methionine (AdoMet). At this stage the pathway is not committed to ethylene formation as AdoMet can participate in a variety of other reactions in the cell (see below). The first committed step is that catalysed by the enzyme ACC synthase. ACC synthase produces ACC by cleaving the MTA moiety from AdoMet. Production of MTA in this reaction is important as methionine can be regenerated from it *via* the Yang cycle. Without this regeneration it is thought that levels of methionine would quickly become limiting in tissue (Baur *et al.*, 1972). Two possible fates await the ACC produced. ACC can either be conjugated to 1-(malonylamino)cyclopropane-1-carboxylic acid (MACC) which appears to be the major ACC-conjugate in plants (Amrhein *et al.*, 1981; Hoffman *et al.*, 1982A). In immature green tomato fruit ACC can also be conjugated to 1-(gamma-L-glutamylamino) cyclopropane-1-carboxylic acid (GACC) (Martin *et al.*, 1995), to a level of about 10 % that of MACC (Peiser and Yang, 1998). If not conjugated, ACC is converted by the action of ACC oxidase to ethylene with the overall result being that ethylene is derived from carbons 3 and 4 of methionine.

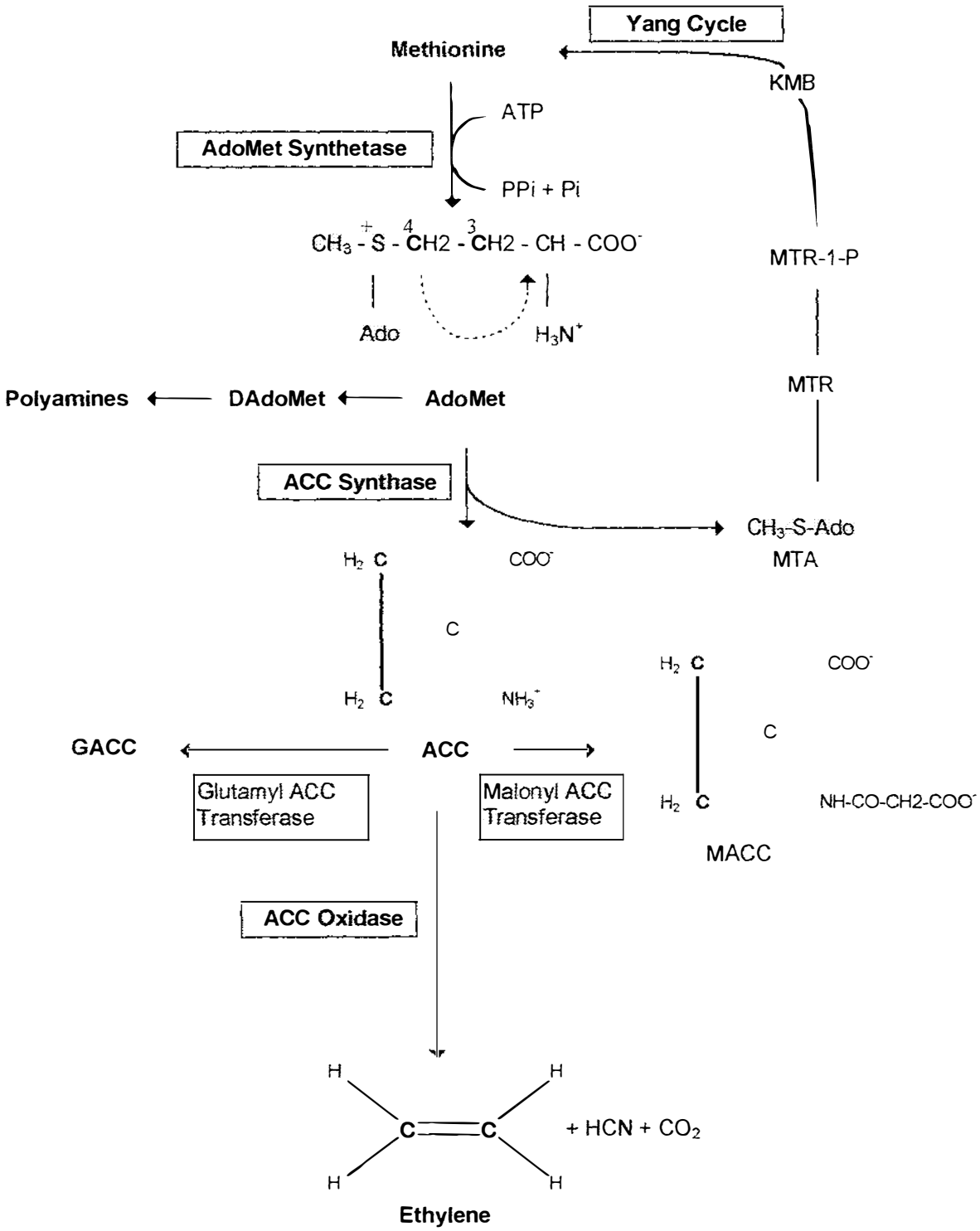

Figure 1. The Ethylene Biosynthetic Pathway.

ACC, 1-aminocyclopropane-1-carboxylic acid; **AdoMet**, *S*-adenosylmethionine; **DAdoMet**, decarboxylated AdoMet; **MTA**, 5'-methylthioadenosine; **MTR**, 5'-methylthioribose; **MTR-1-P**, 5'-methylthioribose-1-phosphate; **KMB**, 2-keto-4-methylthiobutyrate; **GACC**, 1- (gamma-L-glutamylamino) cyclopropane-1-carboxylic acid; **MACC**, 1- (malonylamino) cyclopropane-1-carboxylic acid.

1.3.2 Enzymes of the ACC-mediated biosynthetic pathway

1.3.2.1 AdoMet synthetase

AdoMet synthetase (EC 2.5.1.6) is a ubiquitous enzyme found in both prokaryotic and eukaryotic organisms (Tabor and Tabor, 1984). AdoMet synthetase is classified as a house-keeping enzyme due to its pivotal role in cellular biochemistry (Fluhr and Mattoo, 1996). It provides AdoMet not only for ethylene production, but for polyamine synthesis, and transmethylation reactions of proteins, carbohydrates, lipids and nucleic acids (Tabor and Tabor, 1984). The link between polyamine production and ethylene biosynthesis is of particular interest as application of polyamines has been shown to inhibit ethylene production in some plants. For example, application of spermine to cut carnation flowers delayed flower senescence, and reduced ethylene production, ACC content, and activities and transcript amounts of both ACC synthase and ACC oxidase (Lee *et al.*, 1997).

Although not a committed enzyme of ethylene biosynthesis, AdoMet synthetase is encoded by a multigene family in plants with the different family members under differential control (Schroder *et al.*, 1997; Peleman *et al.*, 1989). The existence of multiple controls on AdoMet synthetase suggests that the level of AdoMet produced by the constitutive enzyme is not always sufficient. In this regard, expression of AdoMet synthetase genes is increased by a variety of environmental factors including drought stress (Mayne *et al.*, 1996), salt stress (Espartero *et al.*, 1994), fungal and bacterial elicitors (Somssich *et al.*, 1989; Gowri *et al.*, 1991; Kawalleck *et al.*, 1992), mechanical stimuli (Espartero *et al.*, 1994; Kim *et al.*, 1994) and ozone exposure (Tuomainen *et al.*, 1996, cited in Gomez-Gomez and Carrasco, 1998), 2,4-dichlorophenoxyacetic acid (2,4-D) application (Gomez-Gomez and Carrasco, 1998) and during fruit ripening (Whittaker *et al.*, 1997). Interestingly, all of these factors are also known to induce ethylene biosynthesis (Abeles *et al.*, 1992). Further, a more direct effect of ethylene on transcript induction has been shown in *Actinidia chinensis* fruit where AdoMet synthetase transcripts were shown to be induced by the exposure to exogenous ethylene (Whittaker *et al.*, 1997). Taken together, these observations suggest that an important role of the enzyme is to replenish AdoMet during periods of enhanced ethylene synthesis (Boerjan *et al.*, 1994; Whittaker *et al.*, 1997).

1.3.2.2 ACC synthase

ACC synthase (S-adenosyl-L-methionine; methylthioadenosine lyase; EC 4.4.1.14), an enzyme found in the cytosolic fraction of plant tissues, converts the aminopropyl group of AdoMet into ACC (Adams and Yang 1979). The enzyme requires pyridoxal-5'-phosphate as a cofactor, and like other enzymes that require pyridoxal-5'-phosphate, is inhibited by AVG and aminooxyacetic acid (AOA) (Imaseki, 1991).

ACC synthase protein was first purified from ripened tomato pericarp after a wounding pretreatment (Bleecker *et al.,* 1986). Subsequently it has been purified from aged mesocarp of *Cucurbita maxima* (Nakajima *et al.,* 1988), hypocotyls of mungbean (Tsai *et al.,* 1988), thin slices of zucchini after induction with indole-3-acetic acid (IAA), benzyl adenine, lithium chloride and AOA (Satoh and Theologis, 1989; Sato *et al.,* 1991) and ripening tomato (Van der Straeten *et al.,* 1990) and apple fruit (Yip *et al.,* 1991).

Low abundance and lability of the enzyme are characteristics of ACC synthase (Acaster and Kende, 1983; Bleecker *et al.,* 1986). The level of ACC synthase protein in ripened tomato pericarp was estimated at 0.0001% of total protein, a level which could be elevated 100-fold by wounding (Bleecker *et al.,* 1986). The lability of the enzyme is due in part to a catalytic-based inactivation where a covalent linkage is formed at the active site between ACC synthase and its substrate AdoMet (Satoh and Esashi, 1986; Satoh and Yang, 1988; Casas *et al.,* 1993). For example, the half-life of a preparation of ACC synthase extracted from mungbean hypocotyls was reduced from 23.5 to 12 min when the concentration of AdoMet was increased from 40 to 150 μM (Satoh and Esashi, 1986).

ACC synthase has been reported to occur as either a monomer or dimer, with the monomer having a molecular mass of 48 kDa (from apple fruit) to 58 kDa (from squash fruit) (Fluhr and Mattoo, 1996). The Km of ACC synthase for its substrate AdoMet is reported to vary between 12 μM for an apple ACC synthase expressed in *E. coli* (White *et al.,* 1994) to 60 μM for the enzyme purified from etiolated hypocotyls of mung bean (Nakajima and Imaseki, 1986). ACC synthase has a pH optima in the alkaline region, with an optima of pH 8.0 and 9.5 reported for the enzyme purified from mung bean hypocotyls (Tsai *et al.,* 1991) and *C. maxima* fruit tissue (Sato *et al.,* 1991) respectively.

Multiple members of ACC synthase have been found in plants, with amino acid sequence identities varying from 48 to 97 % (Woltering and de Vrije, 1995). Seven members have

been identified in tomato (Oetiker *et al.,* 1997), seven in mung bean (Yu *et al.,* 1998), four in *Stellaria longipes*; five in *A. thaliana* (Liang *et al.,* 1992), three in potato (Destefano-Beltran *et al.,* 1995); and two in carnation (Park *et al.,* 1992).

ACC synthase is widely regarded as the major rate determining enzyme of the ethylene biosynthetic pathway (Kende, 1993). This was initially suggested by the finding that ethylene production increased in plant organs (excluding preclimacteric fruits and flowers) after application of ACC (Hoffman and Yang, 1980), and that levels of endogenous ACC were highest in tissue that produced high amounts of ethylene, for example, at certain stages of development (fruit ripening, and flower senescence), and in response to stress (wounding, waterlogging, chilling and pathogen attack) and auxin application (Yang and Hoffman, 1984). Furthermore, application of AVG prevented both the increase in endogenous ACC and the concomitant ethylene production (Yang and Hoffman 1984).

Measurement of ACC synthase activity *in vitro* has confirmed that enzyme activity is higher in tissues that have elevated levels of endogenous ACC and ethylene. This has been shown in ripening fruits of tomato (Boller *et al.,* 1979), in etiolated mung-bean hypocotyls treated with auxin (Yu *et al.,* 1979), in senescing petals of carnation flowers (Park *et al.,* 1992), in the stigma of petunia flowers following pollination (Pech *et al.,* 1987), in bean leaves treated with cadmium (Fuhrer, 1982) and in potato tubers and mesocarp tissue of *C. maxima* following mechanical wounding (Burns and Evensen 1986; Hyodo *et al.,* 1989).

The availability of cDNA probes for ACC synthase has enabled further analysis of the regulation of ACC synthase activity at the molecular level. It is now apparent that the ability of different stimuli to influence the activity of ACC synthase is not through multiple regulation of the same gene, but through the regulation of distinct genes which may or may not have similar regulatory elements. For example, different members of the multigene family are expressed differentially in response to wounding, anaerobiosis, lithium chloride, and auxin treatments in etiolated *A. thaliana* seedlings (Liang *et al.,* 1992), in response to treatment with a yeast elicitor in tomato suspension cells (Oetiker *et al.,* 1997), in response to wounding in tomato fruit tissue (Lincoln *et al.,* 1993), in different tissue of carnation flowers (Ten Have and Woltering, 1997), in response to photoperiod and temperature in *S. longipes* (Kathiresan *et al.,* 1998), in response to lithium chloride and IAA in mung bean hypocotyls (Kim *et al.,* 1997; Yu *et al.,* 1998), in response to fungal infections in tomato

plants (Spanu *et al.,* 1993), and in response to ethylene application of the wounded mesocarp tissue of *C. maxima* (Nakijima *et al.,* 1990).

In many instances, ethylene production rates positively correlate with ACC synthase transcription (Sato and Theologis, 1989; Huang *et al.,* 1991; Olson *et al.,* 1991; Rottmann *et al.,* 1991; Kim *et al.,* 1992; Park *et al.,* 1992; Harpster *et al.,* 1996) suggesting that ethylene production is controlled by ACC synthase activity regulated at the level of gene transcription.

There are, however, examples where ethylene production does not correlate with the accumulation of the ACC synthase transcript, for example, in the styles of cut carnation flowers (Ten Have and Woltering, 1997), during elicitor-based induction of ethylene in tomato suspension cultures (Spanu *et al.,* 1993; Oetiker *et al.,* 1997), in response to wounding of carnation flowers (Park *et al.,* 1997), in response to benzyl adenine treatment of *A. thaliana* plants (Vogel *et al.,* 1998) and during the circadian-based ethylene production of *S. longipes* (Kathiresan *et al.,* 1998). This may be due to the presence of yet unidentified ACC synthase genes, the occurrence of differential transcription, post-transcriptional processing and post-translational modifications of the enzyme, conjugation of the ACC produced, or due to the influence of ACC oxidase. Examples of all of these mechanisms have been reported and will be discussed.

In terms of transcriptional processing, an auxin-inducible ACC synthase gene transcript of pea (Ps-ACS1), was found to recognise two RNA transcripts (*ca.* 1.6 and 1.9 Kb) on northern blots. The larger transcript was not considered to be due to incomplete processing of introns, but due to the presence of an alternative promoter within the sequence of the larger transcript (Peck and Kende, 1998). The reason for differential transcription of the same gene remains unclear.

Post-transcriptional processing involving incomplete RNA splicing (incomplete removal of introns) has been reported for transcripts of ACC synthase isolated from flooded roots of tomato (Olson *et al.,* 1995). This was shown for the LE-ACS3 transcript by probing poly (A^+) RNA of tomato with sequences specific to introns one and three of the LE-ACS3 gene and identifying distinct transcripts that differ by the size expected if the introns were removed. The authors proposed that differential splicing of the ACC synthase gene transcript may represent a form of post-transcriptional control. However, this remains to be proven.

The increase in ethylene production of tissue may not always be regulated by increased transcription of ACC synthase, but by post-translational modification or increased translation of the protein. For instance, both the length and primary sequence of the COOH-terminal region of various ACC synthases is hypervariable despite a high degree of similarity in the rest of the protein (Theologis, 1992). Further, it has been shown in a heterologous *E. coli* expression system that a deletion of 46 to 52 amino acids at the COOH-terminal region results in an enzyme with nine times higher affinity for AdoMet than wild type (Li and Mattoo, 1994). Evidence that modification at the COOH-terminal region can regulate ACC synthase activity in the plant has come from a study that identified a cytokinin-responsive ACC synthase in *A. thaliana* (Vogel *et al.,* 1998). The gene was identified by T-DNA tagging a population of *Arabidopsis* plants that lacked a triple response in the presence of cytokinin. The gene was found to encode ACS5 (Liang *et al.,* 1996), the same gene in which a lesion results in the 20-fold overproduction of ethylene observed in the *eto2* mutant plants. The *eto2* phenotype was found to be due to a single base pair mutation, 35 bp upstream of the stop codon of ACS5 (Vogel *et al.,* 1998). As cytokinin application resulted in only a modest transient increase in ACS5 transcription (less than 2-fold after 1 h), yet ethylene biosynthesis increased more than 8-fold over four days, it was proposed that cytokinin may act by relieving the negative influence of the COOH-terminal region of the ACS5 protein.

Increased translation from pre-existing mRNA is implicated in the carbon dioxide mediated increase in ethylene production of cucumber (Mathooko *et al.,* 1998). The increase required protein kinase activity (which indicates signal transduction), but the activation did not require transcription *de novo* as shown by the non effect of transcriptional inhibitors. Instead a requirement for protein synthesis was demonstrated (cycloheximide inhibited the increase in activity) suggesting that carbon dioxide may act by increasing the translation of the enzyme.

1.3.2.3 ACC conjugation

ACC can be conjugated into either MACC by N-malonyltransferase (Amrhein *et al.,* 1981; Hoffman *et al.,* 1982) or GACC by glutamyl ACC transferase (Martin *et al.,* 1995; Fluhr and Mattoo, 1996). MACC is found throughout the plant, including vegetative tissue, seeds and ripening fruit (Amrhein *et al.,* 1982; Satoh and Esashi, 1984; Yang *et al.,* 1993). It is synthesised in the cytosol and stored in the vacuole (Bouzayen *et al.,* 1989).

N-malonyltransferase has now been partially purified from etiolated hypocotyls of mung bean (Guo *et al.*, 1992; Benichou *et al.*, 1995) and tomato fruit (Martin and Saftner, 1995). Two isoenzymes have been discovered in mung bean that have different molecular weights and kinetic parameters. A 36 kDa isoenzyme exhibits a lower temperature optimum (40°C) and a seven- and three-fold lower apparent Km for ACC (68 μM) and malonyl-Co (74 μM) respectively when compared with a 55 kDa isoenzyme (Benichou *et al.*, 1995). In tomato, N-malonyltransferase activity was found to be enhanced by exposure to ethylene in immature green and mature green, but not ripening, tomato fruit (Martin and Saftner, 1995).

The physiological significance of ACC conjugation for controlling ethylene production is still unclear. In some plant tissues, MACC is considered to be the inactive end product of ACC, and is not oxidised to ethylene (Hoffman *et al.*, 1983). It therefore could act to control ethylene production by sequestering the ACC produced by ACC synthase in an irreversible reaction. For example, during ripening of bananas the peel produces up to 80-fold less ethylene than the pulp even though it has seven-fold more ethylene forming activity (Dominguez and Vendrell, 1993). This was proposed to be due to the greater amount of ACC conjugation observed in the peel as compared with the pulp.

However, it has been shown in vegetative (tobacco leaf discs and watercress stems; Jiao *et al.*, 1986) and floral tissues (senescing carnation flowers; Hanley *et al.*, 1989) that MACC can be hydrolysed and serve as a source of ACC for ethylene production. In watercress stems, the hydrolysis of MACC to ACC was confirmed by radiolabelling MACC. However, only *ca.* 2 % of the MACC was converted to radiolabelled ACC and the hydrolysis required a long incubation time (several hours) as well as high concentrations of MACC (the Km of the putative hydrolase was estimated to be 0.45 mM) (Jiao *et al.*, 1986). Further work, therefore, is required to demonstrate unequivocally the significance of ACC conjugation in plant tissues.

1.4 ACC oxidase

1.4.1 Identification of EFE as ACC oxidase

Characterisation of ACC oxidase (formerly the ethylene-forming-enzyme, EFE) has lagged behind ACC synthase due to the difficulty, until comparatively recently, to assay the enzyme *in vitro*. EFE could be readily assayed *in vivo* by administration of its substrate, ACC, to a wide variety of tissue (Cameron *et al.*, 1979).

Although EFE could be assayed *in vivo*, obtaining authentic activity *in vitro* was difficult as tissues known to produce high amounts of ethylene, quickly lost this ability upon homogenisation. It appeared that to function, EFE required cellular integrity, as the presence of detergents (Tween 20 and Triton X-100) or osmotic shock treatment, both of which can modify membrane structure, greatly reduced activity (Yang and Hoffman, 1984).

Numerous candidates were initially suggested for the EFE. Enzymes such as a peroxidase, an IAA-oxidase, a carnation microsomal enzyme, a pea microsomal enzyme, and an enzyme from a pea seedling extract could convert ACC to ethylene in the presence of various cofactors. Although these systems were oxygen-dependent and heat-denaturable, they displayed other characteristics which did not resemble those of the natural system *in vivo* (Yang and Hoffman, 1984; Venis, 1984). For example, the reported Km for the pea microsomal enzyme ranged between 15 mM to 400 mM, values that were much higher than the Km of 66 μM reported for the enzyme *in vivo* from pea epicotyl (McKeon and Yang, 1984). It was suggested, therefore, that the pea microsomal enzyme was converting ACC to ethylene by a free radical based mechanism (Yang and Hoffman, 1984). Further criteria that were established for authentic EFE activity *in vitro* by the study of the enzyme *in vivo* were inhibition by cobalt ions, production of equimolar amounts of ethylene, CO_2 and cyanide from ACC, and stereospecificity for ACC (Yang and Hoffman, 1984).

The test for stereospecificity was based on ACC possessing reflective symmetry but not rotational symmetry, meaning that the two methylene groups of ACC could be distinguished by an enzyme which stereodifferentiates. Ethyl substitution at each of the four methylene hydrogens of ACC results in four stereoisomers. An enzyme that stereodifferentiates would not convert these four stereoisomers into 1-butene with equal efficiency, and so conversion of these stereoisomers could be used to validate the authenticity of the enzyme activity *in vitro*. Administration of the four stereoisomers *in*

vivo to post climacteric apple fruit, excised preclimacteric cantaloupe and etiolated mung bean hypocotyls, confirmed that for authentic EFE only one stereoisomer, (+) - allocoronamic acid, was favoured (Hoffman *et al.,* 1982). It was shown subsequently that neither the peroxidase, carnation microsomal enzyme, pea microsomal enzyme, IAA-oxidase, or the pea seedling extract were able to stereodiscriminate (Venis, 1984), suggesting their action might be through activating molecular oxygen probably to free radicals such as 0^{2-} and HO, which in turn react with ACC non-enzymatically to form ethylene (Yang and Hoffman, 1984).

Little progress was made throughout the 1980s in measuring authentic EFE activity *in vitro.* Vacuoles isolated from leaf-mesophyll protoplasts of pea and bean were the smallest cellular entities that exhibited EFE activity *in vitro* that was both stereospecific and had the expected Km for ACC. Although the vacuoles accounted for *ca.* 80 % of the EFE activity of the protoplast (Guy and Kende, 1984), the protoplast itself retained only a very small percentage (< 5 %) of the EFE activity observed in plant tissue *in vivo* and so a significant proportion (96 %) of the EFE remained unaccounted for (Porter *et al.,* 1986).

The breakthrough that led Ververidis and John (1991) to obtain complete recovery of the EFE *in vitro* can be credited to D. Grierson and associates. It began in 1985, with their interest in identifying ripening related genes and how they are regulated by ethylene. When a cDNA library made from ripe tomato fruits was differentially screened with cDNA sequences from mature green and ripe fruit, nineteen non-homologous groups of ripening related clones were identified (Slater *et al.,* 1985). One clone, designated pTOM13, was shown to be homologous to a mRNA that also accumulated after mechanical wounding of unripe tomato pericarp and leaf tissue, prior to the wound-induced peak in ethylene production (Smith *et al.,* 1986). It was suggested that the pTOM13 transcript might either be involved in ethylene production or be a transcript that was rapidly induced by ethylene. It was subsequently shown that it was both induced by ethylene in mature green tomato fruit (Maunders *et al.,* 1987) and involved in ethylene biosynthesis (Hamilton *et al.,* 1990).

This evidence for involvement of pTOM13 in ethylene formation came from insertion of its sequence in the antisense orientation into tomato plants (Hamilton *et al.,* 1990). When introduced, the pTOM13 cDNA decreased ethylene synthesis in both wounded leaf tissue and ripening fruit in a dose-dependent manner indicating that it played a role in either ethylene production, perception, or metabolism (Hamilton *et al.,* 1990). It appeared from

the sizes of purified ACC synthases from zucchini fruit (53 kDa; Satoh and Theologis, 1989) that the protein encoded by pTOM13 (35 kDa; Smith *et al.,* 1986) was too small to be an ACC synthase (Hamilton *et al.,* 1990). To test whether pTOM13 could encode EFE, an assay *in vivo* was carried out on leaf discs excised from both control and antisense plants, and it was shown that EFE was inhibited only in the antisense plants, and in a gene-dosage dependent manner (Hamilton *et al.,* 1990).

Ultimate verification came from the heterologous expression in yeast of a corrected clone of pTOM13 (2 bases were found to be missing in the original fragment of pTOM13) designated pRC13. The yeast cells transformed with pRC13 were shown to convert exogenously applied ACC to ethylene, whereas untransformed yeast cells could not (Hamilton *et al.,* 1991).

The identification of the cDNA for the EFE together with the sequence homology it shared with another enzyme (flavanone-3-hydroxylase) led biochemists to recover and assay the recalcitrant EFE *in vitro.* The predicted amino acid sequence of pTOM13 was found to have 33 % identity and 58 % similarity to flavanone-3-hydroxylase from *Antirrhinum majus*, an enzyme known to require anoxic conditions during extraction, and iron and ascorbate when assayed (Britsch and Grisebach, 1986). Using these same extraction and assay conditions, EFE was successfully recovered from the soluble fraction of melon fruit (Ververidis and John, 1991). Of significant note was that there was no obligate requirement for an intact membrane. The complete loss of ACC oxidase activity previously observed in tissue homogenates has now been attributed to the loss of iron and ascorbate during extraction, and the low activity of intact protoplasts and vacuoles being due to the integral membrane structure maintaining these cofactors in sufficiently high concentrations (Fernandez-Maculet and Yang, 1992).

Confirmation that the activity *in vitro* was representative of activity *in vivo* was achieved by finding a parallel increase in both activities in preclimacteric apple fruits treated with ethylene (Fernandez-Maculet and Yang, 1992), and by the stereospecificity of the reaction (Ververidis and John 1991; Kuai and Dilley 1992; Fernandez-Maculet and Yang, 1992; Dong *et al.,* 1992). The stoichiometry of the reaction was then determined (Dong *et al.,* 1992) (Figure 2) and as a consequence of this, EFE was renamed ACC oxidase.

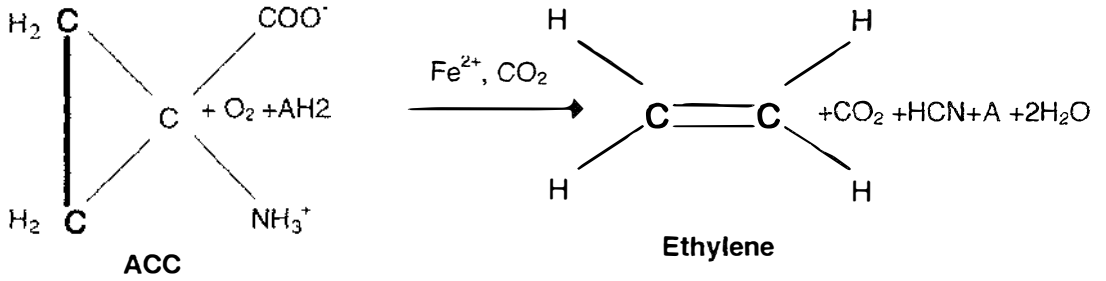

Figure 2. Stoichiometry of reaction catalysed by ACC oxidase.

AH2 and A stand for ascorbate and dehydroascorbate respectively.

1.4.2 Biochemical characterisation of ACC oxidase

ACC oxidase (EC 1.4.3) is now classed as a 2 oxo-acid dependent dioxygenase (2-ODD) (Prescott and John, 1996). Two-ODDs are soluble enzymes that require Fe^{2+} and ascorbate for optimal substrate conversion *in vitro*. Most 2-ODDs have an absolute requirement for 2-oxoglutarate, but ACC oxidase appears to be unique in this family in that it uses ascorbate not 2-oxoglutarate as a cosubstrate (Prescott and John, 1996). It has been proposed that ACC oxidase originated by an alteration in the substrate specificity of the closely related 2-oxoacid dependent dioxygenase (John, 1997).

ACC oxidase has been partially purified from fruits of melon (4-fold; Smith *et al.*, 1992), apple (10-fold; Kuai and Dilley 1992) and cherimoya (41.4-fold; Escribano *et al.*, 1996), and purified to electrophoretic homogeneity in fruits of apple (21-fold; Pirrung *et al.*, 1993), (180-fold; Dong *et al.*, 1992) (171.5-fold; Dupille *et al.*, 1993), and banana (145-fold; Moya-Leon and John, 1995).

The molecular weight of ACC oxidase has now been determined from many tissues and shown to range from 35 kDa for the enzyme from banana fruit (Moya-Leon and John, 1995) to 41 kDa for the enzyme from melon (Smith *et al.*, 1994). ACC oxidase is a basic protein having an isoelectric point at pH 4.35 for the enzyme from cherimoya fruit (Escribano *et al.*, 1996) and pH 4.9 for that of banana fruit (Moya-Leon and John, 1995).

The optimal pH for activity is near neutral but becomes more acidic if carbon dioxide is present. The pH optimum has been shown to vary from as low as pH 6.7 (at 20 % carbon dioxide level) in apple to pH 7.5 (ambient carbon dioxide) in melon.

ACC oxidase requires ascorbate, bicarbonate and Fe^{2+} in the reaction mix for maximal activity. If any one of these compounds is omitted, the activity is greatly reduced. Maximal activity is generally attained over a broad concentration of these cofactors and cosubstrate. For the partially purified enzyme of banana, activity was maximal at concentrations of 20 to 50 mM ascorbate, 0.05 to 0.4 mM Fe^{2+}, and 10 to 40 mM bicarbonate (Moya-Leon and John 1995). These concentrations are similar to those reported for the enzyme of cherimoya fruit (Escribano *et al.,* 1996) and carnation petals (Nijenhuis-De Vries *et al.,* 1994). There are reports that supraoptimal concentrations of cofactors and cosubstrates reduce activity of ACC oxidase. For example, the activity of the enzyme from winter squash mesocarp tissue was reduced by 50 % when the concentration of Fe^{2+} was increased from 20 mM to 500 mM, and reduced by 80 % when the concentration of ascorbate was increased from the optimal 10 mM to 100 mM (Hyodo *et al.,* 1993).

Km values for ACC oxidase for ACC have been reported to range from 6.4 μM for the partially purified enzyme from apple (Kuai and Dilley, 1992), to 425 μM for the enzyme in the crude homogenate of carnation petals (Nijenhuis-De Vries *et al.,* 1994). However, the value of the Km is dependent upon the concentration of carbon dioxide/ bicarbonate in the assay mix. For example, if 30 mM sodium bicarbonate is omitted from the reaction mix in the carnation petal extract, the Km for the enzyme is reduced from 425 μM to 30 μM (Nijenhuis-De Vries *et al.,* 1994). Similarly, the Km value of the partially purified enzyme from cherimoya fruit for ACC is reduced from 194 μM to 82 μM when 20 mM sodium bicarbonate is omitted from the reaction mix (Escribano *et al.,* 1996).

The mechanism by which carbon dioxide activates ACC oxidase has been examined by site directed mutagenesis (Kadyrzhanova *et al.,* 1997; John *et al.,* 1997; Charng *et al.,* 1997). The mechanism was proposed to be similar to the CO_2 activation of RUBISCO which is through the formation of a carbamate at a lysine residue. The lysine residues in ACC oxidase considered as potential carbamylation sites were identified by their conservation in all ACC oxidase sequences. Seven were identified. However, none of the seven lysine residues, when changed to another residue such as arginine (which does not form a carbamate adduct; Charng *et al.,* 1997), or to other residues (Kadyrzhanova *et al.,* 1997; John *et al.,* 1997) prevented the activation of the enzyme by carbon dioxide.

The putative Fe^{2+} ligands of ACC oxidase have been identified as (Histidine[177], Aspartate[179] and Histidine[234]) by comparison with the secondary structure of the related isopenicillin-N-synthase. Site directed mutagenesis of the ACC oxidase protein expressed in *E. coli* has confirmed that the three putative Fe^{2+} ligand residues of ACC oxidase are essential for activity (Kadyrzhanova *et al.*, 1997).

ACC oxidase is unstable during catalysis (Smith *et al.*, 1994; Barlow *et al.*, 1997; Zhang *et al.*, 1997), and has been studied using tomato ACC oxidase purified from *E. coli* transformed with the cDNA clone pRC13 (the corrected version of pTOM13). The catalytic lability of the ACC oxidase encoded by pRC13 was shown to result from at least three discrete processes:

- Partial unfolding of the catalytically active conformation. This was the slowest inactivation mechanism ($t_{1/2}$ > 1 h). This occurred in the absence of cofactors and substrates and did not result in fragmentation of the enzyme.
- Oxidative damage which may or may not occur at the active site of the enzyme. The damage is catalase-protectable and therefore thought to be due to the generation of hydrogen peroxide. This inactivation mechanism is thought to be due to the interaction of Fe^{2+} and ascorbate in aerobic conditions [Udenfreind's reagent] which can produce hydrogen peroxide (Udenfreind *et al.*, 1954, cited in Barlow *et al.*, 1997).
- Oxidative damage to the active site which is not catalase protectable. This is due in part to metal catalysed oxidative cleavage close to the active site (as determined by comparison to the secondary structure of isopenicillin-N-synthetase; Roach *et al.*, 1995). Metal catalysed oxidative damage is considered to be a biochemical 'ageing' process with modified enzymes being apparently more susceptible to protease-mediated degradation (Stadtman and Oliver, 1991). The fragmentation occurs in the absence of ACC, but additional fragments are observed when ACC is present. No fragmentation is observed if the enzyme is denatured prior to addition of ascorbate and iron suggesting a correctly folded enzyme is required for fragmentation to proceed (Barlow *et al.*, 1997).

1.4.3 Localisation of ACC oxidase

ACC oxidase has been localised to both the cytosol and cell wall in tissue. A cytosolic location was initially suggested by recovery of ACC oxidase in the soluble fraction of melon (Ververidis and John, 1991), avocado (McGarvey and Christoffersen, 1992) and

mandarin fruits (Dupille and Zacarias, 1996). Dupille and Zacarias (1996) found that addition of Triton X-100 (a detergent which aids solubilisation of enzymes from membranes) did not increase recovery of the enzyme from the peel of mandarin. In cell suspension cultures of tomato, cell fractionation techniques (which included protoplast and vacuolar preparations) together with activity and immunoblot analysis has localised ACC oxidase to the cytoplasm (not vacuole or cell wall) (Reinhardt *et al.*, 1994). Consistent with these findings, is the absence in ACC oxidase of an N-terminal signal sequence which is considered to be required for targeting of ACC oxidase to the cell wall *via* the endoplasmic-reticulum pathway (Balague *et al.*, 1993).

It appears however, that in apple, ACC oxidase is more readily associated with the pellet than the soluble fraction, as addition of either 0.1 % (v/v) Triton X-100 (Dong *et al.*, 1992; Fernandez-Maculet and Yang, 1992) or 5 % (w/v) polyvinyl polypyrillidone (Kuai and Dilley, 1992; Fernandez-Maculet and Yang, 1992) greatly improves recovery of the enzyme. In addition, using immunogold-labelled secondary antibodies ACC oxidase in ripening apple fruits has been localised to the cell wall (Rombaldi *et al.*, 1994).

1.4.4 ACC oxidase activity during plant development

Biochemical and physiological studies have examined changes in the activity of ACC oxidase during organ development and in response to wounding. In climacteric fruit, ACC oxidase activity is typically low in early unripe green fruit and rises to be highest during ripening, before declining again at the over-ripe stage (Ververidis and John, 1991; Moya-Leon and John, 1994). Comparison of activity between different climacteric fruit is difficult, as not all assays are performed under optimal conditions, but increases in activity from *ca.* 2 to 35 nL g^{-1} FW h^{-1} (pulp) and *ca.* 35 to 130 nL g^{-1} FW h^{-1} (peel) have been reported for ripening banana fruit (Moya-Leon and John, 1994), <5 to *ca.* 260 nL g^{-1} FW h^{-1} for ripening melon fruit (Ververidis and John, 1991) and 10 to 196 mg^{-1} protein h^{-1} for ripening tomato fruit (Barry, *et al.*, 1996).

Wounding has also been shown to increase ACC oxidase activity in fruit tissues when measured *in vivo.* For instance, ACC oxidase activity increases steadily from *ca.*1 to 6 nL g^{-1} FW h^{-1} in flavedo discs of mandarin fruit during a 24 hour incubation (Dupille and Zacarias, 1996) with the increase being 4-fold higher (up to 22 nL g^{-1} FW h^{-1}) if the tissue is incubated in the light. Similarly, ACC oxidase activity increases from 2.5 to 10 nmol g^{-1}

FW h^{-1} in wounded mesocarp tissue of *C. maxima* during a 40 hour incubation (Hyodo *et al.*, 1993). This increase in enzyme activity was effectively prevented by the presence of NBD.

Differences in the affinity of ACC oxidase for carbon dioxide and ascorbate have been used to indicate the existence of distinct isoenzymes in the roots and leaves of sunflower and corn seedlings (Finlayson *et al.*, 1997). In the leaf, where carbon dioxide concentrations are low and ascorbate concentrations are high (as compared with the root), the enzyme has a higher affinity for carbon dioxide (lower Km) and a lower affinity for ascorbate as compared with the enzyme of the root. The authors conclude that specific isoforms of ACC oxidase may exist in plants that are tailored to the environmental and physiological status of each organ. Additional and complementary information on the existence of isoenzymes of plant tissues can be obtained by molecular analysis.

1.4.5 Molecular characterisation of ACC oxidase

Multiple gene members of ACC oxidase have been identified in plants by screening genomic libraries, including four members in petunia (Tang *et al.*, 1993), three members in tomato (Bouzayen *et al.*, 1993), three members in tobacco (Kim *et al.*, 1998), and three members in melon (Lasserre *et al.*, 1996). Multiple ACC oxidase gene transcripts have been identified in other plants by screening cDNA libraries. For example, using this approach two members were discovered in mung bean (Kim and Yang, 1994), three members in sunflower seedlings (Liu *et al.*, 1997), and two members in broccoli (Pogson *et al.*, 1995).

Sequence data from more than thirty ACC oxidase gene members have revealed there is high sequence conservation (70-80 % nucleotide sequence homology) both within a family and between gene families (Lasserre, *et al.*, 1996). The gene families of tomato and petunia are particularly similar with the three gene members of tomato showing 88 to 94 % similarity to each other, and just as high similarity to the three gene members of petunia (88 to 95 %), when amino acid sequences are compared (Lasserre *et al.*, 1996). In contrast, both the 5'- and 3'-untranslated regions (UTRs) show significant sequence divergence (Barry, *et al.*, 1996; Tang, *et al.*, 1993; Kim and Yang, 1994). For example, in tomato, the three isoforms of ACC oxidase show 58 to 65 % homology in their 5'-UTRs and 44 to 52 % homology in their 3-UTRs (Barry, *et al.*, 1996). Similarly, in *P. hybrida,* the isoforms

show greater than 84 % sequence homology in their coding frames, but only 42 to 43 % homology in their 5'- and 50 to 57 % homology in their 3'-UTRs (Tang *et al.,* 1994).

Different members of the ACC oxidase gene families are expressed in response to different endogenous and exogenous cues. For example, the CM-ACO1 and 3 gene transcripts in leaves of melon increase in response to salt and drought stress (Guis *et al.,* 1997), and the expression of the LE-ACO1 GUS-promoter fusion construct in tomato (Blume *et al.,* 1997) and the pVR-ACO1 gene transcript of mung bean (Kim and Yang, 1994) both increase in response to methyl jasmonate application. Different members of the ACC oxidase gene families are also expressed in response to ethylene treatment and wounding in a variety of tissue.

Ethylene treatment increases accumulation of ACC oxidase transcripts in banana (Lopez-Gomez *et al.,* 1997), and *A. chinensis* fruit (Whittaker *et al.,* 1997), in mungbean hypocotyls (Kim and Yang, 1994; Kim *et al.,* 1997), in etiolated pea seedlings (Peck and Kende, 1995), in leaves of tobacco (Kim *et al.,* 1998) and in corollas but not leaves of petunia (Tang *et al.,* 1994). Ethylene has been shown to specifically enhance the accumulation of the LE-ACO1 isoform in tomato fruits (Nakatsuka *et al.,* 1997; Barry *et al.,* 1996); and the ACC Ox2 transcript in broccoli (Pogson *et al.,* 1995). The level of ethylene required to induce ACC oxidase transcripts has been reported to be as little as 0.1 $\mu L\ L^{-1}$ for intact leaves of tobacco treated for 24 h (Kim *et al.,* 1998).

Wounding leaf tissue increases the accumulation of the ripening-related ACC oxidase transcript of peach (Callahan, 1992), tomato (Barry *et al.,* 1996), banana (Lopez-Gomez *et al.,* 1997) and melon (Lasserre *et al.,* 1996). Wounding also increases ACC oxidase mRNA levels in hypocotyls of sunflower seedlings (Liu *et al.,* 1997). Because wounding increases ethylene production, an increase in ACC oxidase activity due to wounding may be mediated through an increase in ethylene production of the tissue. However, in melon at least, the wounding induced transcript accumulation has been shown, using 1-MCP, to be independent of ethylene, and separate wound and ethylene response motifs in the promoter region have been identified (Bouquin *et al.,* 1997).

ACC oxidase activity appears to be controlled at the level of transcription. Increased ACC oxidase activity has been correlated with increased transcript accumulation during ripening of tomato (Barry *et al.,* 1996), apple (Dong *et al.,* 1992) and melon fruit (Lasserre *et al.,* 1996), during senescence of carnation (Nijenhuis-De Vries *et al.,* 1994) and petunia (Tang

et al., 1994), in wounded leaves of tomato (Barry *et al.,* 1996) and melon (Lasserre *et al.,* 1996), and in wounded hypocotyls of sunflower seedlings (Liu *et al.,* 1997). However although wounded sunflower hypocotyls had increased levels of ACC oxidase mRNA and activity, the authors found no evidence for elevated levels of ACC oxidase protein. To explain this, the authors proposed an, as yet undefined, translational control mechanism (Liu *et al.,* 1997).

Members of the ACC oxidase gene families are also under different spatial control. In sunflower seedlings, RT-PCR showed that ACCO3 was expressed equally in roots, leaves and hypocotyls, but only constituted a small amount of the total ACC oxidase transcripts. In contrast, ACCO1 and ACCO2 were differentially expressed in these organs. ACCO1 is the predominant homologue in roots, while ACCO2 was the major homologue in leaves and hypocotyl (Liu *et al.,* 1997). This study is complementary to that of Finlayson *et al.,* (1997) who presented evidence based on biochemical data for the existence of different isoenzymes in roots and leaves of sunflowers. It appears then, that the enzyme encoded by an ACCO1-homologue may represent the predominant isoform Finlayson *et al.,* (1997) were examining in leaf tissue, while an ACCO2-homologue encoded enzyme was the isoenzyme identified in roots. In melon, the CMe-ACO1 isoform is the predominant homologue expressed. It is expressed in flowers, leaves, roots, and etiolated hypocotyls (Lasserre *et al.,* 1996). Expression of CM-ACO2, in contrast, is limited to etiolated hypocotyls, while CM-ACO3 is the predominant isoform in flowers with very little transcript present in leaves and etiolated hypocotyls. ACC oxidase activity assayed *in vitro* in these organs correlated well with gene transcript expression suggesting that in melon, activity is being controlled at the level of transcription. In tomato flowers, ACO1 is predominantly expressed in the petals and stigma and style, while ACO2 expression is mainly restricted to tissues associated with the anther cone, and ACO3 transcripts accumulate in all floral parts except for the sepals (Barry *et al.,* 1996). Taken together, these studies suggest tight spatial control of ACC oxidase expression in plants.

Members of the ACC oxidase gene families are also expressed differentially during development. In all but one study (tobacco leaves; Kim *et al.,* 1998), one gene is predominantly induced during organ ageing. For example, during fruit ripening of tomato (LE-ACO1; Barry *et al.,* 1996; Nakatsuka *et al.,* 1997) and melon (CM-ACO1; Lasserre *et al.,* 1996) and during corolla senescence of petunia flowers (PH-ACO1; Tang *et al.,* 1994).

These genes are all inducible by ethylene, and in tomato and melon have been shown to be wound-inducible as well, an induction which is independent of ethylene

ACC oxidase promoter:β-glucuronidase (GUS) fusion studies in tomato and melon have confirmed that differential expression of the ACC oxidase genes is conferred by their promoter regions and is not a result of differential mRNA stability (Blume *et al.*, 1997; Lasserre *et al.*, 1997). In tomato, using the promoter region of the LE-ACO1 gene (the wound and ripening related gene), GUS activity has been localised to the pericarp of ripening fruit, abscission zones of senescent petioles and unfertilised flowers, and at wound sites (Blume *et al.*, 1997). In tobacco, GUS expression was examined with fusion constructs containing the promoter regions of the melon CM-ACO1 and CM-ACO3 genes. The CM-ACO1 gene promoter was able to drive expression of GUS in response to mechanical wounding, ethylene and copper sulphate treatments and in response to inoculation with a bacterium (known to elicit a hypersensitive response). The CM-ACO3 gene promoter was not expressed in response to infection, but was during flower development.

In many of the above examples, transcript accumulation and activity of ACC oxidase increases to be high at times when ethylene production is known to be high in tissue, for example, during fruit ripening and flower senescence. Yet, ACC oxidase for many years has been considered as an enzyme that has little function in controlling ethylene production (Kende, 1993). As there are now an increasing number of studies appearing that suggest otherwise, it is appropriate to reexamine evidence for ACC oxidase catalysing a rate determining step in the pathway.

1.4.6 ACC oxidase: A rate limiting enzyme

The view that ACC oxidase plays little part in controlling ethylene production arose initially from physiologically based studies where production of ethylene was quickly elevated by application of ACC to tissue (Cameron *et al.*, 1979) and by finding a strong correlation between levels of ACC in ripening fruit and ethylene production (Hoffman and Yang, 1980). Studies then continued to confirm the importance of ACC synthase. ACC synthase has characteristics expected of a regulatory enzyme, as it is present in very low amounts, can be rapidly induced, is labile, and ethylene production has often been positively correlated with its activity (see section 1.3.2.2).

However, as the following four examples show, activity of ACC oxidase is important and, in some instances, more closely correlates with ethylene production than ACC synthase.

ACC oxidase mRNA accumulation and activity can be correlated with ethylene production and internodal growth in deepwater rice stimulated by partial submergence (Mekhedov and Kende, 1996). By contrast, ethylene biosynthesis during this time does not correlate with either increased mRNA or activity of ACC synthase (Mekhedov and Kende, *pers. comm.* cited in Mekhedov and Kende, 1996). So it is proposed that ethylene biosynthesis in internodes of deepwater rice is controlled, at least in part, at the level of ACC oxidase.

S. longipes exhibits a diurnal rhythm of ethylene production that correlates well with both mRNA and activity of ACC oxidase (Kathiresan *et al.*, 1996), but not with levels of ACC content (Emery *et al.*, 1997) or any of the four ACC synthase transcripts identified (Kathiresan *et al.*, 1998).

Wild type tomato plants respond to flooding with increased rates of ethylene production which is considered to be the cause of the epinastic curvature of leaf petioles. This was examined in a transgenic plant of tomato containing the ACO1 gene in antisense orientation. Both antisense and wild type plants had elevated levels of ACC oxidase activity in the leaves of flooded plants. However, the levels of ACC oxidase activity in the antisense plants were always lower than wild type. The extent of epinasty could be correlated with the activity of ACC oxidase suggesting that the extent of epinasty was at least in part being controlled by activity of ACC oxidase (English *et al.*, 1995).

Activity of ACC oxidase may be rate limiting for the IAA-induced ethylene production of etiolated pea hypocotyls (Peck and Kende, 1995). The application of IAA induces ACC synthase gene expression and activity within 1 h of application, yet ethylene production does not increase until after 2 h. This delay correlates with the time when ACC oxidase mRNA accumulation and activity is increasing, suggesting that basal levels of ACC oxidase were not sufficient for converting the increase in ACC content into ethylene. To further examine the potential of ACC oxidase in controlling ethylene production, Peck and Kende (1997) attempted to eliminate the 2 h lag between auxin application and increasing ethylene production by pre-elevating ACC oxidase activity. This was achieved by pretreatment with ethylene which had been shown to enhance expression of the transcript (Peck and Kende, 1995). Ethylene pretreatment did reduce the lag period, suggesting that ACC oxidase activity is limiting for ethylene production, but a caveat was that upon IAA treatment, ACC

synthase transcript and activity was superinduced, meaning that the faster increase in ethylene evolution may also have been due to more ACC synthase activity (Peck and Kende, 1997).

Taken together, these examples provide strong evidence for ACC oxidase activity constituting an extra tier of control of ethylene biosynthesis.

1.4.7 Role of ethylene in leaf maturation and senescence

Ethylene can modify programmed leaf senescence. The relationship between ethylene and leaf senescence has been studied in the *A. thaliana* mutant, ETR1 (Bleecker *et al.,* 1988). This mutant was found to lack a number of responses (see section 1.2) including acceleration of leaf senescence by comparison with wild type. A subsequent study has shown that both visual signs of leaf senescence and the appearance of senescence-associated genes (SAGs) in this mutant are delayed by one week compared with wild type (Grbic and Bleecker, 1995). Furthermore, while treatment of ethylene had no effect on SAG and photosynthetic associated gene (PAG) expression in ETR1 plants, but in wild type plants ethylene hastened both SAG expression and senescence, and decreased expression of PAGs. This effect was age-dependent. In mature leaves ethylene induced greater SAG expression than in just fully expanded leaves and did not elevate SAG expression in younger leaves despite being able to increase expression of another non-SAG related ethylene-inducible gene. It was noted that although ETR1 leaves showed a delay in leaf chlorosis and lived approximately 30 % longer than wild type, the extended period of leaf longevity was associated with low levels of photosynthetic activity suggesting that the leaves had functionally senesced (as determined by carboxylase activity).

This study suggests that ethylene can modulate the timing of leaf senescence by controlling the expression of SAGS rather than acting as an initiator of the process, but only in developmental stages that are responsive (proposed to be due to the presence of age-dependent factor(s)) (Grbic and Bleecker, 1995).

Changes in ethylene production have been examined during leaf maturation and senescence. Production of ethylene has been shown to increase during chlorosis of attached leaves of tobacco (Alejar *et al.,* 1988) and cotton (Morgan *et al.,* 1992), detached leaves of China tree (Morgan and Durham, 1980) and oat (Gepstein and Thimann, 1981), in leaf discs of tobacco and sugar beet (Aharoni *et al.,* 1979), but not in leaf discs of *Phaseolus vulgaris* (Roberts and Osborne, 1981).

In these plants (except *P. vulgaris*), the period of most rapid chlorophyll loss is paralleled by the period of most rapid ethylene evolution (i.e. the rapid increase occurs after chlorophyll levels have begun to decline). This is further supported by the study of Alejar *et al.*, (1988) who compared different cultivars for their rates of ethylene production and senescence. The leaves of the cultivars that yellowed fastest were those that had the highest rates of ethylene production. What then controls this ethylene production?

Unlike ripening fruits and senescing flowers, comparatively few studies have examined the regulation of ethylene production during leaf maturation and senescence. Much of our knowledge has relied on physiologically based studies done in the late 1970s and early 1980s, in which ACC, or inhibitors of ACC synthase or ACC oxidase were applied to leaf tissue and the effect on chlorosis measured. The application of ACC to leaf tissue of detached oat leaves in the light brought forward the period of most rapid chlorophyll loss by one day (Gepstein and Thimann, 1981), whereas application of 10 μM Co^{2+} (an inhibitor of ACC oxidase) and 0.2 M AVG greatly reduced chlorophyll loss in the oat leaves after a four day incubation in the light (Gepstein and Thimann, 1981).

Recently, antisense technology has been able to confirm in tomato that the increased ethylene production observed during leaf chlorosis was due to increased activity of the ACC-mediated biosynthetic pathway. For instance, ethylene production was only 5 % of wild type in chlorotic leaves of LE-ACO1 antisense tomato plants compared with wild type (John *et al.*, 1995).

More recently, in concert with our interest, research groups are beginning to examine changes in gene expression of ACC oxidase during leaf maturation and senescence.

1.5 ACC oxidase during leaf maturation and senescence

Changes in ACC oxidase gene expression during leaf maturation and senescence has now been examined in tomato (Barry *et al.*, 1996; Blume *et al.*, 1997), melon (Lasserre *et al.*, 1996) and tobacco (Lasserre *et al.*, 1997; Kim *et al.*, 1998).

In tobacco, all three ACC oxidase genes are up-regulated in older leaves as compared with younger tissue (Kim *et al.*, 1998). In contrast, in tomato, leaf senescence (as judged by chlorosis) is accompanied predominantly by an increase in expression of only one isoform (ACO1; Barry *et al.*, 1996). Levels of ACO1 mRNA increased 27-fold at the onset of senescence before declining slightly at the most advanced stage examined. The expression

of ACO3 also increased. However, the increase was transient and the levels of the transcript only accumulated to a level approximately half that of the ACO1 message. No ACO2 gene expression could be detected in leaves by the ribonuclease protection assay method. In leaf tissue of melon, quantitative RT-PCR has shown that expression of the two ACC oxidase isoforms is differentially regulated during leaf development and senescence. The steady-state levels of one isoform, CM-ACO3, is highest in young leaves and then declines in green adult to be lowest in yellow-green adult leaves (the most senescent stage examined). While in contrast, the level of CM-ACO1 is lowest in young leaves, then increases to be highest at the onset of chlorophyll loss (similar to ACO1 accumulation in tomato leaves) before declining again during the later stages of senescence.

Studies of ACC oxidase gene expression during leaf maturation and senescence have been extended through the use of GUS-promoter fusion analysis. The promoter of the ageing-related ACC oxidase (ACO1) was used to direct expression of GUS in both tomato and tobacco (Blume *et al.,* 1997). In young leaves of both tomato and tobacco, levels of GUS were virtually non detectable, but increased considerably (150 to 300-fold) at the onset of senescence (chlorosis). These results confirm that it is the promoter driving the increased accumulation of ACC oxidase gene transcript during leaf senescence, and also that it can retain this ability even in a heterologous system (Blume *et al.,* 1997). Similarly, the ACC promoters from the ACC oxidase genes, CM-ACO1 and CM-ACO3, from melon have been used to direct the expression of GUS in tobacco (Lasserre *et al.,* 1997). Expression of GUS activity broadly matched the accumulation of the two transcripts as measured by RT-PCR, thus confirming the importance of the promoters for directing expression of the transcripts during leaf maturation and senescence.

These studies have indicated that changes in gene expression of ACC oxidase may be important for controlling ethylene production during leaf senescence, but they have neglected to report on changes in protein accumulation and activity during the leaf maturation. Coupling gene expression studies with measurements of both protein accumulation and activity are essential if we are to judge the control of ACC oxidase on leaf senescence. There are, for instance, reported cases where huge-fold increases in transcript have resulted in very minimal increases in the activity of ACC oxidase (e.g. ethylene treatment of mungbean hypocotyls; Kim and Yang, 1994), and where ACC oxidase enzyme activity was found to be highest in tissue that had the lowest levels of ACC oxidase mRNA (basal portion compared with tip of sunflower root; Finlayson *et al.,* 1996).

Clearly, measurement of transcript levels alone are not always adequate as there is no means for determining the influence of any post-transcriptional/ post-translational control on the process being measured.

This thesis, therefore, focuses on understanding the role of ACC oxidase during leaf maturation and senescence by coupling studies of gene expression with measurements of protein accumulation and activity.

1.5.1 White clover and leaf senescence

White clover (*Trifolium repens* L.) is the plant used for studying expression of ACC oxidase during leaf maturation and senescence in this thesis. *T. repens* is the most agronomically important member of the 200 to 300 species comprising the genus *Trifolium,* and is considered the most important pasture legume in many temperate climates throughout the world (Baker and Williams, 1987). In New Zealand, it is grown in combination with rye grass to provide nitrogen to the pasture ecosystem and high quality feed for livestock (Brougham, Ball and Williams, 1978).

In pasture, white clover has a stoloniferous growth habit. The basic structure of the stolon consists of a series of internodes separating the nodes which form as a result of growth at the apical bud. Present at each node is a single trifoliate leaf and two root primordia. The uppermost root primordium typically remains dormant while the lower primordium, in moist conditions, gives rise to a fibrous root. At each node is also an axillary bud which either can remain dormant, produce an inflorescence, or produce a lateral stolon. The growth of a stolon is indeterminate with plants in summer often possessing up to six orders of branching (Brock *et al.,* 1988). However, during spring many stolons senesce and fragment to produce a higher proportion of plants with first order branching (Hay *et al.,* 1989).

Stolon fragmentation is thought to be the end result of photosynthate (carbohydrate) reallocation from the old stolon material to the apex (Chapman and Robson, 1992). This change from a reservoir of carbohydrate to exporter is probably closely linked to changes of associated leaves from exporters of carbohydrate to exporters of minerals into the stolon. The change in leaves from a producer of photosynthate to an exporter of minerals is considered part of the senescence syndrome (Thomas and Stoddart, 1980). It can be initiated by a variety of environmental cues such as shading, drought, mineral deficiency and pathogen infection (Thomas and Stoddart, 1980). In the absence of such stimuli, leaf

senescence is regulated in an age-dependent manner (Lohman *et al.* 1994), which may have evolved to prevent maintenance of a leaf past its average time of usefulness for supplying carbohydrate to the increasingly distant apex (Bleecker and Patterson, 1997).

The sequential nature of white clover leaf senescence has been utilised by Butcher (1997) for the development of a model system for studying changes in ethylene physiology associated with leaf ontogeny. In this system, vegetatively propagated individual stolons are grown over a dry substratum (to inhibit nodal root formation) and all axillary buds removed. The rooting at a single node and subsequent outgrowth of a single stolon of white clover over a dry substratum produces a full programme of leaf development along the stolon from initiation at the apex through maturation, senescence and then necrosis. Growth in this system also produces plants at which the number of leaves attached to the stolon reaches a constant number as the production rate is balanced by the rate of senescence.

Using this system, Butcher (1996) has shown that leaf senescence of white clover (as judged by chlorophyll loss) is accompanied by an increase in ethylene evolution levels by the tissue, and that this increase is most probably due to increased activity of the ACC-mediated biosynthetic pathway. In support of this, endogenous levels of ACC were found to both increase and precede the increase in ethylene evolution (Butcher *et al.*, 1996).

These findings will be examined further as part of this thesis as a prelude to more detailed analysis on the contribution of ACC oxidase to ethylene production during leaf maturation and senescence.

1.5.2 Thesis Aims

- To measure changes in ACC oxidase activity *in vitro* during leaf maturation and senescence.
- To isolate gene sequences encoding ACC oxidase and examine changes in gene expression during leaf maturation and senescence.
- To examine factors that regulate the expression of these ACC oxidase genes
- To produce antibodies against ACC oxidase proteins when expressed in *E. coli* and,
- To examine changes in protein accumulation of ACC oxidase during leaf maturation and senescence

2. MATERIALS AND METHODS

2.1 Propagation and Harvesting Methods

2.1.1 Plant material

The white clover genotype 10 F of cultivar Grasslands Challenge (AgResearch, Grasslands, Palmerston North, NZ) was used for all manipulations and experimental analysis in this thesis.

2.1.2 Plant growth conditions

Plants were propagated in horticultural grade bark/ peat/ pumice (50:30:20) (Dalton Nursery Mix, Tauranga, NZ) supplemented with nutrients (Table 1) and grown in temperature controlled greenhouses.

Table 1. Nutrient addition to horticultural grade bark base.

Nutrient	rate(g/L)
Dolomite	3.0
Agricultural lime	3.0
Iron sulphate	0.5
Osmocote	50

The greenhouses were maintained at a minimum temperature of 15 °C and vented at 25°C. Automated watering was at 8 am and 5 pm for 5 min each. The insecticide Attack® (Crop Care Holdings Ltd., Richmond, Nelson, NZ) was used to control aphids and whitefly, and Pyranica® (Mitsubishi Kasei Corporation) was used to control mite infestations. Blackspot was irradicated by application of Benlate (Du Pont de Nemours and Co., In., Wilmington, Delaware, USA).

2.1.3 Plant propagation

2.1.3.1 Stock Plants

To propagate the single genotype, apical cuttings containing two or three leaves were placed in trays containing bark/ nutrient mix and grown under greenhouse conditions until

required. Five trays were maintained in this way, with new cuttings routinely taken to maintain a continual supply of stock material.

2.1.3.2 Model System

To initiate single stolons, apical cuttings containing two or three leaves were excised from the stock plants, all the leaves except the terminal bud and first leaf were removed, and the cuttings placed in bark/nutrient potting mix in the greenhouse. After establishment of root growth (usually four weeks), the most homogeneous cuttings were transferred into trays containing fresh bark/nutrient mix (six per tray). As the cuttings grew, each stolon arising from a single cutting was trained out of the tray onto a dry substratum (upturned tray covered with white polyethylene) to inhibit nodal root formation, and all axillary shoots and flowers were routinely removed. (Figure 3). Stolons were grown until a consistent pattern of leaf development (from initiation through to senescence) was achieved. This was usually after a minimum of three months.

Figure 3.

A. The author amongst stolons of white clover (genotype 10 F) growing in one of the greenhouses of the Plant Growth Unit, Massey University, Palmerston North, New Zealand.

B. Plants of white clover ready for harvesting.

2.1.4 Leaf harvesting

Leaves were excised at the junction of the lamina and petiole, weighed, placed either individually into labelled microfuge tubes or as pooled leaves into 50 mL Nunc™ centrifuge tubes (Nalge Nunc International, Naperville, USA), snap frozen in liquid air and stored at -80°C. When pooled leaf tissue was to be used in multiple analyses, the tissue was removed from the -80°C, powdered and apportioned into measured amounts in separate prechilled, thick-walled plastic containers.

2.1.5 Leaf wounding

Detached leaves were wounded by making approximately *ca.* 2 mm wide parallel excisions along the length of the lamina. Attached leaves were wounded by making two parallel excisions on each leaflet of each trifoliate leaf.

2.1.6 Experimental conditions used for wounding experiments

2.1.6.1 Conditions used for detached leaves

Detached leaves were housed in C68 (125 mL) glass bottles (Arthur Holmes Ltd., Wellington, NZ) at 20°C for the appropriate times. Each jar was housed in its own covered 9 L polystyrene container. In the bottom of the polystyrene containers was placed moistened paper towels. The glass bottles containing the leaves were only sealed (with lids containing rubber bungs) thirty minutes prior to the removal of the 1 mL gas sample. After removal of the gas sample for ethylene analysis using the PhotoVac (section 2.2.3.2), the tissue was immediately snap-frozen in liquid air, and stored at -80°C until required. This tissue was then used for northern, western and activity analyses.

If the treatment included Purafil™, a bag containing 30 g of Purafil was placed in the polystyrene container, and an additional 5 g bag placed in the C68 glass jar. Duplicate sets of tissue were used for treatments containing Purafil. One set was sealed for 30 min to let ethylene accumulate, as described in the preceding paragraph. The other set, incubated in parallel, was not sealed to let ethylene accumulate. It was this non-sealed tissue that was used subsequently for northern and activity analyses.

Notes:

- Purafil is a solution of $KMnO_4$ applied to an inert support to increase the surface area and ease of handling (Abeles, *et al.*, 1992). $KMnO_4$ is very toxic, so precautions are necessary when handling it. In all experiments it was encased in bags made of

polyethylene and Tyvek™ (Dupont, USA). Tyvek (Type 10, style, 1073b) is a spun-bound olefin, which is readily permeable to ethylene.

2.1.6.2 Conditions used for attached leaves

Four trays each containing six independent stolons were transferred from the greenhouse to the lab 48 h prior to beginning the treatments. Two of the trays were then placed in a 470 L growth cabinet with 1 ppm 1-MCP for 30 min. After which, all four trays were placed under six TRUE-LITE® 40 W fluorescent lights and the appropriate leaves wounded (section 2.1.5). The room housing the plants was kept at a constant temperature of 20°C.

2.2 Biochemical and physiological methods

2.2.1 Chemicals

Unless otherwise stated, the chemical reagents used were analytical grade, obtained from either BDH Laboratory Supplies (Poole, Dorset, England), or Sigma Chemical Company (St. Louis, Mo., USA). The laboratory supply of purified water used for making solutions was itself produced by reverse-osmosis (RO), followed by microfiltration (Milli-Q, Millipore Corp., Bedford, MA, USA).

2.2.2 Chlorophyll quantitation

Reagents:

- DMF

Chlorophyll was extracted from leaves with the solvent N, N-dimethylformamide (DMF) as described by Moran and Porath, (1980). Typically, leaf tissue was powdered under liquid N_2 in a mortar and 50 to 200 mg of the powdered leaf material extracted with 1 mL of DMF for between 2 h and 16 days at 4°C in the dark. Prior to chlorophyll determination, samples were vigorously mixed by vortexing and the cellular debris pelleted by centrifugation at 20 800 x g for 5 min at room temperature. A 200 µL aliquot of the supernatant was then added to 2 mL of DMF in a glass cuvette and the absorbance read at both 647 nm and 665 nm in an LKB Novaspec®II spectrophotometer (Pharmacia LKB, Biochrom Ltd., Cambridge, England) in the fumehood. The spectrophotometer was blanked only at 647 nm with DMF. All the samples measured at 665 nm had 0.007 absorbance units added to their values as this was the difference in the blank at 647 nm when compared with 665 nm.

Chlorophyll concentrations were calculated using the formulae described by Inskeep and Bloom (1985) which corrected for errors incorporated in the original formulae described by Moran (1982).

Chlorophyll a = $12.7\ A_{664.5} - 2.79A_{647}$ (mg /mL)

Chlorophyll b = $20.7\ A_{647} - 4.62A_{664.5}$ (mg /mL)

Total Chlorophyll = $17.9A_{647} - 8.08A_{664.5}$ (mg/ mL

2.2.3 Ethylene analysis

2.2.3.1 Measurement of ethylene by Gas Chromatography

The concentration of ethylene in gas samples produced by the ACC oxidase or ACC chemical degradation assays were analysed using a Shimadzu Model GC-8A Gas Chromatograph (Shimadzu Corporation, Kyoto, Japan) fitted with a flame ionisation detector. The 2.5 m * 3 mm (I.D.) glass column (Shimadzu 8G2 6-2.0) came prepacked with Porapak Q with a mesh size of 80/100 (Alltech Associates Inc., Deerfield, II., USA). The carrier gas was nitrogen with a flow rate of 50 ml min^{-1}. The flame was generated by hydrogen and air at 50 kPa respectively. The column was initially conditioned at 200°C for 5 h and thereafter for approximately 0.5 to 1 h before use. For measurement of samples, the oven was set to a temperature of 85°C and the injector/detector to 150°C.

One ml of sample gas was injected onto the column and the ethylene peak was identified by comparison with the retention time of an ethylene standard (0.99±0.01ppm) obtained from BOC Gases (NZ) Ltd., Palmerston North, New Zealand. Ethylene had a retention time of 1 min 30 s.

2.2.3.2 Measurement of ethylene by PhotoVac

Ethylene evolution from leaves attached to the stolon was measured with a portable PhotoVac™10S50 (PhotoVac™, Markham, Canada). Initially integration was performed using an inbuilt integrator, but eventually an external Hewlett Packard 3390A integrator (Hewlett-Packard Company, Avondale, PA, USA) was used. An external supply of carrier gas (air at 40 psi) was passed through a column of Purafil™ (Papworth Engineering, Cambridge, NZ; Faubian and Kader, 1996), before entering the PhotoVac. Ethylene was found to have a peak retention time between 0.78-0.82 min. Peak height rather than area was used to measure the concentration of ethylene.

The PhotoVac instrument was calibrated with an α-standard calibration gas (0.101 ppm ethylene in nitrogen (BOC Gases (NZ) Ltd.)

2.2.4 Ethylene Calculations

The concentration of ethylene in the headspace of containers was determined in ppm by comparison to the peak height obtained from a 1 mL injection of an α-standard calibration gas (0.101 ppm or 0.99 ± 0.01 ppm [mole per mole] ethylene in nitrogen). The number of moles of ethylene this represented could then be determined by calculating the total number of moles present within the headspace of the container with the ideal gas equation and multiplying this value by the concentration of ethylene in ppm.

$$n = \frac{PV}{RT} \times \text{ppm} \times 10^{-6}$$

where:

- n = total number of moles in headspace or vessel containing tissue
  P = pressure (101325 Pa)
  V = volume of headspace or vessel containing tissue (m^3)
  R = universal gas constant, 8.314
  T = temperature (normal temperature and pressure [NTP] = 298 K)

To convert to L, the number of moles is multiplied by 22.4 as 1 mole occupies 22.4 L at standard temperature and pressure (STP).

2.2.5 Measurement of ethylene evolution from attached leaves of white clover

Ethylene evolution of attached leaves of white clover was measured by the method of Butcher (1996). Individual leaves still attached to the stolon were enclosed in 32 mL plastic screw top containers that had a slot cut in the screw top lid to accommodate the petiole. The remaining air gap around the petiole was sealed with silicon sealant. After 1 h, and before the accumulation of significant wound ethylene which occurs after 1.5 h, a 1 mL sample of gas was withdrawn through a rubber bung fitted to the bottom end of the container. The concentration of ethylene in the sample was then determined using the PhotoVac (section 2.2.3.2).

2.2.6 ACC quantitation

ACC concentration of leaf tissue extracts was determined essentially as described by Lizada and Yang (1979). Either fresh or tissue stored at -80°C was used for analysis

2.2.6.1 ACC extraction for leaf tissue down the stolon

Reagents:

- 96 % (v/v) ethanol
- chloroform

Typically a single trifoliate leaf (*ca.* 300-500 mg) was powdered in liquid N_2 and extracted in 10 mL of 96% (v/v) ethanol at 80°C for 20 min in a 15 mL centrifuge tube. The cell debris was pelleted by centrifugation at 5000 x g for 10 min at room temperature and the supernatant collected. The pellet was again resuspended in 10 mL of 96 % (v/v) ethanol and incubated at 80°C. After 20 min, the cell debris was pelleted as before and the supernatants combined. The combined extracts were dried in a rotary evaporator (Rotovapour; Buchi Laboratoriums, Technik Ag., Flawil/Schweiz, Switzerland) at 42 °C. The dried product was dissolved in 2 mL water, half a volume of chloroform added, the mixture vortexed, and the phases separated by centrifugation at 26 000 x g for 10 min at room temperature. The aqueous supernatant was assayed for ACC content (section 2.2.6.3).

When the extraction was scaled up for paper chromatography, leaves were extracted in seven volumes of 96 % (v/v) ethanol at 80°C, evaporated to dryness, redissolved in water and partitioned twice with chloroform. The aqueous extract was stored at -20°C until required.

2.2.6.2 Paper chromatography

Reagents:

- Butanol
- glacial acetic acid

Samples containing putative ACC were resolved by paper chromatography using a butanol: glacial acetic acid: water (8:3:10) solvent system. The chromatography apparatus was pre-equilibrated with the solvent prior to resolving the samples. Each sample (200 µL) was applied along a 2.5 cm pencil line drawn *ca.* 10 cm from the top of a 46 x 57 cm sheet of Whatman® 3MM Chr chromatography paper (3 MM paper; Whatman International Ltd.,

Maidstone, England). Each sample was applied with capillary tubing and was dried between applications. The samples were resolved for 14 h, after which time the solvent front was marked and the paper chromatogram dried in a fume hood. Each lane was then sectioned into 14 (1.5 cm x 4.5 cm) squares, each square cut smaller to fit into a single microfuge tube, and ACC eluted with 700 µL water at 4°C overnight. The cut squares were then pelleted by centrifugation at 20 800 x g for 10 min, 300 µL of the supernatant transferred to a fresh tube, the paper again resuspended with 700 µL water, incubated at room temperature for 20 min, pelleted by centrifugation and the supernatants pooled. ACC was then measured in the pooled supernatant by the method of Lizada and Yang (1979) (section 2.2.6.3)

2.2.6.3 ACC assay

Samples (sections 2.2.6.1 and 2.2.6.2) were analysed for ACC by the method of Lizada and Yang (1979). This method uses sodium hypochlorite which reacts with α-amino acids (for example, ACC) to form N-chloroamine as an intermediate, and this is chemically degraded to ethylene, ammonia, and carbon dioxide with a yield of about 13 %. In the presence of heavy metal ions (particularly mercury), the yield of the ethylene increases up to 80 %. In the assay described, the concentration of the mercury catalyst (50 mM) was higher than that used originally by Lizada and Yang (30 mM), as the higher mercury concentration has been reported to reduce interference by protein contaminants (Coleman and Hodges, 1991).

Reagents:

- 50 mM $HgCl_2$
- 3.15 % NaOCl solution (Janola®; Marketed by Reckitt and Coleman (NZ) Ltd., Auckland New Zealand
- NaOH (saturated solution)

An aliquot of the sample (800 µL) was placed in a 4.5 mL Vacutainer® tube (Becton Dickensen Medical, Singapore) on ice, 100 µL of $HgCl_2$ added and the tube sealed with a rubber stopper. A 100 µL aliquot of an ice cold mixture of 2:1 (v/v) NaOCl: NaOH was then injected through the rubber stopper, the tube immediately vortexed for 5 s, incubated on ice for 2 min, revortexed for 5 s and a 1 mL gas sample withdrawn for analysis by gas chromatography (section 2.2.3.1) or PhotoVac (section 2.2.3.2).

2.2.7 Measurement of ACC Oxidase activity

2.2.7.1 Extraction procedure

ACC oxidase was extracted from leaf tissue of white clover by a procedure derived from McGarvey and Christoffersen (1992) and Fernandez-Maculet and Yang (1992).

2.2.7.1.1 Extraction procedure 1.

Reagents:

- Extraction buffer: (0.1 M Tris-HCl, pH 7.5, 10 % (v/v) glycerol, 2 mM DTT, 30 mM sodium ascorbate)

Leaf tissue was powdered and extracted in two volumes of extraction buffer. Typically, to obtain enough enzyme to perform a single determination in triplicate, 1 g of powdered sample was scraped directly into 2 mL of chilled extraction buffer, the tissue extracted on ice for 45 min, and then filtered through two layers of Miracloth (Calbiochem-Novabiochem Corporation, La Jolla, CA, USA) into 2 mL pre-cooled microfuge tubes until 1.4 mL (measured as grams) had been transferred. After centrifugation at 20 800 x g for 10 min at 4°C, the supernatant was passed through a column of Sephadex® G-25 (Pharmacia Biotech AB, Upsala, Sweden; section 2.2.4.2) and the resulting eluate apportioned into a 700 µL aliquot for measurement of ACC oxidase activity. The excess extract was aliquotted into a separate tube to be used for measurement of protein (section 2.2.8) and for analysis by sodium dodecyl sulphate-polyacrylamide gel electrophoresis (SDS-PAGE; section 2.2.9).

2.2.7.1.2 Extraction procedure 2.

Reagents:

- Extraction Buffer: (0.1 M Tris-HCl, pH 7.5, 10 % (v/v) glycerol, 2 mM DTT, 30 mM sodium ascorbate)
- Ammonium sulphate
- Resuspension Buffer: (50 mM Tris-HCl, pH 7.5, 10 % (v/v) glycerol, 2 mM DTT)

A 2 g aliquot of powdered leaf tissue was extracted in six volumes of extraction buffer on ice for 45 min and filtered through two layers of Miracloth to a constant weight as described above (section 2.2.7.1.1). After centrifugation at 26 000 x g for 10 min at 4°C ,

the supernatant was decanted, the volume adjusted to 30 % saturation (164 g L^{-1} at 0°C) with solid ammonium sulphate, and the extract incubated on ice for 30 min. Nucleic acid and residual cellular debris was then pelleted by centrifugation at 26 000 x g for 10 min at 4°C, the supernatant transferred to a fresh tube, and adjusted to 90 % saturation (at 0°C) by the addition of 402 g L^{-1} salt. After incubation on ice for 1 h, protein was pelleted by centrifugation at 26 000 x g for 10 min at 4°C, the supernatant discarded, the protein precipitate resuspended in 1 volume of resuspension buffer (i.e. 1 g of leaf tissue to 1 mL resuspension buffer), and then desalted by passage through a column containing Sephadex G-25 (section 2.2.7.2). The resulting eluate was apportioned into a 700 µL aliquot for measurement of ACC oxidase activity. The excess extract was aliquotted into a separate tube to be used for measurement of protein (section 2.2.8) and for analysis by sodium dodecyl sulphate-polyacrylamide gel electrophoresis (SDS-PAGE; section 2.2.8).

2.2.7.2 Preparation of Sephadex G-25 spin columns

Proteins were desalted and any putative low molecular weight inhibiting substances removed using a method modified from that described by Neal and Florini (1973).

Reagents:

- Sephadex G-25
- Resuspension buffer: (50 mM Tris-HCl pH 7.5, 10 % (v/v) glycerol, 2 mM DTT)

Spin columns were prepared by placing three layers of GF-A glass microfibre filter paper (Whatman) in the bottom of 10 mL disposable syringe barrels (Becton Dickensen). The tips of the barrels were sealed with parafilm, the barrels filled with Sephadex G-25 pre-equilibrated with resuspension buffer (five volumes Sephadex G-25 to one volume enzyme extract). The syringe barrels were then placed in 50 mL centrifuge tubes, the parafilm removed, and the column conditioned by spinning at 178 x g for exactly 1 min at 4°C. After removal of the excess buffer collected at the bottom of the tube, the sample was carefully loaded and the columns centrifuged again at 178 x g for 1 min at 4°C , and the eluant collected.

2.2.7.3 Assay procedure

Reagents:

- 1 M Tris-HCl, pH 7.5
- 0.667 mM $FeSO_4.7H_2O$ (made fresh)
- 4 mM ACC (stored frozen)
- 1 M DTT (stored frozen)
- 1 M $NaHCO_3$ (made fresh)
- 1 M sodium ascorbate (made fresh)

ACC oxidase activity of triplicate 200 µL volumes of a 700 µL enzyme preparation, pre-equilibrated at 30°C for 3 min, were aliquotted into 4.5 mL vacutainer tubes containing 0.8 mL of reaction mix (pre-equilibrated at 30 °C) to give a final concentration of 50 mM Tris-HCl, pH 7.5, 1 mM ACC, 10 % (v/v) glycerol, 2 mM DTT, 30 mM sodium ascorbate, 20 µM FeSO4.$7H_2O$ and 30 mM $NaHCO_3$. The vacutainers were sealed, incubated with shaking at 175 rpm for 20 min at 30°C, after which 1.0 mL of the gas phase was removed and the ethylene content determined by gas chromatography (section 2.2.3.1).

For the determination of the pH optimum, different aliquots of the standard buffer (50 mM Tris-HCl, pH 7.5) (typically used at a 2 X concentration) were adjusted to either pH 7.5, 8.0, and 8.5 with HCl prior to addition to the reaction mix. For pH values of 6.5, 7.0 and 7.5 the Tris-HCl buffer was replaced with 50 mM Na(3-[N-Morpholino]propanesulphonic acid) (MOPS). The pH of each solution was further checked once all components of the reaction mix had been added and adjusted if necessary.

2.2.8 Protein quantitation

Reagents:

- Coomassie Brilliant Blue G-250 concentrate dye preparation (Bio-Rad, Richmond, CA, USA)
- BSA: (Bovine serum albumin, Fraction V, standard grade, Serva Feinbiochemica, Heidelberg, Germany)

Protein concentration was estimated by a microassay version of Bradford's method (Bradford 1976), using a commercially available dye concentrate (Bio-Rad). Typically, extracts were diluted 1:10 with water before protein measurement. Aliquots (5 to 10 µL) of the diluted extract were pipetted into wells of a microtitre plate, in triplicate, and made

up to 160 µL with water. After which, 40 µL of Bio-Rad Reagent was added and mixed in with the micropipette. After standing for 5 min, the protein content was determined at 595 nm using an Anthos htII platereader (Anthos Labtech Instruments, Salzburg, Austria) by comparison to a protein standard (BSA) measured in parallel. Only absorbances within the linear region of the standard curve were used for protein estimation.

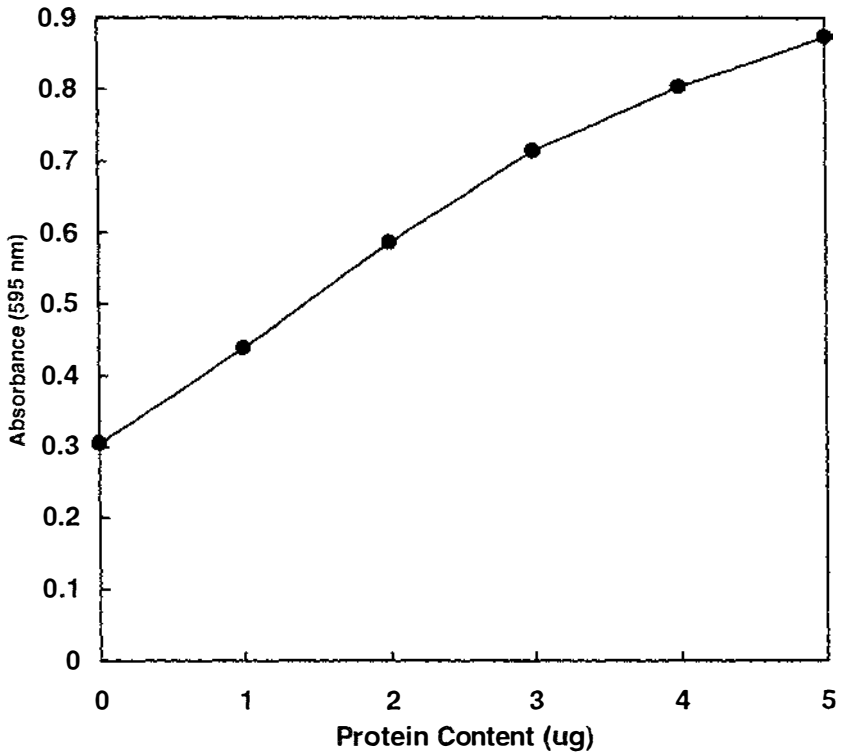

Figure 4. A typical standard curve for the Bio-Rad protein assay microassay procedure.

2.2.9 SDS-PAGE of Protein

SDS-PAGE, originally described by Laemmli (1970), separates protein on the basis of molecular mass.

2.2.9.1 Linear slab gel SDS-PAGE using the BioRad Mini-Protean apparatus.

Reagents:

- 40 % (w/v) acrylamide stock solution (Bio-Rad))
- 4 X resolving gel buffer: (1.5 M Tris-HCl, pH 8.8, 0.4 % (w/v) SDS).
- 4 X stacking gel buffer: (0.5 M Tris-HCl, pH 6.8, 0.4 % (w/v) SDS).
- 10 % (w/v) APS (ammonium persulphate ; Univar, Auburn, NSW, Australia) Aliquots stored at -20°C
- TEMED (N,N,N',N - tetramethylethylenediamine) (Riedel-de haen ag seelze, Hannover, Germany).
- 10 X SDS running buffer: (30 g Tris, 144 g glycine, 10 g SDS, water to 1 L). (pH should be approximately 8.3, stable indefinitely at room temperature).
- 5 X SDS gel loading buffer: (60 mM Tris-HCl pH 6.8, 25 % (v/v) glycerol, 2 % (w/v) SDS, 14.4 mM 2-mercaptoethanol, 0.1 % (w/v) bromophenol blue). (stable for weeks in the refrigerator or months at -20°C).

Table 2. Composition of resolving and stacking gels used for SDS-PAGE with the Mini-Protean apparatus.

Order of addition	Components	Resolving Gel Solution (mL)	Stacking Gel Solution (mL)
1.	**water**	3.5	6.5
2.	**4 X resolving gel buffer**	2.5	
3.	**4 X stacking gel buffer**		2.5
4.	**acrylamide stock solution**	4	1
5.	**APS**	0.1	0.1
6.	**TEMED**	0.01	0.01

A resolving gel solution was prepared by mixing the components in the order outlined in Table 2. The solution was then transferred between glass plates of a gel sandwich until the level was *ca.* 1 cm below where the bottom of the well-forming comb sits. Water was then layered onto the gel surface to protect from atmospheric oxidation and the gel allowed to polymerise for *ca.* 30 min. The layer of water was discarded, the well-forming comb inserted, and gel stacking solution added. After polymerisation for *ca.* 30 min, the gel

sandwich apparatus was placed in the electrophoresis chamber, running buffer added to both inner and outer chamber and the comb removed in preparation for loading.

Samples were prepared for loading by adding one fifth volume of 5 x gel loading buffer, boiling for 3 min (except for samples that contained imidazole [i.e. fractions off the affinity column] which instead were heated at 37°C for 10 min), and then centrifuging at 20 800 x g for up to 1 min. All samples were made to the same volume with sample buffer. Routinely, one lane was reserved for an aliquot (10 µL) of prestained molecular weight standards (Low Range [20.5 to 111 kDa], Bio-Rad). Empty lanes were loaded with 1 X gel loading buffer. Electrophoresis was conducted at 200 V for a minimum of 50 to 75 min.

2.2.9.2 Gradient (8-15 %) slab gel SDS-PAGE

Reagents

- sucrose
- 2 X stacking buffer: (250 mM Tris-HCl, pH 6.8, 0.2 % (w/v) SDS)

An 8-15 % linear gradient gel of acrylamide was produced by mixing two solutions containing different concentrations of acrylamide as they were pumped by peristalsis into the glass plate assembly. One solution termed the resolving gel heavy solution had the highest concentration of acrylamide and also contained sucrose (Table 3)

Table 3. Composition of resolving and stacking gel solutions used in the SDS-PAGE gradient gels.

Reagents	Resolving Gel Heavy Solution (15 %) (mL)	Resolving Gel Light Solution (8 %) (mL)	Stacking Gel Solution (mL)
1. Sucrose	3 g		
2. Water	7.5	11	8
3. 4 X resolving gel buffer[1]	5	5	
4. 2 X stacking gel buffer			10
5. Acrylamide stock (40 %)[1]	7.5	4	2
6. APS[1]	0.1	0.1	0.2
7. TEMED[1]	0.003	0.003	0.02

[1] see reagents listed in section 2.2.9.1

After the separating gel was poured , a layer of water was pipetted onto the gel surface and the gel allowed to set for *ca.* 30 min. The layer of water was then discarded, the top of the gel rinsed briefly with stacking buffer, and the remaining liquid removed with a piece of

3MM paper. After insertion of the well-forming comb the stacking gel solution was pipetted onto the resolving gel and allowed to set for *ca.* 30 min. Samples were prepared for loading as described in section 2.2.9.1. Electrophoresis was conducted at 65 mA through the stack and 25 mA through resolving gel, and was usually terminated after 4 to 5 h. For composition of running buffer, see section 2.2.9.1.

2.2.9.3 Staining of gels after SDS-PAGE

Reagents

- CBB stain: (0.1 % (w/v) Coomassie Brilliant Blue R-250, 40 % (v/v) methanol, 10 % (v/v) acetic acid)
- CBB destain: (30 % (v/v) ethanol)
- modified CBB stain (0.2 % (w/v) Coomassie Brilliant Blue R-250, 20 % (w/v) methanol, 0.5 % (v/v) acetic acid)
- modified destain (30% (v/v) methanol)

SDS-PAGE gels were immersed in Coomassie Brilliant Blue (CBB) stain for 20 min with gentle agitation and then rinsed with several changes of CBB destain until the background became clear. When the protein was to be excised from the gel for sequencing the modified CBB stain and destain were used.

2.2.9.4 Drying of gels after SDS-PAGE

Polyacrylamide gels were air dried by placing between sheets of GelAir Cellophane Support (Bio-Rad).

2.2.10 Western analysis of SDS-PAGE gels

2.2.10.1 Production of primary antibodies

Polyclonal antibodies were raised against the translation products of cloned cDNA sequences expressed in *E. coli.* The cDNA sequences were generated by reverse transcriptase polymerase chain reaction (RT-PCR) (section 2.3.6), ligated into the GIBCO BRL pPROEX ^{TM}-1 plasmid expression vector (Life Technologies Inc. Gathersburg, MD USA) (section 2.3.2.9.2) and then transformed into a suitable strain of *E. coli* (section 2.3.2.10.2). Translation of the cloned cDNA sequences in *E. coli* harboring the recombinant plasmid was induced with isopropyl-β-D-thiogalactopyranoside (IPTG), the protein then isolated by cellular disruption of the bacteria followed by metal-chelate affinity chromatography and the affinity purified protein used to immunise either rats or rabbits for production of polyclonal antibodies.

2.2.10.1.1 Preliminary induction of His-tagged fusion proteins in E. coli

Reagents:

- LB : (Luria-Bertani broth; see section 2.3.2.1)
- 100 mM IPTG
- 2 X SDS-PAGE gel loading buffer: (0.22 M Tris-HCl, pH 6.8, 27 % (w/v) glycerol, 5.5 % (w/v) SDS, 5 % (v/v) 2-mercaptoethanol, 0.01 % (w/v) bromophenol blue)

The ability of *E. coli* transformed with recombinant pPROEX to translate the cDNA insert upon treatment with IPTG, was initially tested on a small scale, by following the procedure accompanying the pPROEX kit.

A single colony of *E. coli,* transformed with recombinant pPROEX was grown at 37°C overnight with agitation in 10 mL of LB broth supplemented with 100 μg mL^{-1} ampicillin (LB Amp^{100}; section 2.3.2.1). An aliquot (0.5 mL) of overnight culture was then used to inoculate 10 mL of fresh broth and incubation continued until the optical density at 590 nm of the bacterial culture reached between 0.5-1.0 (usually 3 h). One mL of the culture was then removed (to serve as an uninduced control), and IPTG added to a final concentration of 0.6 mM to the remaining culture. The culture was incubated for a further 3 h, during which 1 ml samples were removed each hour. At conclusion of the sampling period, the bacteria were pelleted by centrifugation at 20 800 x g for 30 s, resuspended in

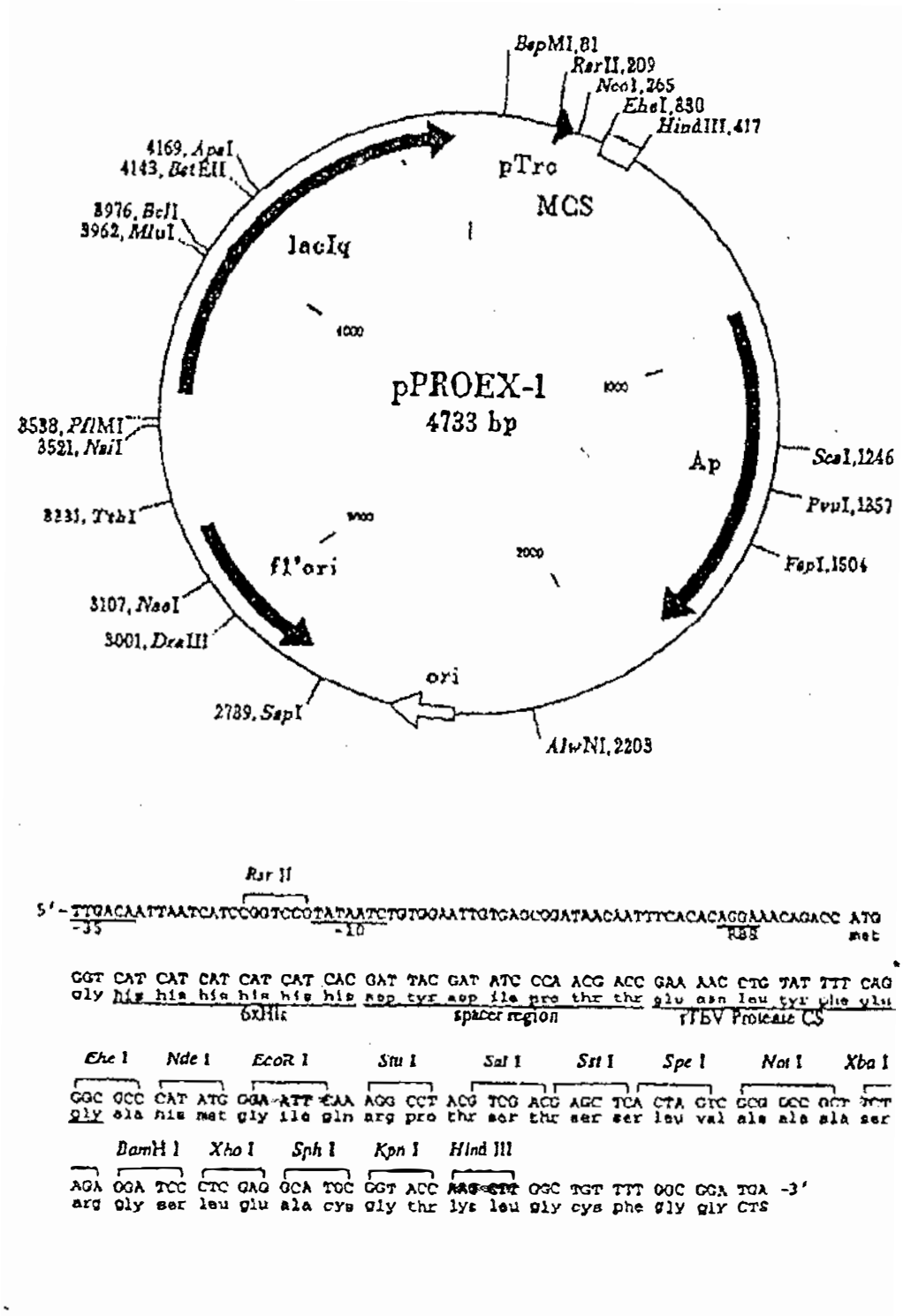

Figure 5. The map and schematic diagram of the pProEX vector and the vector multiple cloning site.

The *Eco*R1 and *Hind* III sites used for inserting TR-ACO1 and TR-ACO2 sequences in-frame into the multiple cloning site (MCS) of pProEX are highlighted. Also indicated are the N-terminal six histidine residues that become fused to the translated sequences and serve to enable purification of the fusion proteins by metal-chelate affinity chromatography.

The figure was reproduced from *Focus* 16 (4).

60 µL of 2 X SDS-PAGE gel loading buffer, boiled for 4 min, centrifuged again for 3 min and loaded into a well of an SDS-PAGE gel. Generally between 3 to 8 µL of sample supernatant was loaded. After completion of electrophoresis, the proteins in the gel were stained with CBB (Section 2.2.9.3) and the protein profile at each time point examined for both induction of the protein of the predicted size, as well as to determine the time at which protein induction was maximal.

2.2.10.1.2 Large scale induction of His-tagged fusion proteins in E. coli

Reagents

- Lysis buffer: (50 mM Tris-HCl, pH 8.0, 0.5 % (w/v) SDS, 1 % (v/v) 2-mercaptoethanol)
- Dialysis membrane: Visking, Size 5, 12 to 14 000 kDa cutoff (Medicell International Ltd., London, UK). Prepared by boiling in 10 mM sodium bicarbonate, 1 mM EDTA for 15 min, then washed with many changes of milliQ water.
- 100 mM IPTG
- 50 mM Tris-HCl, pH 8.0

After IPTG had been shown to induce a protein of predicted size and the time of its maximal induction determined, the procedure was scaled up to produce large amounts of the putative fusion protein. Broths were inoculated with *E. coli* and grown overnight as described above (section 2.2.10.1.1). An aliquot of overnight culture was then used to inoculate 1 to 2 L of fresh broth (one part overnight culture to 100 parts fresh broth) and incubation continued until the bacterial culture reached an optical density at 590 nm of between 0.5-1.0. One mL of the culture was then removed (to serve as an uninduced control), and IPTG added to a final concentration of 0.6 mM to the remaining culture. Incubation was then continued until the time of maximal induction was completed (based upon the result of the small scale induction). The cultures were then transferred to pre-weighed centrifuge tubes, the bacteria pelleted by centrifugation at 10 000 x g for 10 min at 4°C, the supernatant decanted, the weight of the bacteria determined, and the cells stored at - 80°C until required.

To prepare a crude protein extract containing the induced protein for subsequent purification, the pelleted bacteria were resuspended in four volumes of cell lysis buffer, apportioned into 4 mL volumes and the protein released by sonication with a MSE Soniprep 150 Ultrasonic Disintegrator (MSE Scientific Instruments, Manor Royal, Sussex, England). The sonicator was fitted with 3 mm diameter probe and used at an amplitude of

14 microns (15 s on, 30 s off, repeated 6 times, with the bacteria kept cooled on ice). After sonication, the cellular debris was pelleted by centrifugation at 10 000 x g for 10 min at 4°C, the supernatant removed and dialysed against 100 volumes of 50 mM Tris, pH 8.0 at room temperature for 7 h to remove SDS (buffer was changed every 2 h).

2.2.10.2 Purification of His-tagged fusion protein by metal chelate affinity chromatography

Reagents

- Buffer A: (20 mM Tris-HCl pH 8.5, 100 mM KCl, 20 mM imidazole, 10 mM 2-mercaptoethanol, 10 % (v/v) glycerol)
- Buffer B: (20 mM Tris-HCl pH 8.5, 1 M KCl, 10 mM 2-mercaptoethanol, 10 % (v/v) glycerol)
- Buffer C: (Tris-HCl pH 8.5, 100 mM KCl, 100 mM imidazole, 10 mM 2-mercaptoethanol, 10 % (v/v) glycerol)

The induced His-tagged fusion protein prepared in section (2.2.10.1.2) was purified away from the bacterial protein contaminants by metal-chelate affinity chromatography according to the instructions in the pPROEX™ -1 Protein Expression System kit.

The affinity column (1 mL) was housed in a 10 mL disposable syringe barrel (Becton Dickensen) fitted with 2 layers of GF-A glass microfibre filter paper, to prevent leakage of the column matrix. Prior to addition of sample, the column was equilibrated with 5 to 10 volumes of Buffer A at a flow rate of 0.5 mL min^{-1}. After which the sample was gently loaded onto the top of the column, allowed to run in, the column washed with ten volumes of Buffer A, two volumes of Buffer B, two volumes of Buffer A, and the fusion protein eluted with five to ten volumes of Buffer C. The eluate was collected in 0.5 to 1.0 mL fractions and 5 µL aliquots of each fraction analysed by SDS-PAGE (section 2.2.9) and the protein quantified (section 2.2.8) to determine which fractions contained the fusion protein. These fractions were then combined.

2.2.10.3 Protein sequencing

Reagents:

- AC: (200 mM ammonium carbonate)
- TFA : (Trifluoroacetic acid)
- Acetonitrile
- Trypsin: (bovine trypsin (Sigma), 250 μg mL^{-1} in AC)
- Tween-20

To confirm that the purified His-tagged fusion protein was the translated product of the cDNA insert cloned, 40 μg of affinity-purified fusion protein was fractionated over 8 lanes of a 16 % SDS-PAGE gel. The fusion protein was then identified on the basis of molecular weight using a modified CBB stain and destain procedure (section 2.2.9.3) and excised. In preparation for digestion, each gel piece was cut into tiny pieces, washed twice with 150 μL of 50 % (v/v) acetonitrile in AC at 30 °C for 20 min and then left at room temperature for *ca.* 10 min to semidry. After which, the pieces were partially rehydrated in 5 μL of AC containing 0.02 % Tween-20, and digested by adding 2 μL trypsin and then 5 μL aliquots of AC until the pieces had rehydrated to their original size. The gel pieces were then completely immersed with AC, and digested further at 30 °C for 4 h and the reaction stopped by the addition of 1.5 μL of TFA. The resulting peptides were then extracted twice with 100 μL of 60 % (v/v) acetonitrile, 0.1 % (v/v) TFA at 30°C with shaking, and the extracts combined and concentrated to *ca.* 20 μL in a SpeedVac® Concentrator (Savant Instruments Inc. Farmingdale, NY, USA)

The peptides eluted from the polyacrylamide gel were separated on a (250 x 4.6 mm) VYDAC 218 TP C18 (10 micron particle size) reverse phase column (Alltech Associates, Applied Science Labs, Deerfield, UK) fitted with a (10 x 4.6 mm) 218TP (10 micron particle size) Direct Connect® HPLC Guard Column Cartridge (Alltech). The peptides were eluted from the column using a linear gradient of acetonitrile and 0.1 % TFA at a flow rate of *ca.* 0.3 mL min^{-1}. Elution of the peptide fragments was monitored at 214 nm using a scale of 0.1 absorbance units, the fractions containing the fragments were collected manually, dried in a SpeedVac and sent away to Ms Catriona Knight, Department of Biochemistry, University of Auckland, for amino acid sequencing.

2.2.10.4 Immunisation of animals with affinity purified His-tagged fusion proteins and collection of antisera

Reagents

- Freund's adjuvant (complete and incomplete; Difco Laboratories, Detroit, Michigan, USA)
- PBSalt (50 mM sodium phosphate, pH 7.4 in 250 mM NaCl)

The affinity-purified fusion proteins were used as the antigen for production of polyclonal antibodies in either rabbits or rats at the Small Animal Production Unit (SAPU), Massey University, Palmerston North, NZ. The primary inoculum consisted of fusion protein, PBS and complete Freund's adjuvant in a ratio of 1:1:2. The inoculum was vortexed vigorously upon addition of the components so that upon sitting it did not separate out into layers. Rabbits were inoculated with 500 µg fusion protein and rats 80 µg as a final volume of 1.0 mL (for rabbits) and 0.5 mL (for rats). Incomplete Freund's adjuvant replaced the complete adjuvant for the boost inoculations.

Table 4. Antibody production: timing of inoculation and collection of antisera.

	Rabbits	Rats
	Time between inoculations	Time between inoculations
Preimmune sera collection		
1º immunisation	1 day	1 day
First boost	4.5 weeks	4.5 weeks
Second boost	4.5 weeks	4.5 weeks
First bleed	4 weeks	4 weeks

Immunisation and bleeds were performed by Mr. Eldon Ormsby, SAPU. Collected blood was clotted at 37 °C for 30 to 60 min in a centrifuge tube, the clot separated from the sides of the tube with a pasture pipette and allowed to clot further at 4°C overnight. The antisera containing the antibodies was then removed from around the clot, any contaminating cells pelleted by centrifugation at 10 000 x g for 10 min and the serum stored at -20°C.

2.2.10.5 Western blotting

2.2.10.5.1 Transfer of proteins from SDS-PAGE gel to membrane support

Reagents:

- Transfer Buffer: (25 mM Tris, 190 mM Glycine)

Proteins separated by SDS-PAGE gel were transferred to a polyvinyl fluoride membrane (PVDF; Immobilin-P, Millipore Corporation, Bedford, MA, USA) using a Trans-Blot Electrophoretic Transfer Cell (Bio-Rad). The transfer cassette holder with gel and membrane was set up as shown in Figure 6.

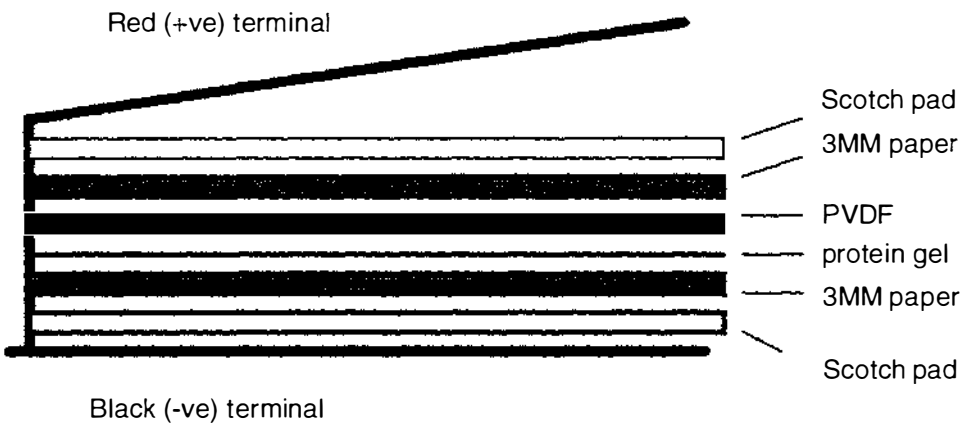

Figure 6. Setting up the cassette for transfer of protein from gel to membrane.

The cassette was set up while partially immersed in transfer buffer so as to exclude air bubbles which can interfere with transfer. The PVDF membrane was soaked for 10 s in 100 % methanol prior to placing on top of the gel. Transfer was performed either at 30 V overnight, or at 100 V for 1 h with stirring in the cold room. Protein transfer from polyacrylamide gel to PVDF membrane was confirmed by staining the gel after transfer with CBB stain (section 2.2.9.3).

2.2.10.5.2 Immunodevelopment of membrane

Reagents:

- PBSalt: (50 mM sodium phosphate pH 7.4 in 250 mM NaCl)
- PBSalt-Tween 20: (0.05 % (v/v) Tween 20 in 1 X PBSalt)
- Goat anti-rabbit IgG antibody (Sigma)
- Goat anti-rat IgG antibody (Sigma)
- Substrate: (150 mM Tris-HCl, pH 9.7 containing 0.01 % (w/v) 5-bromo-4-chloro-3-indoyl phosphate (BCIP), 0.02 % (w/v) *p*-nitro blue tetrazolium chloride (NBT), 1 % (v/v) dimethyl sulphoxide (DMSO); 8 mM $MgCl_2$)

After the conclusion of transfer, the membrane was peeled from the gel, placed protein-side up into an appropriate sized container and blocked in 0.5 % (w/v) I-Block™ (Tropix, Bedford, MA, USA) at room temperature for 1 h, or at 4°C overnight. The blocking solution was then discarded, and the PVDF membrane rinsed briefly with PBSalt-Tween 20. The membrane was then bathed with a solution of either rabbit-raised primary antibody at a concentration of 1: 2000 (diluted in PBSalt-Tween 20) or the rat primary antibody at a concentration of 1: 1000 in PBSalt-Tween 20 either at room temperature or at 37°C for 1 h with gentle shaking. After which, the primary antibody was discarded and the membrane washed three times for 10 min with PBSalt-Tween 20 and the secondary antibodies (either goat anti-rabbit alkaline phosphatase or goat anti-rat alkaline phosphatase) at a concentration of 1:10 000 in PBSalt-Tween 20 added. After incubation at room temperature for 1 h, the membrane was washed three times for 10 min with PBSalt-Tween 20, twice with 150 mM Tris pH 9.7 for 5 min, the substrate added, and the reaction allowed to continue in the dark. The reaction was stopped when sufficient colour had developed by discarding the substrate solution and rinsing the membrane several times in RO water.

2.2.10.5.3 Estimation of protein molecular mass

Protein size was estimated by comparison to the electrophoretic mobility of the size standard marker proteins. In detail, the distance between the origin and the centre of each of the marker proteins was used to plot a calibration curve. A regression equation was fitted to the calibration curve using the computer programme SlideWrite™ (Advanced Graphics Software Inc., Carlsbad, CA, USA) and the size of the protein of interest determined from the regression curve (using the Function Evaluator option of the programme).

2.2.10.5.4 Quantification of protein accumulation in western blots by image analysis

Quantification of protein on western blots by image analysis was carried out by Dr. Donald Bailey at the Institute of Fundamental Sciences, Massey University, Palmerston North, NZ. The alkaline phosphatase product was imaged with a Sony DXC-3000P video camera and the image captured into a PC using the Visionplus-AT Colour Frame Grabber. For each band of product deposition, the maximum pixel was found. The programme then moved left and right until a local minimum was found in each direction, which delineated the front and back edges of the band. The pixel values between the front and back are summed to give the integrated density.

2.3 Molecular methods

2.3.1 Chemicals

Unless otherwise stated, molecular biology or analytical grade chemicals and reagents supplied by BDH or Sigma were used, and all solutions were made with milli-Q water. Solutions were sterilised in a bench pressure cooker or by autoclaving at 103 kPa for times dependent upon the volume of liquid (500 mL or less, 20 min; 1 L, 30 min; 2 L, 45 min), or filter sterilised through a 0.22 μM nitrocellulose filter (Millex®-GS sterilising filter unit, Millipore).

2.3.2 DNA cloning procedures

2.3.2.1 Growth conditions for bacteria

Reagents:

- LB (Luria-Bertani) pH 7.5: (1 % (w/v) bacto-tryptone, 0.5 % (w/v) bacto-yeast extract, 1 % (w/v) NaCl).
- $Amp^{50 or 100}$: Ampicillin (50 or 100 mg mL^{-1})

E. coli cultures were grown with vigorous shaking (200-230 rpm) at 37 °C in LB broth. *E. coli* cultures were maintained and single colonies isolated on solid LB. Media were supplemented with antibiotics as required. In this study, ampicillin at a final concentration of 50 or 100 μg mL^{-1} ($Amp^{50 or 100}$) was typically used.

E. coli cultures maintained on solidified media were stored at 4°C and subcultured approximately every four to six weeks. Every three to five months, the stored cultures on

solidified media were replaced by fresh inoculations from frozen long-term storage cultures.

In order to store bacteria longer term, the bacterial cells were preserved as frozen glycerol stocks. Typically an 800 µL aliquot from a 10 mL LB overnight culture was added aseptically to a pre-sterilised cryotube (Nunc) containing 200 µL of 100 % (v/v) glycerol, the tube snap frozen in liquid N_2 and immediately placed at -80°C.

2.3.2.2 Plasmid isolation from E. coli by the alkaline lysis method

Reagents:

- Alkaline Lysis, Solution A: (25 mM Tris-HCl, pH 8.0, 50 mM glucose, 10 mM EDTA)
- Alkaline Lysis, Solution B: (0.2 M NaOH, 1% (w/v) SDS)
- Alkaline Lysis, Solution C: (3 M potassium acetate, 2 M glacial acetic acid)
- Isopropanol
- 80 % (v/v) ethanol

Plasmid DNA was isolated from *E. coli* by the alkaline lysis method of Sambrook *et al.*, (1989). Typically, a 10 mL LB Amp^{100} broth was inoculated with *E. coli* by stabbing a single colony with a sterile toothpick and breaking off the lower portion of the toothpick directly into the broth. After incubation at 37°C overnight with shaking, the cells were pelleted by centrifugation at 3 000 x g for 5 min at room temperature, the supernatant drained, and the pellet resuspended completely in 200 µL of freshly prepared alkaline lysis solution A. After transferring to a microfuge tube, the cells were lysed with 400 µL of freshly prepared Alkaline Lysis Solution B by mixing with gentle inversion and a 10 min incubation on ice. The contaminating chromosomal DNA and protein was then precipitated by addition of 300 µL of freshly prepared alkaline lysis solution C. After the solution was shaken vigorously and incubated on ice for 5 min, the precipitate was pelleted by centrifugation at 20 800 x g for 5 min at room temperature, and the supernatant removed to a fresh tube. If the plasmid was to be used in ligation reactions, an equal volume of chloroform: isoamyl alcohol (24:1) was added to the supernatant, the aqueous and organic phases mixed by vortexing and separated by centrifugation at 20 800 x g for 5 min at room temperature, after which the top aqueous phase was removed. The plasmid DNA was then precipitated by the addition of an equal volume of isopropanol, the DNA pelleted by centrifugation at 20 800 x g for 10 min at room temperature, the pellet rinsed with ice-cold

80 % (v/v) ethanol, and dried briefly in a SpeedVac (section 2.3.2.3). Typically the pellet was redissolved in 40 to 50 µL of sterile water.

2.3.2.3 Precipitation of DNA and RNA with ethanol or isopropanol

Reagents:

- 3 M sodium acetate pH 5.2
- 100 % (v/v) ethanol: (99.7 to 100 % (v/v) ethanol)
- 80 % (v/v) ethanol

Nucleic acid was routinely precipitated from solutions by adding 0.1 volumes of 3 M NaOAc and either 2.5 volumes (for DNA) or three volumes (for RNA) of ice cold 100 % (v/v) ethanol. Precipitations were performed at 4°C on ice or for times dependent upon the estimated concentration of nucleic acid. If the concentration was considered to be 1 µg mL^{-1} or greater (for example in plasmid preparations) then the nucleic acid was centrifuged immediately, while if thought to be below 0.5 µg ml^{-1}, the nucleic acid was incubated overnight (for maximal yield) prior to centrifugation. The nucleic acid precipitate was then pelleted by centrifugation at 20 800 x g for 10 to 15 min at room temperature (or 4°C), the supernatant discarded, residual salts removed by rinsing the pellet with 80 % (v/v) ethanol. After discarding the 80 % (v/v) ethanol any residual ethanol still adhering to the walls of the microfuge tube was collected by pulse-centrifugation and removed with a micropipette. The pellet was then dried at 40°C in a heating block for *ca.* 4 min.

In some instances when volume quantities were limiting, 0.6 to one volume of isopropanol was added rather than ethanol. However, ethanol was preferred as isopropanol is less volatile and tends to co-precipitate solutes, for example, NaCl, which can inhibit re-dissolution of the nucleic acid pellet.

2.3.2.4 DNA quantitation

DNA was quantified by diluting an aliquot (typically 5 µL) of DNA to 1 mL with water, placing in a 1 cm light path quartz cuvette, and comparing the absorbance at 260 nm against a water blank. The absorbance reading at 260 nm enabled calculation of the concentration of nucleic acid present in the sample since an OD of 1 corresponds to approximately 50µg/ mL double stranded DNA (Sambrook *et al.* 1989)

$A_{260\,nm}$ X dilution factor X 50 = conc. DNA in µg/ mL

Purity of nucleotide solutions can be gauged by examining the A_{260nm}/A_{280nm} (Sambrook *et al.*, 1989) and A_{260nm}/A_{230nm} ratios (Dong and Dunstan, 1996).

Relatively pure DNA solutions have an A_{260nm}/A_{280nm} ratio of 1.8, a value that decreases with the presence of contaminants such as proteins, phenol and surfactant, or if nucleic acid is not fully resuspended (Teare *et al.*, 1997).

Relatively pure DNA solutions have an A_{260nm}/A_{230nm} ratio > 2, a value that decreases with the presence of polysaccharides.

2.3.2.5 Restriction digestion of DNA

Unless otherwise stated, DNA was digested with GIBCO BRL restriction enzymes (Life Technologies) in the recommended buffer. The total concentration of glycerol in the digestion reactions was always kept at 5 % (v/v) or below and the enzyme never exceeded 100 U μg^{-1} to reduce the incidence of "star" activity, whereby endonucleases cleave sequences similar, but not identical to their defined cleavage sites.

Reagents:

- Restriction enzyme
- 10 X Restriction buffer
- RNase A (10 mg mL^{-1} stock) (Sigma)
- 10 X SUDS: (0.1 M EDTA pH 8.0, 50 % (v/v) glycerol, 1 % (w/v) SDS, 0.025 % (w/v) bromophenol blue)

Digestion of DNA with restriction endonuclease enzymes was performed for a number of different reasons.

1. To prepare plasmid and insert for cloning

DNA was digested serially when more than one restriction enzyme was used. Plasmid DNA obtained from a 10 mL culture of bacteria by alkaline lysis (section 2.3.2.2) was divided in half, one half digested with the first restriction enzyme, and the other with the second enzyme in reaction mixes containing 40 U restriction enzyme, 0.1 volumes of 10 X restriction buffer, 20 µg RNase A and sterile water to 40 µL. After incubation at 37°C for 3 h, an aliquot (2µL) of each digestion mix was resolved in a 1 % (w/v) agarose gel (section 2.3.2.6) to confirm that both enzymes were cutting effectively and to assess whether the enzymes had cut to completion (by the presence of linearised plasmid). After

digestion had proceeded to completion with the first restriction enzymes, the linearised plasmid from each mix was precipitated with ethanol (section 2.3.2.3), resuspended in sterile water and digested with the other restriction enzyme (except no RNase was added). After digestion at 37°C for 3 h was completed, the double digested plasmid was gel- (section 2.3.2.6) and column-purified in preparation for ligation (section 2.3.2.8.1).

PCR products (amplified using the primers described in section 2.3.6.2.3) were also digested serially with the appropriate restriction enzymes in preparation for cloning. The DNA from a single 100 µL volume amplification mix (section 2.3.6.2.5) was precipitated with ethanol, resuspended in 20 µL sterile water and digested with 200 U of the first restriction enzyme in a reaction mix containing 0.1 volumes of 10 X restriction buffer and sterile water to 200, µL at 37°C for 3 h. The DNA was then precipitated as before, resuspended in 20 µL sterile water and digested with the second restriction enzyme using the same reaction conditions as for the first digestion. On completion of digestion, the double digested DNA was again precipitated with ethanol, resuspended in sterile water, and gel- (section 2.3.2.6) and column purified (section 2.3.2.8.1).

2. To confirm that plasmids of transformed bacteria contained the inserts of expected size.

Typically, 1 to 2 µg plasmid DNA obtained by alkaline lysis (section 2.3.2.2) was digested in a reaction mix containing 5 U of restriction enzyme, 0.1 volumes of 10 X restriction buffer, 10 µg RNase A and sterile water to 10 µL at 37°C for 1 to 3 h. The reaction was terminated by the addition of 0.1 volumes of 10 X SUDS and the digested DNA resolved by electrophoresis (section 2.3.2.6).

If excision of the insert required the action of two restriction enzymes, and both enzymes were able to cut effectively in a common buffer (for example, *Hin*d III and *Eco*R1 both cut 100 % in the *Hin*d III buffer), then digestion was performed in a single reaction volume.

3. To produce quantities of insert for radiolabelling

Larger amounts of insert were obtained by digesting all the plasmid DNA purified from a 10 mL culture in a reaction mix containing 20 U of restriction enzyme, 0.1 volumes of 10 X restriction buffer, 20 µg RNase A and sterile water to 80 µL at 37°C for 3 h. The excised insert was gel-purified in a 1 % (w/v) agarose gel (section 2.3.2.6) and the insert isolated by the freeze-squeeze method (section 2.3.2.8.2).

2.3.2.6 Agarose gel electrophoresis of DNA

Reagents:

- 10 X TAE Buffer: (0.4 M Tris, 0.2 M glacial acetic acid, 10 mM EDTA pH 8.0)
- 10 X SUDS: (0.1 M EDTA pH 8.0, 50 % (v/v) glycerol, 1 % (w/v) SDS, 0.025 % (w/v) bromophenol blue)
- Ethidium bromide: (10 mg mL^{-1})
- Gibco BRL UltraPURE™ agarose (Life Technologies)

DNA fragments generated by PCR (section 2.3.6.2) and restriction digestion (sections 2.3.2.5 and 2.3.4.3) were routinely analysed by separation through horizontal 1X TAE, 0.8 to 1.2 % (w/v) agarose gels. Electrophoresis was routinely performed using a Bio-Rad DNA Mini Sub Cell™ (70 cm^2 gel bed; 30 mL volume) for plasmid and PCR generated DNA, or a Bio-Rad DNA Sub Cell™ (225 cm^2 gel bed; 100 mL volume) for plant genomic DNA.

The gel solution was made by adding 1 X TAE running buffer to the appropriate amount of agarose. The weight of the flask and contents were then noted, the gel mix heated to dissolve the agarose, the flask reweighed and any water that had evaporated replaced. After the gel solution had cooled to touch, ethidium bromide was added to a final concentration of 0.15 μg mL^{-1} and the solution immediately poured into a gel-forming apparatus. No ethidium bromide was added to the gel solution used for genomic analysis. Instead the gel was stained after electrophoresis with 0.1 μg mL^{-1} ethidium bromide for 20 min and then destained (with water) for a further 20 min.

DNA samples were weighted with 0.1 volumes of 10 X SUDS, loaded, and separated by electrophoresis at 5 to 10 V cm^{-1} for plasmid and PCR-generated DNA or at 5 V cm^{-1} for plant genomic DNA. After electrophoresis, the DNA fragments were visualized on a short-wavelength (340 nm) UV Transilluminator (UVP Inc., San Gabriel, CA, USA), and photographed either digitally with an Alpha Imager™ 2000 Documentation and Analysis System (Alpha Innotech Corporation, San Leandro, CA, USA) or using a Polaroid Land Camera with Polaroid 667 film (Fabrique au Royanne-Uni. UK, Ltd., Hertfordshire, England).

2.3.2.7 Size determination of nucleic acid

The sizes of nucleic acid fragments were determined from their mobility relative to that of known standards resolved on the same gel. This data was entered into a computer programme, DNAFIT (National Institute of Health, Bethesda, MD, USA) employing a four-parameter logistic model to describe the relationship between electrophoretic mobility and the $\log_{10}$ molecular size (Oerter *et al.*, 1990).

2.3.2.8 DNA recovery from agarose gels

DNA fragments generated by PCR (section 2.3.6.2) or produced by restriction endonuclease digestion of plasmid inserts (section 2.3.2.5) were isolated for use in ligation or labelling reactions by either the spin-column or freeze-squeeze methods.

2.3.2.8.1 Spin column method

Reagents:

- Wizard™ MiniPreps DNA Purification System (Promega Corporation, Madison, WI USA)
- Column wash solution: (8.3 mM Tris-HCl, pH 7.5, 80 mM KOAc, 40 µM EDTA, pH 8.0, 55 % (v/v) ethanol)
- 6 M NaI

DNA fragments were isolated from agarose gels for ligation reactions using the spin column method. DNA was separated by electrophoresis in a 1 % (w/v) agarose gel (section 2.3.2.6), the desired fragment identified under long-wave UV, excised from the gel with a sterile scalpel blade and placed in a pre-weighed microfuge tube. Three volumes of 6 M NaI were added per gram of excised gel and the gel heated at 55°C for 15 min or until the gel had completely melted. One mL of thoroughly resuspended DNA purification resin was then added and the resin/DNA mix transferred to a 3 mL syringe barrel (Becton Dickensen) attached to a minicolumn on a Vac-Man™ Laboratory Vacuum Manifold (Promega). The resin/DNA mix was then drawn onto the column by vacuum, flushed with 2 mL of column wash solution, and dried by continuing the vacuum for an additional 30 s. After transfer of the column to a microfuge tube, residual wash solution was removed by centrifugation at 3 800 x g for 1 min. An aliquot (50 µL of sterile water preheated to 70°C) was then added to the column and after 1 min the DNA eluted by centrifugation at 18 000 x g for 20 s.

2.3.2.8.2 Freeze-squeeze method

This very simple and quick method was used to isolate DNA templates for labelling. DNA was separated by electrophoresis and the fragment isolated as before (section 2.3.2.8.1). The excised gel piece was then snap-frozen in liquid N_2 , the agarose pelleted by centrifugation at 20 800 x g for 10 min at room temperature, and the supernatant containing the DNA collected. A variation of the method which resulted in higher yields, involved adding 1 volume of sterile water to the excised gel and melting at 50°C for 15 min prior to snap-freezing of the gel in liquid N_2.

Notes:

- In this study, the DNA purified by this method could not be ligated.

2.3.2.9 DNA Ligation

2.3.2.9.1 DNA ligation using linearised T-Vector

Sequences generated by PCR were ligated into the pCR®2.1 linearised T-vector plasmid (Figure 7) by essentially following the method provided with the TA-Cloning® kit (Invitrogen, Leek, The Netherlands). The technique relies on the ability of the PCR amplification enzyme, *Taq* polymerase, which has terminal transferase activity, to add a single deoxyadenosine to the 3'-ends of duplex molecules. These 3'-A overhangs can then be used to insert the PCR product into a vector which contains single 3'-T overhangs at its insertion site.

The amount of PCR product (for a 1:3 molar ratio) required for ligation was calculated using the equation supplied with the TA-cloning Kit.

$$X\ ng = 3\frac{(Y\ bp\ PCR\ Product)(50\ ng\ pCR\ 2.1\ Vector)}{(\text{size in bp of pCR 2.1 Vector})}$$

Reagents:

- T4 DNA ligase (Invitrogen)
- 10 X ligation buffer (Invitrogen)

The PCR product was ligated with 50 ng linearised pCR 2.1 vector in a reaction mix that contained 2µL T4 DNA ligase, 0.1 volumes of 10 X ligation buffer and sterile water to 20 µL. The ligation was conducted at 14°C overnight in a PTC-200 Peltier Thermal Cycler (MJ Research, Inc., Watertown, Massachusetts, 02172 USA).

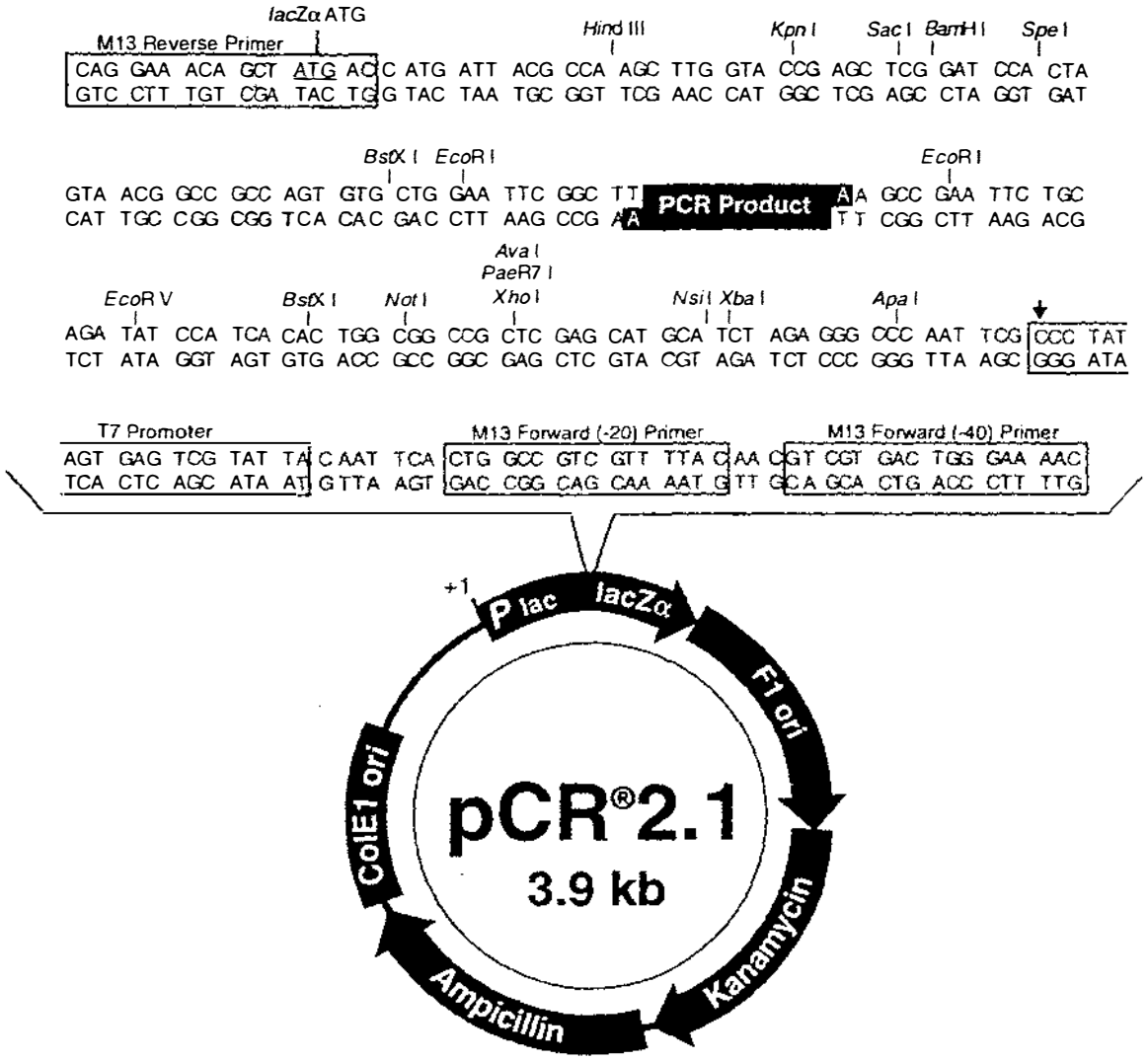

Figure 7. Diagram of the pCR 2.1 plasmid used for TA-cloning PCR generated sequences.

The sequence of the multiple cloning site is shown with a PCR product inserted by TA-cloning. The inserted PCR product is flanked on each side by *Eco*R1 sites that were used to cut out the insert from the plasmid. The M13 Forward and Reverse Primers used in sequencing are indicated.
This figure is reproduced from the TA-cloning® Instruction manual.

2.3.2.9.2 DNA ligation using restriction digested vector

For ligations not involving the pCR 2.1 vector, a 1:3 molar ratio of vector to insert was also used, but the quantity of vector and product used was calculated visually by resolving an aliquot of vector and PCR product on the same 1 % (w/v) agarose gel and estimating from the ethidium bromide staining intensities. This simple method works because plasmid vectors are often four times larger than their inserts.

Reagents:

- Gibco BRL T4 DNA Ligase (1 U μL^{-1}) (Life Technologies)
- 10 X Ligation buffer (supplied with Ligase)

The appropriate amount of PCR product was ligated with typically between 10 to 50 ng of vector in a reaction mix that contained 2µL T4 DNA ligase, 0.1 volumes of 10 X ligation buffer and sterile water to 20 µL. The ligation was conducted at 14°C overnight in a PTC-200 Peltier Thermal Cycler

2.3.2.10 Transformation of E. coli

2.3.2.10.1 Preparation of competent cells

Cells used for transformation in this thesis were either TA-Cloning®OneShot™ competent cells supplied with the TA-Cloning kit, or *E. coli* strain DH-5α cells (Life Technologies) made competent using $CaCl_2$.

Reagents:

- 60 mM $CaCl_2$
- glycerol
- LB broth: (refer section 2.3.2.1)

Ten mL of LB broth was inoculated with a single colony of *E. coli*, incubated at 37°C overnight with shaking, and 0.4 ml removed to inoculate 40 mL of fresh LB broth. Incubation was continued at 35°C until the optical density at 600 nm had reached 0.4, the culture was then poured into a prechilled centrifuge tube and the bacteria pelleted by centrifugation at 2000 x g for 5 min at 4°C. After discarding the supernatant, the bacterial pellet was resuspended in 10 mL ice-cold 60 mM $CaCl_2$, a further 10 mL $CaCl_2$ added and the cells placed on ice for 30 min. After which time, the cells were pelleted as before, the

supernatant discarded, the cells resuspended in 4 mL $CaCl_2$, 15 % (v/v) glycerol, and stored at -80°C in 300 µL aliquots.

Three different transformation methods were used in this thesis to transform competent cells. Lab stocks of DH-5α cells made competent (section 2.3.2.10.1) were either transformed with the standard heat shock protocol (section 2.3.2.10.2) or the faster 5 min transformation protocol of Pope and Kent (1996) (section 2.3.2.10.3). Both methods worked equally well in this thesis. When TA-cloning was performed with the One Shot™ competent cells supplied in the kit, the transformation protocol recommended by the manufacturer was followed (section 2.3.2.10.4).

2.3.2.10.2 Transformation by standard heat shock protocol

Reagents:

- LB broth: (refer section 2.3.2.1)

A 300 µL aliquot of DH-5α cells made competent (section 2.3.2.10.1) was thawed on ice, ca 10 ng (10 µL) of plasmid DNA added, and incubation on ice continued for a further 30 min. After which time the cells were heat-shocked at 42°C for 2 min, placed back on ice for 2 min, 0.7 mL of LB added, and the transformation mix incubated with shaking at 37°C for 1 h. Putative transformants were selected by spreading 25 µL and 100 µL volumes of the transformation mix onto LB plates supplemented with antibiotics (typically Amp^{50}), and incubating the plates at 37°C overnight. The plasmids of the resultant single colonies (isolated by alkaline lysis, section) were then evaluated for the presence of insert of the expected size by restriction endonuclease digestion (section 2.3.2.5).

2.3.2.10.3 Transformation by 5-minute protocol

In this thesis, the 5 min transformation method of Pope and Kent (1996) was found to work equally well with competent cells prepared by the $CaCl_2$ method. Ten ng of plasmid DNA was added to 300 µL of competent DH-5α cells, the mix incubated on ice for 5 min and a 100 µL aliquot then spread directly onto an LB Amp^{50} plate that had been preincubated at 37°C. The plate was incubated at 37°C overnight and the resultant colonies checked for the presence of plasmid and insert as described above (section 2.3.2.5).

Notes:

- Does not work with plasmids that are selected with Kanamycin sulphate (Pope and Kent (1996).

2.3.2.10.4 Transformation by TA cloning kit protocol

Reagents:

- 0.5 M 2-mercaptoethanol: (supplied in kit)
- SOC medium: (supplied in kit): (2 % (w/v) tryptone, 0.5 % (w/v) yeast extract, 10 mM NaCl, 10 mM $MgSO_4$, 20 mM glucose)
- Ampicillin: (50 μg ml^{-1})

Two μL of 0.5 M 2-mercaptoethanol was added to a vial of One Shot™ competent cells (Invitrogen) that had been thawed on ice, and mixed in gently by swirling of the pipette tip. Five μL of the ligation reaction was then added and the transformation mix incubated on ice for 30 min, the mix was then heat shocked at 42°C for exactly 30 s, placed back on ice for 2 min, and 250 μL of SOC medium added. The putatively transformed bacteria were then shaken at 37°C for 1 h, placed on ice and aliquots of 50 and 200 μL spread onto LB Amp^{50} plates. Plates were incubated at 37°C overnight and the resultant colonies checked for the presence of plasmid and insert as described above (section 2.3.2.5).

2.3.3 DNA sequencing procedures

2.3.3.1 Purification of DNA for sequencing

Plasmid DNA isolated from a 10 mL culture of *E. coli* by alkaline lysis (section 2.3.2.2) was made up to 100 μL with sterile water or TE buffer, and 10 μL (50 μg) of RNase added. After incubation at 37°C for 10 min, 1 mL of thoroughly resuspended Wizard™ MiniPreps DNA purification resin was added, and the plasmid column-purified (section 2.3.2.8.1) except that the centrifugation step at 3 800 x g for 1 min was replaced by centrifugation at 18 000 x g for 2 min.

2.3.3.2 Manual sequencing

Double-stranded DNA was sequenced with a Sequenase™ Version 2.0 DNA Sequencing Kit (United States Biochemicals, Cleveland, Ohio, USA: Amersham) that was developed from the chain-termination method (Sanger *et al.*, 1977) using a modified Sequenase™ T7 DNA polymerase (Tabor and Richardson, 1989). The enzyme has been genetically modified to remove the 3' to 5' exonuclease repair activity, is reported to be very stable and have high specific activity.

Reagents:

- 2N NaOH
- 0.5 M EDTA
- 2 M ammonium acetate pH 4.6
- 100 % (w/v) ethanol
- 75 % (w/v) ethanol
- [α-^{35}S]-dATP (Amersham International, Plc., Amersham, Buckinghamshire, England)
- Sequenase version 2 sequencing kit
- 5 X labelling mix: (7.5 μM dGTP, 7,5 μM dCTP, 7.5 μM dTTP)
- Enzyme dilution buffer: (10 mM Tris-HCl, pH 7.5, 5 mM DTT, 0.5 mg mL^{-1} BSA)
- 2 X stop solution: 95 % (v/v) formamide, 20 mM EDTA, 0.05 % (w/v) bromophenol blue, 0.05 % (w/v) xylene cyanol FF)

Typically, 4 μg of plasmid DNA was denatured by adding one-tenth volume of 2 M NaOH, 2 mM EDTA and incubating at room temperature for 5 min. The mixture was neutralised by adding a one-tenth volume of 2 M ammonium acetate pH 4.6 and the DNA precipitated with two to four volumes of 100 % (v/v) ethanol at -80°C for 10 min. After the DNA was pelleted by centrifugation at 18 000 x g for 10 min and rinsed with ice-cold 75 % (v/v) ethanol, the DNA was dried briefly under vacuum in a SpeedVac.

The dried DNA pellet was redissolved in 6 μL of sterile water and 2 μL of 5 X T7 Sequenase Reaction Buffer and 2 μL of sequencing primer (either M13 Universal Forward or Reverse) added. The DNA strands were then melted at 65°C for 5 min in a heating block, and then the temperature was rapidly reduced to 37°C and the primer annealing continued at 37°C for a further 15 min. The annealed DNA mixture was then placed on ice while the reaction mix was prepared.

Prior to combining the components of the reaction mix the T7 DNA polymerase was diluted 1:7 with enzyme dilution buffer, and the labelling mix diluted 1:4 with sterile water and both placed on ice until required. The reaction mix was then prepared by combining 1 µL DTT, 2 µL diluted labelling mix, 2 µL diluted Sequenase T7 DNA polymerase, and 0.5 µL 1000 Ci mmol^{-1} [α-^{35}S]-dATP (Amersham).

The reaction mix was then added to the ice-cold annealed DNA mixture, and the mix incubated at room temperature for 2 to 5 min to initiate polymerisation and label the sequencing product a short distance from the primer. After which time, the tube was cooled on ice until the dideoxy-nucleotide termination reaction tubes were prepared. The termination tubes were prepared by aliquotting 2.5 µL of each dideoxy-nucleotide into a separate labelled tube. Aliquots (3.5 µL) of the labelling reaction were transferred to each tube, and the tubes incubated at 37°C for 5 min. After which time, the reactions were stopped by the addition of 4µL of stop solution, and stored on ice or at -20°C until required.

2.3.3.3 Sequencing gels

Reagents:

- 10 X TBE: (1.3 M Tris-base, 450 mM boric acid, 25 mM EDTA)
- 40 % (w/v) acrylamide
- 10 % (w/v) APS
- TEMED
- Urea

Termination reactions were analysed by electrophoresis through a vertical 6 % (w/v) polyacrylamide denaturing gel containing 8.3 M urea in 1 X TBE buffer. The gel mix consisted of 15 mL of 40 % (w/v) acrylamide, 10 mL of 10 X TBE, 50 g of urea and water to 100 mL. The solution was mixed for at least 1 h to dissolve the urea, and then filtered through Whatman No. 1 filter paper prior to the addition of 1 mL of fresh 10 % (w/v) APS and 50 µL of TEMED. After addition of the TEMED, the gel mix was quickly injected into the gel plate assembly which consisted of two GIBCO BRL Model S2 glass sequencing plates (Life Technologies) separated by 0.4 mm thick spacers (Life Technologies) and sealed at the base and sides with Sleek™ medical tape (Smith and Nephew, Ltd., Hull, UK). Two 14 cm GIBCO BRL vinyl doublefine sharkstooth combs (Life Technologies Inc.)

were then inserted between the plates, into the gel to a depth of *ca.* 2 mm and the combs completely covered with excess acrylamide to exclude air. After polymerisation was complete (at least 1 h), the combs and basal tape were removed, and the plates installed into the GIBCO BRL Model S2 Sequencing Gel Electrophoresis System (Life Technologies). TBE buffer (running buffer) was added to both chambers and the inverted combs removed and reinserted teeth downward until the teeth had just made contact with the gel surface. The gel wells were then flushed with running buffer to remove any accumulated urea in preparation for loading. The stopped termination reactions were then heated at 70°C for 3 min, rapidly cooled on ice, and loaded into the wells. The sequencing products were initially separated at 1650 V, 40 mA and 65 W for 3 h by electrophoresis, then a second loading from each reaction was performed in separate wells and electrophoresis continued for another 2 h. At completion of electrophoresis, the gel plate assembly was dismantled and the gel fixed in a solution of 5 % (v/v) acetic acid: 5 % (v/v) methanol for 20 min. The gel was then transferred onto 3MM paper, covered with clingfilm, dried in vacuum gel-drier at 80°C for 1.5 h, and placed in a Hypercassette™ (Amersham) with NIF RX Fuji Medical X-ray film (Fuji Photo Film Co., Ltd.) and the radiolabelled fragments visualised by autoradiography.

2.3.3.4 Automated DNA sequencing

Plasmid DNA was prepared for automated sequencing as described in section (2.3.3.1) at a concentration of 200 ng μL^{-1} and sent to Ms Lorraine Berry, MUSeq, Institute of Molecular BioSciences, Massey University, Palmerston North, NZ for automated sequencing. The plasmid DNA was sequenced using the ABI PRISM™ Dye Terminator Cycle Sequencing Ready Reaction Kit with AmpiTaq®DNA Polymerase, FS (Perkin Elmer, Foster City, CA, USA), and the products analysed with an automated ABI PRISM™ 377 DNA Sequencer (Applied Biosystems, Foster City, CA, USA)

2.3.3.5 Sequence alignment

Alignment of sequences obtained with manual and automated sequencing was achieved either using the Align Plus Sequence Alignment Program version 2 (Science and Educational Software, State Line, PA, USA) or Clustal X (Thompson *et al.,* 1994). Sequence identity comparisons with other organisms was performed using Basic Local Alignment Sequence Tool (Blast-N ; Altschul *et al.,* 1990).

2.3.3.6 Sequence phylogeny

A majority rule consensus tree was built using a heuristic search with default parameters of a pre-release β-version of the computer programme Phylogenetic Analysis Using Parsimony (Paup version 4.0 od64, Sinaur Assoc, Inc. Publishers, Sunderland Massachusetts© 1998 Smithsonian Institute).

2.3.4 Southern analysis procedures

Two different phenol-based methods for isolating genomic DNA were used in this thesis. The first method which used less phenol and chloroform appeared to produce DNA that was restriction-digested just as well as the more time consuming second method.

2.3.4.1 Genomic DNA isolation method 1.

Reagents:

- Extraction buffer: (50 mM Tris-HCl, pH 8.0, 0.25 M NaCl, 20 mM EDTA, 0.5% (w/v) SDS) and 0.01% (v/v) 2-mercaptoethanol added just before use
- Tris-buffered phenol: (6 mL of 1 M Tris-HCl, pH 8.0, 7.5 mL 2M NaOH, 130 mL H_2O, 500 g commercial phenol crystals)
- TE Buffer: (10 mM Tris-HCl, pH 8.0, 1 mM EDTA, pH 8.0)
- RNase A: (10 mg/ mL)

Genomic DNA was isolated from leaf tissue using the method of Michaels *et al.*, (1994). This involved extracting approximately 3 g of powdered leaf material in 10 mL of extraction buffer at 60°C for 5 min. Six mL of Tris-buffered phenol was then added to the extraction mix and incubation continued for a further 5 min. After this time, an equal volume of chloroform: isoamylalcohol (24:1) was mixed in by inversion, the aqueous phase separated from the organic phase by centrifugation at 4 000 x g for 10 min at 4°C and transferred to a fresh tube. Contaminating polysaccharides were precipitated by adding slowly, but with rapid mixing, 0.35 volumes of 100 % (v/v) ethanol and incubating the solution on ice for 15 to 20 min. After pelleting the polysaccharides by centrifugation at 4 000 x g for 10 min at 4°C, the aqueous supernatant containing the nucleic acids was collected, and the nucleic acids precipitated on ice for 15 min after the addition of an equal volume of isopropanol. The precipitated nucleic acid was then pelleted by centrifugation at 4 000 x g for 10 min, the supernatant discarded, the pellet was washed once with 80% (v/v) ethanol and once with 100% (v/v) ethanol before being resuspended in 3 mL of TE

buffer. Contaminating RNA was removed by incubating the nucleic acid with 3 μg of RNase A at 37°C for 1 h and the DNA precipitated by incubation at room temperature for 15 min after the addition of one third volume of 8 M ammonium acetate and 2.5 volumes of 100% (v/v) ethanol. The DNA was then pelleted by centrifugation at 4 000 x g for 15 min at 4°C, washed in 80 % (v/v) ethanol, resuspended in 25 to 400 μL of TE buffer and stored at - 20°C .

Notes:

- The temperature of the Tris-buffered phenol extraction mix must be below 60°C when the chloroform is mixed in, as chloroform boils at 61.7°C

2.3.4.2 Genomic DNA isolation method 2

Genomic DNA was isolated from leaf tissue by a modified method of Junghans and Metzlaff, (1990) (A. Griffith, AgResearch, Grasslands, Palmerston North, NZ, *pers. comm.*).

Reagents:

- Lysis buffer: (50 mM Tris-HCl, pH 7.6, 100 mM NaCl, 50 mM EDTA, 0.5 % (w/v) SDS), 0.01 % (v/v) 2-mercaptoethanol may be added to the lysis buffer immediately prior to DNA extraction
- Tris-buffered phenol: (6 mL 1 M Tris-HCl, pH 8.0, 7.5 mL 2M NaOH, 130 mL H_2O, 500 g commercial phenol crystals)
- TES: (10 mM Tris-HCl, pH 8.0, 100 mM NaCl, 1 mM EDTA
- RNase A: (10 mg/ mL)
- TES/RNase: (25 mL TES, 40 μL RNase)

Approximately 1.6 g of powdered leaf tissue was added to 10 mL of lysis buffer and 10 mL of Tris-buffered phenol. The mix was then shaken vigorously for 3 min to obtain a good emulsion, 5 mL of chloroform: isoamyl alcohol (24:1) added, and the mixing continued for a further 3 min. The cellular debris was then pelleted by centrifugation at 26 000 x g for 10 min at 4°C, the aqueous supernatant transferred to a new centrifuge tube containing 5 mL of Tris-buffered phenol, and the phenol mixed in by shaking for 3 min. Five mL of chloroform: isoamyl alcohol (24:1) was then added and the mixture shaken again for 3 min. The aqueous and organic phases were then separated by centrifugation at 26 000 x g for 10 min and the aqueous supernatant removed to a fresh tube, 10 mL of chloroform: isoamyl alcohol (24:1) added, the contents mixed for 3 min and the aqueous phase separated and

removed to a new tube as before. The nucleic acid was precipitated by the addition of 0.67 volumes of isopropanol and then pelleted by centrifugation at 26 000 x g for 10 min. After which time, the pellet was rinsed with 80 % (v/v) ethanol, dried at 40°C for 5 min, and resuspended in 4 mL TES/RNase solution. After incubation at 37°C for 25 min to digest the contaminating RNA, the nucleic acid was transferred into a fresh centrifuge tube that contained 2 mL phenol, the solution shaken vigorously for 3 min, 2 mL chloroform: isoamyl alcohol (24:1) added and the tube shaken for a further 3 min. The aqueous phase was separated by centrifugation as before, transferred into a fresh tube that contained 4 mL chloroform: isoamyl alcohol (24:1), shaken for 3 min, and the centrifugation repeated. The nucleic acid in the aqueous phase was precipitated with ethanol (section 2.3.2.3), resuspended in 500 µL of 0.25 M NaCl, and 0.35 volumes of 100 % (v/v) ethanol added slowly but with rapid mixing to precipitate polysaccharide contaminants. After incubation on ice for 15 min, the polysaccharide precipitate was pelleted by centrifugation at 20 800 x g for 5 min at 4°C, the supernatant removed, the DNA precipitated with ethanol, resuspended in sterile water, quantified (section 2.3.2.4) and stored in aliquots at -20°C

2.3.4.3 Restriction Digestion of Genomic DNA

Reagents:

- Gibco BRL *Eco*R1: (10 U μL^{-1}) (Life Technologies)
- Gibco BRL *Xba* I: (10 U μL^{-1}) (Life Technologies)
- Gibco BRL *Hind* III: (10 U μL^{-1}) (Life Technologies)
- 10 X Restriction buffer: (supplied with the appropriate restriction enzyme)

Genomic DNA was digested with three restriction endonuclease enzymes in separate reaction mixes. Each digestion mixture consisted of 30 µg DNA, 80 U of restriction enzyme, 20 µL of 10 X restriction buffer and sterile water to 200 µL. Digests were incubated at 37°C overnight, after which an additional 30 U of enzyme was added and the DNA digested further for 3 to 5 h. The DNA was then precipitated with ethanol overnight (section 2.3.2.3), resuspended in 20µL sterile water, weighted with one-tenth volume of 10 X SUDS and resolved by agarose gel electrophoresis (section 2.3.2.6).

2.3.4.4 Southern (capillary) blotting of genomic DNA

Genomic DNA fragments resolved by agarose gel electrophoresis (section 2.3.2.6) were transferred to a nylon membrane by the downward alkaline capillary transfer method of Chomczynski (1992), except for an additional depurination step.

Reagents:

- Depurination solution: (0.25 M HCl)
- Denaturation solution: (1.5 M NaCl, 0.4 M NaOH)
- Transfer solution (pH 11.4 to 11.45): (3 M NaCl, 8 mM NaOH)
- 5 X SSPE: (50 mM $Na_2PO_4.2H_2O$, pH 7.7, 0.9 M NaCl, 5 mM EDTA)

Following electrophoresis (section 2.3.2.6), the gel was immersed in depurination solution with gentle agitation for 7 min. The depurination solution was then discarded, the gel rinsed twice with RO water, placed in denaturation solution for 1 h, washed twice more with RO water and immersed in transfer solution for 15 min.

The blotting system (Figure 8) was constructed while the gel was being prepared for transfer. A gel-sized piece of 3MM paper, pre-soaked in transfer solution, was placed on a glass plate. Upon this was placed a gel-sized sheet of Hybond^{TM}-N^+ membrane that had been pre-soaked in transfer solution for 5 min. The gel was then placed on the membrane to exclude air bubbles, and a piece of gel-sized 3MM paper, pre-soaked in transfer solution, laid on top. The whole assembly was transferred onto four pieces of dry 3MM paper which sat upon a 3 to 5 cm high stack of paper towels, and the gel was surrounded by strips of laboratory sealing film (Whatman) to ensure that all capillary movement of the transfer solution would pass through the gel. Two more pieces of gel-sized 3MM paper pre-soaked in transfer solution were placed on top of the assembly and a wick constructed from 4 strips of 3MM paper presoaked in transfer solution. The whole construction was then covered in clingfilm to prevent evaporation of transfer solution from the wick and transfer occurred overnight. Upon completion of transfer, the apparatus was dismantled, the membrane immediately placed, DNA side up, upon 3MM paper soaked in 0.4 M NaOH and the membrane left for 20 min. The membrane was then neutralised in 5 X SSPE for 5 min, dried at 70°C for 10 min, and sealed in a plastic bag at 4°C until required.

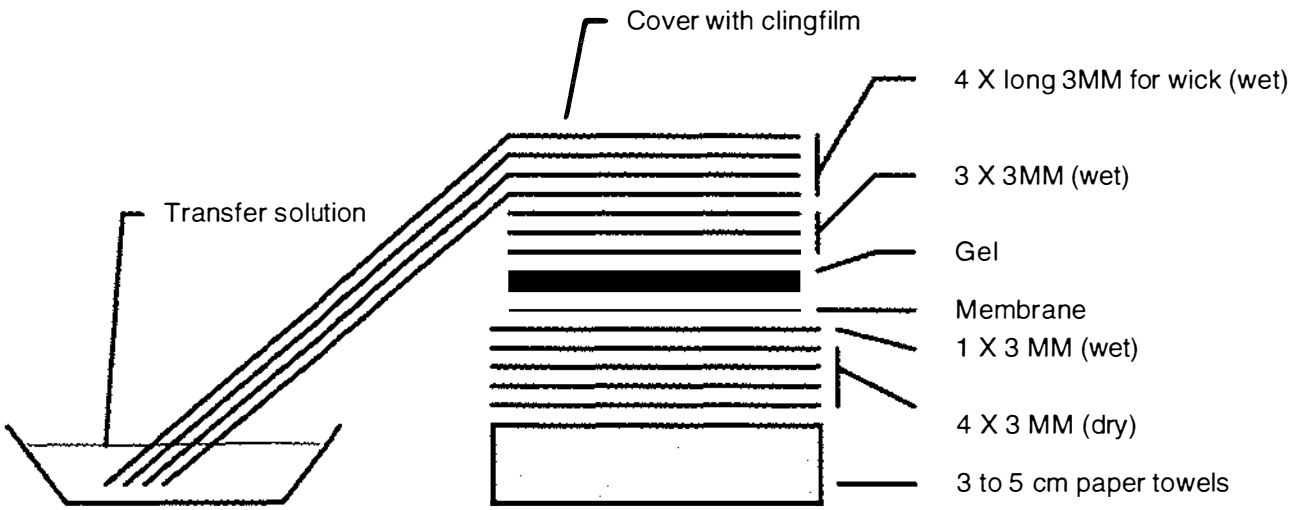

Figure 8 Arrangement of the apparatus used to transfer DNA and RNA samples to Hybond-N$^+$ membranes

2.3.4.5 Southern (capillary) blotting of cDNA fragments

Reagents:

- Transfer solution: (0.4 M NaOH, 1.5 M NaCl)
- Neutralisation solution: (0.1 M $Na_2PO_4.2H_2O$, pH 7.2)

Aliquots (50 ng) of DNA fragments generated by the polymerase chain reaction or restriction digestion of plasmids were transferred to Hybond-N$^+$ by the downward alkaline capillary transfer method of Chomczynski (1992) as described for Southern blotting (section 2.3.4.4), except the gel was not depurinated or denatured before transfer, and the transfer was carried out in 0.4 M NaOH and 1.5 M NaCl for 4 h. After transfer, the membrane was incubated for 10 min in neutralisation solution and stored moist at 4°C until required.

2.3.4.6 Labelling Probe DNA for use in Southern and northern analysis

2.3.4.6.1 Labelling DNA with the Ready-To-Go™ [α-^{32}P]-dCTP DNA Labelling Kit

Reagents:

- Ready-To-Go™ DNA Labelling Kit (Pharmacia Biotech)
- TE: (10 mM Tris-HCl, pH 8.0, 0.1 mM EDTA)
- [α-^{32}P]-dCTP (Amersham)

DNA was labelled with [α-^{32}P]-dCTP using the Ready-To-Go™ DNA Labelling Kit. An aliquot of DNA (25-50 ng) was diluted with either sterile water or TE, denatured in a boiling water bath for 2 to 3 min and then immediately chilled on ice for 2 min. The denatured DNA was collected at the bottom of the tube by pulse centrifugation and added to the Ready-To-Go reagent bead. After gently resuspending the bead with the DNA, 5µL of [α-^{32}P]-dCTP (3 000 Ci/ mmol) was added and the labelling reaction allowed to proceed either at room temperature or 37°C for 15 min. During this time, the ProbeQuant™ Sephadex G-50 Micro Column (Pharmacia Biotech) was prepared. This involved vortexing the column to resuspend the Sephadex, loosening the lid, snapping off the bottom closure and centrifugation of the column in a microfuge tube at 735 x g for 1 min to remove the void volume. The column was then transferred to a new microfuge tube in readiness for sample application. After completion of the labelling reaction, the sample was carefully layered onto the Sephadex and the sample purified away from unincorporated nucleotides, reaction dyes and salts by centrifugation at 735 x g for 2 min. The labelled DNA collected at the bottom of the microfuge tube was then denatured in a boiling water bath for 2 min, quick-chilled on ice for 2 min and added directly to the hybridisation solution (pre-equilibrated at 65°C) bathing the membrane (section 2.3.4.7).

2.3.4.6.2 Labelling DNA with the Megaprime™ [α-^{32}P]-dATP DNA Labelling Kit

Reagents:

- Megaprime™ DNA Labelling Kit (Amersham)
- [α-^{32}P]-dATP (Amersham)
- 0.2 M EDTA, pH 8.0
- Reaction buffer: (supplied in kit)

DNA was labelled with [α-^{32}P]-dATP using the Megaprime™ DNA Labelling Kit. DNA was first diluted to a concentration of *ca.* 5 ng μL^{-1}, and 5 μL of this diluted DNA combined with 5 μL of nonamer primers. The DNA was then denatured in a boiling water bath for 3 min, the contents collected by a brief centrifugation and 4μL each of the unlabelled nucleotides (dGTP, dCTP and dTTP) added. The labelling reaction was initiated with 5 μL of [α-^{32}P]-dATP (specific activity 3 000 Ci/ mmol) after the addition of 5 μL of reaction buffer, 17 μL of sterile water, and 2 μL of enzyme. The reaction was continued at 37°C for 15 min, then stopped by the addition of 5 μL 0.2 M EDTA, pH 8.0, after which the radiolabelled DNA was purified through a ProbeQuant Sephadex G-50 Micro Column as described in section 2.3.3.7.1. The radiolabelled DNA was then denatured for 3 min in a boiling water bath, cooled on ice for 2 min and either 25 or 50 μL of the labelled DNA added directly to the hybridisation solution (pre-equilibrated at 65°C) bathing the membrane (section 2.3.4.7).

2.3.4.7 Hybridisation and washing of DNA and RNA blots

Reagents:

- Church hybridisation solution: (0.25 M $Na_2PO_4.2H_2O$, pH 7.2, 7 % (w/v) SDS, 1 % (w/v) BSA fraction V, 1 mM EDTA, pH 8.0)
- Hybridisation wash solution 1.: (20 mM $Na_2PO4._2H_2O$, pH 7.2, 5 % (w/v) SDS, 0.5 % (w/v) BSA fraction V, 1 mM EDTA, pH 8.0)
- 20 X SSPE: (0.2 M NaH_2PO_4 'pH 6.5, 3.6M NaCl, 20 mM EDTA).
- 2 X SSPE wash: (2 X SSPE pH 6.5, 0.1% (w/v) SDS).
- 1 X SSPE wash: (1 X SSPE pH 6.5, 0.1% (w/v) SDS)
- 0.2 X SSPE wash: (0.2 X SSPE pH 6.5, 0.1% (w/v) SDS).
- 0.1 X SSPE wash: (0.1 X SSPE pH 6.5, 0.1% (w/v) SDS)

Labelling and washing of Hybond-N$^+$ membranes was performed essentially as described by Church and Gilbert (1984). The membrane was rolled up, nucleic acid facing inwards, and placed inside a Hybaid™ screw top glass tube (Hybaid Ltd., Teddington, Middlesex, UK), then rinsed with RO water, and bathed with 25 mL of Church hybridisation solution in a rotary oven at 65°C. The denatured labelled DNA probe, prepared as described in sections 2.3.4.6, was then added to the hybridisation solution bathing the membrane and hybridisation allowed to occur overnight at 65°C. The membrane then underwent a series of washes at 65°C. The first was for 20 min in *ca.* 100 mL of hybridisation wash solution

1. This was followed by 20 min in 2 X SSPE wash, 20 min in 1 X SSPE wash, 20 min in 0.2 X SSPE wash and finally 30 to 60 min in the 0.1 X SSPE wash. The membrane was then wrapped in clingfilm, or heat-sealed in a plastic bag, and placed in a X-OMATIC cassette (Eastman Kodak Company, Rochester, NY, USA) containing a single X-OMATIC intensifying screen and XAR-5 X-ray film (Kodak). After exposure for a suitable period of time at -70°C , the film was developed in the dark by incubation for 5 min in developer solution (HC110, Kodak), then rinsed briefly with water and fixed for 1 to 2 min in a fixative solution (Rapid Fixer Solution A, Kodak).

2.3.4.8 Stripping Southern and northern blots

Reagents:

- Stripping solution: (0.1 X SSPE, 0.1 % (w/v) SDS)
- 0.1 X SSPE

Blots were stripped according to the method of Memelink *et al.,* (1994). Stripping solution was boiled for *ca.* 5 min in a gas pressure cooker with the pressure cap removed and the solution poured onto the membrane and allowed to cool to room temperature. This procedure was repeated (typically twice) until counts were low. The membranes were given a final rinse in 0.1 X SSPE to remove the SDS.

2.3.5 RNA Isolation

RNA is tolerant of a variety of solvent, salt and temperature conditions. It is highly resistant to shear and can be vortex-mixed without detriment (Strommer *et al.,* 1993). The major concern of working with RNA is the presence of contaminating ribonucleases, both endogenous (mainly located in vacuoles) and in the environment, which can be difficult to eliminate or inactivate.

In this study, endogenous ribonucleases were inactivated during extraction by the use of an extraction buffer with high pH, and the inclusion of a chelating agent, a detergent, and organic solvents.

Care was taken to avoid the introduction of ribonucleases from external sources such as hands and dust. Disposable gloves were always used and regularly changed. Unless otherwise stated, solutions were made from analytical grade chemicals that were reserved for RNA use only. Chemicals were dispensed by pouring or by using spatulas that had

been baked at 180 °C for a minimum of 4 h. Only new sterile plasticware or glassware that had been baked at 180°C for at least 4 h were used for storing solutions for RNA, and water used for making the solutions was obtained directly from the Milli-Q water source. If pH adjustment of a solution was necessary, the pH electrode was incubated in 50 mM NaOH for 10 to 15 min and rinsed with sterile water. Any gel apparatus used was sterilized with 0.1 M NaOH for a minimum of 20 min.

2.3.5.1 Isolation of total RNA

Reagents:

- Extraction buffer: (100 mM Tris-HCl, pH 8.0, 100 mM LiCl, 10 mM EDTA, 1% (w/v) SDS)
- Tris-buffered phenol: (6 mL of 1 M Tris-HCl, pH 8.0, 7.5 mL of 2M NaOH, 130 mL of H_2O, 500 g of commercial phenol crystals)
- Extraction buffer/ phenol: (extraction buffer: Tris-buffered phenol [1:1])

Extraction of RNA was accomplished essentially by scaling up the procedure described by Van Slogteren *et al.* (1983). Aliquots (1 to 4 g) of powdered leaf material was extracted in five volumes of extraction buffer/ phenol, pre-equilibrated at 80°C, in a fume hood. The extraction mix was vortexed for 30 s, 2.5 volumes of chloroform: isoamyl alcohol (24:1) added and the vortexing repeated. The extraction mix was then incubated at 50°C for 15 min and the cellular debris and denatured proteins pelleted by centrifugation at 4 000 x g for 30 min at 4°C. The aqueous supernatant was transferred to a fresh tube, the RNA precipitated at 4°C overnight by the addition of an equal volume of ice cold 4 M LiCl, and the precipitate pelleted by centrifugation at 4 000 x g for 45 min at 4°C. The pellet was resuspended in sterile water, an equal volume of chloroform: isoamyl alcohol (24:1) added, the aqueous and organic phases mixed by vortexing and then separated by centrifugation at 20 800 x g for 3 min at room temperature. The aqueous phase was removed to a new tube and the RNA precipitated with ethanol (section 2.3.2.3), resuspended in a small volume of sterile water, quantified (section 2.3.5.3) and stored at -80°C until required.. For 1 g extractions this was typically 40 µL , and for 4 g extractions 250 µL. For long term storage, RNA was stored at -80°C as an ethanol precipitate.

Notes:

- The final chloroform step added to this method was especially important for large extractions as it improved final dissolution of the RNA pellet.

- If the RNA pellet was hard to dissolve, it was heated at 65°C for 10 min

2.3.5.2 Isolation of poly (A)+ RNA

Reagents:

- PolyATtract mRNA Isolation System IV Kit (Promega)
- 20 X SSC, pH 7.0 (supplied in kit): (17.53 % (w/v) NaCl, 8.82 % (w/v) sodium citrate)

Poly $(A)^+$ mRNA was purified from total RNA using biotinylated oligo(dT) bound to Streptavidin MagneSphere™ particles, following the protocol supplied with the PolyATtract mRNA Isolation System IV Kit.

Total RNA (100 to 1000 µg: section) was made to a volume of 500 µL with sterile water in a microfuge tube and the solution heated at 65°C for 10 min to denature the RNA. An aliquot of the biotinylated 17 mer oligo (dT) primer (dT) oligonucleotide (3µL) and 13 µL of 20 X SSC was added and mixed, and the solution incubated at room temperature for 10 min. The Streptavidin MagneSphere® Particles (SA-PMPs) were resuspended by flicking the bottom of the tube, and then captured on a magnetic stand. The preservative solution was carefully removed, and the SA-PMPs washed 3 times with 300 µL of 0.5 X SSC by first resuspending the particles and then capturing them on the magnetic stand. Following the third wash, the SA-PMPs were resuspended in 100 µL of 0.5 X SSC, and the entire contents of the RNA/ oligo (dT) annealing reaction added. The reaction was incubated at room temperature for 10 min to allow binding between the biotin and streptavidin components, the SA-PMPs captured on the magnetic stand and the supernatant removed. The SA-PMPs were washed 4 times by resuspending them in 300 µL of 0.1 X SSC, capturing the particles on the magnetic stand, and removing the supernatant. On the last wash, care was taken to remove as much of the supernatant as possible.

The poly (A)+ RNA was recovered by resuspending the SA-PMPs in 100 µL of sterile water, incubating for 5 min at room temperature, and capturing the particles with the magnetic stand. The supernatant was transferred to a fresh microfuge tube. The SA-PMPs were again resuspended in 150 µL sterile water, incubated for 5 min and the particles captured with the magnetic stand. The supernatant was removed, added to the first supernatant and the RNA quantified (section 2.3.5.3), snap-frozen in liquid air and stored at -80 until required.

2.3.5.3 RNA Quantitation

To measure total RNA concentration, the procedure as described for DNA (section) was used. For RNA, an OD_{260} of 1.0 corresponds to approximately 40 μg mL^{-1} (Sambrook *et al.*, 1989).

$A_{260\,nm}$ X dilution factor X 40 = conc. RNA in μg/ mL

Poly $(A)^+$ mRNA was quantified in a 250 μL volume, 1 cm light path, quartz cuvette that had been incubated with concentrated HCl for 15 min. Initially 50 mM NaOH was used to denature the RNases, but was discontinued as NaOH can etch the face of glass and quartz cuvettes (Dr. Christine Voisey, AgResearch, Grasslands, Palmerston North, NZ, *pers. comm.*). After incubating with concentrated HCl, the cuvette was rinsed with copious volumes of sterile water and the samples measured. The cuvette was rinsed three times with sterile water in between sample measurements.

The purity of the RNA was determined as for DNA by measuring the A_{260nm}/A_{280nm} ratio. Relatively pure solutions of RNA have an A_{260nm}/A_{280nm} ratio of 2.0, a value that decreases with the presence of contaminants such as proteins and phenol.

2.3.6 Amplification of DNA by RT-PCR

2.3.6.1 Reverse Transcriptase Synthesis of cDNA

Reagents:

- GIBCO BRL Superscript™ II RNase H- Reverse Transcriptase (200 U μL^{-1}) (Life Technologies)
- Gibco BRL 5 X first strand buffer: (supplied with Superscript)
- 0.1 M DTT (supplied with Superscript)
- GIBCO BRL cloned Ribonuclease Inhibitor (10 U μL^{-1}) (Life Technologies)
- Gibco BRL 10 mM dNTP mix (10 mM each dATP, dGTP, dCTP and dTTP at neutral pH) (Life Technologies)

First strand copy DNA (cDNA) synthesis was performed using GIBCO BRL Superscript™ II RNase H- Reverse Transcriptase. Five μL (5μg) of total RNA was denatured with 0.5 μL (500 ng) of 17 mer oligo (dT) primer in a microfuge tube at 80 °C for 5 min and the contents collected by centrifugation at 20 800 x g for 5 min at room temperature. Two μL of 0.1 M DTT, 4 μL of 5 X first strand buffer, 1 μL of 10 mM dNTP mix, 2 μL of ribonuclease inhibitor and 1 μL of reverse transcriptase were then added to the RNA/

primer mix and the volume made to 20 µL with sterile water. The contents were then carefully mixed and incubated at 42 °C for 1.5 h, after which the mix was diluted 1:4 with sterile water and heated at 70°C for 10 min to denature the enzyme.

For 3'-RACE, 5 µL of a 10 µM stock of the oligonucleotide primer ADAPdT (Fig) replaced the 500 ng 17 mer oligo (dT) primer. ADAPdT (Figure 9) was used instead of the 17 mer oligo (dT) primer when gene specific primers were used for 3'-RACE, as at the higher temperatures used for PCR, multiple T residues serve as a poor primer (Frohman *et al.*, 1988).

5'-GTGGATCCTACTGCAGCTAATTTTTTTTTTTTTTTT-3'
BamH I *Pst I*

Figure 9. Sequence of the ADAPdT primer

2.3.6.2 PCR amplification of DNA

2.3.6.2.1 Primers

GIBCO BRL primers (Life Technologies Inc.) were dissolved in sterile water at a concentration of 100 µM and stored at -20°C. A working stock was prepared by dissolving one part primer to two parts water which gave a concentration of 33 µM. Typically 1 µL of primer was used per 100 µL volume of PCR mix to give a final concentration of 330 nM.

2.3.6.2.2 Degenerate primers used in RT-PCR

Nested degenerate oligonucleotide primers known to bound a highly conserved region amongst ACC oxidase genes were provided by Professor S.F. Yang (University of California, Davis, USA). The sequence of each primer is given in Figure 10.

ACOF1: First round forward primer (Shifted by 3 nucleotides in 5' direction for E101)

```
                                  Q
                                  H
Amino acids        D    A    C    E    N    W    G
5' GTGAATTC GAY GCN TGY SAN AAY TGG GG 3'
     EcoR1         2    4    2 2  4    2          ←—— Degeneracy = 256 X
```

ACOR1: First round reverse primer (Shifted by 12 nucleotides in 3' direction for E102)

```
5' TCG TCT AGA TC RAA NCK MGG YTC YTT 3'
     Xba I         2    4    4    2    2    2    ←—— Degeneracy = 256 X
```

E101: Second round forward primer

```
                       Q
                  A    C    E    N    W    G    F
5' GTGAATTC GCN TGY GAR AAY TGG GGH TT 3'
     EcoR1        4    2    2    2              3  ←—— Degeneracy = 96 X
```

E102: Second round reverse primer

```
5' TCG TCT AGA GYT CYT TNG CYT GRA AYT T 3'
     Xba I        2    2    4    2    2    2    ←—— Degeneracy = 256X
```

Where: R= A,G; H= A,C,T; W= A,T; D= A,G,T; Y= C,T; S= C,G; N= A,C,G,T; M=A,C

Figure 10. Sequence of the primers used in RT-PCR to amplify putative ACC oxidase sequences.

2.3.6.2.3 Primers used for in-frame cloning into the pPROEX™-1 vector

The GIBCO BRL pPROEX ™-1 protein expression system was used to translate foreign gene sequences in *E. coli* (section 2.2.10). This requires that the cDNA template be inserted in the correct orientation and in-frame into the pPROEX plasmid vector. To accomplish this, new primers (Figure 11) were designed by Dr. Michael T. McManus and used in PCR with a plasmid cDNA template to generate sequences that contained a different restriction site at their 5' and 3'ends. These two restriction sites could then be used to directionally clone the DNA fragment into the multiple cloning site of the pPROEX vector. The primers were also designed (where necessary) to contain spacer nucleotides between the coding frame portion of the primer and the restriction site so that the when inserted into pPROEX the sequence would be in-frame. Another important aspect of primer design was the requirement for additional nucleotides to cap the restriction site. This was necessary because restriction enzymes cut very poorly at the ends of DNA fragments (New England Biolabs Catalogue, 1993). For instance, *Eco*R1 requires the addition of a single nucleotide to cap the restriction site for the enzyme to cut, while *Hin*d III will not cut unless there is a minimum of three nucleotides capping its restriction site.

ACOFE: E101 derivative (first round forward primer)

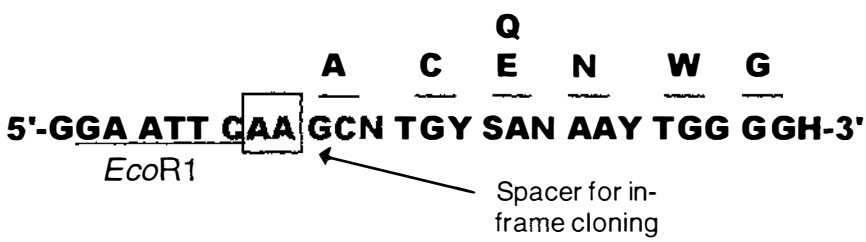

ACORH: E102 derivative (first round reverse primer)

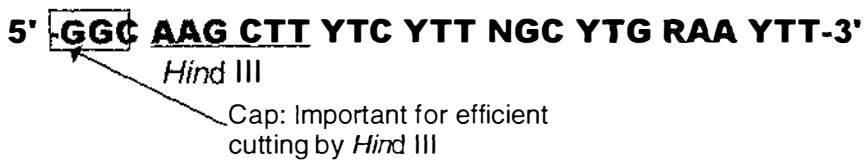

Figure 11. Primers used for amplification of sequences for directional in-frame cloning into the pProEX vector.

2.3.6.2.4 Primers used for 3'-RACE

Primers used in 3'-RACE were identified using the Primer 2, Primer Designer programme (Scientific and Educational Software) together with the following criteria: (i.) The 3'-end of the primer should be unique in the sequence to eliminate the chance of secondary priming, and (ii.) The 3'-end should be somewhat unstable, finishing in A's and T's, which effectively prevents false priming as well as broadening the optimal annealing temperature (Rychlik, 1993). The primers used in 3'-RACE are given in Figure 12.

ACOF2: First round forward primer

(Primer designed to region common to both TR-ACO1 and 2)

5' -GGTGACCAGCTCGAGGTAAT-3'

ACOF4: First round forward primer

(Primer designed to region specific to TR-ACO1)

5' -GTTATCTATCCAGCAACAAC-3'

ACOF4^{A} : second round forward primer (shifted 5 residues at 5' end of ACOF4)

(Primer designed to region specific to TR-ACO1)

5' -CTATCCAGCAACAACATTGA-3'

ACOF4B : (First round forward primer)

(Primer designed to generate the 3'-UTR TR-ACO2 probe)

5' -CTTGGTTCAATTGCAACAGT-3'

ACOF2B : (First round forward primer)

(Primer designed to generate the 3'-UTR TR-ACO1 probe)

5' -CAAGCTAAGGAACCAAGAT-3'

ADAP: reverse primer

5' -GTGGATCCTACTGCAGCTAA-3'

Bam HI *Pst* I

Figure 12. Primers used in 3'-RACE

2.3.6.2.5 PCR conditions

Reagents:

- Expand™ High Fidelity system (Boehringer Mannheim, GmbH, Mannheim, Germany)
- 10 X PCR buffer (supplied with Expand)
- Gibco BRL 10 mM dNTP mix (10 mM each dATP, dGTP, dCTP and dTTP at neutral pH)

PCR was performed in 100 µL volumes using the Expand High Fidelity system as described by the manufacturer. Two separate master mixes were prepared on ice. Master Mix 1 consisted of 2 µL of 10 mM dNTP mix, 1 µL of 33 µM upstream primer, 1 µL of 33 µM downstream primer, DNA template (see below) and sterile water to 50 µL. Master Mix 2 consisted of 1 µL of Expand High Fidelity enzyme mix, 10 µL of 10 X PCR buffer with 15 mM $MgCl_2$ and sterile water to 50 µL. The two mixes were combined, placed into a PTC-200 Peltier Thermal Cycler and the PCR carried out for thirty cycles, each consisting of 1 min at 92°C (denaturation), 1 min at 42°C* (annealing), and 1 min 40s at 72°C (extension) with a final extension time of 10 min at 72°C.

The DNA template used in PCR was either (i.) 10 µL of the diluted (1:4) first strand cDNA template produced in section, (ii.) 1 µL of spin-column purified (section 2.3.2.8.1) plasmid. (iii.) 2 µL of first round amplification mix.

*The temperature of annealing was raised from 42°C to 50 °C for plasmid templates and raised to 55°C for amplification with gene-specific-primers used 3'-RACE procedure.

2.3.7 Northern Analysis Procedures

2.3.7.1 Electrophoresis of RNA

Reagents:

- 37 % (v/v) formaldehyde
- 10 X MSE: (200 mM MOPS, 50 mM NaOAc, 10 mM EDTA)
- Gibco BRL UltraPURE™ Agarose
- Running buffer: (0.22 M formaldehyde in 1 X MSE)
- Formamide/BB/XC: (0.01 % (w/v) bromophenol blue, 0.01 % (w/v) xylene cyanol in formamide)
- Loading buffer: (For 1 mL: Dissolve 625 µL formamide/BB/XC stock, 212.5 µL of formaldehyde, 125 µL MSE, and 5 µL ethidium bromide. Use at minimum ratio of 2 (Load buffer):1 (RNA)

- Gibco BRL 0.24 to 9.5 Kb RNA Ladder (Life Technologies)

Total and Poly $(A)^+$ RNA were resolved by formaldehyde agarose gel electrophoresis in a Bio-Rad DNA Sub Cell™ (225 cm^2 gel bed; 100 mL volume). The 1 % (w/v) agarose gel solution was made by adding 95 mL of 1 X MSE to 1 g of agarose. The weight of the flask and contents noted, the gel mix heated to dissolve the agarose, the flask reweighed and any water that had evaporated replaced. The gel solution was then cooled to *ca.* 55°C in a water bath, taken to a fume hood and 5 mL of 37 % (v/v) formaldehyde added and the solution poured into the gel forming apparatus. After the gel had set, running buffer was added to the gel apparatus and the RNA samples loaded.

Typically 40 µg of total RNA or 1 to 1.5 µg of Poly $(A)^+$ RNA was loaded into each gel well. If the concentration of RNA in a sample was too dilute, it was concentrated by aliquotting the required amount of RNA into a microfuge tube, snap-freezing in liquid air and lyophilising in a SpeedVac to a volume of 10 µL or less. Twenty µL of RNA loading buffer was then added to each sample of RNA, including the GIBCO BRL 0.24 - 9.5 Kb RNA Ladder (Life Technologies), the RNA denatured at 65°C for 15 min, cooled on ice for 2 min, and then loaded into the wells.

Electrophoresis was conducted at 80 V for 5 h, after which the gels were visualized using a short-wave (340 nm) UV transilluminator, the distance the molecular weight markers migrated marked and the gels photographed either digitally with an Alpha Imager 2000 Documentation and Analysis System or by with a Polaroid Land Camera using Polaroid 667 film. The RNA was then transferred to a Hybond-N^+ membrane either for 4 h in alkaline conditions (section 2.3.7.2) or overnight in 10 X SSPE (section 2.3.7.3).

2.3.7.2 Northern (capillary) blotting by downward alkaline transfer

Reagents:

- Neutralisation solution: (0.1 M $Na_2PO_4.2H_2O$, pH 7.2)
- Transfer solution (pH 11.4-11.45): (3 M NaCl, 8 mM NaOH)

RNA was transferred to a Hybond-N^+ membrane by the downward alkaline capillary method of Chomczynski (1992) as described for Southern blotting of genomic DNA (section 2.3.4.4), except there was no pretreatment of the gel in depurination or

denaturation solutions, transfer was carried out for no longer than 4 h, the membrane was incubated in neutralisation solution for 10 min, and stored moist at 4°C until required.

2.3.7.3 Northern (capillary) blotting by downward SSPE transfer

Reagents:

- 10 X SSPE: (0.1 M NaH_2PO_4, pH 7.7, 1.8 M NaCl, 10 mM EDTA).

RNA was also transferred to Hybond-N^+ using the method described in section 2.3.4.4, except the transfer solution was changed to 10 X SSPE pH 7.7 and the transfer time extended from 4 h to overnight. After transfer, the membrane was immediately placed DNA side up on 3MM paper and UV cross-linked using the autocross-link function of a UV Stratalinker. The membrane was then stored dry until required.

3. RESULTS

3.1 Stolon growth of white clover

Plants of white clover (genotype 10F, cv. Grasslands Challenge) grown by the method of Butcher (1997) (section 2.1.3.2), produced stolons that, at harvest time, possessed leaf tissue representing all stages of development from leaf initiation, through maturation to senescence (Figure 13A). In the current study, leaves at nodes 1 to 16 (designated leaves 1 to 16) were used for analysis. Leaf 1 represents the first apical leaf whose leaflets remain folded but which is clearly separated from the apex by a horizontal petiole, while leaf 16 represents the most chlorotic leaf examined.

The growing method used produced a highly reproducible pattern of leaf development along the stolon. This is indicated by the consistent change in fresh weight found for leaves along the stolon in two independent harvests (Figure 14A and B). The weights of the newly initiated leaves were low (leaf 1, *ca.* 0.05 g) but increased to between 0.35 to 0.38 g at leaves 6 to 7. The weights of leaves 7 to 10 remained similar (between 0.35 and 0.38 g). In leaves 11 to 14, the fresh weight of the tissue increased further to 0.42 to 0.45 g, before declining again at leaves 15 and 16 .

3.2 Chlorophyll content of leaf tissue during leaf initiation, maturation and senescence of white clover

In this study, the onset of leaf senescence was determined both visually (initial yellowing at leaf margins) and, more accurately, by quantification of chlorophyll loss (section 2.2.2) since chlorosis is thought to be an early event in the senescence syndrome (Thomas and Stoddard, 1980). Changes in leaf chlorophyll content of a typical harvest are presented in Figure 13B. Chlorophyll concentration increased as newly initiated tissue unfolded and expanded, from 877 $\mu g\ g^{-1}$ FW at leaf 1 to a plateau of between 1590 to 1650 $\mu g\ g^{-1}$ FW at leaves 4 to 8 (designated the mature green stage). Typically leaves 9 to 11 were the first to display visual signs of chlorosis (yellowing at leaf margins), designated in this study as the onset of the senescence stage. The chlorophyll concentration of the tissue then declined further as the tissue aged (leaves 12 to 16; designated the senescent stage) to a level of *ca.* 400 $\mu g\ g^{-1}$ FW.

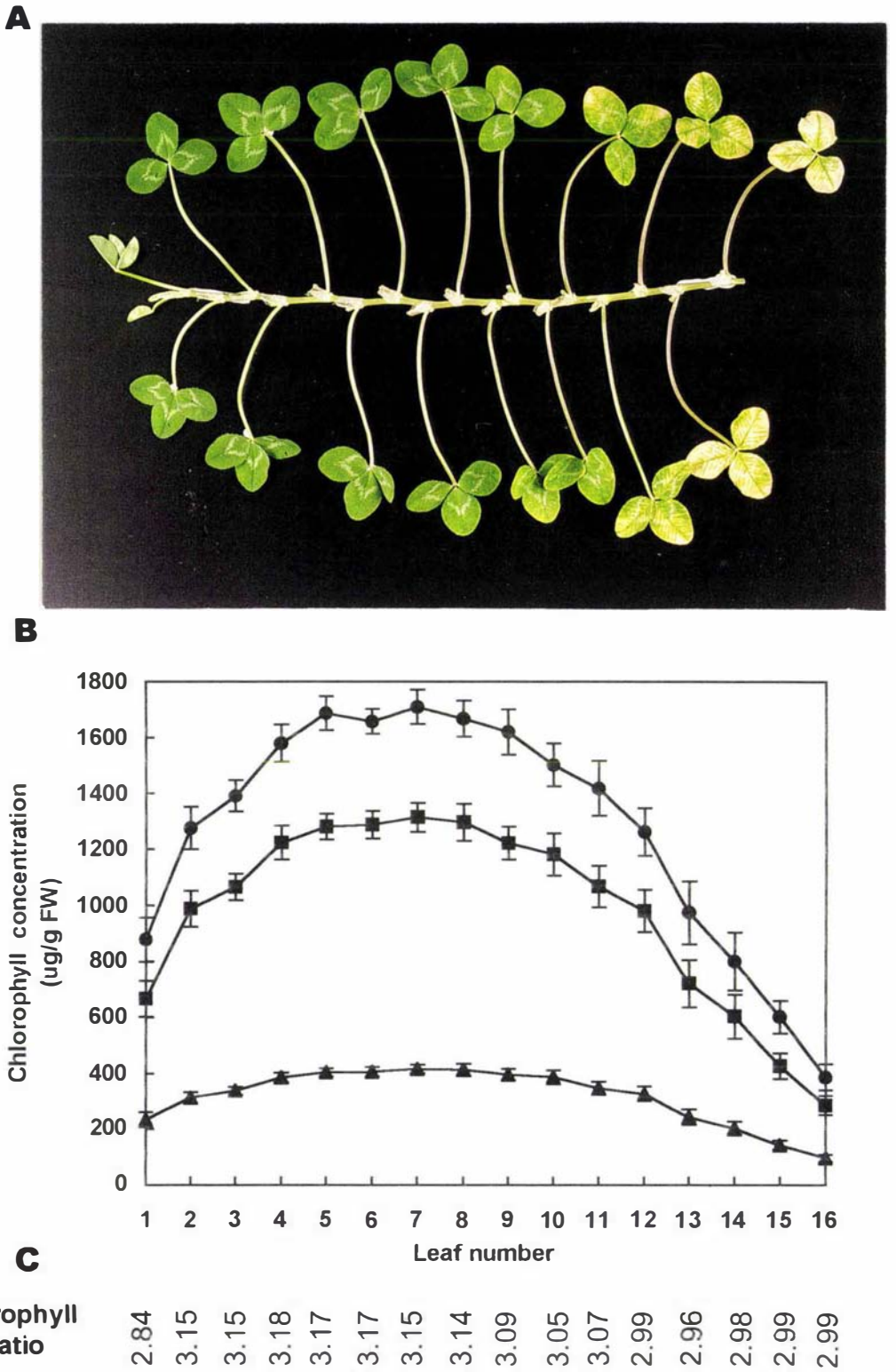

Figure 13. Chlorophyll concentration as an indicator of senescence

A. An individual stolon containing leaf tissue at various stages of development and senescence.
B. Chlorophyll concentration of the leaves.
C. Ratio of chlorophyll a:b.

Where indicated the error bars are ± 1 sem from leaves of 12 independent stolons.
(--●--) Total chlorophyll (--■--) Chlorophyll *a* (--▲--) Chlorophyll *b*

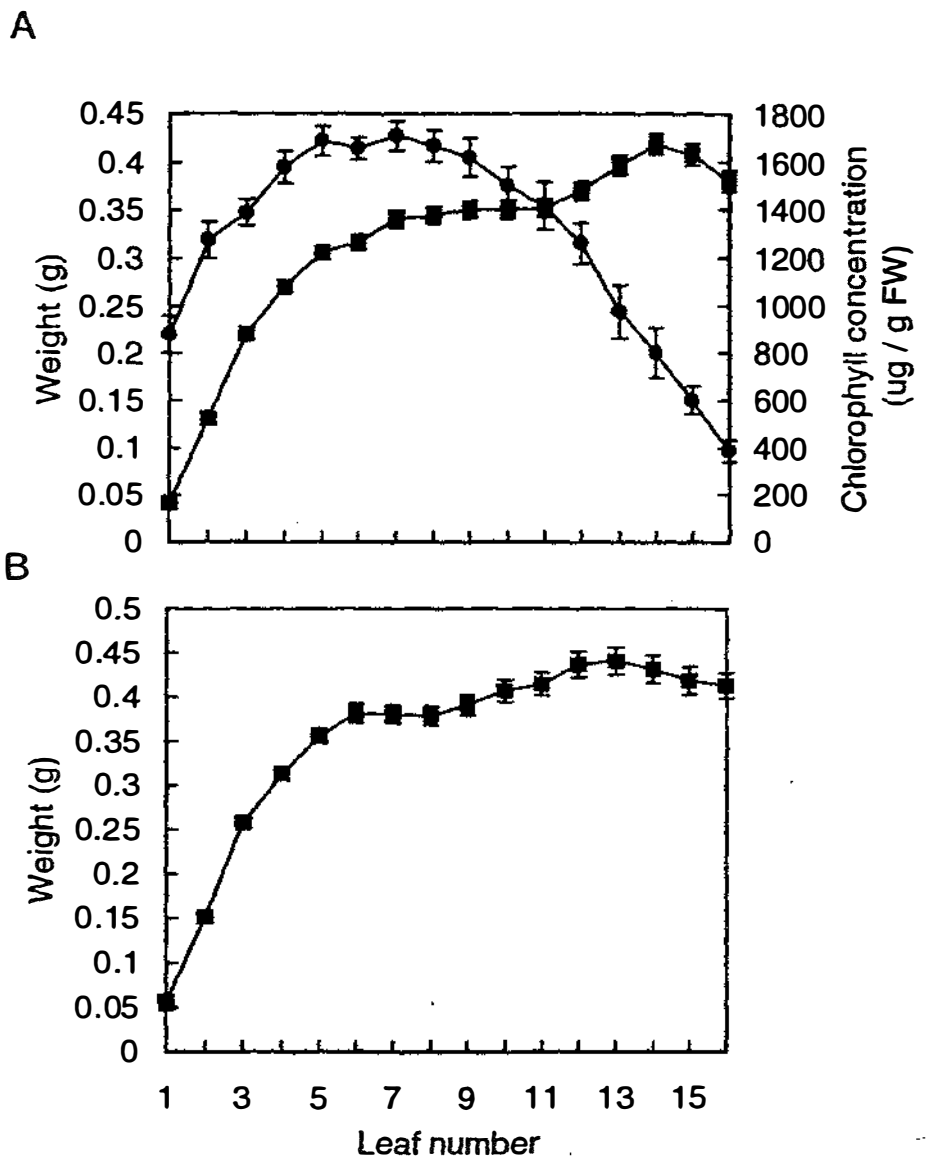

Figure 14. Fresh weights of leaves of white clover during leaf ontogeny.

A. (--■--) Fresh weight of leaf tissue harvested in November 1995 (Greenhouse 9).
Error bars = ± 1 sem for leaves of 97 stolons.
(--●--) Chlorophyll concentration of leaves of this harvest.
Error bars = ± 1 sem for leaves of 12 stolons.

B. (--■--) Fresh weight of leaf tissue harvested in December 1995 (Greenhouse 8).
Error bars = ± 1 sem for leaves of 93 stolons.

Partitioning of total chlorophyll into its two components *a* and *b* showed that approximately 75 % of the chlorophyll being measured was chlorophyll *a* and 25 % chlorophyll *b* (Figure 13B). As the tissue aged, chlorophyll *a* was degraded slightly faster than chlorophyll b indicated by a consistent but slight decrease in the ratio of chlorophyll *a*:*b* from 3.18 at leaf 4 to 2.99 at leaf 16 (Figure 13C). A preferential loss of chlorophyll *a* in senescing (yellowing) leaf tissue has been reported in a study of 25 deciduous plants (Wolf, 1956, cited in Butcher, 1997), but not for the monocots *Lolium temulentum* (Thomas, 1990) or wheat (Ferguson *et al.,* 1993) where chlorophyll *b* is preferentially degraded.

3.3 Changes in evolved ethylene during leaf initiation, maturation and senescence of white clover

Ethylene evolution of attached leaves of white clover was measured (section 2.2.5.1) and found to be highest both in newly initiated and chlorotic leaf tissue (Figure 15). The newly initiated tissue evolved ethylene at 0.7 nL g^{-1} FW h^{-1}. Ethylene evolution then declined, as the leaves increased in fresh weight from *ca.* 0.14 to 0.3 g (leaves 2 to 4), to a low basal level of *ca.* 0.25 nL g^{-1} FW h^{-1} at the mature green stage (leaves 4 to 9). The second increase in ethylene evolution of leaves 11 to 16 was observed after chlorophyll levels had begun to decline (leaf 10), so that by leaf 16, ethylene levels being evolved were *ca.*7-fold greater (2.05 nL g^{-1} FW h^{-1}) than that from mature green tissue. These values are consistent with those reported by Butcher (1997)

3.4 Changes in ACC content during leaf initiation, maturation and senescence of white clover

ACC levels remained comparatively low (30 to 45 pmol g^{-1} FW) in newly initiated and mature green leaf tissue (leaves 1 to 8) (Figure 16). At leaf 9, (designated the onset of chlorosis by visual analysis), the level of ACC in the leaf tissue began to increase, and this increase continued so that by leaf 16, the level of ACC measured was 1590 pmol g^{-1} FW. The increase in ACC levels was co-incident with the rise in measured ethylene evolution.

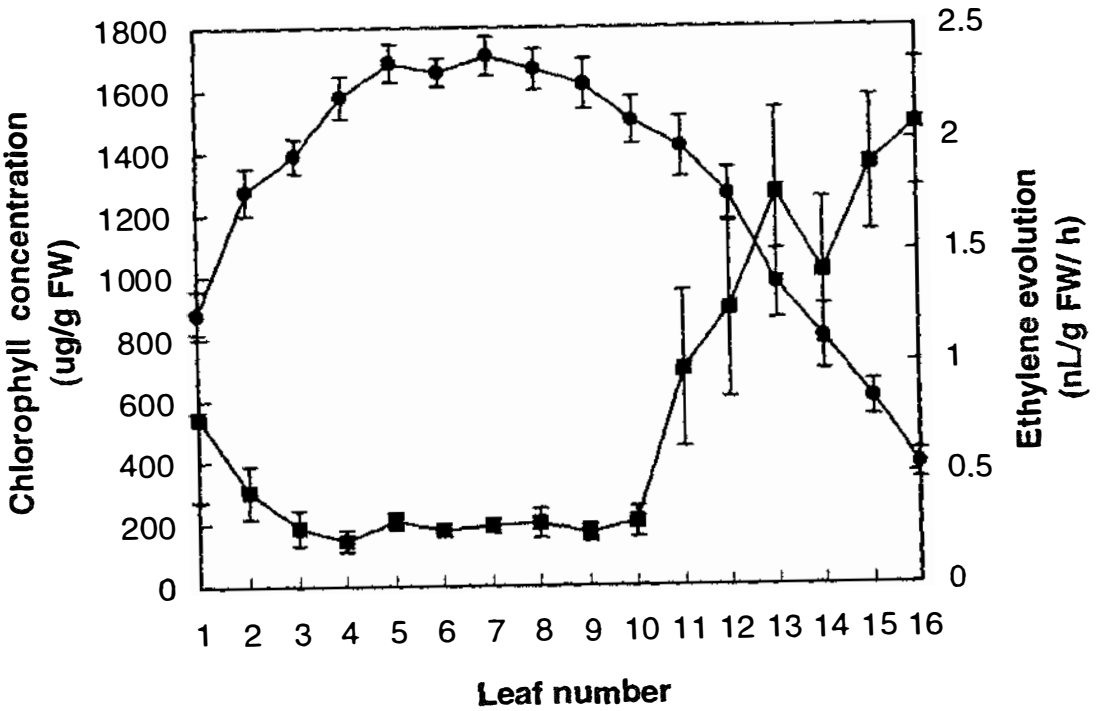

Figure 15. Ethylene evolution and chlorophyll content in leaves at nodes 1 to 16.

(--■--) Ethylene evolution from individual attached leaves.
Error bars = ± 1 sem for leaves of 6 stolons.
(--●--) Total chlorophyll of leaves used for ethylene evolution.
Error bars = ± 1 sem for leaves of 12 stolons.

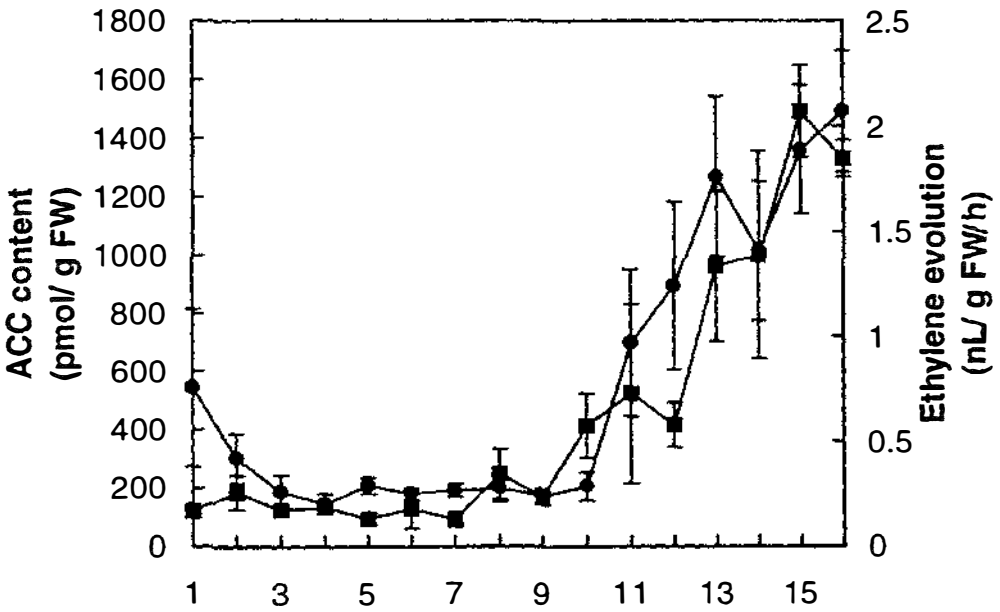

Figure 16. ACC content, and ethylene evolution during leaf ontogeny

(--■--) ACC content.
Error bars = ± 1 sem for 3 independent experiments.
(--●--) Ethylene evolution from leaves.
Error bars = ± 1 sem for leaves of 6 stolons.

ACC was measured by a method that relies on the chemical conversion of ethanolic-extracted ACC to ethylene (Lizada and Yang, 1979). Since the publication of the Lizada and Yang method, further studies have shown that the assay is subject to interference by phenolics (Sitrit, 1988), mono and dialkyl amines (Nieder, *et al.*, 1986), ethanol and other unidentified substances (Bufler and Mor, 1980). Using a paper chromatographic method, Bufler and Mor reported that unidentified compound(s) in senescing flower extracts of carnations led to a 50-fold overestimation of ACC content. In this thesis, therefore, paper chromatography was also used to confirm the specificity of the Lizada and Yang (1979) assay for the measurement of ACC content in leaf extracts of white clover.

The ability of the paper chromatographic technique to accurately quantitate known concentrations of ACC was examined initially. This was accomplished by fractionating authentic ACC (between 500 and 2500 pmol; dissolved in water) and then eluting the resolved ACC from the paper and assaying it by the method of Lizada and Yang (1979). Using this method, a linear and quantitative recovery of approximately 60 % of the ACC applied was achieved (Figure 17).

The paper chromatographic method was then used to fractionate the putative ACC in mature green and senescent extracts prior to elution, and assay by the method of Lizada and Yang (1979) (Figure 18). The tissue extracts that were examined for ACC content included those from mature green leaves, mature green leaves after a 2.5 h wounding treatment, senescent leaves, senescent leaves extracted together with authentic ACC, and authentic ACC dissolved in water.

All the elutions from the lane where the mature green tissue extract was fractionated produced very little ethylene upon oxidation (2 to 14 pmol g^{-1} FW). In contrast, elutions from the lane where the senescent extract had been fractionated produced comparatively higher amounts of ethylene at two distinct regions on the paper chromatogram. The first region produced the greatest amount of ethylene (1778 pmol g^{-1} FW) and arose from a substance that had relatively low mobility in the paper chromatography system (R_f 0.32). The second region (R_f 0.49) produced approximately 3-fold less ethylene (740 pmol g^{-1} FW), but this region was closer to where authentic ACC (dissolved in water) was found to resolve to (R_f, 0.59). Of the 10000 pmoles of this authentic ACC applied to the paper chromatogram, *ca.* 8100 pmol was recovered after elution and assay, representing a recovery rate of *ca.* 80 %. The recovery rate was probably higher than reported in the

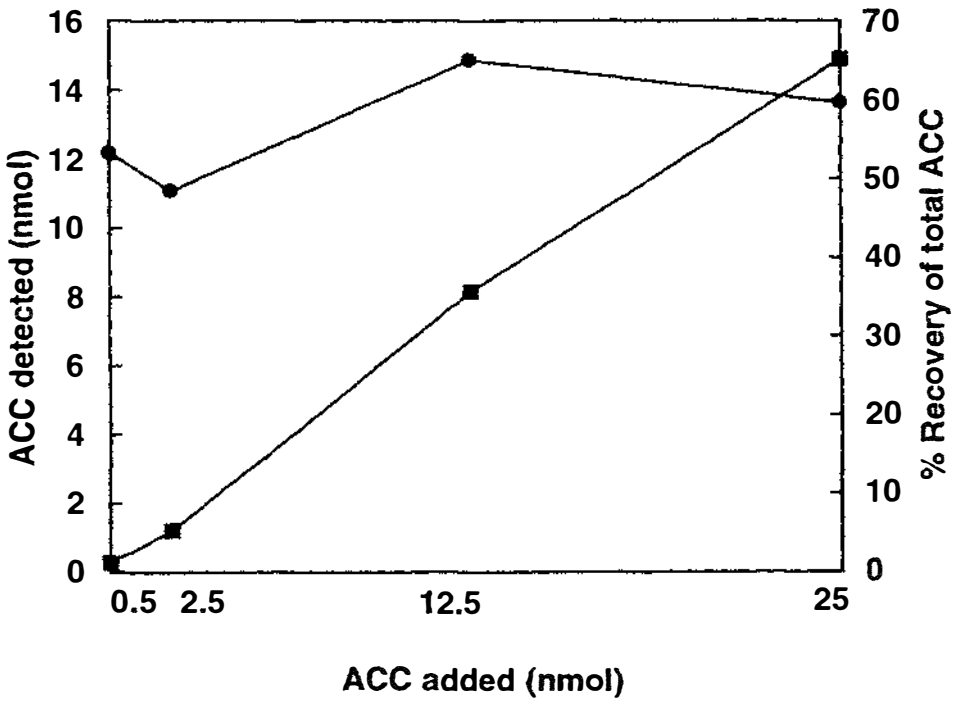

Figure 17. Assessment of paper chromatography as a quantitative tool for measuring ACC content

Different amounts of authentic ACC (dissolved in water) were resolved by paper chromatography then eluted, and assayed by the method of Lizada and Yang (1979). The number of moles added to the paper chromatogram is compared with the number of moles detected and the percentage recovery calculated.
(--■--) nmol ACC detected. (--●--) % recovery.

preliminary experiment (*ca.* 60 %; Figure 17) due to the elution from this chromatography of a larger area of the lane in which the ACC was resolved.

To determine whether the difference in mobility between authentic ACC (R_f 0.59) and the R_f 0.49 peak in the senescent extract was due to substances retarding the movement of endogenous ACC in the paper chromatogram, a known amount of authentic ACC (12 nmol) was extracted together with the senescent material and resolved on the paper chromatogram. Separation of the senescent extract with no added authentic ACC, produced two peaks of ethylene production at R_f 0.32 and R_f 0.49. Addition of authentic ACC to the senescent extract did not result in greater levels of ethylene being detected at the region where ethylene production was highest (R_f 0.32). However, an extra 465 pmol g^{-1} FW of ethylene was detected at R_f 0.49 which was the region closest to where authentic ACC (dissolved in water) resolves to (R_f 0.59). Given the probable losses of ACC during extraction, elution and assay, it is likely that this value (465 pmol g^{-1} FW) is representative of the 900 pmol of ACC that would be expected if 100 % recovery had been achieved. Furthermore, as the region was at R_f 0.49, not R_f 0.59, it appears that during the chromatographic separation the mobility of the putative ACC is being retarded by components (possibly pigments) present in the senescent extract. This is further suggested by the finding that only a comparatively small amount of ethylene (50 pmol g^{-1} FW) is evolved at R_f 0.59.

An additional approach to determine the specificity of the Lizada and Yang method for ACC involved wounding mature green leaves to elevate levels of endogenous ACC, as wounding has been shown to elevate ACC levels in other tissues (Yu and Yang, 1980). Leaves were harvested 2.5 h after wounding as this is the time of maximal wound ethylene production; refer Figure 61). Extracts of both wounded and non-wounded leaves were then partitioned by paper chromatography and regions of the chromatogram assayed for ethylene evolution (Figure 18). In contrast to the mature green extract which produced only low levels of ethylene from anywhere within the fractionated lane (2 to 14 pmol g^{-1} FW), the wounded mature green leaf tissue produced comparatively high levels of ethylene (160 pmol g^{-1} FW) at R_f 0.32. This was not the region (R_f 0.49) of the chromatogram where it was concluded that ACC in the senescent extract separated to (judged by the mobility of authentic ACC in senescent extract), or where authentic ACC separated to. However, since it was the same region which produced the most ethylene in the senescent extract after elution and assay, it was concluded that the ethylene was non-ACC derived.

Figure 18. Specificity of Lizada and Yang method for determination of tissue ACC content

Leaf-tissue extracts as well as an ACC-standard were fractionated by paper chromatography, and regions of the chromatogram assayed for ethylene production.

A. Paper chromatogram after separation of the extracts overnight.
   Lane 1. Fractionation of 9900 pmol of authentic ACC in water.
   Lane 2. Fractionation of the extract produced by extracting senescent leaves together
   with authentic ACC.
   Lane 3. Fractionation of the senescent leaf extract.
   Lane 4. Fractionation of the extract of wounded mature green leaves.
   Lane 5. Fractionation of the mature green leaf extract.

B. The amount of ethylene produced from regions of the chromatogram after fractionation of the extracts.
   (--O--) Authentic ACC dissolved in water; (--●--) Senescent leaves extracted together with authentic ACC; (--▲--) Senescent leaf extract; (--■--) Extract of wounded mature green leaves; (--◆--) Mature green leaf extract.

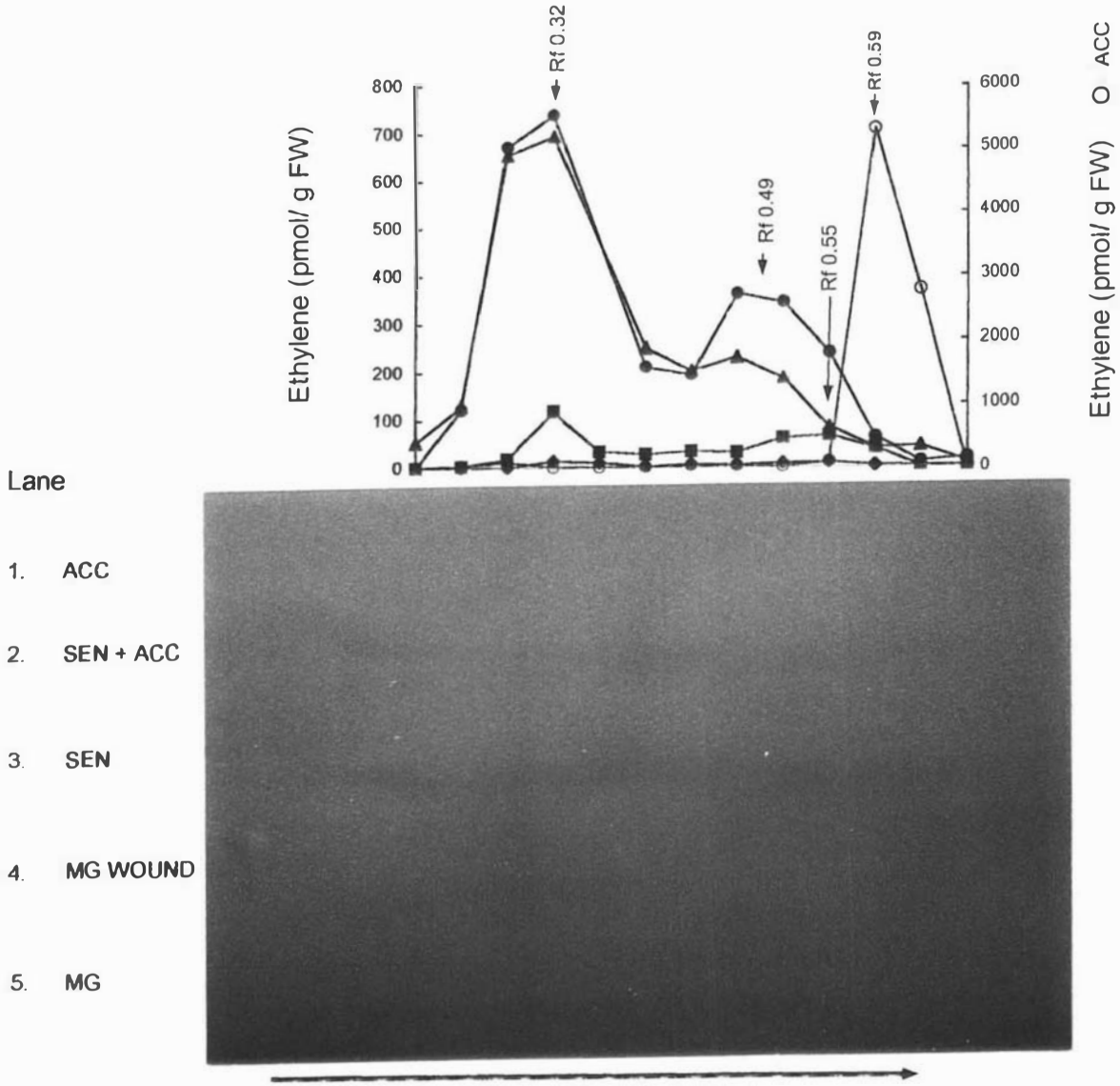
Rf 0.32
Rf 0.49
Rf 0.55
Rf 0.59
Ethylene (pmol/ g FW)
800
700
600
500
400
300
200
100
0
6000
5000
4000
3000
2000
1000
0
Ethylene (pmol/ g FW) O ACC
Lane
1. ACC
2. SEN + ACC
3. SEN
4. MG WOUND
5. MG

A similar amount of ethylene production (156 pmol g^{-1} FW) was observed at a position (R_f 0.55). This may represent the region at which endogenous ACC in the mature green extract resolved to, as the nature of the retarding substance(s) in this extract may differ from that in the senescent extract. However, addition of authentic ACC to the wounded mature green extract would be needed to show this unequivocally.

The results of the paper chromatography experiments do support the trend determined by the Lizada and Yang method in which ACC levels are higher in the chlorotic leaf tissue than mature green. Therefore, the higher levels of ethylene being evolved from this tissue are probably due to greater activity of the ACC-mediated biosynthetic pathway. Yet, there are no reports on the changes in activity (*in vivo* or *in vitro*) of either ACC synthase or ACC oxidase during leaf maturation and senescence.

The next section examines changes in ACC oxidase activity, assayed *in vitro*, during leaf maturation (leaves 4 to 8) and senescence (leaves 9 to 16) in the model system.

3.5 Changes in activity of ACC oxidase during leaf maturation and senescence of white clover

3.5.1 Optimisation of ACC oxidase extraction and assay *in vitro*

A series of experiments were performed to characterise aspects of the extraction and assay of ACC oxidase in mature green tissue prior to examining enzyme activity during leaf maturation and senescence. This was useful as maximising the amount of activity per unit fresh weight reduces the requirement for large amounts of tissue which can be a limiting factor, and identifying factors important for activity will also identify aspects of the assay that may need to be tightly controlled in order to obtain reproducible results.

Initial attempts at measuring ACC oxidase activity in a crude tissue homogenate of mature green leaf tissue of white clover failed. However, activity could be measured after passage of the crude tissue homogenate through Sephadex G-25 (as described in section 2.2.7.1.1) which suggested that there may be putative low molecular weight inhibitors (MW < 5000) present in the crude extract of the leaf tissue (data not shown).

The linearity of the ACC oxidase catalysed reaction was examined because the initial rate of an enzymatic reaction can only be accurately determined if the accumulation of product is linear during the time period the enzyme is measured. Production of ethylene by ACC

oxidase activity *in vitro* was found to be linear within the first 20 min (Figure 19A) after which activity decreased with a half life of 22 min (Figure 19B).

To further confirm that an assay time of 20 min enabled an accurate measure of the initial rate of ACC oxidase activity, the mature green tissue extract was diluted to provide a series of concentrations from 1.04 mg mL^{-1} protein to 0.13 mg $mL^{-1}$and then assayed for activity (Figure 19c). The highest concentration (1.04 mg mL^{-1}) represented the protein concentration typically obtained when the mature green tissue was extracted with two volumes of extractant per gram fresh weight (section 2.2.7.1.1). The lowest concentration (0.13 mg mL^{-1}) represents an *ca.* 8-fold dilution of this concentration. It was found that within the range of 0.13 to 1.04 mg mL^{-1} protein, activity remained proportional to protein concentration. This suggests firstly, that 20 min enabled an accurate measure of the initial rate of activity and secondly, that even if the protein concentration of mature green tissue extracts was diluted 8-fold from that normally obtained by the standard extraction procedure, the activity remained proportional and therefore comparable. Henceforth, a reaction time of 20 min was used for all subsequent assays.

ACC oxidase activity could be increased 5-fold by shaking the enzyme/ reaction mix at 175 rpm during the incubation at 30°C for 20 min when compared with a static incubation (Figure 20A). However, more vigorous mixing (vortexing) did not increase enzyme activity, but rather reduced it. This reduction was as great as 50 % if the enzyme/ reaction mix was vortexed prior to the 20 min incubation time at 30°C (with shaking at 175 rpm) (Figure 20B).

Ageing of the reaction mix (i.e. storing for use in multiple serial assays) was also examined to determine if it would affect enzyme activity. This was considered necessary as the reaction mix did not appear to be stable (as judged by the fading of the pink coloration of the freshly prepared mix with time). The reaction mix was preincubated for different times for up to 1 h at 30°C, prior to addition of the enzyme extract and subsequent assay (which involved a further incubation at 30°C for 20 min). It was found that the reaction mix could be preincubated at 30 °C for up to 30 min without a reduction in detectable ACC oxidase activity upon subsequent assay (Figure 20C). However, addition of enzyme to a reaction solution preincubated at 30°C for 45 and 60 min resulted in a decrease in activity of 30 and 35 % respectively.

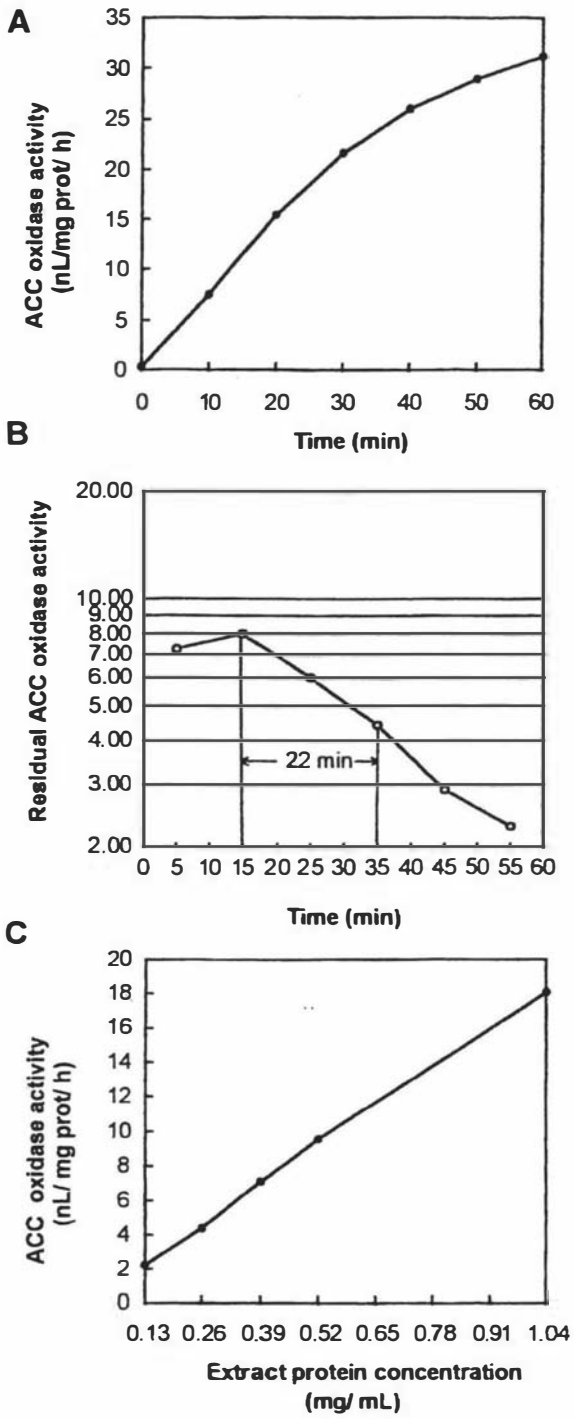

Figure 19. Time course of ACC oxidase activity and effect of extract concentration on ACC oxidase activity measured *in vitro*.

A. Linearity of ACC oxidase activity with time.
B. Half-life of ACC oxidase activity during incubation. The rate per unit 5 min was calculated over times spanning 60 min and plotted as residual ACC oxidase activity.
C. Correlation between concentration of enzyme extract (mg mL^{-1} protein) and amount of ethylene produced by the ACC oxidase assay.

Figure 20. Optimisation of ACC oxidase activity measured *in vitro*.

A. Effect of shaking the enzyme/ substrate mix on ACC oxidase activity. After addition of the enzyme to the substrate mix the reaction was either incubated with shaking at 175 rpm (shaken) or incubated without shaking (static).

B. Effect of vortexing the enzyme substrate mix on ACC oxidase activity. After addition of the enzyme to the substrate mix, the reaction was either not vortexed before incubation (none) , was vortexed 5s prior to incubation at 30°C (start), vortexed both prior to and after incubation at 30°C (start/ end), or vortexed after incubation (end). Error bars = ± 1 sem for 3 internal replicates of 4 independent experiments.

C. Effect of preincubating substrate mix at 30°C before addition of enzyme extract. Activity was measured after a further incubation time of 20 min.
Error bars = ± 1 sem for 3 internal replicates of 2 independent experiments.

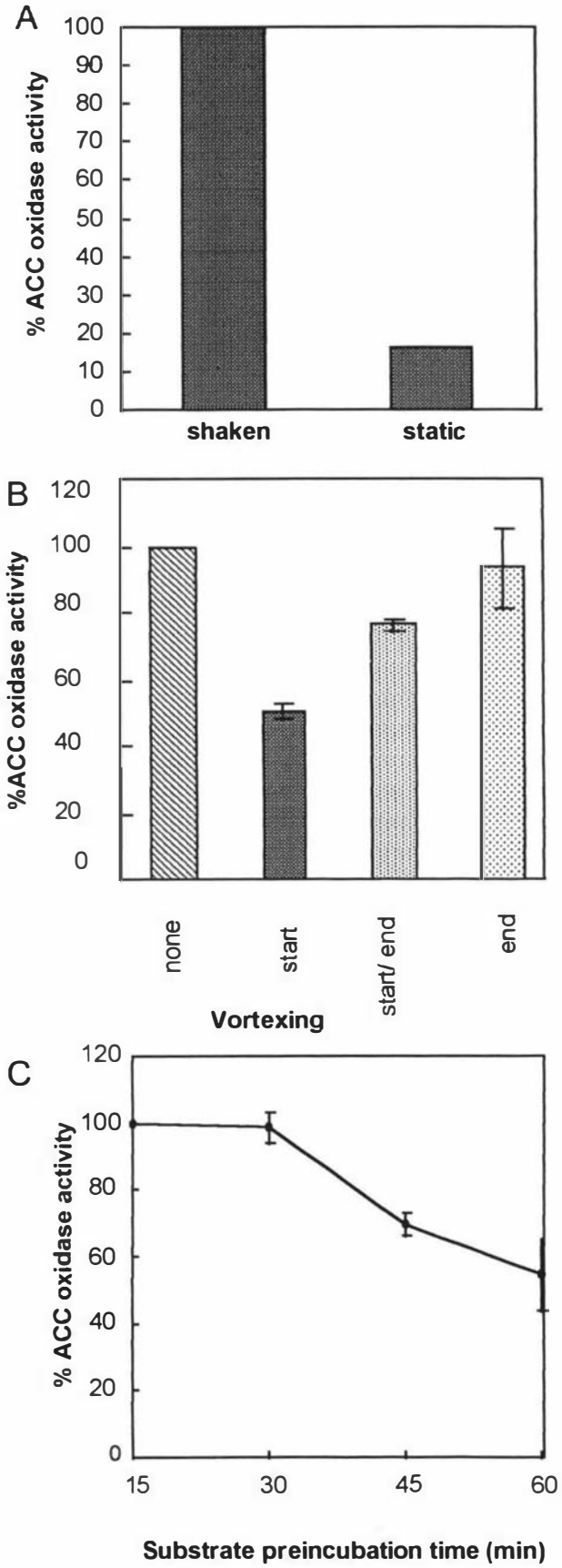
A
% ACC oxidase activity
100
90
80
70
60
50
40
30
20
10
0
shaken
static
B
%ACC oxidase activity
120
100
80
60
40
20
0
none
start
start/ end
end
Vortexing
C
% ACC oxidase activity
120
100
80
60
40
20
0
15
30
45
60
Substrate preincubation time (min)

To determine the importance of extraction time on obtaining maximum and reproducible ACC oxidase activity, pooled mature green leaf tissue was extracted for different times over a 1 h time period and the activity compared (Figure 21). Expression of ACC oxidase activity on both a fresh weight (Figure 21A) and protein basis (Figure 21B), indicated that an extraction time of 15 min was sufficient to recover most of the enzyme.

The optimum pH for ACC oxidase activity of mature green leaves assayed *in vitro* was found to be pH 7.5 (Figure 22). Activity at pH 6.5 and 8.5 was only 64 % and 62 %, respectively, of that obtainable at pH 7.5.

The effect of the freeze-thaw process on ACC oxidase activity was examined as, for convenience, the enzyme extracts were to be snap-frozen in liquid air and stored at -80°C. When mature green extracts of leaf tissue were pooled, aliquotted into separate microfuge tubes, snap-frozen in liquid air and then quick-thawed at 30°C, the activity of the enzyme was reduced by less than 10 % (Figure 23).

The composition of the extraction medium was tested for its ability to recover maximal yields of ACC oxidase activity as the literature suggested that a number of additions to the Tris-glycerol buffer (used originally by Ververidis and John (1991) to extract activity from melon fruit) could improve recovery. The recovery achieved by the addition of various components to the extraction buffer was compared to that achieved by a buffer chosen from a consensus of published studies (0.1 M Tris-HCl, pH 7.5, 2 mM DTT, 2 % (w/v) PVPP and 10 % (v/v) glycerol) (Figure 24). The Tris-glycerol buffer of Ververidis and John was comparatively poor at recovering ACC oxidase activity in leaf tissue of white clover (only 40 % of that obtainable with the above buffer), while inclusion of DTT and sodium ascorbate appeared to be important for maximum recovery of activity. PVPP was not found to increase recovery of ACC oxidase. In contrast, its presence in the extraction buffer was slightly inhibitory and therefore it was subsequently omitted. The composition of the extraction buffer that gave maximum recovery of ACC oxidase from leaf tissue of white clover was 0.1 M Tris-HCl, pH 7.5, 2 mM DTT, 30 mM ascorbate, and 10 % (v/v) glycerol, and this buffer was used for all further experiments.

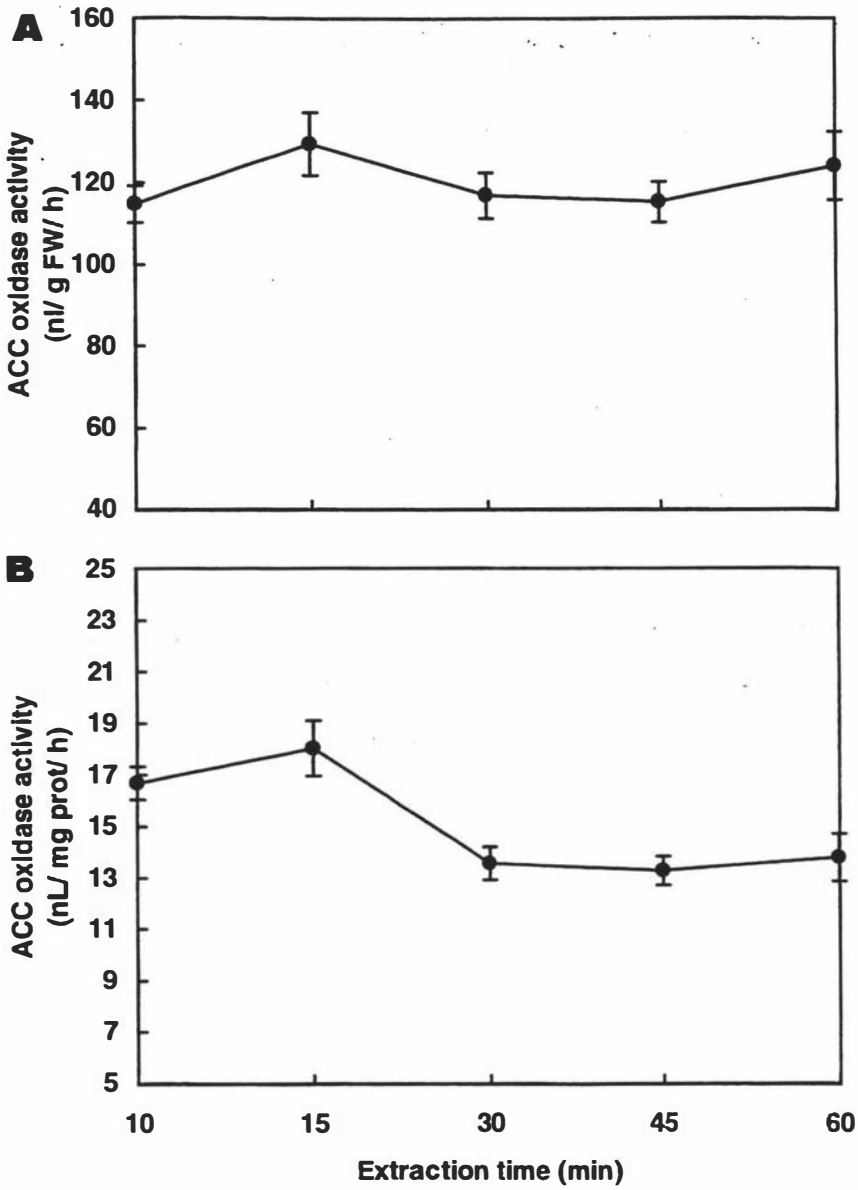

Figure 21. Effect of extraction time on ACC oxidase activity.

Mature green leaves were extracted for various times up to 1 h and assayed for ACC oxidase activity *in vitro*.

A. Activity expressed on a per unit fresh weight basis.

B. Activity expressed on a per unit protein basis.

Error bars = ± 1 sem for 3 internal replicates.

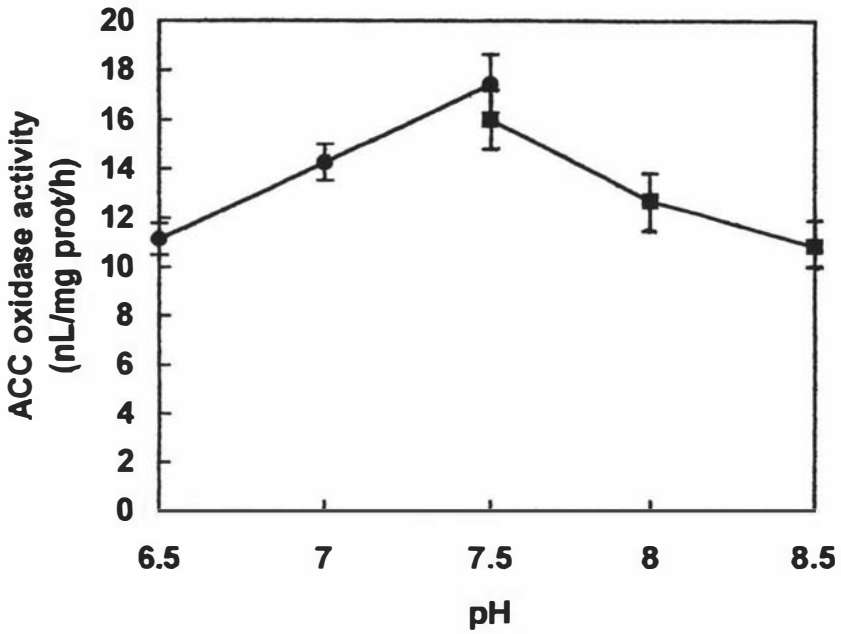

Figure 22. Effect of assay buffer pH on ACC oxidase activity.

(—●--) 50 mM MOPS buffer, pH 6.5 to 7.5.
(--■--) 50 mM Tris-HCl buffer, pH 7.5 to 8.5.
Error bars = ± 1 sem for 3 internal replicates of 2 independent experiments.

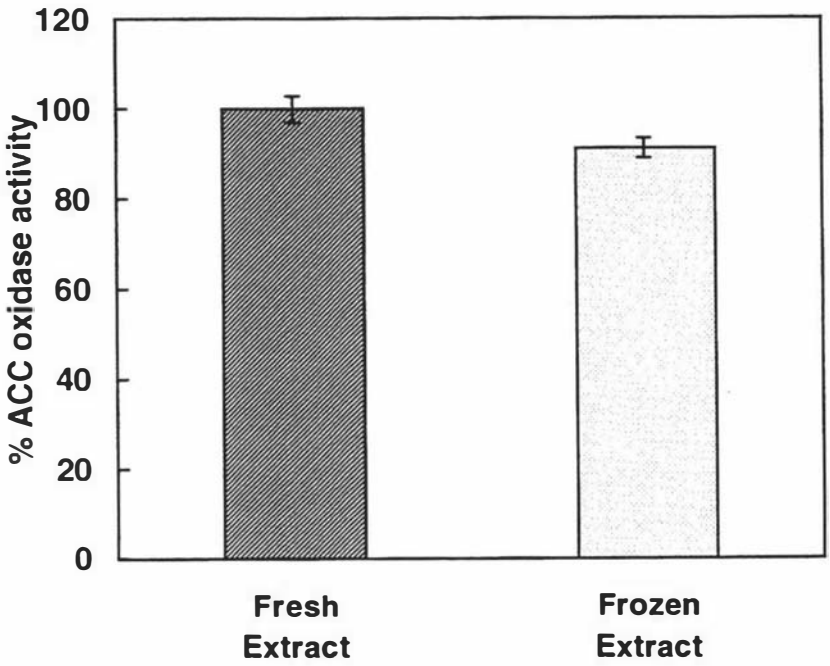

Figure 23. Effect of freeze/ thaw on ACC oxidase activity.

Extracts of mature green leaves were snap-frozen in liquid N_2, thawed at 30°C, immediately placed on ice and then assayed together with samples that had remained on ice.
Error bars = ± 1 sem for 3 internal replicates of 4 independent experiments.

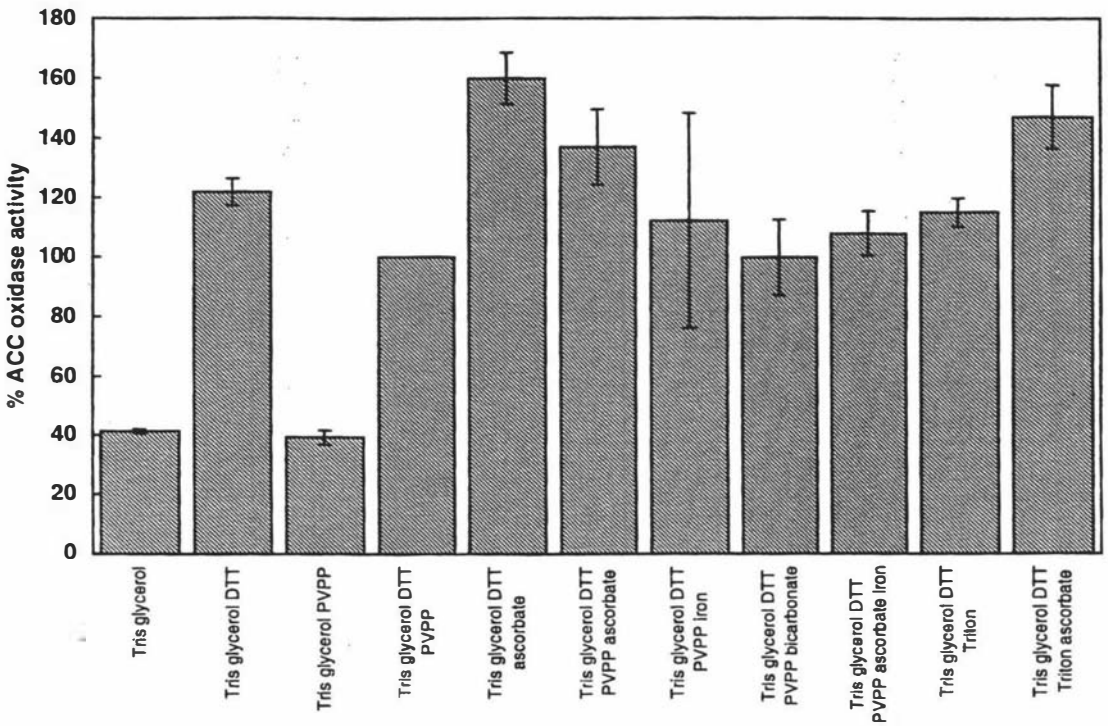

Figure 24. Extraction requirements for ACC oxidase.

The effect of various extraction mediums on recovery of ACC oxidase activity measured *in vitro* from mature green leaves. The concentration of the components were as follows: 0.1 M Tris-HCl, pH 7.5, 2 mM DTT, 2 % (w/v) PVPP, 10 % (v/v) glycerol, 30 mM sodium ascorbate, 20 µM iron sulphate, 30 mM sodium bicarbonate, 0.1 % (v/v) Triton X-100.

Error bars = ± 1 sem for 3 internal replicates of 3 independent experiments.

3.6 Activity of ACC oxidase during leaf maturation and senescence of white clover

The previous section identified aspects of the extraction and assay that were important determinants of reproducibility and yield of ACC oxidase activity *in vitro* from leaf tissue of white clover. This section now examines changes in activity *in vitro* of ACC oxidase during leaf maturation and senescence in the model system.

Mature green (pooled leaves, 4 to 7), onset (pooled leaves, 9 to 11) and senescent (pooled leaves, 13 to 16) leaf tissue was powdered in liquid N_2 , each developmental stage divided in half, and each half extracted and assayed in parallel for activity.

ACC oxidase activity was highest in the pooled mature green leaf tissue, lower in tissue starting to show symptoms of chlorosis and lowest in tissue at an advanced stage of chlorosis, irrespective of whether expressed on a per unit fresh weight or protein basis (Figure 25). Although, the decline in activity as the tissue became chlorotic was greatest when expressed on a per unit fresh weight basis (6-fold; Figure 25A) as compared to per unit protein (2-fold; Figure 25B). The parallel extraction and assay gave very similar results confirming both the reliability of the extraction and assay.

The stability of ACC oxidase was assessed as ACC oxidases extracted from other plant tissue have been reported to lose activity upon storage at 2 °C for 5 h (Fernandez-Maculet and Yang, 1992). To determine the stability of ACC oxidase, extracts were incubated on ice for 3 h before being re-assayed (Figure 25). Detectable ACC oxidase activity did not change in extracts of leaf tissue at the mature green or onset stage after a 3 h incubation on ice. In contrast, the activity from the extracts of leaf tissue at the senescent stage decreased by about 43% which suggested that ACC oxidase was less stable in these extracts.

ACC oxidase activity was then examined in individual leaves from nodes 4 to 16 of the model system (Figure 26). Activity was highest in mature green leaves (leaves 4 to 9) when expressed either on a per unit fresh weight (Figure 26A) or per unit protein basis (Figure 26B) compared with chlorotic leaves (leaves 10 to 16). The decline in activity in leaves was concomitant with chlorophyll loss in the tissue and was greater when expressed on a per unit fresh weight basis (8-fold; from leaf 8 to leaf 16) as compared with a per unit protein basis (3-fold).

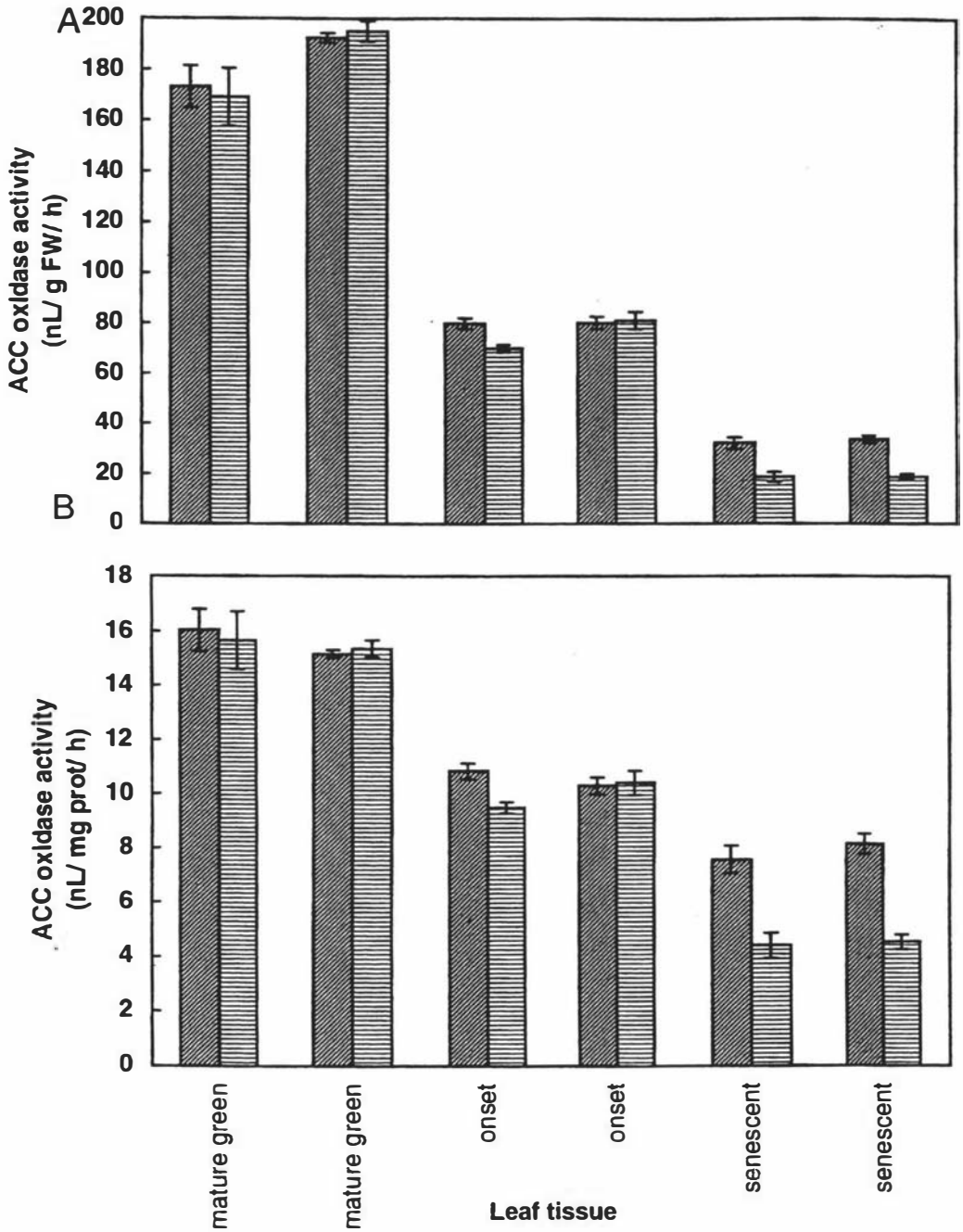

Figure 25. Activity of ACC oxidase in leaves at mature green, onset and chlorotic stages, and after a 3 h storage on ice.

Parallel extractions and assays were performed as a measure of the reliability of the procedures and determinations for both are included.

▨ Activity measured initially. ▤ Activity after a 3 h incubation on ice.

A. ACC oxidase activity in leaves expressed on a per unit fresh weight basis.

B. ACC oxidase activity in leaves expressed on a per unit protein basis.

Error bars = ± 1 sem for triplicate measurements of a single experiment.

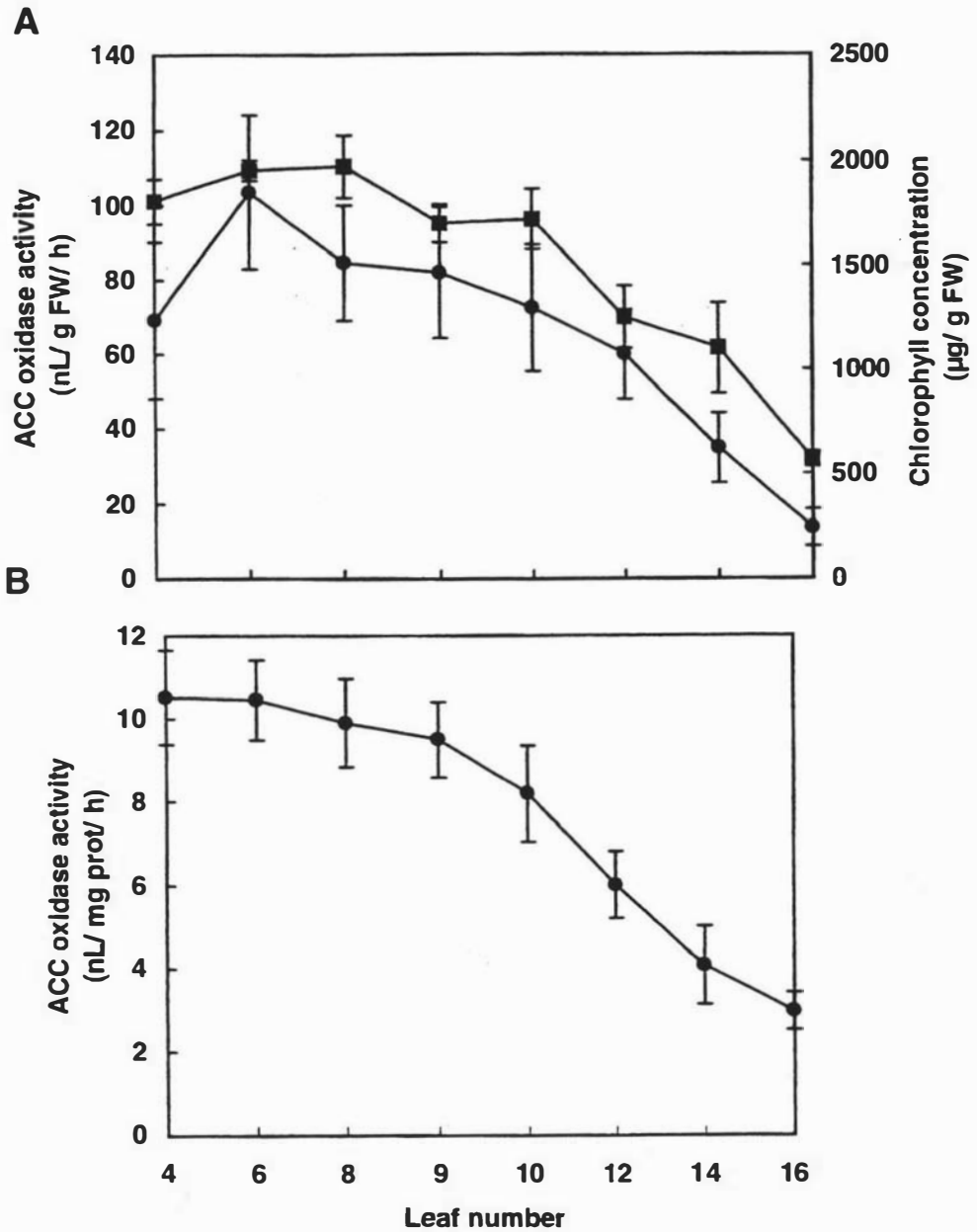

Figure 26. Activity of ACC oxidase at individual nodes in mature and senescing leaves

A. (—●--) Activity expressed on a per unit fresh weight basis.
(--■--) Total chlorophyll content measured in the same leaves.

B. (—●--) Activity expressed on a per unit protein basis.

Error bars = ± 1 sem for triplicate measurements of 3 independent experiments.

Since it has been suggested in the literature that ACC oxidase activity is often controlled at the level of gene transcription (see section 1.4.5), a study of ACC oxidase gene expression during leaf maturation and senescence in white clover was initiated. The main aim was to determine whether ACC oxidase gene expression supported the observed changes in ACC oxidase activity *in vitro*.

3.7 Gene expression of ACC oxidase during leaf maturation and senescence of white clover.

Initially, putative ACC oxidase cDNA sequences of leaf tissue were generated by the reverse transcriptase-polymerase chain reaction (RT-PCR) by Dr. Michael T. McManus at the University of California, Davis using RNA isolated by Dr. Stephen Butcher, and primers provided by Professor Shang Fa Yang. TA-cloning of these sequences yielded twelve colonies which were subsequently brought back to New Zealand for further analysis as part of this thesis.

3.7.1 Confirmation of putative ACC oxidase sequences by manual sequencing

Bacteria from nine of these twelve colonies were grown overnight, their plasmids isolated by alkaline lysis, column purified, and their inserts (of *ca.* 840 bp) sequenced with both forward and reverse M13 Universal Primers. Approximately 200 to 300 bp at each end of the putative ACC oxidase inserts were sequenced manually (section 2.3.3.2). An alignment comparison of all nine sequences generated by RT-PCR revealed that they shared greater than 94 % similarity in their nucleotide composition (Table 5). In this study, sequences amplified by RT-PCR that showed greater than 94 % similarity were considered to be representative of the same gene transcript, as errors in the sequence are produced during both generation and identification of PCR sequences. For example, errors can occur both during first strand synthesis of cDNA by reverse transcriptase, during PCR by the DNA polymerases and by the DNA polymerase during sequencing. The consensus sequence generated by RT-PCR from RNA of mature green leaf tissue of white clover showed greatest sequence identity (> 75 %) to ACC oxidases identified from other organisms in the GenBank database and was therefore designated TR-ACO1 (data not shown).

Table 5. Percentage homology comparison of sequences amplified from mature green leaves of white clover by RT-PCR and designated TR-ACO1.

Sequences were aligned using the Align+ program and the percentage homologies compared to the sequence designated TR-ACO1.

Sequence	bp sequenced	% homology
TR-ACO1	1-264	
ACO2	1-274	98
ACO3	1-278	95
ACO4	1-270	95
ACO5	1-299	98
ACO6	1-285	96
ACO7	1-277	95
ACO8	1-269	95
ACO9	1-270	96

3.7.2 RT-PCR amplification of putative ACC-oxidase gene transcripts

RT-PCR (section 2.3.6) performed on RNA extracted from mature green leaf tissue identified a single isoenzyme of ACC oxidase. There may have been other isoenzymes in the mature green tissue that were missed due to the low number of transformants screened. In addition, there may have been isoenzymes in white clover leaf tissue that were missed due to being expressed in chlorotic tissue, and so it was considered important to repeat the PCR. Total RNA was extracted from mature green (leaf 4), onset of chlorosis (leaf 9) and chlorotic (leaf 14) leaves. Putative sequences of ACC oxidase were then amplified from the RNA by RT-PCR using nested degenerate primers (see Figure 10) made to conserved domains among ACC oxidase sequences and known to amplify a product of *ca.* 840 bp.

The first round primers (ACOF1 and ACOR1) generated a cDNA fragment during PCR of the expected size (*ca.*840 bp) from all three RT reactions (Figure 27A). An aliquot from each of the first round PCR mixes was then used as a template for amplification with the second round primers (E101 and E102; Figure 10). Amplification with these second round primers further increased the amount of the *ca.* 840 bp product in each of the mixes (data not shown). The amplified products from all three PCR mixes (representative of leaves 4, 9, and 14) were then individually TA-cloned into the pCR 2.1 vector and transformed into *E. coli* DH-5α. Subsequently, the plasmids were isolated by alkaline lysis and checked for the presence of the *ca.* 840 bp insert by restriction digestion (Figure 27B). The *ca.* 840 bp insert from a selection of clones (representative of nodes 4, 9, and 14) was then sequenced using an automated DNA sequencer.

3.7.3 Confirmation of putative ACC oxidase gene transcripts by sequence analysis

A total of 16 clones was sequenced: four (leaf 4), six (leaf 9), and six (leaf 14). Some of these sequences showed no homology to anything in the GenBank database and were discarded, while others showed highest sequence homology with ACC oxidase sequences and were then compared by alignment.

An alignment comparison revealed that the sequences could be separated into two distinct groups. Each of the sequences within a group showed greater than 94 % homology and so both groups were considered to represent two distinct cDNA products. One of the cDNA products had the same sequence as TR-ACO1 identified earlier (Figure 28), the other cDNA product did not and so was designated TR-ACO2 (Figure 29).

TR-ACO2 was the predominant cDNA sequence amplified from leaves in this study. Ten out of 13 sequences (three of the 16 sequences showed no homology to anything in the database) were TR-ACO2 sequences while only three were TR-ACO1 (two from leaf 4, (mature green), and one from leaf 14, (chlorotic)). It appears then, that both sequences are able to be generated by RT-PCR in both mature green and chlorotic leaf tissue. Rather than screen more clones for the presence of additional isoenzymes of ACC oxidase, the decision was made to focus further work on the analysis of TR-ACO1 and TR-ACO2.

TR-ACO1 is 84 % homologous to TR-ACO2 at the nucleotide level (Figure 30) and 87 % identical at the amino acid level (Figure 31). TR-ACO1 (804 bp) is shorter than TR-ACO2 (816 bp) by 12 bp due to a deletion at nucleotides 724 to 736 of TR-ACO2, a region shown to be highly variable among ACC oxidases (Figure 31).

Both TR-ACO1 and TR-ACO2 contain the amino acids hitherto shown to be important for maximal activity of the enzyme by structure function analysis (refer Figure 28 and 29) (Kadyrzhanova *et al.,* 1997). These include the lysine residues at positions 158, 230, 199 and a fourth residue that varies slightly in position in TR-ACO1 and TR-ACO2. It occurs at position 289 in TR-ACO1 and 293 in TR-ACO2. Other residues also shown to be important for maximal activity are the histidine residue at position 39, the cysteine residue at position 165, and the putative Fe ligands (Histidine^{177} [H^{177}], Aspartate^{179} [D^{179}], and Histidine^{234} [H^{234}]) which have been shown to be essential for activity. The presence of these residues in TR-ACO1 and TR-ACO2 strongly suggest that both transcripts encode functional ACC oxidases.

A phylogenetic tree constructed from an alignment of TR-ACO1 and 2 with eighteen other ACC oxidases and two other 2-ODDs (flavanone-3-hydroxylase and isopenicillin-N-synthetase) clustered TR-ACO1 and 2 with ACC oxidases within a single branch of a trifurcating tree (Figure 32). This is further evidence for TR-ACO1 and 2 representing authentic ACC oxidase sequences. The tree also suggests that the senescence-associated TR-ACO2 is more similar to TR-ACO1 than to other senescence-associated ACC oxidases (LE-ACO1 of tomato, Barry *et al.,* 1996; and CM-ACO1 of melon, Lasserre *et al.,* 1997) characterised thus far.

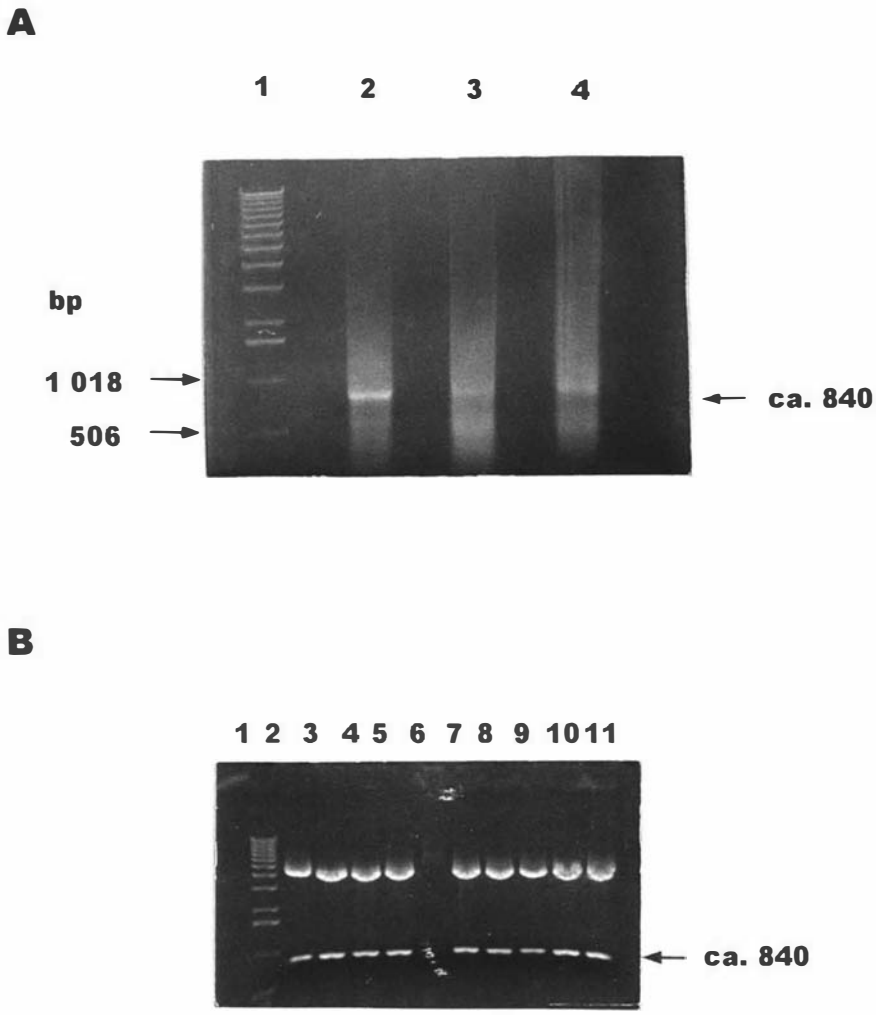

Figure 27. First round PCR amplification of putative ACC oxidase cDNA sequences and restriction digests of plasmids cloned with these sequences.

A. RT-PCR with first round primers on RNA extracted from leaves 4, 9, and 14.
Lane 1. Gibco BRL 1Kb DNA Ladder. The molecular weight of the standards is indicated to the left of the figure. The size of the amplified cDNA fragment is indicated by an arrow to the right of the figure.
Lane 2. 20 μL of 100 μL PCR of leaf 4 RT mix, 333 nM ACOF1, 333 nM ACOR1.
Lane 3. 20 μL of 100 μL PCR of leaf 9 RT mix, 333 nM ACOF1, 333 nM ACOR1.
Lane 4. 20 μL of 100 μL PCR of leaf 14 RT mix, 333 nM ACOF1, 333 nM ACOR1.
B.Restriction digestion of isolated plasmids to confirm presence of *ca.* 840 bp cDNA fragment.
Lane 1. Gibco BRL 1 Kb DNA Ladder. The size of the amplified cDNA fragment (*ca.* 840 bp) is indicated by an arrow to the right of the figure.
Lanes 2 to 11. Restriction digest of plasmids isolated from *E. coli* to confirm cloning of the *ca.* 840 bp cDNA fragment.

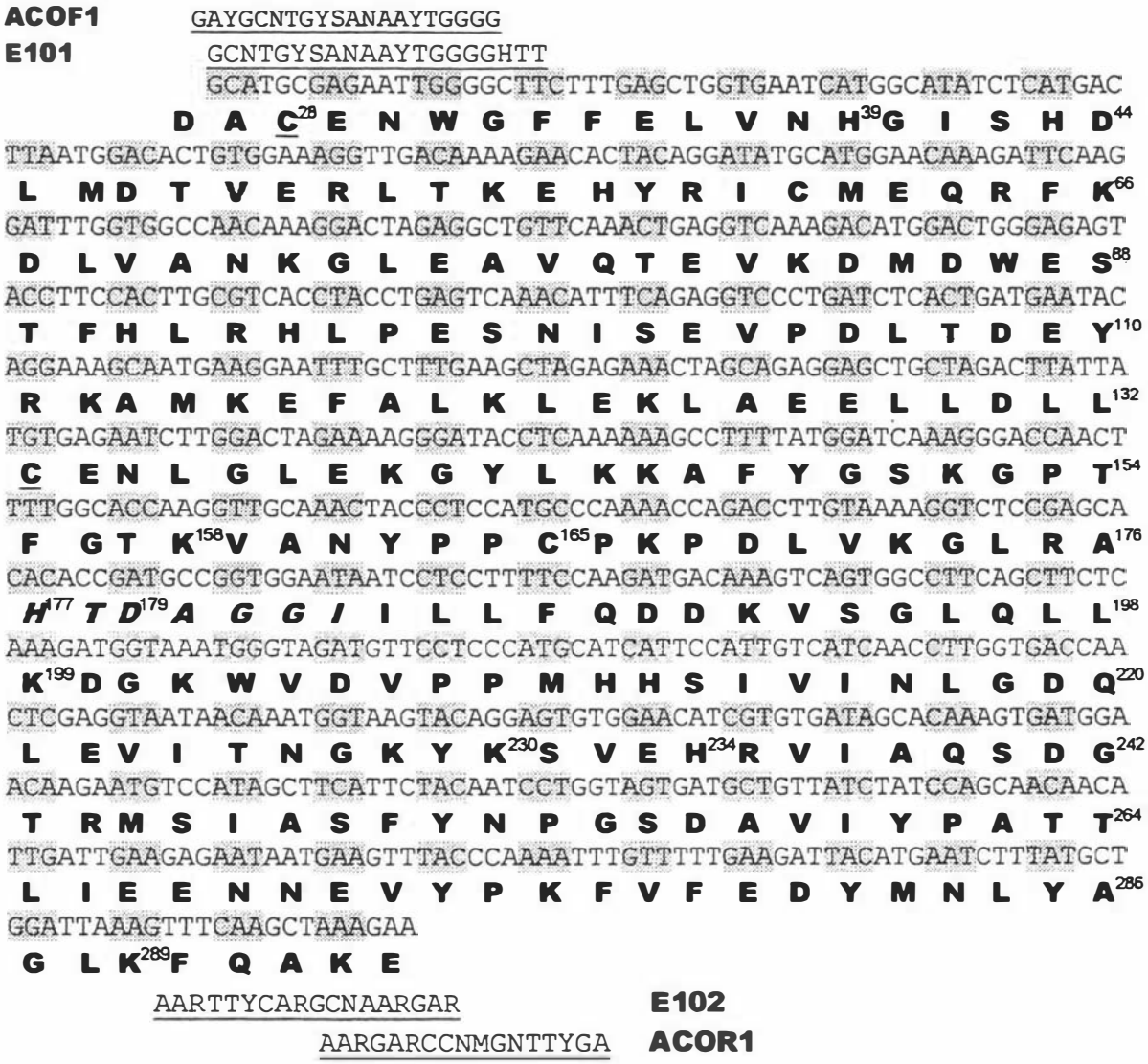

Figure 28. Nucleotide and deduced amino acid sequence of TR-ACO1

The sequences of the primers used for first round (ACOF1, ACOR1) and second round (E101, E102) are underlined. The first cysteine in the sequence is designated at position 28 in the sequence as determined by a consensus of published studies. Residues shown to be important for maximal enzyme activity by structure function analysis are indicated ^{num}. The three cysteine residues found to be conserved among ACC oxidases are underlined. The 7 amino acids that are *italicised* were identified by protein sequencing of the putative TR-ACO1-His tagged fusion protein (see section 3.13.4). One letter abbreviations for amino acids: Ala, A; Arg, R; Asp, D; Cys, C; Gln, Q; Glu, E; Gly, G; His, H; Ileu, I; Leu, L; Lys, K; Met, M; Phe, F; Pro, P; Ser, S; Thr, T; Trp, W; Tyr, Y; Val, V

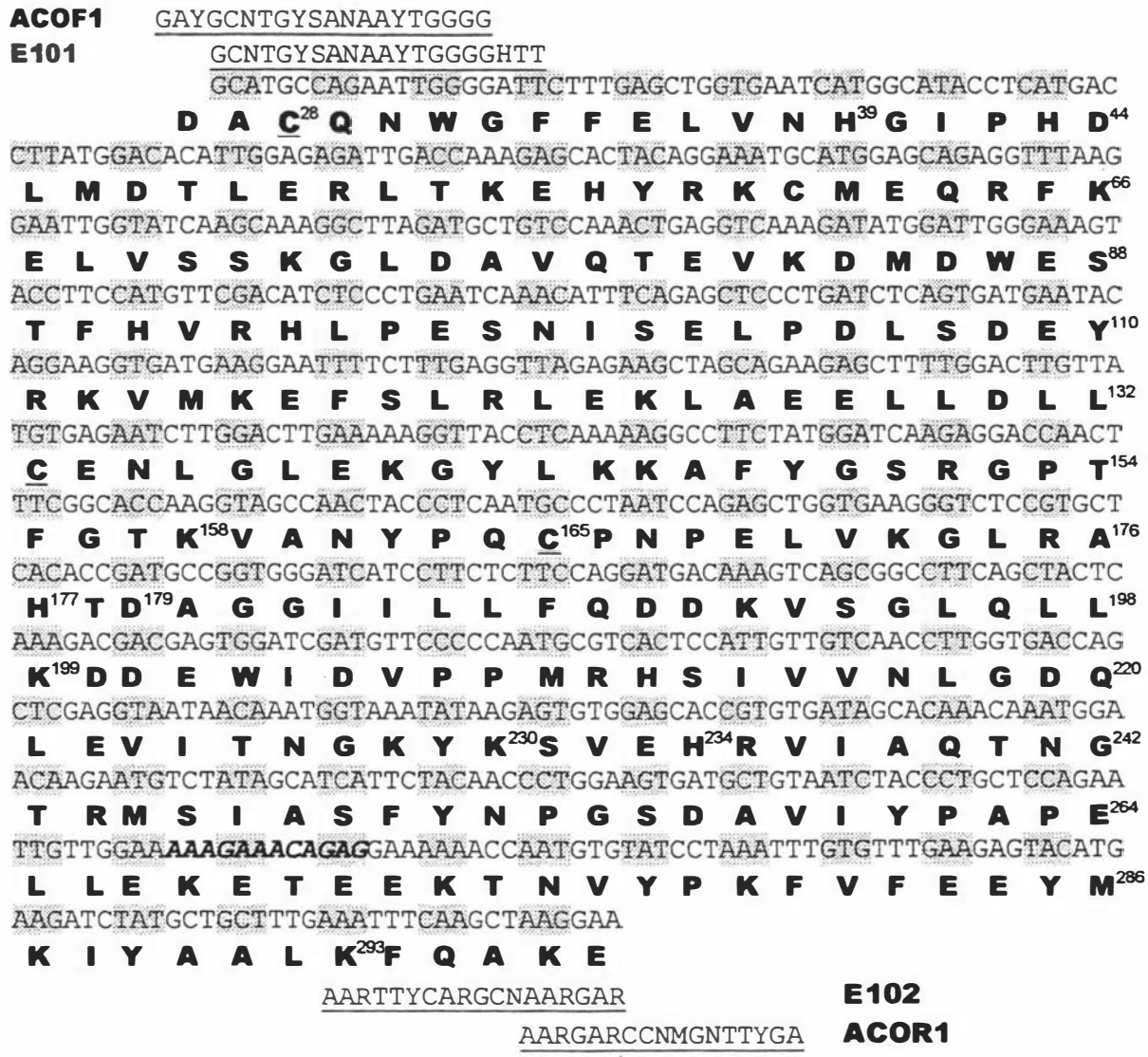

Figure 29. Nucleotide and deduced amino acid sequence of TR-ACO2

The sequences of the primers used for first round (ACOF1, ACOR1) and second round (E101, E102) are underlined. The first cysteine in the sequence is designated at position 28 in the sequence as determined by a consensus of published studies. Residues shown to be important for maximal enzyme activity by structure function analysis are indicated ^{num}. The three cysteine residues found to be conserved among ACC oxidases are underlined. The nucleotide region which is found to be deleted in TR-ACO1 is indicated (**bold**, ***italicised***). This region corresponds to a highly variable region among ACC oxidases.

Reference molecule: **TR-ACO1**1 - 804 (804 bps) Homology
Sequence 2: **TR-ACO2**1 - 816 (816 bps) 84%

```
ACOF1  GAYGCNTGYSANAAYTGGGG
E101       GCNTGYSANAAYTGGGGHTT

TR-ACO1    GCATGCGAGAATTGGGGCTTCTTTGAGCTGGTGAATCATGGCATATCTCATGACTTA
TR-ACO2    GCATGCCAGAATTGGGGATTCTTTGAGCTGGTGAATCATGGCATACCTCATGACCTT

TR-ACO1    ATGGACACTGTGGAAAGGTTGACAAAAGAACACTACAGGATATGCATGGAACAAAG
TR-ACO2    ATGGACCAATTGGAGAGATTGACCAAAGAGCACTACAGGAAATGCATGGAGCAGAG

TR-ACO1    ATTCAAGGATTTGGTGGCCAACAAAGGACTAGAGGCTGTTCAAACTGAGGTCAAAG
TR-ACO2    GTTTAAGGAATTGGTATCAAGCAAAGGCTTAGATGCTGTCCAAACTGAGGTCAAAG

TR-ACO1    ACATGGACTGGGAGAGTACCTTCCACTTGCGTCACCTACCTGAGTCAAACATTTCA
TR-ACO2    ATATGGATTGGGAAAGTACCTTCCATGTTCGACATCTCCCTGAATCAAACATTTCA

TR-ACO1    GAGGTCCCTGATCTCACTGATGAATACAGGAAAGCAATGAAGGAATTTGCTTTGAAG
TR-ACO2    GAGCTCCCTGATCTCAGTGATGAATACAGGAAGGTGATGAAGGAATTTTCTTTGAGG

TR-ACO1    CTAGAGAAACTAGCAGAGGAGCTGCTAGACTTATTATGTGAGAATCTTGGACTAGAA
TR-ACO2    TTAGAGAAGCTAGCAGAAGAGCTTTTGGACTTGTTATGTGAGAATCTTGGACTTGAA

TR-ACO1    AAGGGATACCTCAAAAAAGCCTTTTATGGATCAAAGGGACCAACTTTTGGCACCAAG
TR-ACO2    AAAGGTTACCTCAAAAAGGCCTTCTATGGATCAAGAGGACCAACTTTCGGCACCAAG

TR-ACO1    GTTGCAAACTACCCTCCATGCCCAAAACCAGACCTTGTAAAAGGTCTCCGAGCACAC
TR-ACO2    GTAGCCAACTACCCTCAATGCCCTAATCCAGAGCTGGTGAAGGGTCTCCGTGCTCAC

TR-ACO1    ACCGATGCCGGTGGAATAATCCTCCTTTTCCAAGATGACAAAGTCAGTGGCCTTCAG
TR-ACO2    ACCGATGCCGGTGGGATCATCCTTCTCTTCCAGGATGACAAAGTCAGCGGCCTTCAG

TR-ACO1    CTTCTCAAAGATGGTAAATGGGTAGATGTTCCTCCCATGCATCATTCCATTGTCATC
TR-ACO2    CTACTCAAAGACGACGAGTGGATCGATGTTCCCCCAATGCGTCACTCCATTGTTGTC

TR-ACO1    AACCTTGGTGACCAACTCGAGGTAATAACAAATGGTAAGTACAGGAGTGTGGAACAT
TR-ACO2    AACCTTGGTGACCAGCTCGAGGTAATAACAAATGGTAAATATAAGAGTGTGGAGCAC
                     ACOF2

TR-ACO1    CGTGTGATAGCACAAAGTGATGGAACAAGAATGTCCATAGCTTCATTCTACAATCCT
TR-ACO2    CGTGTGATAGCACAAACAAATGGAACAAGAATGTCTATAGCATCATTCTACAACCCT
                                          ACOF4

TR-ACO1    GGTAGTGATGCTGTTATCTATCCAGCAACAACATTGATTGAA----------GAG
TR-ACO2    GGAAGTGATGCTGTAATCTACCCTGCTCCAGAATTGTTGGAAAAAGAAACAGAGGAA
                                    ACO4A

TR-ACO1    AATAATGAAGTTTACCCAAAATTTGTTTTTGAAGATTACATGAATCTTTATGCTGGA
TR-ACO2    AAAACCAATGTGTATCCTAAATTTGTGTTTGAAGAGTACATGAAGATCTATGCTGCT

TR-ACO1    TTAAAGTTTCAAGCTAAAGAA
TR-ACO2    TTGAAATTTCAAGCTAAGGAA
           AARTTYCARGCNAARGAR                    E102
                    AARGARCCNMGNTTYGAACOF2
```

Figure 30. Alignment of coding frame regions of TR-ACO1 and TR-ACO2 gene transcripts.

TR-ACO1 and 2 coding frame sequences were aligned by the Align^{+} program. First round and second round primers used to generate the sequences are indicated in **bold**. Regions differing in homology are highlighted in grey The position of the primers used subsequently for 3'-RACE are indicated (**Bold Underlined**).

Reference molecule:	**TR-ACO1**	1 - 268 (268 aa)	Homology
Sequence 2:	**TR-ACO2**	1 - 272 (272 aa)	87%
Sequence 3:	**Consensus Seq.**	1 - 271 (271 aa)	85%

```
TR-ACO1A C E N W G F F E L V N H G I S H D L M D T V E R L T K
TR-ACO2A C Q N W G F F E L V N H G I P H D L M D T L E R L T K
CONS.  A C e N W G F F e l v n H G i p h e l m D t V E k m T k

TR-ACO1E H Y R I C M E Q R F K D L V A N K G L E A V Q T E V K
TR-ACO2E H Y R K G M E Q R F K E L V S S K G L D A V Q T E V K
CONS.  e H Y k k c m E q r F k e l v a s k g l e a v q a e v t

TR-ACO1D M D W E S T F H L R H L P E S N I S E V P D L T D E Y
TR-ACO2D M D W E S T F H V R H L P E S N I S E L P D L S D E Y
CONS.  D l D W E S T F f l r H l P v S N i s e v p D l d d e y

TR-ACO1R K A M K E F A L K L E K L A E E L L D L L C E N L G L
TR-ACO2R K V M K E F S L R L E K L A E E L L D L L C E N L G L
CONS.  re v M k d F a k r l E k L a E e l L d L L C E N L G L

TR-ACO1E K G Y L K K A F Y G S K G P T F G T K V A N Y P P C P
TR-ACO2E K G Y L K K A F Y G S R G P T F G T K V A N Y P Q C P
CONS.  E k g Y L K k a F y G s k g P n F G T K V S N Y P p C P

TR-ACO1K P D L V K G L R A H T D A G G I I L L F Q D D K V S G
TR-ACO2N P E L V K G L R A H T D A G G I I L L F Q D D K V S G
CONS.  kP d l i K G L R A H t D A G G i i L L F Q D d k V s G

TR-ACO1L Q L L K D G K W V D V P P M H H S I V I N L G D Q L E
TR-ACO2L Q L L K D D E W I D V P P M R H S I V V N L G D Q L E
CONS.  L Q L L K D g q W i D V P P m r n s I V v N I G D Q I E

TR-ACO1V I T N G K Y R S V E H R V I A Q S D G T R M S I A S F
TR-ACO2V I T N G K Y K S V E H R V I A Q T N G T R M S I A S F
CONS.  V I T N G k Y K S V m H R V i a Q t d G t R M S I A S F

TR-ACO1Y N P G S D A V I Y P A T T L.....I E E N N E V Y P
TR-ACO2Y N P G S D A V I Y P A P E L L E K E T E E K T N V Y P
CONS.  Y N P g s D a v I y P a p a l v e k l e a e k  g v Y P

TR-ACO1K F V F E D Y M N L Y A G L K F Q A K E
TR-ACO2K F V F E E Y M K I Y A A L K F Q A K E
CONS.  kF V F d D Y M k L Y a g I K F Q a K E
```

Figure 31. Alignment comparison of the deduced polypeptide sequences of TR-ACO1 and TR-ACO2 with a consensus sequence derived from 23 ACC oxidases

Capital letters represent amino acids completely conserved in all 23 ACC oxidases and lower case letters represent the most commonly occurring amino acid. Also indicated (underlined) is a small highly variable region found within the coding region of ACC oxidases. Regions of differences are highlighted in grey.

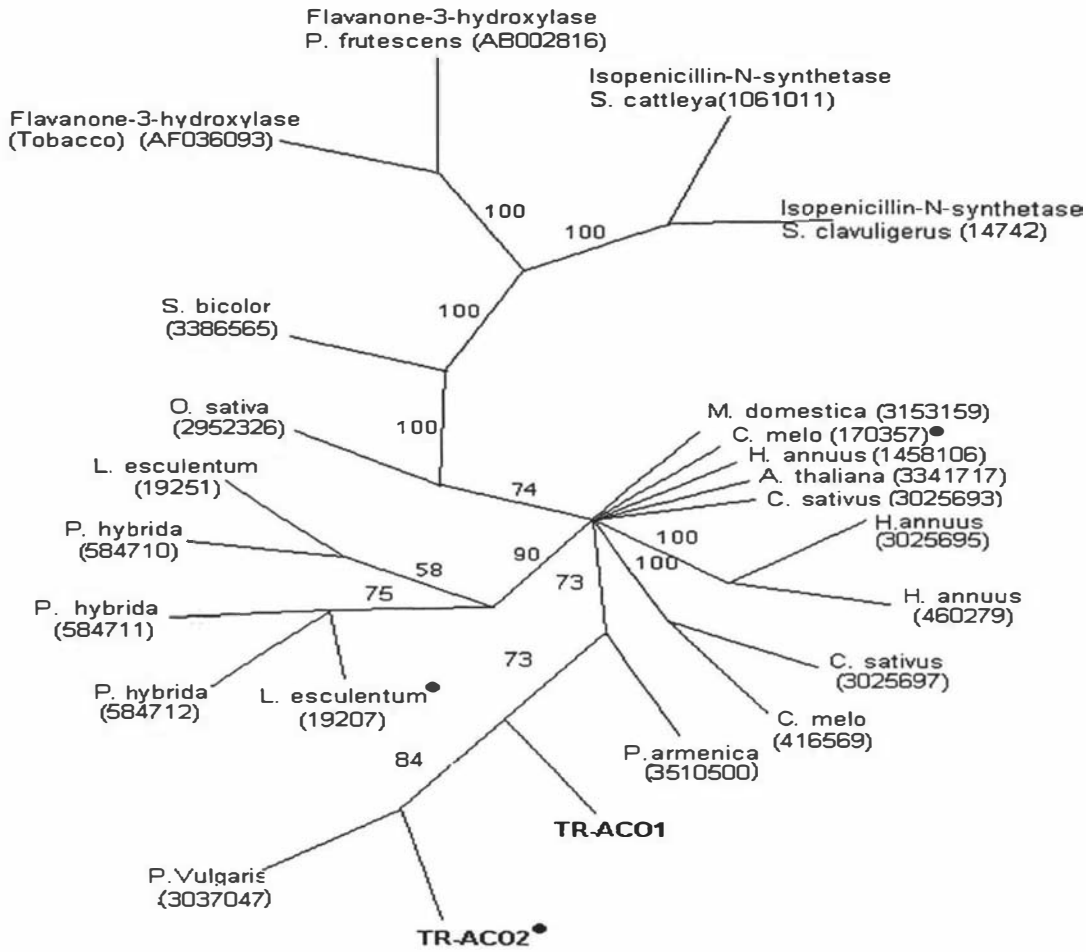

Figure 32. Phylogenetic analysis of amino acid sequences of 2-ODD members

Majority rule consensus tree using parsimony. Bootstrap values for internal splits are shown. These give an indication of the strength of the signals within the data that separate the grouping of taxa on one side of the split from taxa on the other side. Internal branches receiving less than 55 % support have been collapsed. (- ● -) Leaf senescence associated sequences.

The numbers in brackets following genera are accession numbers. P(*Phaseolus*) *vulgaris* (3037047 = ACO1); P (*Prunus*) *armenica*; H (*Helianthus*) *annuus* (1458108 = ACO2); P (*Petunia*) *hybrida* (58712 = ACO4; 584711 = ACO3; 584710 = ACO1); L (*Lycopersicon*) *esculentum* (19207 = ACO1; 19251 = ACO2); C (*Cucumis*) *melo* (416569 = ACO1; 1703057 = ACO3); C (*Cucumus*) *sativus* (3025697=ACO3; 3025693= ACO2); M (*Malus*) *domestica*; A (*Arabidopsis*) *thaliana* (ACO2); O (*Oryza*) *sativa* (2952326 = ACO1); S (*Sorghum*) *bicolor* (3386567 = ACO2) S(*Streptomyces*) *cattleya*; N (*Nicotiana*) *tabacum*; P (*Perilla*) *frutescens*; S (*Streptomyces*) *clavuligerus*.

3.8 Confirmation by genomic Southern analysis that TR-ACO1 and TR-ACO2 are encoded by distinct genes

As a prelude to genomic Southern and northern analysis of TR-ACO1 and TR-ACO2, their specificity for their own sequence in blotting analysis was examined. This was undertaken because they are very similar in nucleotide sequence (84 %, Figure 30) and so have the potential to cross-hybridise to each others sequence. Duplicate blots containing DNA from TR-ACO1 and TR-ACO2 were probed with either [α-^{32}P]-dCTP labelled TR-ACO1 or TR-ACO2 sequences and then washed at high stringency (0.1 X SSPE, 0.1 % (w/v) SDS at 65°C). At this stringency, TR-ACO1 and TR-ACO2 showed high specificity for their own cognate sequences (Figure 33). Henceforth, these washing conditions were used in subsequent DNA and RNA blot analysis.

Southern analysis of digested genomic DNA (section 2.3.4) confirmed that TR-ACO1 and TR-ACO2 were encoded by distinct genes, as both TR-ACO1 and TR-ACO2 [α-^{32}P]-dCTP labelled probes hybridised to different genomic sequences on the Southern blot (Figure 34A and B). However, each probe also hybridised to multiple sequences in each lane despite not having internal restriction sites for any of the enzymes used. Potentially, these multiple sequences could be caused by

i. incomplete digestion,

ii. the presence of restriction sites for the *Eco*R1, *Hin*d III, and Xba I within putative introns,

iii. the presence of closely related genes (possibly through gene duplication), or

iv. polymorphic alleles.

It is unlikely that incomplete digestion is the cause of the multiple banding pattern in each lane, as ethidium bromide staining revealed an even smear of digested genomic DNA throughout each lane with little high molecular weight DNA (greater than 12 000 Kb) evident (Figure 34C). Each of the other possibilities is discussed later.

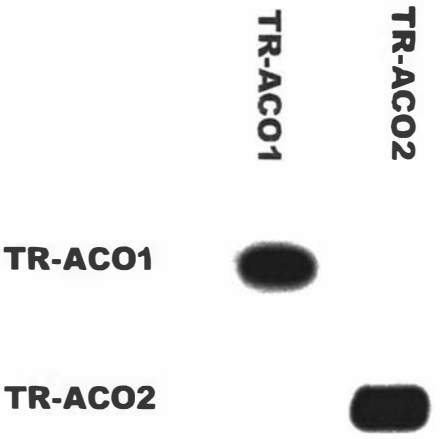

Figure 33 Specificity of TR-ACO1 and TR-ACO2 (coding-frame probes) in blotting analysis.

50 ng of TR-ACO1 and TR-ACO2 cDNA sequences were subjected to Southern analysis. The blots were washed at high stringency (0.1 X SSPE, 0.1% (w/v) SDS at 65 °C).

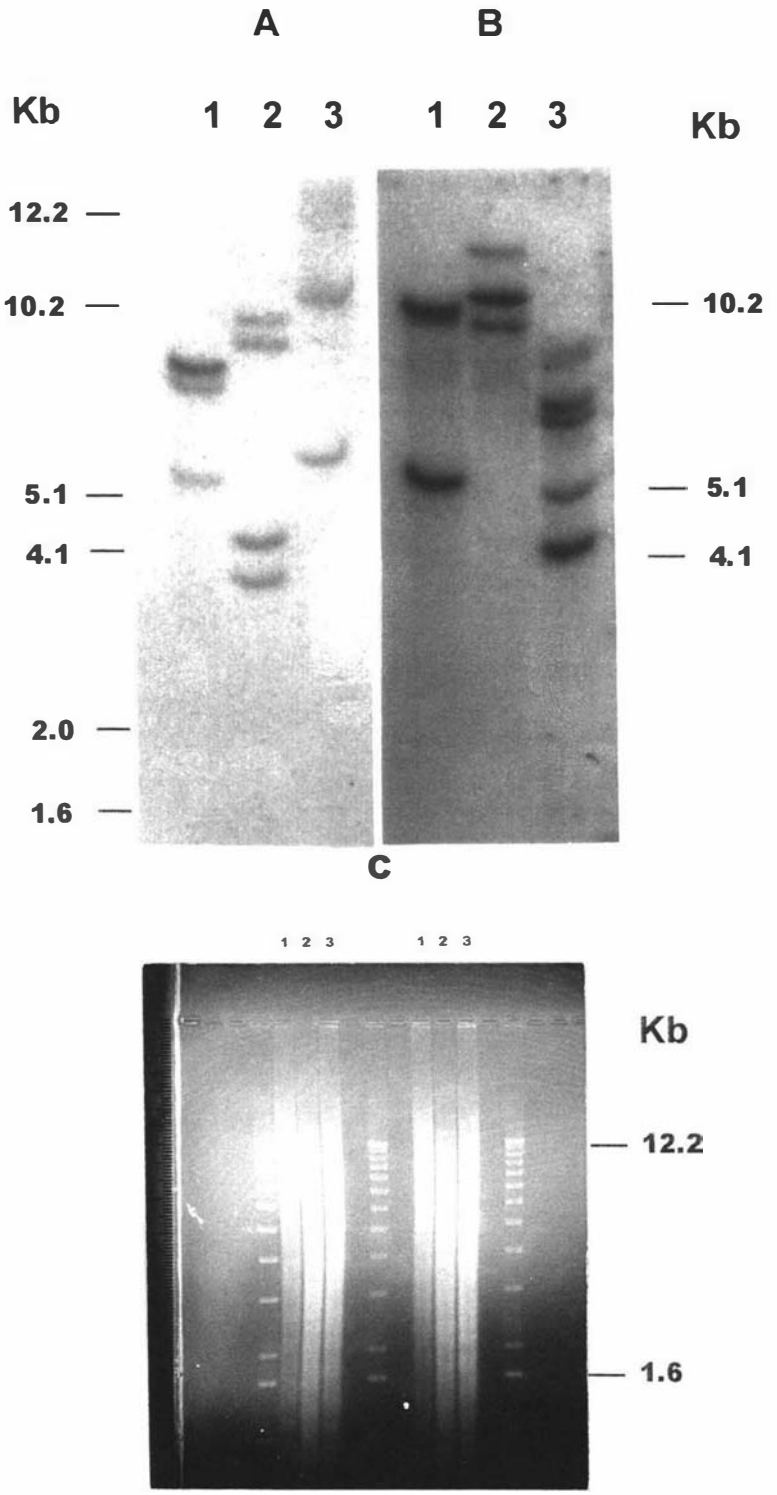

Figure 34. Southern analysis of white clover genomic DNA

A. Hybridisation pattern of [α-^{32}P]-dCTP labelled TR-ACO1.
B. Hybridisation pattern of [α-^{32}P]-dCTP labelled TR-ACO2.
C. Digested DNA visualised by ethidium bromide staining.
Lane 1, DNA cut with *Eco*R1, Lane 2, DNA cut with *Hin*d III , Lane 3, DNA cut with *Xba*I. Molecular weight markers are indicated.

With the completion of Southern analysis, the next section of the thesis involved the use of the TR-ACO1 and TR-ACO2 coding regions as probes to examine changes in expression of these genes during leaf maturation and senescence. A differential expression pattern may also confirm that TR-ACO1 and TR-ACO2 are encoded by distinct genes.

3.9 Changes in gene transcript expression of ACC-oxidase during leaf maturation and senescence of white clover by northern analysis

Prior to northern analysis, the amount of RNA able to be extracted from leaves at different stages of maturation and senescence was examined (Figure 35). The greatest amount of RNA (on a per gram fresh weight basis) was extracted from leaves that had just fully unfolded (*ca.* 550 μg g^{-1} FW; leaf 4). The level of extractable RNA then declined from leaf 5 to 8, so that by leaf 8 (mature green), only *ca.* 240 μg of RNA per gram fresh weight could be extracted. For leaves 8 to 12 (onset of chlorosis), the quantities of RNA extracted remained constant at *ca.* 240 μg g^{-1} FW. Then, as the leaves became more chlorotic, the amount of RNA obtainable from the tissue declined further, as has also been observed in senescing leaf tissue from other species (Lohman, *et al.,* 1994; Buchanan-Wollaston, 1997).

3.9.1 Gene expression of TR-ACO1 and TR-ACO2 during leaf maturation and senescence

Gene expression of TR-ACO1 and TR-ACO2 was examined in leaves 6 to 16, on a per unit fresh weight basis (Figure 36), a per unit total RNA basis (Figure 37) and a per unit poly A^+ basis (Figure 38) using northern analysis (section 2.3.7).

The TR-ACO1 sequence hybridised to a single RNA transcript on all three northern blots of *ca.* 1.35 Kb in size. The steady-state levels of this transcript were similar in mature green leaf tissue (leaves 6 to 10), but declined as the tissue became chlorotic (leaves 12 to 16) irrespective of whether expressed on a per unit fresh weight basis (no RNA for leaf 11 is present on this blot), total RNA basis, or poly A^+ RNA basis. In contrast, the TR-ACO2 sequence hybridised to two distinct RNA transcripts (1.35 Kb and 1.17 Kb) with similar intensity. This is most clearly seen on the poly A^+ RNA blot (Figure 38). Both of these transcripts were enhanced equally as the leaf tissue aged (became chlorotic), irrespective of whether expressed on a per unit fresh weight, total RNA, or poly A^+ RNA basis. Further,

the increased accumulation of the TR-ACO2 transcripts began at leaf 8 which was before visual and quantitative symptoms of chlorosis were evident (leaf 11). The gels used for analysis of RNA that were loaded by total RNA and by fresh weight and stained with ethidium bromide are also presented. Of particular interest is the gel loaded by total RNA, where it can be seen that the differential transcript accumulation patterns of TR-ACO1 and TR-ACO2 were not caused by uneven loading of the RNA.

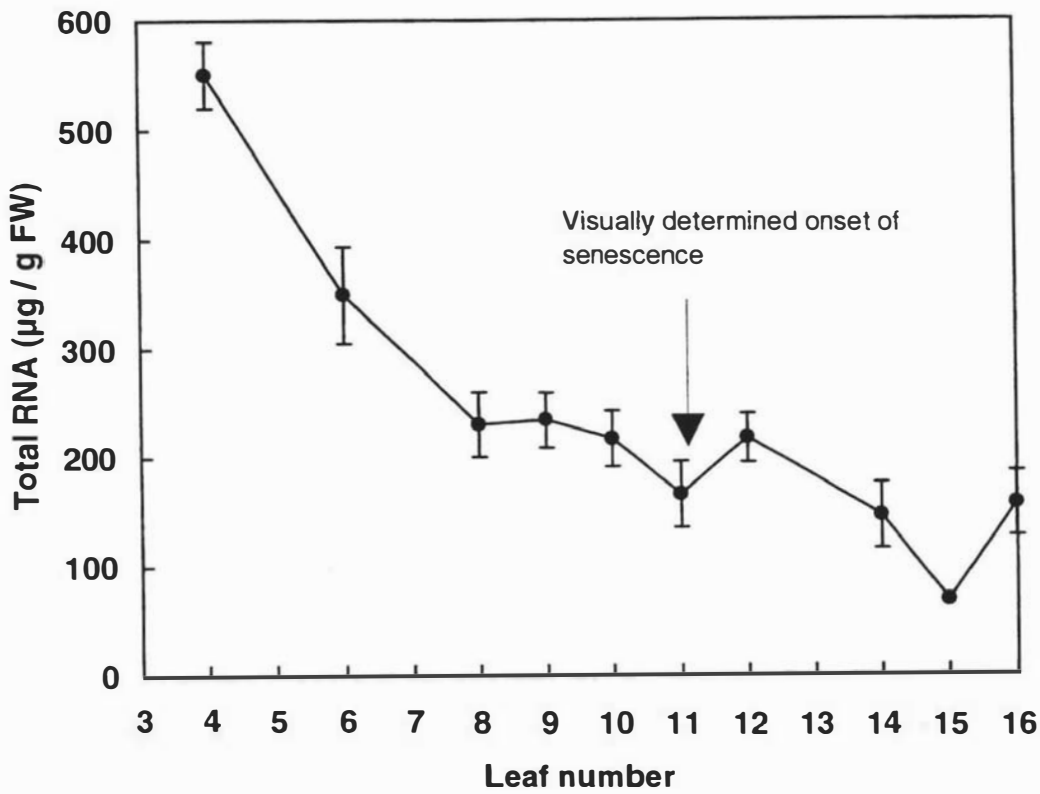

Figure 35. Concentration of total RNA extracted from mature and senescing leaves of white clover

The leaf at which chlorosis (corresponding to approximately 5 % or less degreening around the leaf margins) occurs is indicated.
Error bars = ± 1 sem. For leaves at node 6,8,9,10, 11, 12, 14, n = 4; node 4, n = 3; node 15 n= 1; and node 16 n = 2.. n = number of independent extractions.

Figure 36. Chlorophyll analysis and northern analysis of ACC oxidase gene expression expressed on a per unit fresh weight basis in mature and senescing leaf tissue of white clover using the coding frame regions of TR-ACO1 and TR-ACO2 as probes.

A. Concentration of chlorophyll in leaves used for northern analysis.
Error bars = ±1 sem for 3 internal replicates.
The leaf at which chlorosis (corresponding to approximately 5 % or less degreening around the leaf margins) is visually apparent is indicated.

B. Northern blot hybridized to either [α-^{32}P]-dCTP labelled TR-ACO1 or TR-ACO2 coding-frame probes (as labelled).

C. RNA of northern gel visualised by ethidium bromide staining. Lane 11 RNA is missing.

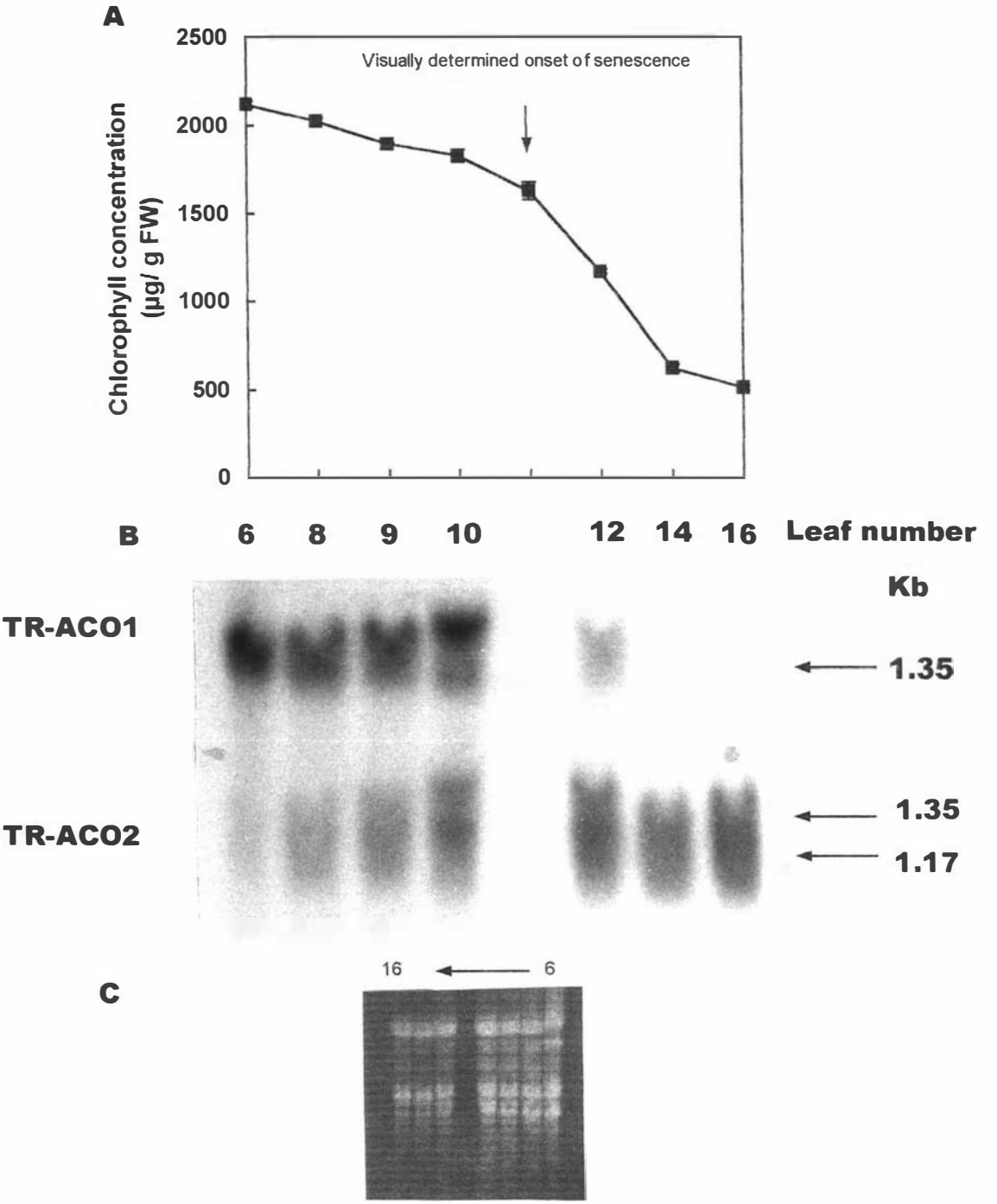
A
2500
2000
1500
1000
500
0
Chlorophyll concentration (µg/ g FW)
Visually determined onset of senescence
B
6 8 9 10 12 14 16
Leaf number
Kb
TR-ACO1
1.35
TR-ACO2
1.35
1.17
C
16
6

Figure 37. Chlorophyll analysis and northern analysis of ACC oxidase gene expression expressed on a per unit total RNA basis in mature and senescing leaf tissue of white clover using the coding frame regions of TR-ACO1 and TR-ACO2 as probes.

A. Concentration of chlorophyll in leaves used for northern analysis.
Error bars = ±1sem for n = 3 internal replicates.
The leaf at which chlorosis (corresponding to approximately 5 % or less degreening around the leaf margins) is visually apparent is indicated.

B. Northern blot hybridized to either [α-^{32}P]-dCTP labelled TR-ACO1 or TR-ACO2 coding-frame probes (as labelled).

C. RNA of northern gel visualised by ethidium bromide staining.

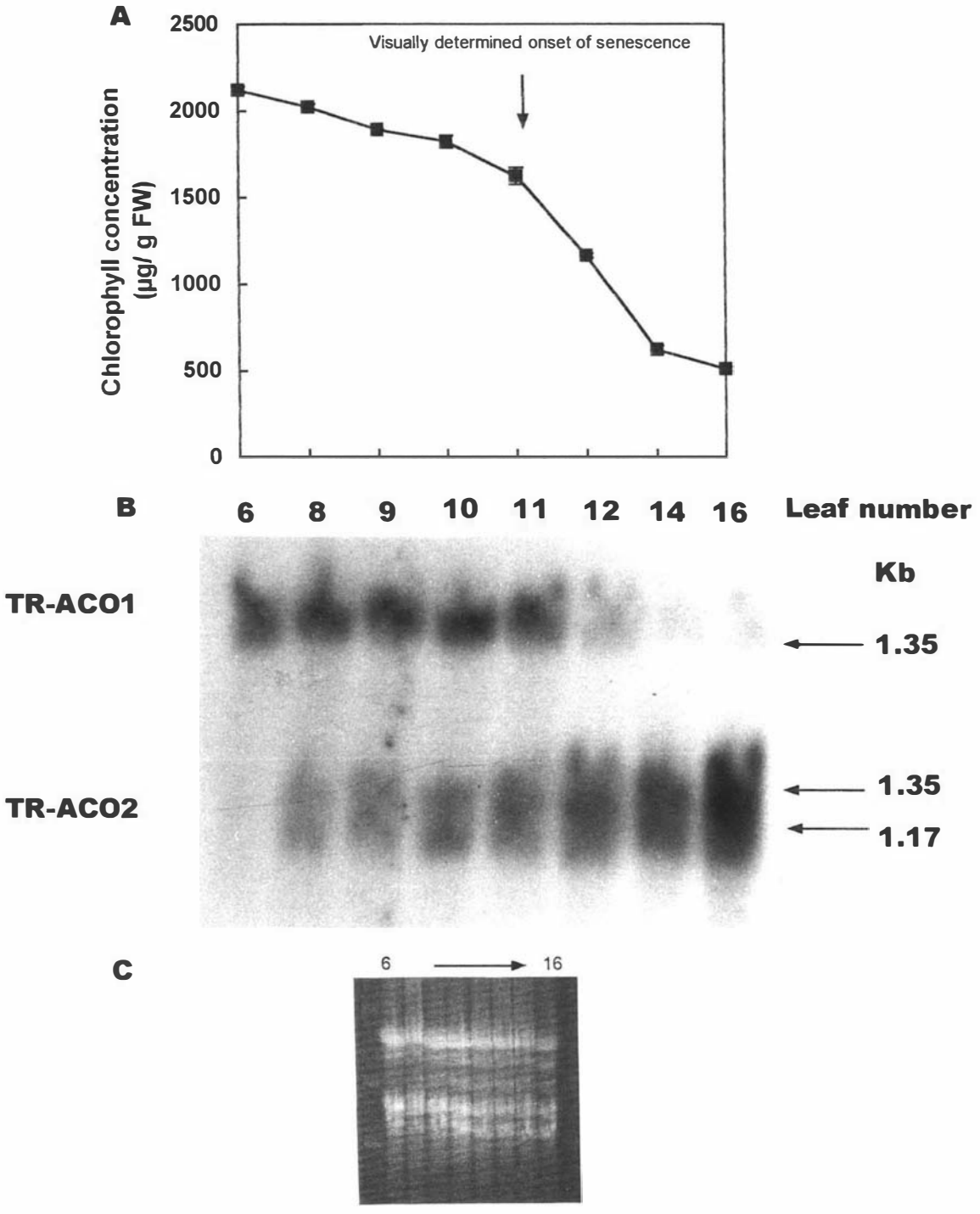
A
2500
2000
1500
1000
500
0
Chlorophyll concentration (µg/ g FW)
Visually determined onset of senescence
B
6 8 9 10 11 12 14 16
Leaf number
Kb
TR-ACO1
1.35
TR-ACO2
1.35
1.17
C
6
16

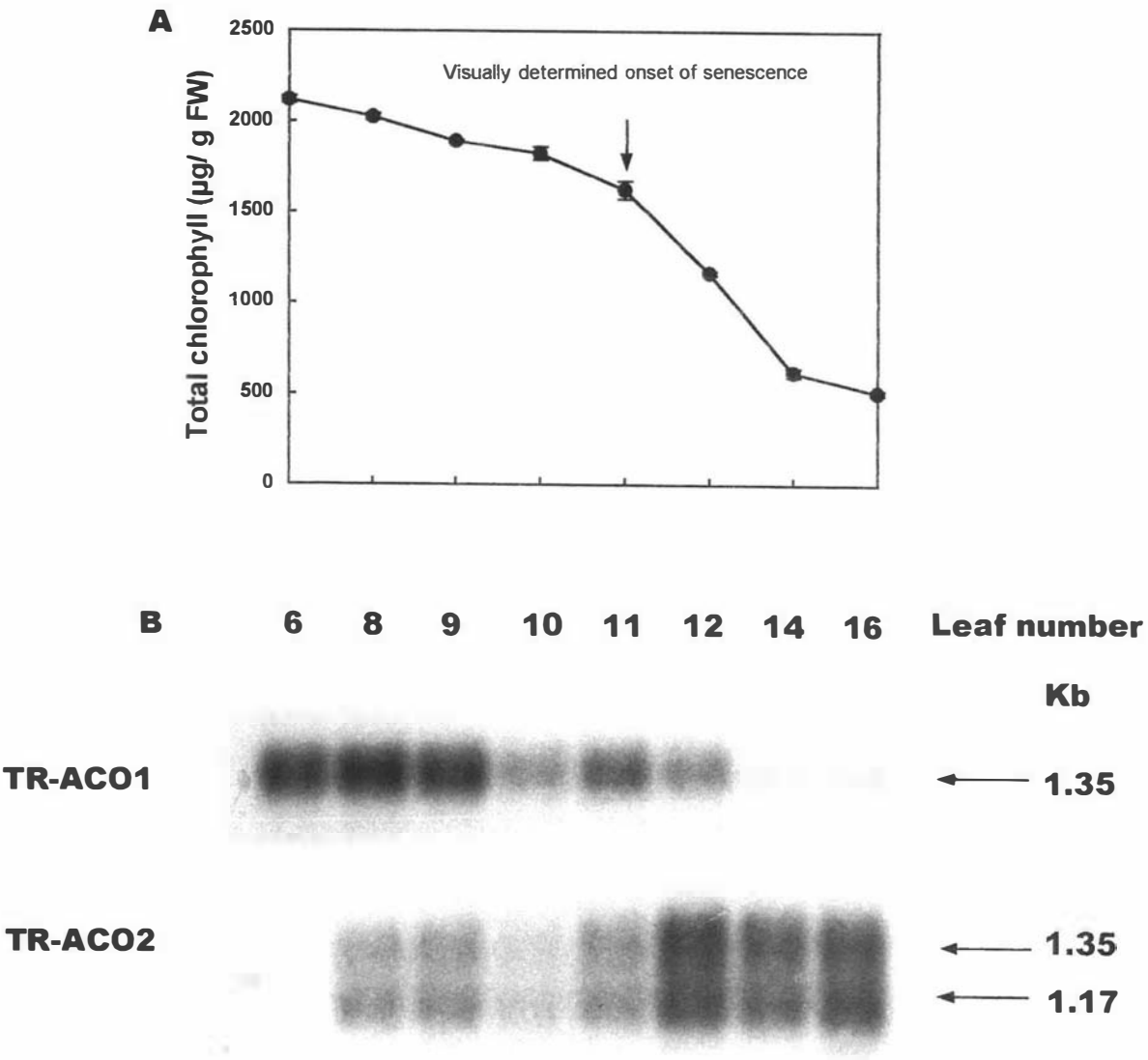

Figure 38. Chlorophyll analysis, and northern analysis of ACC oxidase gene expression expressed on a per unit poly A$^+$ RNA basis in mature and senescing leaf tissue of white clover using the coding frame regions of TR-ACO1 and TR-ACO2 as probes.

A. Concentration of chlorophyll in leaves used for northern analysis.
Error bars = ±1sem for n = 3 internal replicates.
The leaf at which chlorosis (corresponding to approximately 5 % or less degreening around the leaf margins) is visually apparent is indicated.

B. Northern blot hybridized to either [α-^{32}P]-dCTP labelled TR-ACO1 or TR-ACO2 coding-frame probes (as labelled).

The discovery that the TR-ACO2 probe recognised two RNA transcripts on the northern blot and that both TR-ACO1 and TR-ACO2 sequences hybridised to multiple genomic sequences on the Southern blot suggests that there may be additional ACC oxidase genes which are closely related to TR-ACO1 and TR-ACO2 but which are not discriminated using the coding regions as probes, even at the highest stringency of washing (0.1 X SSPE, 0.1 % (w/v) SDS at 65°C). Alternatively, the 1.17 Kb transcript may be a product of post-transcriptional processing, whereby the 3'-UTR is truncated due to the presence of an alternative polyadenylation site.

This was examined further by repeating the Southern and northern analysis with probes generated to a more divergent region of the TR-ACO1 and TR-ACO2 gene transcripts.

The 3'-untranslated region (3'-UTR) has been identified as a region of high sequence divergence among ACC oxidase gene transcripts (Barry *et al.*, 1996; Kim and Yang 1994; Tang *et al.*, 1993). For example, while ACO1 and ACO3 of tomato share greater than 94 % nucleotide sequence homology over an extensive area of the coding frame, the similarity is only 65 % and 47 % in the 5'- and 3'-UTRs respectively, and therefore it is these regions that have been used as gene-specific probes to discriminate expression of ACO1 and ACO2 in tomato tissue (Barry *et al.*, 1996).

The next section describes the amplification and sequencing of the 3'-UTRs of TR-ACO1 and TR-ACO2 and their use as probes in both Southern and northern analysis.

3.10 Confirmation of Southern and Northern analysis using 3'-RACE

The 3'-UTRs of TR-ACO1 and TR-ACO2 were generated using 3'-RACE (Randomly Amplified cDNA Ends). RACE is an RT-PCR technique first described by Frohman *et al.*, (1988) for the amplification of either the 5'-UTR or the 3'-UTR of mRNA. The main difference between 3'-RACE and conventional RT-PCR is that the downstream (3') primer is replaced by a primer rich in T residues which binds to the poly A^+ tail of the mRNA and acts as the primer for the RT reaction.

3.10.1 Identification of the 3'-UTRs of TR-ACO1 and TR-ACO2

3.10.1.1 Development of 3'-RACE:degenerate primer approach

Initially, RT-PCR (section 2.3.6) was performed using the degenerate upstream primers previously used to generate the TR-ACO1 and TR-ACO2 coding regions, but with the downstream primers (ACOR1 and E102, see Figure 10) replaced with the 17 mer oligo d(T) primer.

3'-RACE was performed on RNA isolated from leaves 9 and 14, as it had been shown previously by RT-PCR that both TR-ACO1 and TR-ACO2 could be amplified from RNA isolated from these leaves. It was predicted from a consensus of published sequences that the amplified products should be *ca.* 1000 to 1200 bp in size , comprising of *ca.* 840 bp coding frame and *ca.* 200 to 300 bp 3'-UTR. For example, the 3-UTR of apple pAE12 is 191 bp (Dong *et al.,* 1992), avocado pAVOe3, 159 bp (McGarvey *et al.,* 1990), *Pelargonium x hortorum* GEFE-1, 249 bp (Wang *et al.,* 1994), *P. hybrida* pPHEFE, 227 bp (Wang and Woodson, 1992), *C. melo* CM-ACO1, 248 bp (Lasserre *et al.,* 1996), peach pch 313, 253 bp (Callahan *et al.,* 1992), and mung bean pVR-ACO1, 317 bp (Kim and Yang, 1994).

Initially, 3'-RACE was performed using different concentrations of both upstream (degenerate) and the downstream 17 mer oligo d(T) primers to determine the conditions needed for formation of a discrete cDNA product(s).

The concentration of the 17 mer oligo d(T) primer was increased in the PCR mix as it has been proposed to improve yields of cDNA product in amplification mixes (Czerny, 1996). However, increasing primer concentration from 250 nM to 1 μM did not result in the formation of discrete products (Figure 39, lane 2 and 3). By contrast, it appeared that non-specific amplification was occurring during the PCR.

The specificity of a PCR may be improved by using nested degenerate primers, and so second round PCR amplification using E101 (the nested primer of ACOF1) was performed on 2 μL of the first round amplification products of lane 2. To increase further the likelihood of a successful PCR, a series of increasing concentrations of the second round primer was used, as it has been suggested that when using degenerate primers higher concentrations of primer (1- 3 μM) should be used (Rychlik, 1993).

Figure 39. Development of 3'-RACE: degenerative primer approach

Lane 1, 4, 8, 12, 16. Gibco BRL 1 Kb DNA Ladder
Lane 2. PCR of leaf 9 RT mix, 333 nM ACOF1, 250 nM oligo d(T).
Lane 3. PCR of leaf 9 RT mix, 333 nM ACOF1, 1 µM oligo d(T).
Lane 5. Second round PCR using 2 µL of lane 2 amplification products as a template, 333 nM E101, 250 nM oligo d(T).
Lane 6. Second round PCR using 2 µL of lane 2 amplification products as a template, 666 nM E101, 250 nM oligo d(T).
Lane 7. Second round PCR using 2 µL of lane 2 amplification products as a template, 3.33 µM E101, 250 nM oligo d(T).
Lane 9. PCR of leaf 9, RT mix 1.667 µM ACOF1, 250 nM oligo d(T).
Lane 10. No template control 1.667 µM ACOF1, 250 nM oligo d(T).
Lane 11. PCR of leaf 14 RT mix , 1.667 µM ACOF1, 250 nM oligo d(T).
Lane 13. Second round PCR using 2µL of lane 9 amplified products as a template, 1.667 nM E101, 250 nM oligo d(T).
Lane 14. Second round PCR using 2 µL of lane 11 amplified products as a template, 1.667 nM E101, 250 nM oligo d(T).
Lane 15. No oligo d(T) control: PCR of 2 µL of lane 9 amplification products, 1.667 nM E101.
Lane 17. PCR using gel-purified amplification products of *ca.* 900 to 1400 bp in size from lane 9 PCR products as template.
Lane 18. PCR using gel purified amplification products of *ca.* 900 to 1400 bp in size from lane 11 PCR products as template.

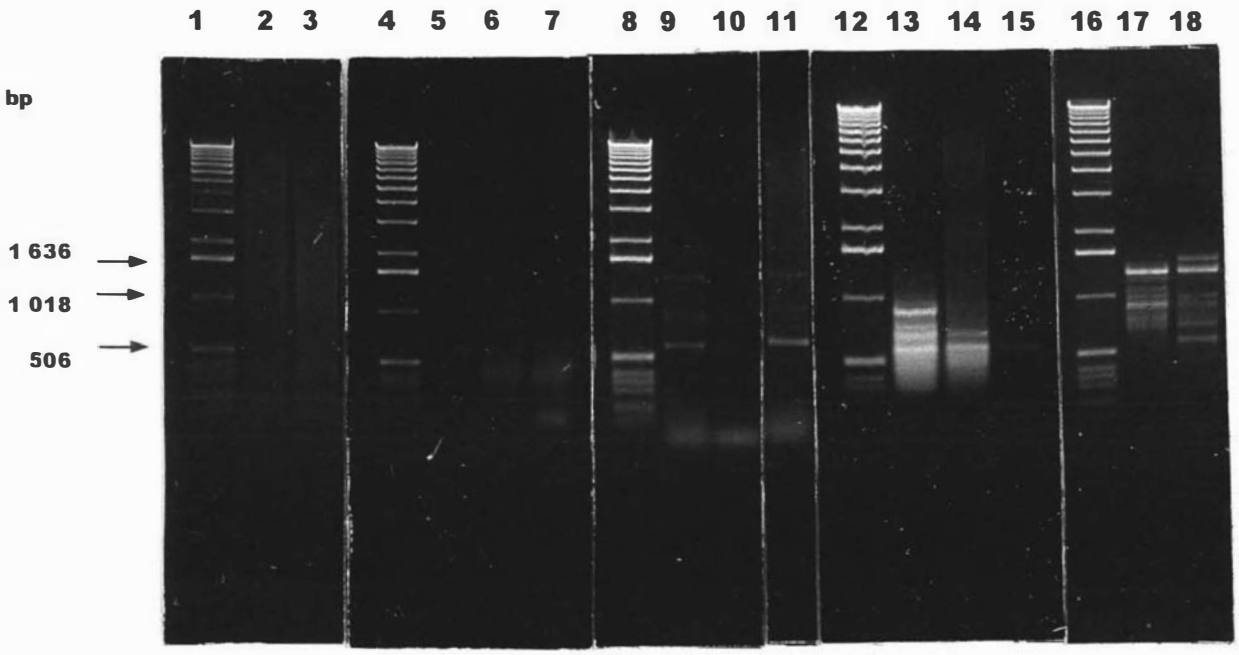
1 2 3 4 5 6 7 8 9 10 11 12 13 14 15 16 17 18
bp
1 636
1 018
506

However, second round PCR with the nested primer (E101) did not increase the specificity of the PCR (i.e. the formation of discrete cDNA products) even if the primer concentration was increased from 333 nM to 3.33 μM (lanes 5 to 7).

The effect of increasing ACOF1 primer concentration in the PCR mix from 333 nM (used in lanes 2 and 3) to 1.667 nM on product formation was further examined in lanes 9 and 11. The increased concentration of ACOF1 in the PCR did produce discrete amplified products of *ca.* 650, 900 and 1380 bp in size. However, the smaller of these fragments (*ca.* 650 and 900 bp) were too small to be putative ACC oxidase sequences as they were smaller than the coding regions of TR-ACO1 and 2 previously generated with ACOF1 (*ca.* 840 bp). Whilst the largest fragment (*ca.* 1380 bp) appeared too large as northern analysis had previously determined the total size of the TR-ACO1 and TR-ACO2 gene transcripts as 1.35 Kb.

A further (second-round) amplification was performed with the nested primer, E101, on the PCR mixes that generated the discrete bands (in lanes 9 and 11) to see whether further amplification would result in products of the expected size. Again an upstream primer concentration in the mix of 1.667 nM was able to generate discrete bands, but all of which were too small (less than 900 bp) to have contained the 3'-UTR (lanes 13 and 14).

A further way by which the specificity of second round amplification may be increased is to excise the region of the gel where the products of the first round amplification were expected, elute the fragments from the gel and perform second round amplification. This was performed by excising a region from *ca.*900 bp to 1400 bp of lane 9 and lane 11, snap-freezing, and repeating the PCR with 1.667 nM E101 (replacing the 1.667 nM ACOF1). Many of the products obtained were smaller in size than the region excised from the gel (lanes 9 and 11) and not around the size expected *ca.* 1000 to 1200 bp (lanes 17 and 18). The major staining fragment (*ca.* 1380 bp) was again the same as observed previously in lanes 9 and 11 which was considered as too large.

It was therefore decided to use a gene-specific primer (GSP) approach at a higher annealing temperature to minimise production of spurious amplification products and specifically amplify the 3'-UTR of TR-ACO1 and TR-ACO2.

3.10.1.2 Development of 3'-RACE:Gene-specific primer approach

A gene-specific primer, designated ACOF2 (see Figure 30), was designed as complementary to a region of 20 bp approximately 250 bp from the 3' end of the coding regions of both TR-ACO1 and TR-ACO2. This region was chosen so that after amplification the 3'-UTRs could easily be associated with their corresponding coding frame by sequence homology. The advantage of using gene-specific primers is that they enable higher annealing temperatures during the PCR, which in turn increases the specificity of the amplification reactions. However, at these higher temperatures the annealing efficiency of the 17 mer oligo d(T) primer to the poly A tails of cDNA sequences is compromised due to the weaker H^+-bonding of A-T residues (Frohman *et al.*, 1988). This problem is circumvented by replacing the downstream 17 mer oligo d(T) primer in the RT reaction with ADAPdT (refer Figure 9). ADAPdT is a hybrid primer which consists of a GC containing oligonucleotide (ADAP) attached to the 5' end of 17 oligo d(T) residues. Hybridisation of ADAPdT to mRNA in the RT-reaction incorporates ADAP into all first strand cDNA species synthesized. A sequence that is complementary to ADAP can then serve as an effective primer in the subsequent PCR.

After first round amplification using ACOF2 (333 nM) and the ADAP (333 nM) as primers and an annealing temperature of 50°C, 5 µL aliquots of each reaction were resolved in a 1 % (w/v) agarose gel. Four discrete cDNA products (*ca.* 250 bp, 400 bp, 500 bp and 600 bp) were amplified from the RT mix of RNA extracted from leaf 9 and 14 (Figure 40, lanes 2 and 3). Approximately 250 bp of the sequence should be coding region due to the position of the ACOF2 priming site in the sequence. This suggested that the size of the *ca.* 250 bp amplified product would be too small to contain the 3'-UTR of either TR-ACO1 or TR-ACO2. The PCR was repeated with a higher annealing temperature (from 50°C to 55°C) to increase the specificity of the amplification (lanes 5 and 6). The 250 bp product was not amplified at this higher temperature, while the three larger cDNA sequences (*ca.* 400 bp, 500 bp, and 600 bp) were amplified from both the leaf 9 and 14 RT mixes. Controls were included for the PCR, such as a PCR with no template (lane 7), a PCR with no upstream primer (ACOF2; lane 8), and a PCR with no downstream primer (ADAP; lane 9). No product was amplified in these controls which indicated that the complete PCR mix was necessary for the amplification of the three cDNA sequences and also confirmed that the products were not artifacts.

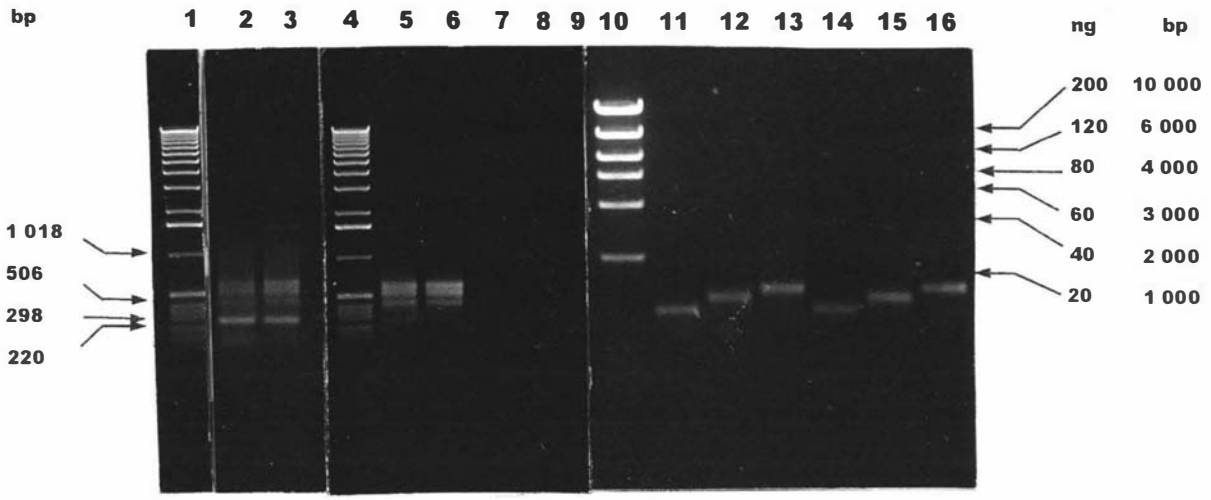

Figure 40. Development of 3'-RACE: gene-specific primer approach

Lane 1. Gibco BRL 1 Kb DNA Ladder.
Lane 2. PCR of leaf 9 RT mix, 333 nM ACOF2, 333 nM ADAP, annealing temp. of 50°C.
Lane 3. PCR of leaf 14 RT mix, 333 nM ACOF2, 333 nM ADAP, annealing temp. of 50°C.
Lane 4. Gibco BRL 1 Kb DNA Ladder.
Lane 5. PCR of leaf 9 RT mix, 333 nM ACOF2, 333 nM ADAP, annealing temp. of 55°C.
Lane 6. PCR of leaf 14 RT mix, 333 nM ACOF2, 333 nM ADAP, annealing temp. of 55°C.
Lane 7. No template control: 333 nM ACOF2, 333 nM ADAP, annealing temp. of 55°C.
Lane 8. No ACOF2 control: PCR of leaf 9 RT mix, 333 nM ADAP, annealing temp. of 55°C.
Lane 9. No ADAP control: PCR of leaf 9 RT mix, 333 nM ACOF2, annealing temp. of 55°C.
Lane 10. Gibco BRL High DNA Mass Ladder.
Lane 11. Gel- and column-purified 400 bp fragment from leaf 9 RT-PCR mix, lane 5.
Lane 12. Gel- and column-purified 500 bp fragment from leaf 9 RT-PCR mix, lane 5.
Lane 13. Gel- and column-purified 600 bp fragment from leaf 9 RT-PCR mix, lane 5.
Lane 14. Gel- and column-purified 400 bp fragment from leaf 14 RT-PCR mix, lane 6.
Lane 15. Gel- and column-purified 500 bp fragment from leaf 14 RT-PCR mix, lane 6.
Lane 16. Gel- and column-purified 600 bp fragment from leaf 14 RT-PCR mix, lane 6.

Molecular size markers are indicated on the left and right of the figure in bp. The mass in ng for each of the molecular size markers in lane 10 is also indicated to the right of the figure.

The PCR mixes containing the amplified products (*ca.* 400, 500 and 600 bp) were precipitated with ethanol, resuspended in sterile water and gel-purified through a 1 % (w/v) agarose gel. The 400 bp, 500 bp, and 600 bp cDNA amplified products were then excised, column-purified and their concentrations estimated by fractionation along side the GIBCO BRL DNA mass ladder (Figure 40; lanes 11 to 16). The amplified products of the putative 3'-UTR of ACC oxidase were then individually TA-cloned into the pCR 2.1 vector and transformed into *E. coli* strain DH-5α. After selection on Amp^{100} LB media, transformants were grown overnight in LB broths, their plasmids isolated by alkaline lysis and the presence of the insert (*ca.* 400 bp, 500 bp, and 600 bp) confirmed by restriction digestion (Figure 41).

The 400, 500 and 600 bp inserts separated from the cut plasmids in 1 % (w/v) agarose gels appeared to be represented as doublets (Figure 41A). It was confirmed that the doublets were probably an artifact of the separation through the 1 % (w/v) agarose gels, by amplifying inserts from plasmids in lane 4, 8 and 13 (Figure 41A) by PCR with ACOF2 and ADAP and checking the products on a 1 % (w/v) agarose gel (Figure 41B, lanes 2 to 4).

*Eco*R1 digests of plasmids that were isolated from bacteria TA-cloned with the 400 bp fragment are shown in lanes 2 to 6, and the inserts in lanes 2, 4, 5, and 6 that were of consistent size were column-purified and sequenced. *Eco*R1 digests of TA-cloned plasmids with the 500 bp fragment are shown in lanes 8 to 12, and the plasmids in lanes 8 and 11 were sequenced. *Eco*R1 digests of TA-cloned plasmids with the 600 bp fragment are shown in lanes 14 to 19, and the plasmids in lanes 14, 15, and 16 were sequenced. The different sizes of the insert in some of the lanes, e.g. lane 3, 10, and 12 (Figure 41A) were assumed to be due to anomalies produced during cloning and so were ignored.

Figure 41. Confirmation of transformed colonies after TA-cloning of putative 3'-UTRs.

Restriction digestion of plasmids containing putative 3'-UTRs of ACC oxidase

Lanes 1, 7, 13. GIBCO BRL 1 Kb DNA Ladder.

Lanes 2 to 6. Digestion of pCR 2.1 plasmids containing a 400 bp putative ACC oxidase 3'-UTRs.

Lanes 8 to 12. Digestion of pCR 2.1 plasmids containing a 500 bp putative ACC oxidase 3'-UTRs.

Lanes 14 to 19. Digestion of pCR 2.1 plasmids containing a 600 bp putative ACC oxidase 3'-UTRs.

B. PCR amplification using 1 µL of a representative plasmid from each transformation.

Lane 1. GIBCO BRL 1 Kb DNA Ladder.

Lane 2. PCR amplification of plasmid from lane 4, containing 400 bp putative ACC oxidase 3'-UTR, 333 nM ACOF2, 333 nM ADAP, annealing temp. of 50°C.

Lane 3. PCR amplification of plasmid from lane 8, containing 500 bp putative ACC oxidase 3'-UTR, 333 nM ACOF2, 333 nM ADAP, annealing temp. of 50°C.

Lane 4. PCR amplification of plasmid from lane 13, containing 600 bp putative ACC oxidase 3'-UTR, 333 nM ACOF2, 333 nM ADAP, annealing temp. of 50°C.

A

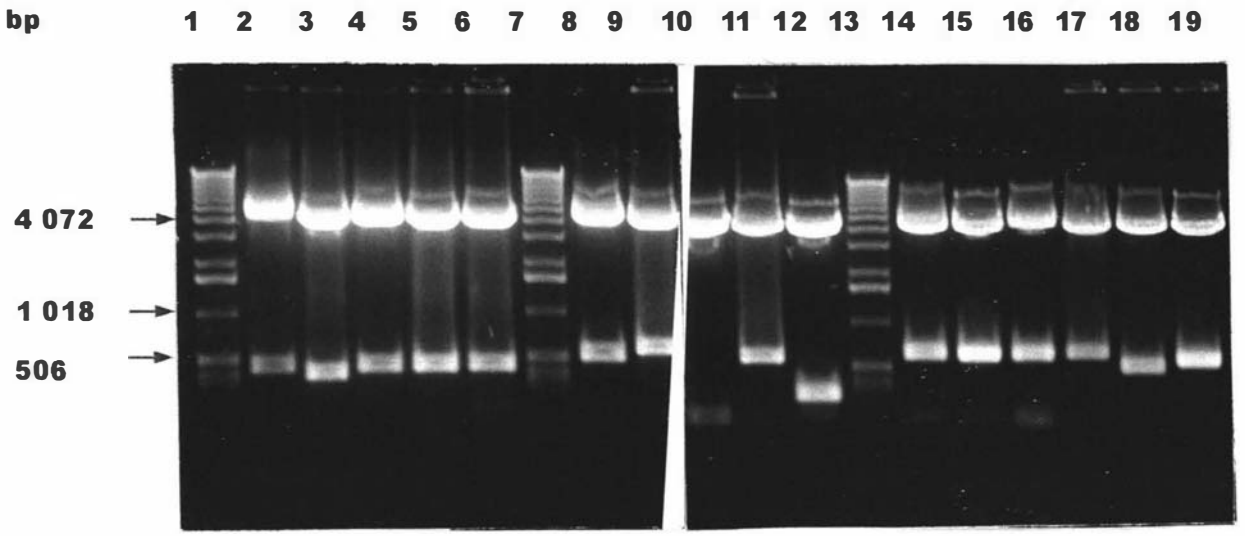
bp
1 2 3 4 5 6 7 8 9 10 11 12 13 14 15 16 17 18 19
4 072
1 018
506

B

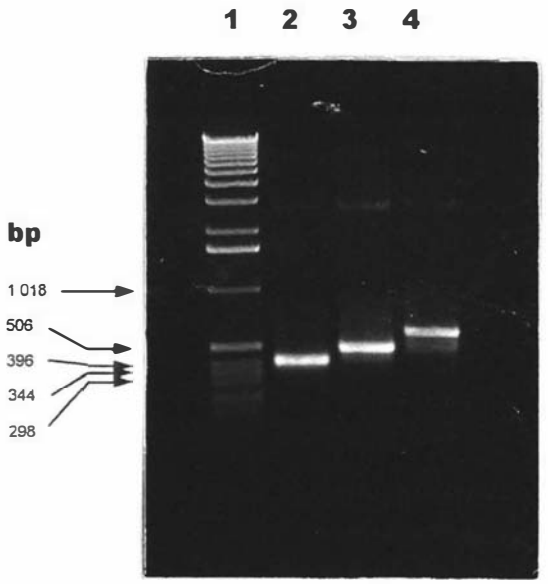
1 2 3 4
bp
1 018
506
396
344
298

3.10.1.3 Confirmation of putative ACC oxidase 3'-UTR gene transcripts by sequence analysis

Sequence alignment identified the two smaller 3'-UTR amplified products of *ca.* 400 and 500 bp to be truncated versions of the larger 600 bp product (Figure 42). The high sequence homology of their coding frame regions with TR-ACO2 suggested that only the 3'-UTR sequence of TR-ACO2 had been cloned. The truncated versions of the 600 bp product may have arisen because the RT reaction was carried out at a relatively low temperature (42°C), since at this temperature a stretch of A residues as short as 6 to 8 nt can serve as a binding site for an oligo d(T)-tailed primer (Frohman, 1993). However, in the 3'-UTR of TR-ACO2 there was only one region that contained six adjacent 'A' residues (position 936-941; Figure 42), and this region was not one of the binding sites for the oligo d(T)-tailed primer (as determined by sequence analysis). This suggests that the 400 bp and 500 bp products are not artifacts produced by non-specific binding of the 17-mer oligo d(T) region of ADAPdT to additional poly A rich regions within the 3'-UTR of TR-ACO2.

The three 3'-UTRs of TR-ACO2 may be explained by the presence of multiple sequences termed Near Upstream Elements (NUE) and Far Upstream Elements (FUE) (Rothnie, 1996) upstream of the polyadenylation sites of TR-ACO2 (Figure 42). These are regions characteristic of certain plant mRNAs that alter the position of attachment of the poly A tail, for example, 14 distinct 3'-end processing sites have been identified in the chloroplast binding protein of tobacco (Klahre *et al.*, 1995).

The 3'-UTRs of gene-transcripts contain, in addition to polyadenylation signaling regions, other motifs that can provide the researcher with additional information on gene regulation. For instance, the pentamer motif (AUUUA) has been implicated in determining the stability of transcripts *in vivo* (Ohme-Takagi *et al.*, 1993), and three such regions can be identified in the 3'-UTR of TR-ACO2.

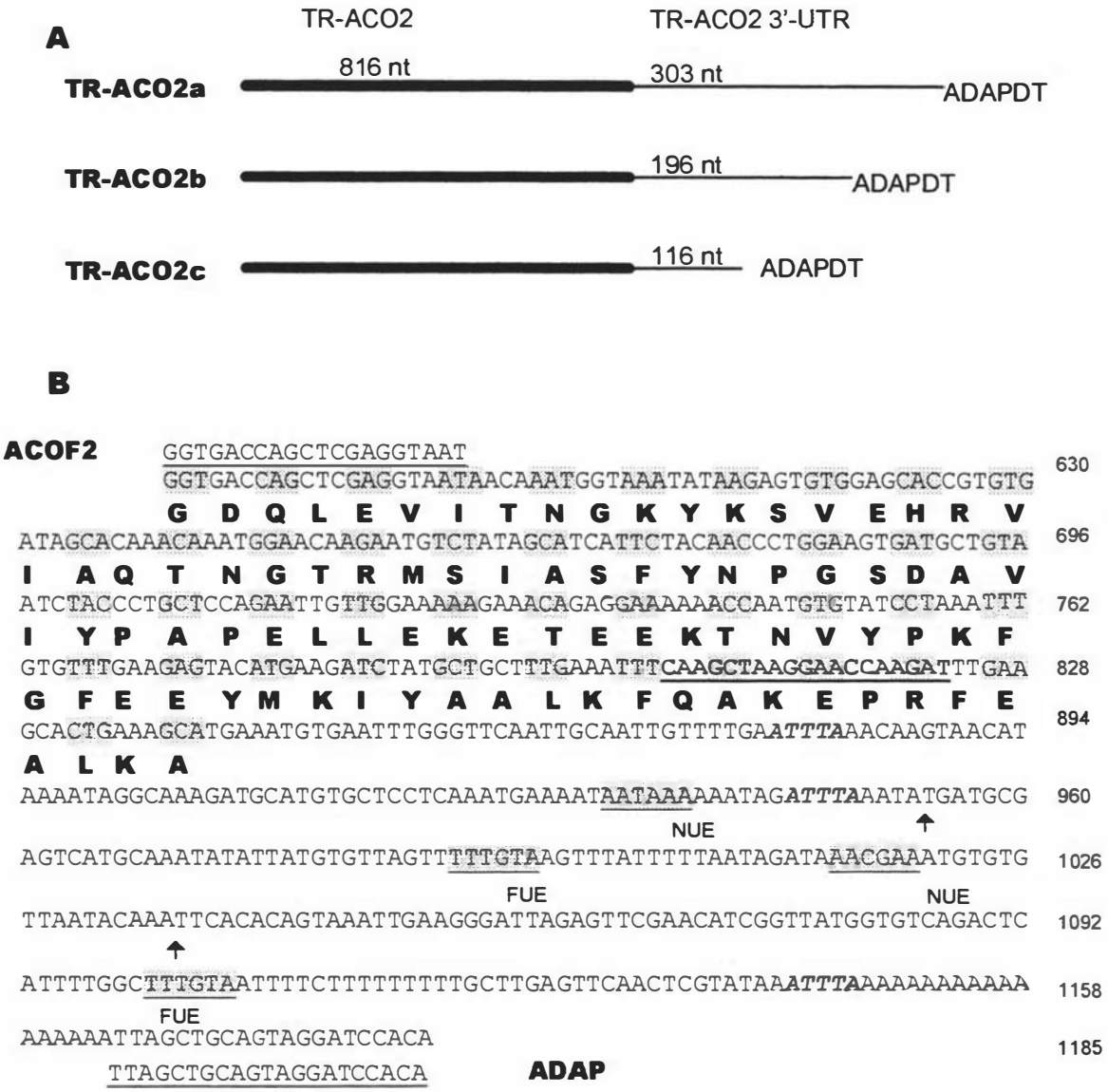

Figure 42. Nucleotide and deduced amino acid sequence of TR-ACO2 3'-translated and untranslated regions generated by 3'-RACE.

The sequences were generated using a gene-specific primer ACOF2 (underlined) and a sequence, ADAP, previously attached during first strand synthesis to the poly-A tail of TR-ACO2.

A. Schematic diagram of the three truncated 3'-UTR's of TR-ACO2.

B. Sequence of the 3'- translated and untranslated regions of TR-ACO2.

The arrows indicate the truncated versions of TR-ACO2 found. Also indicated is ACOF2b (**bold underlined**), the primer used subsequently with ADAP for TR-ACO2 probe generation. Three AUUUA pentamers (***bold,italics***), Near upstream elements (NUE) and far upstream elements (FUE) (highlighted, underlined) are indicated. The NUE designated at position 1213 is potentially another slight variation of NUEs documented so far (the U nt replaced by C).

A total of 21 clones (i.e. nine inserts (400 bp), six inserts (500 bp), and six inserts (600 bp) product) were eventually sequenced and all 21 identified as TR-ACO2 sequences. It appeared that the ACOF2 primer, although made complementary to a region present in both TR-ACO1 and TR-ACO2 sequences, was predominantly amplifying TR-ACO2 sequences.

To increase the chance of amplifying the 3'-UTR of TR-ACO1, 3'-RACE was repeated on RNA isolated from leaves at node 6, as northern analysis had previously shown in leaves at this node, that transcript levels of TR-ACO1 were high, while in contrast, transcript levels of TR-ACO2 were low (refer Figure 38). In order to increase further the specificity of the PCR, nested gene-specific primers made to a complementary region specific to TR-ACO1 were used .

3.10.1.4 Isolation of TR-ACO1 3'-UTR by the GSP approach

Two rounds of PCR were performed, and the upstream primer ACOF2, replaced with the nested primers, ACOF4 and ACOF4a (see Figure 30).

After amplification had been completed, aliquots (5 μL) of both first and second round mixes were separated in adjacent lanes of a 1 % (w/v) agarose gel (Figure 43; lanes 2 and 3). Amplification with the first round primer, ACOF4, did not produce a discrete cDNA product (lane 2), but upon further amplification with the second round primer, ACOF4a, an *ca.* 400 bp fragment was generated (lane 3).

The nucleic acid from the second round amplification mix was precipitated with ethanol, the *ca.* 400 bp DNA fragment gel- and column-purified and TA-cloned into *E. coli* strain DH 5α. DNA inserts from six transformed colonies were sequenced.

Sequence alignment of the coding frame portion with the 3'-terminal coding frame region of TR-ACO1 confirmed that 3'-RACE (with ACOF4 and ACOF4a as primers) was successful at generating the 3'-UTR (233 bp) of TR-ACO1 (Figure 43).

Putative cis-acting motifs for poly A signaling were also identified, but unlike TR-ACO2 there was not multiple NUEs and FUEs in the 3'-UTR and this may explain why only one discrete sequence was amplified. Another difference between the 3'-UTR of TR-ACO1 and TR-ACO2 was the complete absence of the putative cis-acting instability motif, AUUUA in TR-ACO1.

A

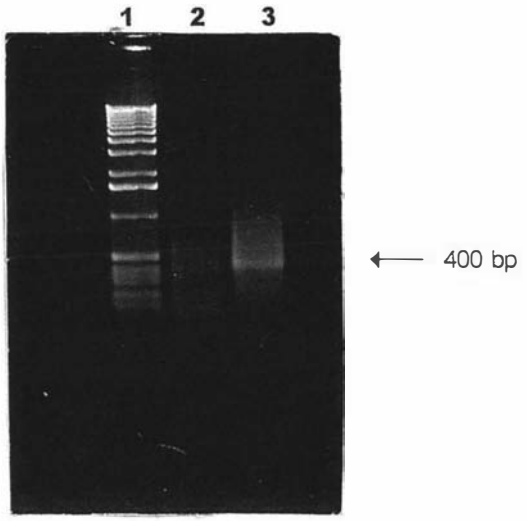

B

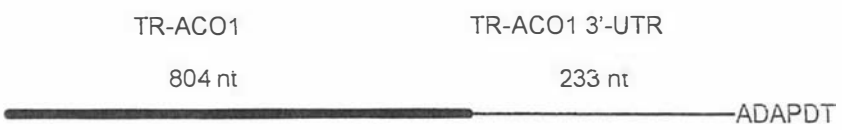

C

ACOF4 GTTATCTATCCAGCAACAAC

ACOF4A CTATCCAGCAACAACATTGA

CTATCCAGCAACAACATTGATTGAAGAGAATAATGAAGTTTACCCAAAATTT 750

Y P A T T L I E E N N E V Y P K F

GTTTTTGAAGATTACATGAATCTTTATGCTGGATTAAAGTTTCAAGCTAAAGAACCAAGATTTGAA 816

V F E D Y M N L Y A G L K F Q A K E P R F E

GCATTTAAGGAATCATCAAATGTTAAA**CTTGGTCCAATTGCAACAGT**TTAATTATGTGTTACTATA 882

A F K E S S N V K L G P I A T V

AATAAATAAAAAATAATATAAATATATGTTAACATGTTTGTTTAAGTGGAAGCAAGCAAAGTAAAA 948

AA***AAGCTT***AAAGTCAAGTGCATAAGTTTCTCAAATTAGTATGTAGTTGTTTACTTACTATATAGTG 1014

AGTGATGTGATGTGATTTTCTTGTATTATTTGTGGAAAAAGTAATATCAATGTTCAATATAATAAT 1080

FUE NUE

AAATATATTATTCAAGTAAAAAAAAAAAAAAAAAATTAGCTGCAGTAGGATCCACA 1135

TTAGCTGCAGTAGGATCCACA **ADAP**

Figure 43 Nucleotide and deduced amino acid sequence of the TR-ACO1 3'-translated and untranslated regions

A. PCR amplification of putative 3'-UTR of TR-ACO1.

Lane 1.1 Kb DNA ladder.

Lane 2.PCR of leaf 9 RT-mix, primers were 333 nM ACOF4 and 333 nM ADAP.

Lane 3.Second round amplification using 2μLof amplified products from lane 2, primers were 333 nM ACOF4A and 333 nM ADAP, annealing temp. of 55°C . The arrow denotes the size in bp of the amplified fragment.

B. Schematic diagram of the 3'-UTR of TR-ACO1.

C. Sequence of the 3'-translated and untranslated regions of TR-ACO1.

The primer used subsequently for TR-ACO1 probe generation with ADAP is indicated (ACOF4b, **bold underlined**). Near upstream elements (NUE) and far upstream elements (FUE) (highlighted, underlined)are indicated. At the position of the A in the FUE (indicated by arrow) is normally found a T (U for mRNA) (Rothnie, 1996). Also indicated is the *Hin*d III restriction site found within the 3'-UTR (***bold, italics***).

3.10.1.5 3'-UTR probe production for blot analysis

TR-ACO1 and TR-ACO2 3'-UTR sequences (minus the majority of the 3' coding region) were generated by RT-PCR from column-purified plasmids containing the cloned sequences using ACOF4b (see Figure 43) and ACOF2b (see Figure 42) respectively as the upstream primers (Figure 44). The sequence homology of TR-ACO1 and 2 was reduced from 84 % in their coding regions (see Figure 30) to 61 % in their 3'-UTRs (Figure 45).

The reduction in homology between the 3'-UTR regions of TR-ACO1 and TR-ACO2 confirmed the greater sequence divergence in the 3'-UTR. These sequences were used as probes to further characterise the expression of TR-ACO1 and 2 during leaf maturation and senescence.

A

ACOF4b CTTGGTCCAATTGCAACAGTT

CTTGGTCCAATTGCAACAGTTTAATTATGTGTTACTATAAATAAATAAAAAATAATA

L G P I A T V

TAAATATATGTTAACATGTTTGTTTAAGTGGAAGCAAGCAAAGTAAAAAAAAAGCTTAAAGTCAAGTGC

ATAAGTTTCTCAAATTAGTATGTAGTTGTTTACTTACTATATAGTGAGTGATGTGATGTGATTTTCTT

GTATTATTTGTGGAAAAAGTAATATCAATGTTCAATATAATAATAAATATATTATTCAAGTAAAAAAA

AAAAAAAAAATTAGCTGCAGTAGGATCCACA

TTAGCTGCAGTAGGATCCACA**ADAP**

B

ACOF2b CAAGCTAAGGAACCAAGAT

CAAGCTAAGGAACCAAGATTTGAAGCACTGAAAGCATGAAATGTGAATTTGGGTTCA

Q A K E P R F E A L K A

ATTGCAATTGTTTTGAATTTAAACAAGTAACATAAAATAGGCAAAGATGCATGTGCTCCTCAAATGAA

AATAATAAAAAATAGATTTAAATATGATGCGAGTCATGCAAATATATTATGTGTTAGTTTTTGTAAGT

TTATTTTTAATAGATAAACGAAATGTGTGTTAATACAAATTCACACAGTAAATTGAAGGGATTAGAGT

TCGAACATCGGTTATGGTGTCAGACTCATTTTGGCTTTGTAATTTTCTTTTTTTTTGCTTGAGTTCAA

CTCGTATAAATTTAAAAAAAAAAAAAAAAAATTAGCTGCAGTAGGATCCACA

TTAGCTGCAGTAGGATCCACA **ADAP**

Figure 44. Nucleotide and deduced amino acid sequence of the 3'-UTR TR-ACO1 and TR-ACO2 sequences generated with the primers ACOF4b (TR-ACO1), ACOF2b (TR-ACO2) and ADAP.

A. TR-ACO1 3'-UTR sequence.

B. TR-ACO2 3'-UTR sequence.

The primers are shown (underlined). The terminal amino acids are indicated as **black bold** capitals.

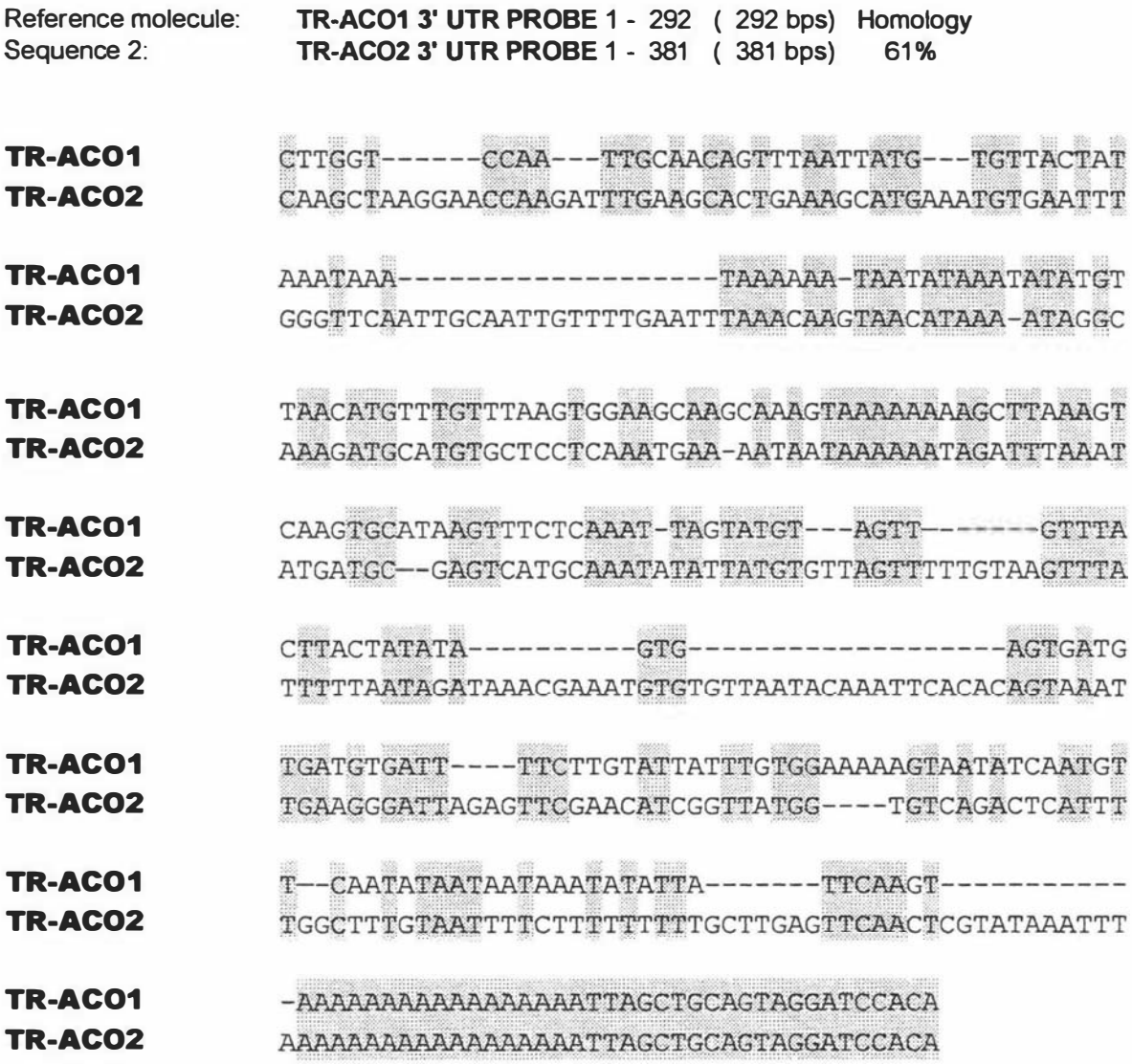

Figure 45. Nucleotide alignment of 3'-UTRs of TR-ACO1 and TR-ACO2 sequences.

Regions of homology are highlighted in grey.

3.10.2 Specificity of TR-ACO1 and TR-ACO2 3'-UTR probes in blotting analysis

Initially, the specificity of TR-ACO1 and TR-ACO2 3'-UTR sequences as probes for their own sequence was examined in nucleic acid blotting analysis. Duplicate blots were probed with either [α-^{32}P]-dCTP labelled TR-ACO1 or TR-ACO2 sequences and then washed at high stringency (0.1 X SSPE, 0.1 % (w/v) SDS at 65°C). At this stringency each sequence showed complete specificity for its corresponding sequence (Figure 46).

3.10.3 Confirmation that the 3'-UTRs of TR-ACO1 and TR-ACO2 identify distinct genes

Genomic Southern analysis was repeated using the 3'-UTRs of TR-ACO1 and TR-ACO2 as probes. Genomic DNA was cut separately with *Hin*d III , *Xba* I or *Eco*R1, probed with either the 3'-UTR of TR-ACO1 or TR-ACO2, and the blots washed at high stringency (0.1 X SSPE, 0.1 % (w/v) SDS at 65°C).

Initially, dCTP was the radiolabelled nucleotide used, but the hybridisation detected was always very low, even if the autoradiograph was left for weeks before being developed (data not shown). This can be explained by the nucleotide composition of the probe sequences (Figure 45), in which the 3'-UTRs of both TR-ACO1 and 2 are adenine/ thymine (A/T) rich. The 3'-UTR of TR-ACO1 has 25 cytosine residues out of a total number of 292 (i.e. 8.6 %), while the 3'-UTR of TR-ACO2 has 42 cytosines out of 381 (11 %). By contrast, the 3'-UTRs of TR-ACO1 and 2 have 123 (42.1 %), and 146 (38 %) adenine residues respectively. Therefore it was decided that the genomic Southern analysis would be undertaken with [α-^{32}P]-dATP labelled TR-ACO1 and 2 probes.

The 3'-UTR TR-ACO1 probe hybridised to multiple genomic fragments in each lane of the Southern blot (Figure 47A), and the hybridisation pattern was very similar to that recognised by the coding frame probe (TR-ACO1; Figure 47C). Additional genomic fragments were recognised in the lane digested with *Hin*d III, but these can be explained by the presence of a *Hin*d III restriction site in the 3'-UTR of the TR-ACO1 sequence (see Figure 43). By contrast, the 3'-UTR TR-ACO2 probe hybridised to single genomic fragments in each lane of the Southern blot (Figure 47B). These fragments were a subset of those recognised by its cognate coding-frame region, TR-ACO2 (Figure 47D).

The multiple bands recognised by the 3'-UTR of TR-ACO1 were not an artifact caused by incomplete digestion. This was shown when the 3'-UTR of TR-ACO1 also recognised the

same (multiple band) hybridisation pattern on a stripped blot that the 3'-UTR of TR-ACO2 had previously identified single bands on (and so the DNA was considered completely digested).

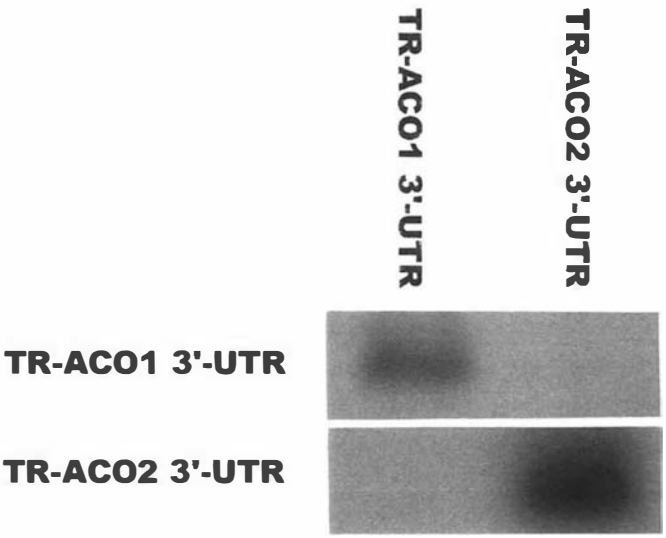

Figure 46. Specificity of TR-ACO1 and TR-ACO2 3'-UTRs in blotting analysis.

Non specific hybridisation was removed by washing at high stringency (0.1 X SSPE, 0.1% (w/v) SDS at 65 °C).

Figure 47. Genomic Southern blot analysis of ACC oxidase genes. A comparison of hybridisation patterns obtained with coding frame regions and 3'-UTRs of TR-ACO1 and TR-ACO2.

A. Membrane probed with [α-^{32}P]-dATP labelled 3'-UTR of TR-ACO1.
B. Membrane probed with [α-^{32}P]-dATP labelled 3'-UTR of TR-ACO2.
C. Membrane probed with [α-^{32}P]-dCTP labelled coding frame region of TR-ACO1 (from Figure 34).
D. Membrane probed with [α-^{32}P]-dCTP labelled coding frame region of TR-ACO2 (from Figure 34)

Membranes were washed at high stringency (0.1 X SSPE, 0.1 % SDS at 65 °C) to remove non-specific binding. Lane 1. DNA digested with *Eco*R1, Lane 2, DNA digested with *Hin*d III, Lane 3. DNA digested with *Xba*I. Molecular weight markers are indicated.

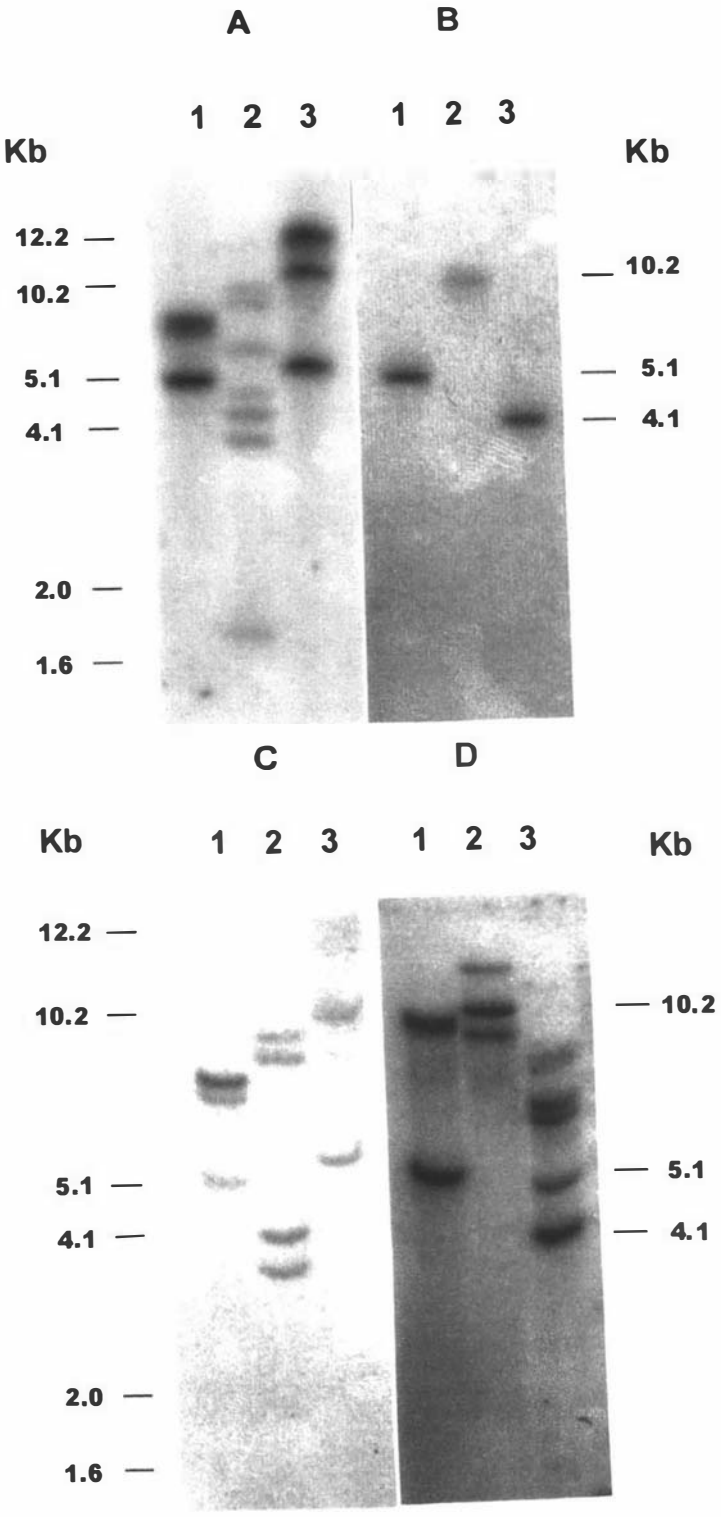
A
B
1 2 3
1 2 3
Kb
Kb
12.2
10.2
5.1
4.1
2.0
1.6
10.2
5.1
4.1
C
D
Kb
1 2 3
1 2 3
Kb
12.2
10.2
5.1
4.1
2.0
1.6
10.2
5.1
4.1

The 3'-UTRs of TR-ACO1 and 2 were found to be more divergent in sequence than their corresponding coding-frame regions. These regions therefore, when used as probes, were more likely to be gene specific. This appeared to be confirmed in Southern analysis by the hybridisation of the 3'-UTR of TR-ACO2 to a subset of the fragments recognised by its cognate coding frame region. This may mean that there are two closely related but distinct TR-ACO2 genes in the genome.

Of further interest then, is whether the 3'-UTR of TR-ACO2 will still hybridise to two RNA transcripts on the northern blot as did its cognate coding frame region. The next section reexamines the gene expression of both TR-ACO1 and TR-ACO2 during leaf maturation and senescence using the 3'-UTRs as probes.

3.10.4 Changes in gene expression of ACC oxidase during leaf maturation and senescence using the 3'-UTRs of TR-ACO1 and TR-ACO2 as probes

Northern analysis was performed on PolyA$^+$ RNA isolated from leaves 4 to 16 and probed with either [α-^{32}P]-dCTP labelled 3'-UTR of TR-ACO1 or TR-ACO2.

The 3'-UTR of TR-ACO1 hybridised to a single RNA transcript of the same size (*ca.* 1.35 Kb) as recognised by its cognate coding frame region (Figure 48B). The levels of this transcript were comparatively high in mature green leaves (leaves 4 to 8), but declined as the leaves became chlorotic (leaves 9 to 16) being virtually undetectable at leaves 11 to 16.

The 3'-UTR of TR-ACO2 hybridised to a single RNA transcript of *ca.* 1.35 Kb (Figure 48B), in contrast to the two RNA transcripts (*ca.* 1.35 and *ca.* 1.17 Kb) recognised by its cognate coding frame region (see Figure 38). The levels of the transcript were comparatively low in mature green leaves (leaves 4 to 8), but increased in chlorotic leaves (leaves 10 to 16). This pattern of expression is the same as that recognised by its cognate coding region. The transcript accumulation patterns of TR-ACO1 and TR-ACO2 were not caused by unequal loading of the RNA into the gel as staining the RNA in the gel with ethidium bromide indicated that equal quantities of Poly A$^+$ RNA had been fractionated in each lane (Figure 48C)..

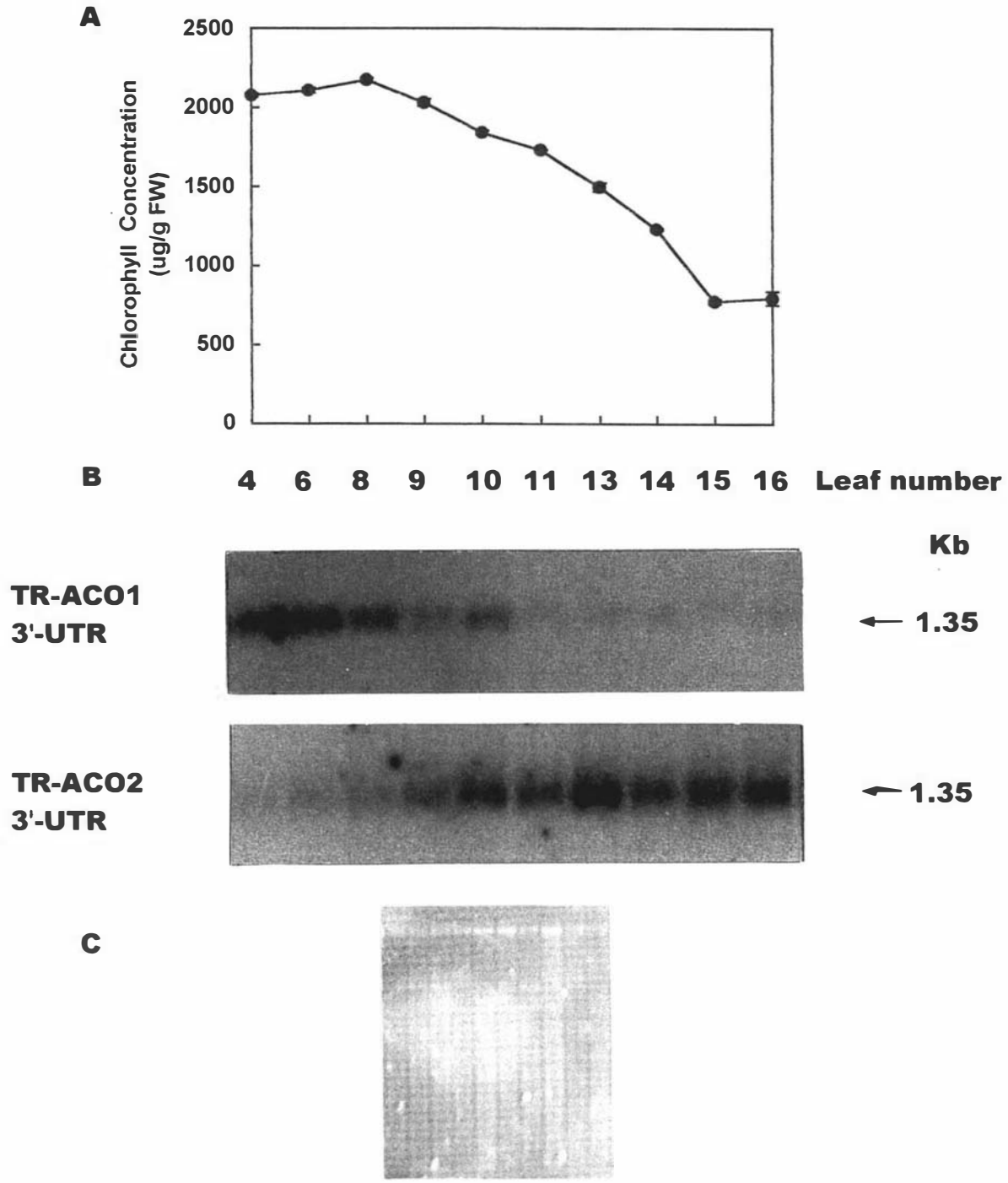

Figure 48. Chlorophyll analysis and northern analysis of ACC oxidase gene expression during leaf maturation and senescence using the 3'-UTRs of TR-ACO1 and TR-ACO2 as probes.

A. Concentration of chlorophyll in leaves used for northern analysis. Error bars = ± 1 sem for 2 internal replicates.

B. RNA isolated from leaves 4 to 16 and hybridised to either the [α-^{32}P]-dCTP labelled 3'-UTR of TR-ACO1 or 2 (as labelled). Membranes were washed at high stringency. (0.1 X SSPE, 0.1 % (w/v) SDS at 65 °C). Sizes of the transcripts are indicated to the right of the blots in Kb.

C. RNA gel used for northern analysis stained with ethidium bromide.

The steady state levels of the TR-ACO1 transcript were consistent with ACC oxidase activity *in vitro* which was high in leaves 4 to 10 and then declined to be lowest by leaf 16. However, expression of TR-ACO2 which is abundant in chlorotic tissue did not coincide with measurable ACC oxidase activity. Since ACC oxidase activity *in vitro* (see Figure 56B) was measured from the same powdered tissue as used for the northern analysis with the 3'-UTRs (Figure 48), it appears that the isoenzyme encoded by TR-ACO2 does not contribute to measured activity *in vitro* of ACC oxidase in the chlorotic tissue. The ACC oxidase coded for by TR-ACO2 does contain all the residues hitherto considered as important for activity (see Figure 29). It may be, therefore, that the method being used to determine ACC oxidase activity *in vitro* does not measure activity of the enzyme encoded by TR-ACO2, because the isoenzyme requires different extraction and/ or assay conditions.

The next section investigates whether the isoenzyme of ACC oxidase from chlorotic tissue has different extraction and assay requirements to the isoenzyme of the mature green leaf tissue, and whether this may explain the lower activity of ACC oxidase *in vitro* detected in the chlorotic leaf tissue.

3.11 Extraction and assay requirements for ACC oxidase activity *in vitro* of mature green and senescent leaf material

Eleven different extraction regimes that had been compared previously for the ability to extract ACC oxidase from mature green tissue (see Figure 24) were now compared for their ability to extract ACC oxidase from chlorotic tissue (Figure 49). The highest recovery of ACC oxidase activity in the chlorotic leaf material was achieved with the same extraction buffer used to recover the highest amount of enzyme from the mature green tissue (0.1 M Tris-HCl, pH 7.5/ 10 % (v/v) glycerol/ 2 mM DTT/ 30 mM ascorbate). The buffer that was least effective (*ca.* 4.5-fold less) for recovery of activity from chlorotic tissue was again the Tris/ glycerol buffer with no added components. The extract made from chlorotic tissue was always browner in colour than the extract made from mature green leaf tissue. Browning of extracts is often a characteristic of polyphenolic production (Loomis, 1974).

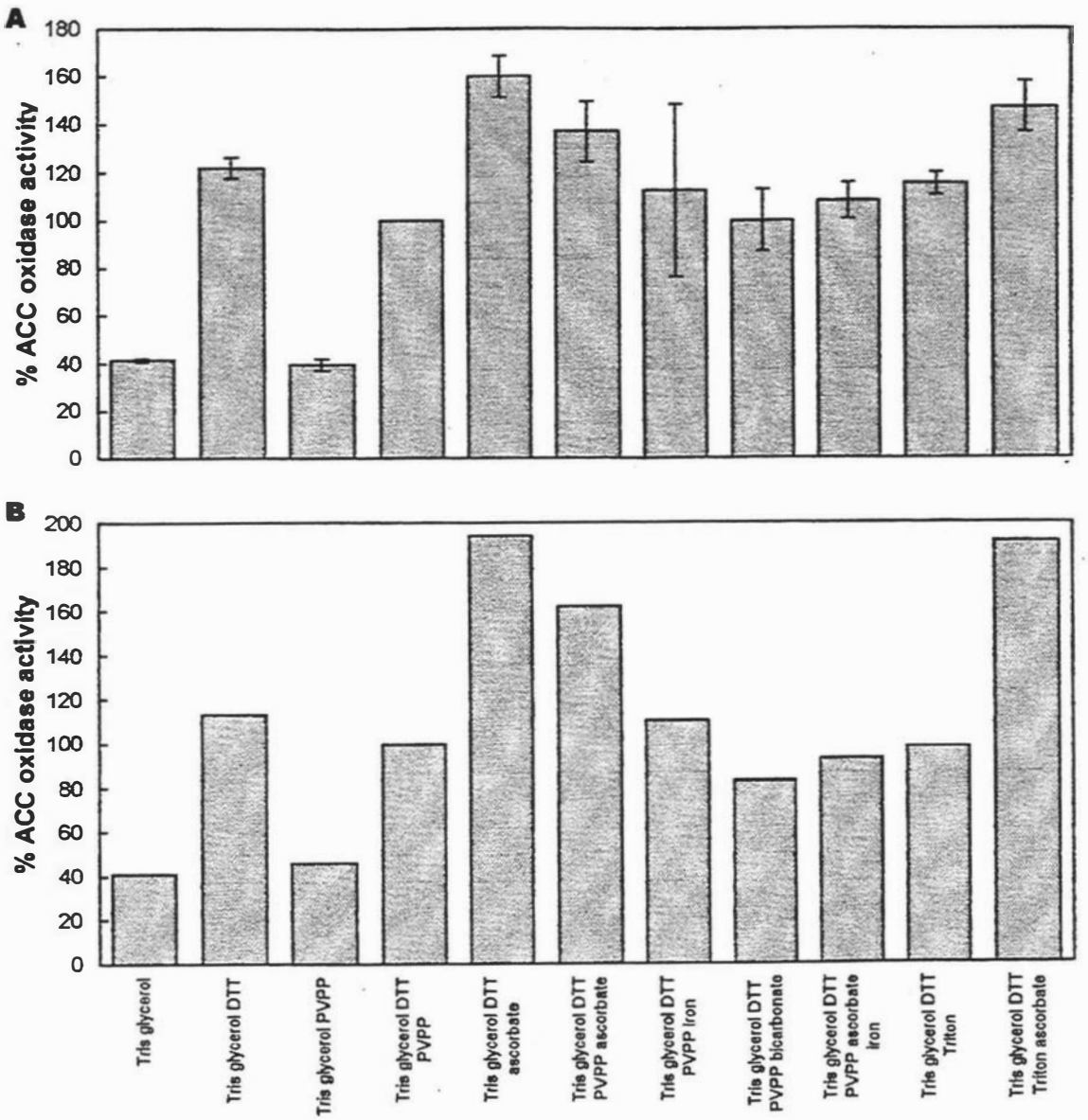

Figure 49. A comparison of extraction requirements of mature green and senescent leaves for recovery of ACC oxidase activity *in vitro*.

A. Effect of extraction regime on recovery of ACC oxidase from mature green leaves. Error bars = ± 1 sem for 3 internal replicates of 4 independent experiments.

B. Effect of extraction regime on recovery of ACC oxidase from senescent leaves. The experiment was performed once in triplicate.

The concentrations of the reagents used are: 0.1 M Tris-HCl, pH 7.5, 10 % (w/v) glycerol, 2 mM DTT, 2 % (w/v) PVPP, 30 mM sodium ascorbate, 20 μM iron sulphate, 30 mM sodium bicarbonate, 0.1 % (v/v) Trtion X-100.

These compounds such as flavanoids and tannins can inhibit enzyme activity by H-bonding with peptide bond oxygens, or by covalent modification of amino acid residues, such as thiol groups, hydroxyls and primary amines (Gegenheimer, 1990). Inclusion of phenol adsorbants such as insoluble PVPP in the extraction media can aid recovery of active enzyme (Loomis, 1974; Gegenheimer, 1990). However, inclusion of PVPP did not increase recovery of ACC oxidase from chlorotic leaf tissue.

To determine whether the lower enzyme activity measured in the chlorotic tissue (leaves 10 to 16, see Figure 26) was due to the conditions of the assay being more optimal for activity of the enzyme from mature green tissue, pH, cosubstrate and cofactor concentrations were altered and the effect on activity of enzyme extracts from both tissues was compared (Figure 50 and 51). The lower activity of the chlorotic extract was not because it required a different pH for optimal activity, as ACC oxidase activity *in vitro* from chlorotic tissue had the same pH optima (7.5) as that of the mature green tissue (Figure 50). The lower activity of the chlorotic extracts also was not due to the enzyme in these extracts requiring different concentrations of cosubstrates and cofactors compared with the mature green extracts, because the effect of altering their concentration on activity was similar for extracts of both tissues (Figure 51). Activity from both tissue extracts showed a rather broad optima for bicarbonate (10 to 50 mM), ascorbate (30 to 90 mM), and iron (40 to 80 μM).

An earlier result (Figure 19) had suggested that the enzyme in the chlorotic extract was more unstable than the enzyme in the mature green extract when the extracts were kept at 0°C (ice) for 3 h before assay. The greater instability of the enzyme of the chlorotic extracts was now confirmed in another experiment (Figure 52) where it was found that the enzyme activity in the chlorotic extract kept on ice for three and six hours before assay decreased by 12.5 % and 24 % respectively, while over the same time period the enzyme activity in the mature green extract did not change. The loss of activity with storage suggests that loss of enzyme activity may be influenced by the time the tissue is extracted for. However, there was only a very small decline in extractable activity from chlorotic tissue after one hour compared to the amount extracted after 15 min (the time over-which most activity could be extracted for (Figure 53)). Since leaf tissue had routinely been extracted for 45 min in the previous assays, any decline in activity due to time of extraction would not be enough to explain the difference in activity *in vitro* of the chlorotic and mature green tissue extracts.

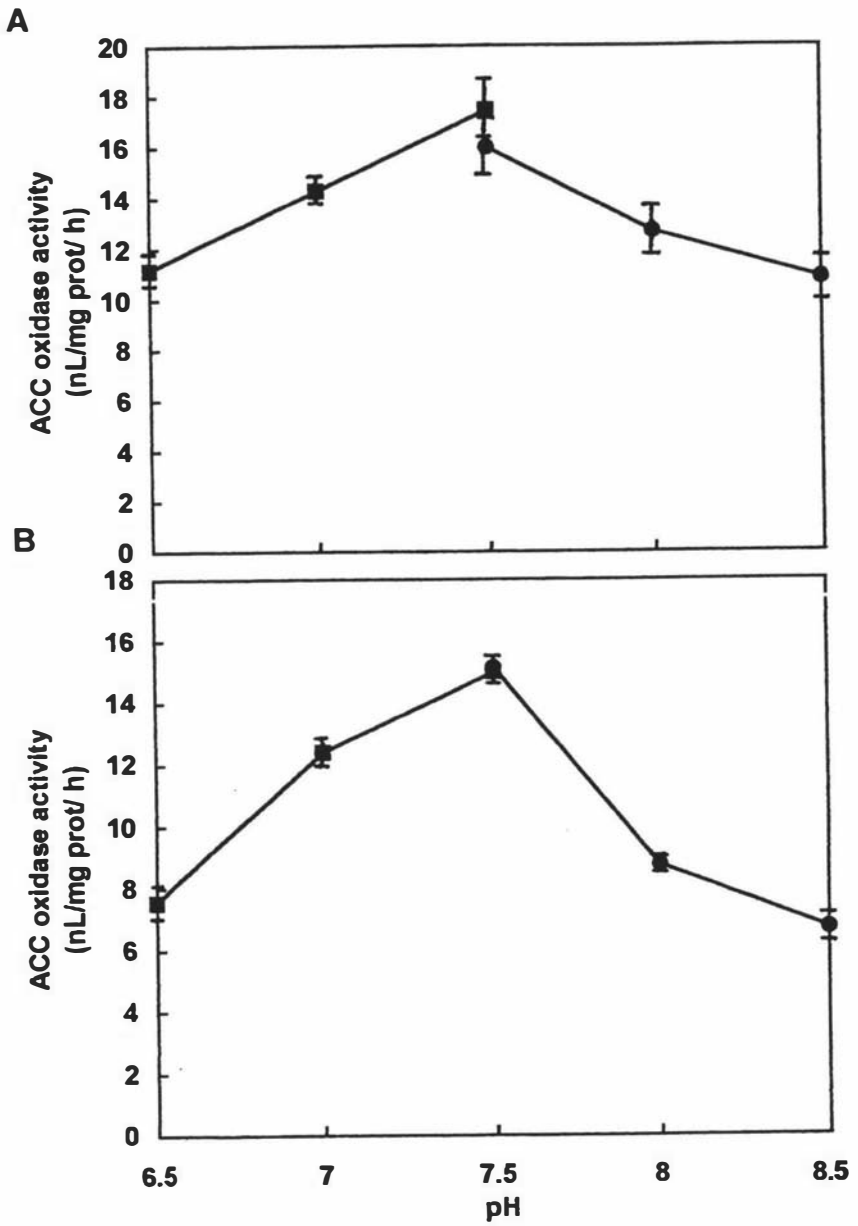

Figure 50. Effect of assay buffer pH on ACC oxidase activity measured *in vitro*.

A. ACC oxidase extracted from mature green leaves and assayed under different pH conditions.

B. ACC oxidase extracted from senescent leaves and assayed under different pH conditions.

(--■–) 50 mM MOPS buffer, pH 6.5 to 7.5; (–●–) 50 mM Tris-HCl buffer, pH 7.5 to 8.5. Error bars are ± 1 sem for 3 internal replicates of 2 independent experiments.

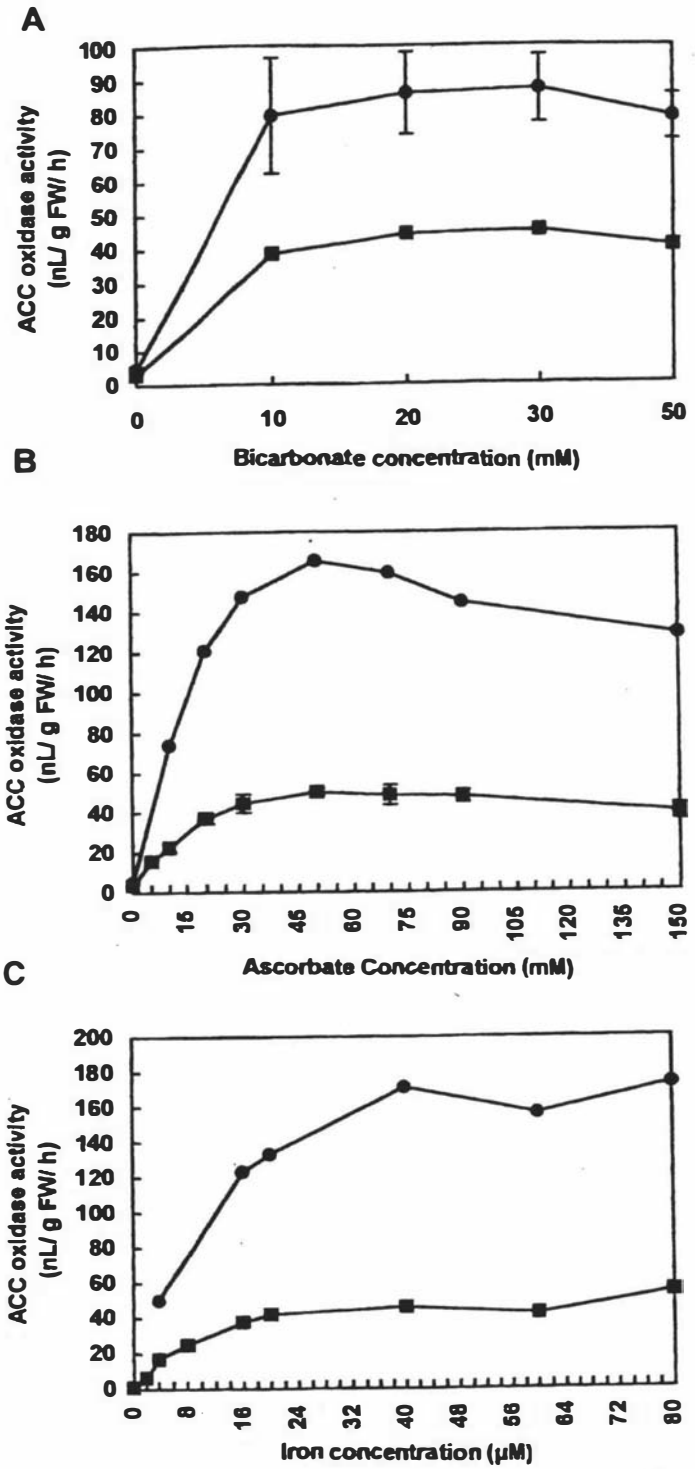

Figure 51. Cofactor and cosubstrate requirements for ACC oxidase extracted from mature green and chlorotic leaves.

A. Effect of varying sodium bicarbonate concentration.
B. Effect of varying sodium ascorbate concentration.
C. Effect of varying iron sulphate concentration.
(—●--) Mature green leaves; (--■--) Senescent leaves.
Where indicated the error bars are ± 1 sem for 3 internal replicates of 3 independent experiments.

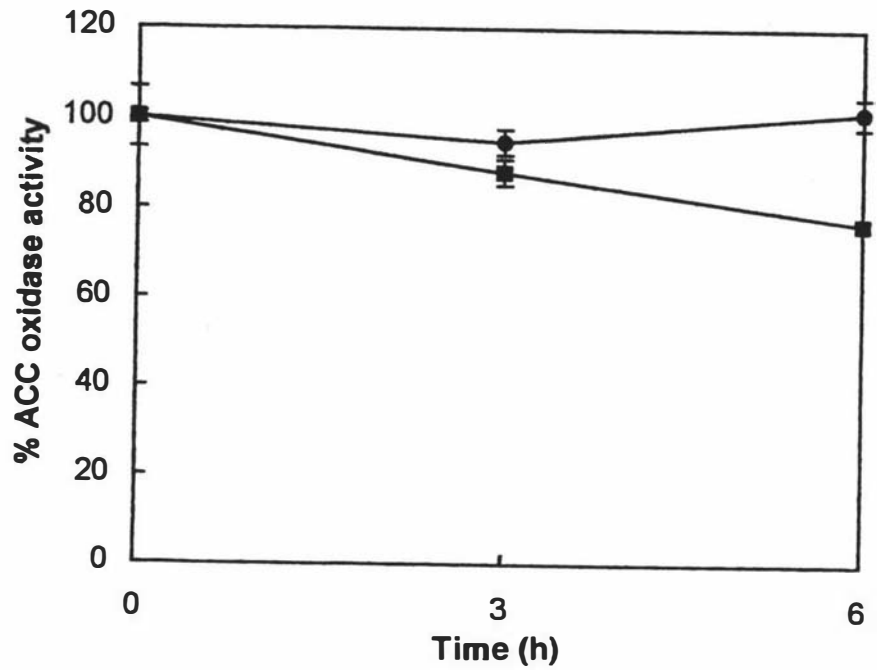

Figure 52. Activity of ACC oxidase after incubation on ice.

Leaf tissue extracts were incubated on ice for up to 6 h before subsequent assay of ACC oxidase activity. (--●--) Mature green leaves; (--■--) Senescent leaves. Error bars are ± 1 sem for 3 internal replicates of a single experiment.

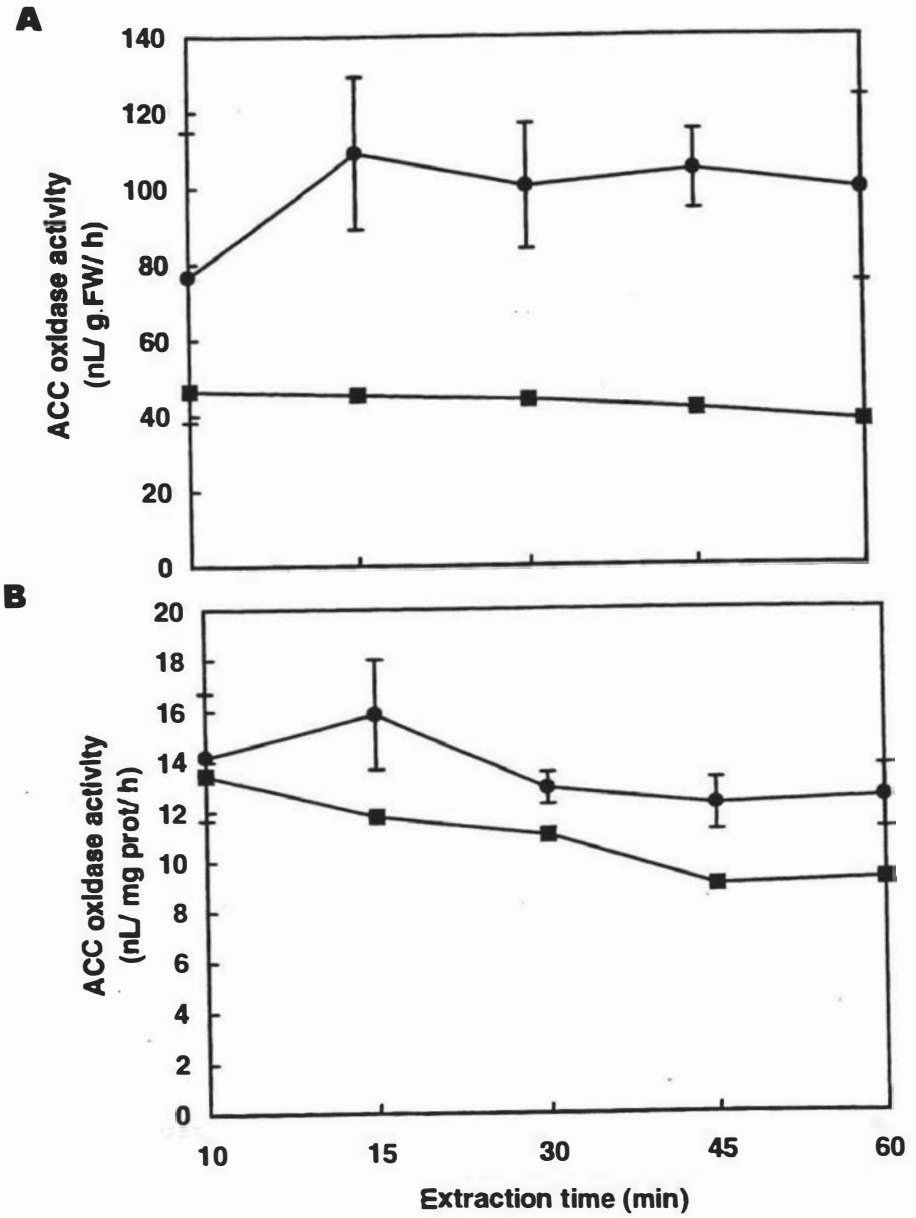

Figure 53. Effect of extraction time on recovery of ACC oxidase.

Mature green and chlorotic leaves were extracted for 10 to 60 min and activity measured.

A. ACC oxidase activity expressed on a per unit fresh weight basis.

B. ACC oxidase activity expressed on a per unit protein basis.

(--●--) Mature green leaves; (--■--) Senescent leaves.

Error bars where indicated are ± 1 sem from 2 independent experiments.

This study has so far shown that the activity of ACC oxidase *in vitro* declines as the leaf tissue becomes chlorotic, and that the pattern of activity correlates well with TR-ACO1, but not TR-ACO2 gene expression. Attempts to explain the comparatively low ACC oxidase activity *in vitro* of the chlorotic leaf extract, by finding factors in the extraction and assay that were not optimal for activity of chlorotic tissue, but were for mature green, were unsuccessful. The enzyme in the chlorotic tissue extract had the same extraction and assay requirements as the enzyme in the mature green tissue extract. Apparently, increased TR-ACO2 gene expression does not result in increased measurable activity *in vitro* of ACC oxidase in the chlorotic tissue. Further aspects of the extraction and assay could be studied to provide a reason for the lower activity of the chlorotic extract, including testing for inhibitory compounds in the chlorotic tissue, and purifying the putative isoenzymes from each tissue and measuring activity. However, an alternative approach (which may be independent of extractable activity) is to measure the pattern of protein accumulation of ACC oxidase during leaf maturation and senescence using antibodies. Western analysis is a well established method for determining changes in protein accumulation. It has been used to study the changes in ACC oxidase protein accumulation in tomato leaves after wounding where a strong correlation between increased transcript (ACO1) and increased protein accumulation and activity *in vitro* of ACC oxidase was found (Barry, *et al.*, 1996).

The next section describes the production of polyclonal antibodies to the translated products of TR-ACO1 and TR-ACO2 expressed in *E. coli* and the results obtained from using these antibodies to examine accumulation of ACC oxidase protein during leaf maturation and senescence.

3.12 Protein accumulation of ACC oxidase during leaf maturation and senescence

The pPROEX ™-1 protein expression system was used to produce the translated products of TR-ACO1 and TR-ACO2 (see section 2.2.10.1). This involved ligating the sequences into the pPROEX vector, transforming the vector into a suitable bacterial host and inducing the host to translate the sequences. The translated proteins (that are fused to a sequence of six histidine residues) were then purified (using the His-tag) by metal-chelate affinity chromatography, and used as antigens for inoculation into rabbits (TR-ACO1) or rats (TR-ACO2), after which antibodies were collected and used in western analysis for

identification and quantification of ACC oxidase protein accumulation during leaf maturation and senescence.

3.12.1 Directional cloning of TR-ACO1 and TR-ACO2 into the pPROEX vector

3.12.1.1 Preparation of cDNA inserts of TR-ACO1 and TR-ACO2 by attachment of restriction sites to their 5' and 3' ends

The coding frame regions of TR-ACO1 and TR-ACO2 were prepared for directional in-frame cloning into the multiple cloning site of pPROEX by using PCR to attach restriction sites to the ends of these sequences. The forward primer (ACOFE, see Figure 11) contained an *Eco*R1 restriction site at its 5'-end, whilst the reverse primer (ACORH, see Figure 11) contained a *Hin*d III site. Column-purified plasmids containing TR-ACO1 and TR-ACO2 sequences were used as the template for amplification. After amplification the fragments of the expected size were gel- and column-purified, and the ends digested with *Eco*R1 and *Hin*d III in preparation for ligation.

3.12.1.2 Preparation of pPROEX vector for ligation by digestion with EcoR1 and Hind III restriction enzymes

Prior to ligation, the pPROEX vector was column-purified and the plasmid then cut in its multiple cloning site (see Figure 5) with *Eco*R1 and *Hin*d III restriction enzymes to provide complementary ends for in-frame insertion of the similarly cut TR-ACO1 and TR-ACO2 sequences. After ligation of the TR-ACO1 and TR-ACO2 sequences into pPROEX, the recombinant pPROEX vectors were transformed into *E. coli* strain DH 5α, and the presence of the insert of appropriate size (*ca.* 840 bp) confirmed by restriction digestion (data not shown)

The bacteria were then induced to translate the TR-ACO1 and TR-ACO2 sequences by incubation with IPTG. Initial attempts to induce expression of TR-ACO1 and TR-ACO2 His-tagged fusion proteins in DH 5α were not successful as determined by the absence of an induced protein of the expected size (*ca.* 38 kDa) in the crude bacterial protein extracts (data not shown). Therefore, the recombinant pPROEX vectors (containing TR-ACO1 and TR-ACO2 sequences) were subsequently transferred into two new strains of *E. coli*, TB-1 and BL-21, as other fusion proteins have been shown to be stable in these genetic backgrounds (Daniel Jeffares, Institute of Molecular BioSciences, Massey University, NZ, *pers. comm.*). No fusion proteins were detected in strain BL-21 after induction (data not

shown), but the *E. coli* strain TB-1 could be induced to produce fusion proteins of *ca.* 38 kDa (TR-ACO1; Figure 54A, lanes 3 to 5) and *ca.* 39 kDa (TR-ACO2; Figure 54B, lanes 1 and 3). These are approximately the sizes predicted from translation of the coding frames of TR-ACO1 (35 474 kDa) and TR-ACO2 (36 250 kDa) with the associated polylinker of pPROEX (3 386 kDa); i.e. TR-ACO1 (38 860 kDa) and TR-ACO2 (39 636 kDa).

3.12.2 Purification of TR-ACO1 and TR-ACO2 His-tagged fusion proteins in preparation for animal inoculations

After confirmation that the strain TB-1 could be induced to produce TR-ACO1 and TR-ACO2 His-tagged fusion proteins of the expected size, the procedure was scaled up and the induced proteins were purified from the crude bacterial extract by metal chelate affinity chromatography.

The elution profile obtained from the affinity column for the TR-ACO2 fusion protein is shown in Figure 55A. The column fractions containing the fusion protein were identified by SDS-PAGE. The TR-ACO2 fusion protein eluted mainly in column fractions 3 to 7 (Figure 55A, lanes 3 to 7; data for TR-ACO1 not shown) and these were pooled and the protein content measured. A total of 1.67 mg of TR-ACO2 fusion protein was obtained from a 1 L broth of TB-1 bacteria harboring the TR-ACO2 sequence, and a total of 3.1 mg of TR-ACO1 protein was obtained from a 2 L broth of TB-1 bacteria harboring the TR-ACO1 sequence. In addition to the induced band of *ca.* 37 kDa, a lower band of approximately 29 kDa was detected by SDS-PAGE. This has been identified previously as a nickel binding protein common to strains of *E. coli* (M. T. McManus, *pers. comm.*).

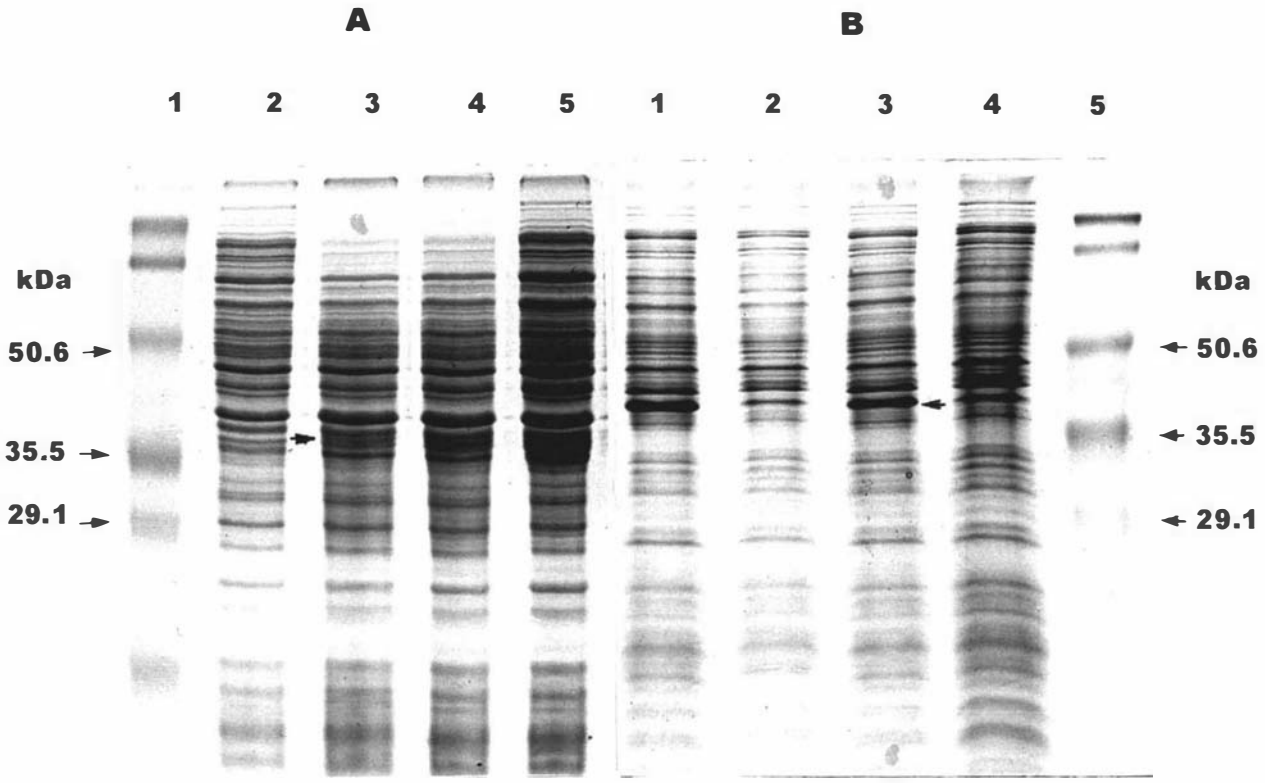

Figure 54. Induction of TR-ACO1 and 2 fusion proteins within the genetic background of *E. coli* strainTB-1.

A. SDS-PAGE analysis of TR-ACO1 induction.
Lane 1.3 µL BioRad pre-stained markers (molecular weights are indicated).
Lane 2.3 µL of TB-1 protein after induction for 0 h.
Lane 3.3 µL of TB-1 protein after induction for 1 h.
Lane 4.3 µL of TB-1 protein after induction for 2 h.
Lane 5.3 µL of TB-1 protein after induction for 3 h.
The arrow denotes the position of the induced TR-ACO1 fusion protein.
B. SDS-PAGE analysis of TR-ACO2 induction.
Lane 1.3 µL of TB-1 protein after 3 h induction
Lane 2.3 µL of TB-1 protein after 0 h induction.
Lane 3.3 µL of TB-1 protein after 3 h induction.
Lane 43 µL of TB-1 protein after 0 h induction.
Lane 5.3 µL BioRad pre-stained markers (molecular weights are indicated).
The arrow denotes the position of the induced TR-ACO2 fusion protein.

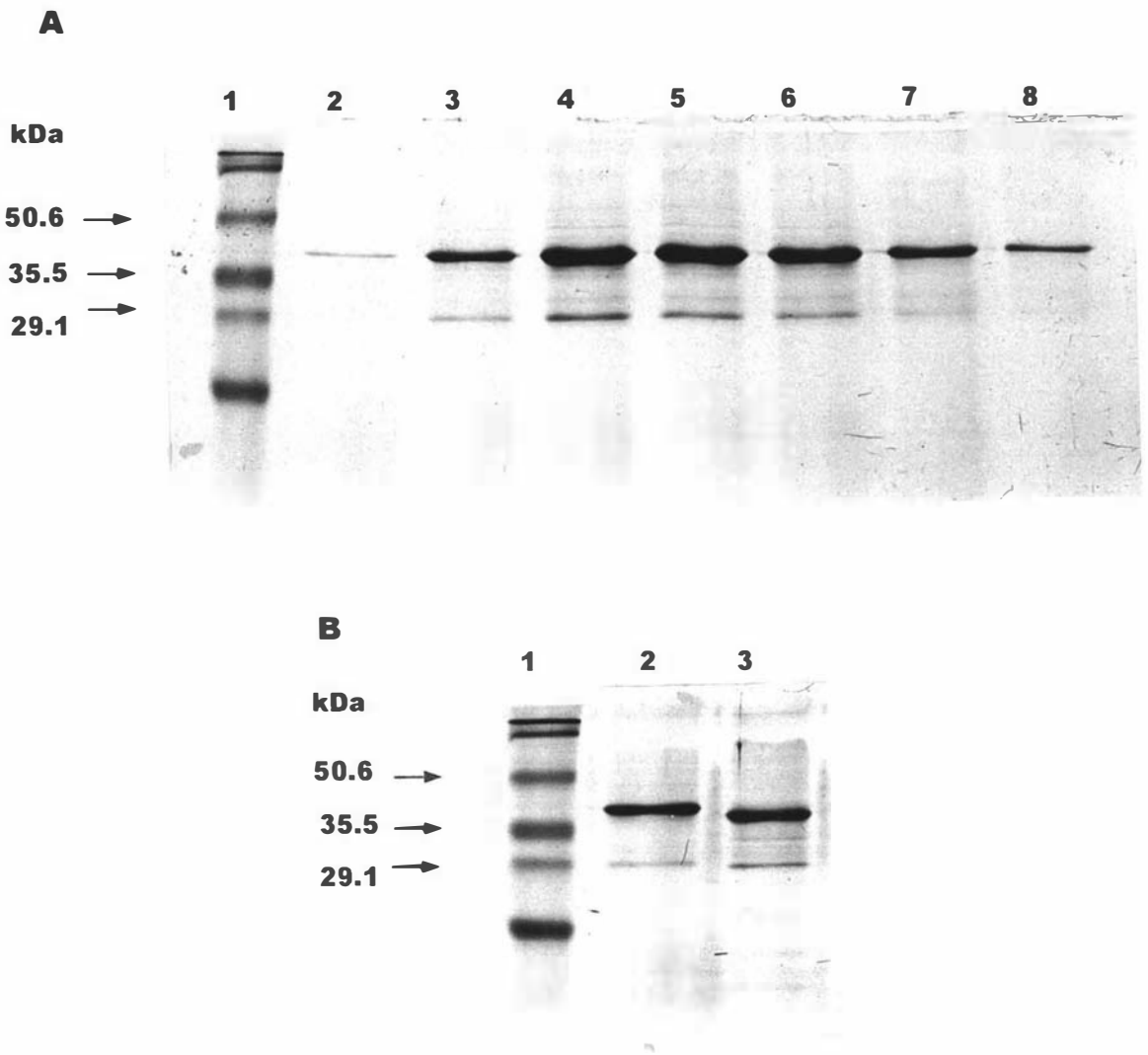

Figure 55. Identification of column fractions that contained the induced TR-ACO2 fusion protein.

A. SDS-PAGE of column fractions containing affinity purified TR-ACO2 fusion protein.
Lane 1.3 µL Biorad pre-stained markers (molecular weights are indicated).
Lane 2 5 µL fraction 1.
Lane 3.5 µL fraction 2., ca. 1 µg TR-ACO2.
Lane 4.5 µL fraction 3., ca. 2.65 µg TR-ACO2.
Lane 5.5 µL fraction 4., ca. 2.05 µg TR-ACO2.
Lane 6.5 µL fraction 5., ca. 1.71 µg TR-ACO2.
Lane 7.5 µL fraction 6., ca. 1 µg TR-ACO2.
Lane8.5 µL fraction 7.
B. Size comparison of affinity purified TR-ACO1 and 2 proteins.
Lane1.3 µL Biorad pre-stained markers. (molecular weights are indicated).
Lane 2.3 µL pooled TR-ACO2 protein, (ca. 1 µg).
Lane 3.3 µL pooled TR-ACO1 protein, (ca. 1.47 µg).

3.12.3 Confirmation that the fusion protein is the translation product of TR-ACO1

Amino acid sequencing of trypsin digested fragments of the TR-ACO1 fusion protein identified a sequence of seven amino acids (H-T-D-A-G-G-I) that could be found within the deduced translated sequence of TR-ACO1 (see Figure 28), which confirmed that the TR-ACO1 sequence had been translated in-frame in *E. coli.* The TR-ACO2 protein was not sequenced, but the size (*ca.* 38 kDa) was approximately the size expected from the translation of the TR-ACO2 sequence (sequence analysis showed that had it not been inserted in-frame, stop codons would have produced severely truncated proteins). Further, polyclonal antibodies eventually made to the TR-ACO2 fusion protein cross reacted with the TR-ACO1 fusion protein (Mr Sang Dong Yoo, Institute of Molecular BioSciences, Massey University, NZ, *pers. comm.*).

3.12.4 Polyclonal antibody production to TR-ACO1 and TR-ACO2 His-tagged fusion proteins

It was predicted that the polyclonal antibodies raised against the TR-ACO1 and TR-ACO2 fusion proteins would cross-react due to the high similarity of their deduced amino acid sequences (see Figure 31). However, it was hoped that they may recognise their target proteins with more avidity (and hence produce a higher detection signal). To increase the likelihood of this, antibodies were raised in different immune systems, rabbits for TR-ACO1, and rats for TR-ACO2, as the immune systems of these animals might be more responsive to a different set of antigenic determinants. The His-tag was not removed prior to injection of the proteins into either of the animals as it has been shown previously to be a poor antigenic determinant (M. T. McManus *pers. comm.*)

Western analysis (section 2.2.10) was then performed on the same tissue previously used in northern analysis with the 3'-UTRs of TR-ACO1 and TR-ACO2 as probes (see Figure 48). Prior to western analysis, changes in chlorophyll concentration, protein concentration, and ACC oxidase activity was also measured.

3.12.5 Changes in chlorophyll concentration, protein concentration and ACC oxidase activity during leaf maturation and senescence

The concentration of protein in the leaves started to decline in leaf 10 which was the leaf where chlorophyll levels had clearly begun to decrease (Figure 56A). ACC oxidase activity *in vitro* was greatest in leaves 4 to 10 (mature green) and also declined around the onset of

chlorosis (leaf 11; Figure 56B). Again the decline was greater when expressed on a per gram fresh weight basis (*ca.* 7-fold) compared to per milligram protein (*ca.* 3-fold).

3.12.6 ACC oxidase protein accumulation during leaf maturation and senescence

Changes in accumulation of ACC oxidase protein during leaf maturation and senescence were examined by western analysis (section 2.2.10). One hundred microgram aliquots of protein extracted from leaves 4 to 16 were fractionated in an 8-15 % gradient SDS-PAGE gel, transferred to a PVDF membrane and the putative ACC oxidase protein detected with polyclonal antibodies raised either to the fusion proteins of TR-ACO1 or TR-ACO2.

The antibodies raised against the TR-ACO1 fusion protein recognised a protein of *ca.* 36.4 kDa (as determined by gradient SDS-PAGE) (Figures 56B and 57) which is in the range reported for ACC oxidases of other organisms (36 to 41 kDa). The pattern of protein accumulation detected by the TR-ACO1 antibodies is seen most clearly using image analysis to quantify signal intensity (Figure 57C). The protein was highest in leaves 4 to 10 (before the onset of chlorosis at leaf 11) and then declined as the leaves became chlorotic (refer Figure 56A). This broadly matched both the transcript accumulation of TR-ACO1 (see Figure 48B) and the detectable ACC oxidase activity *in vitro* for the same leaf tissue (Figure 57A).

Antibodies raised against the TR-ACO2 fusion protein did not recognise a protein in leaves 4 to 16 that had a pattern of accumulation consistent with TR-ACO2 transcript accumulation. The antibodies did recognise a protein in the leaf extracts that had both the same size (*ca.* 36.4 kDa) and pattern of accumulation, as that recognised by the TR-ACO1 raised antibodies. However, a longer time was necessary in order to detect the protein by the GARAP (goat-anti-rat-alkaline phosphatase) reaction. Taken together, these observations suggest that the antibodies raised against the TR-ACO1 and TR-ACO2 fusion proteins recognise the same protein in the plant extracts, particularly since it has been shown also that each antibody is able to recognise the fusion protein from both genes.

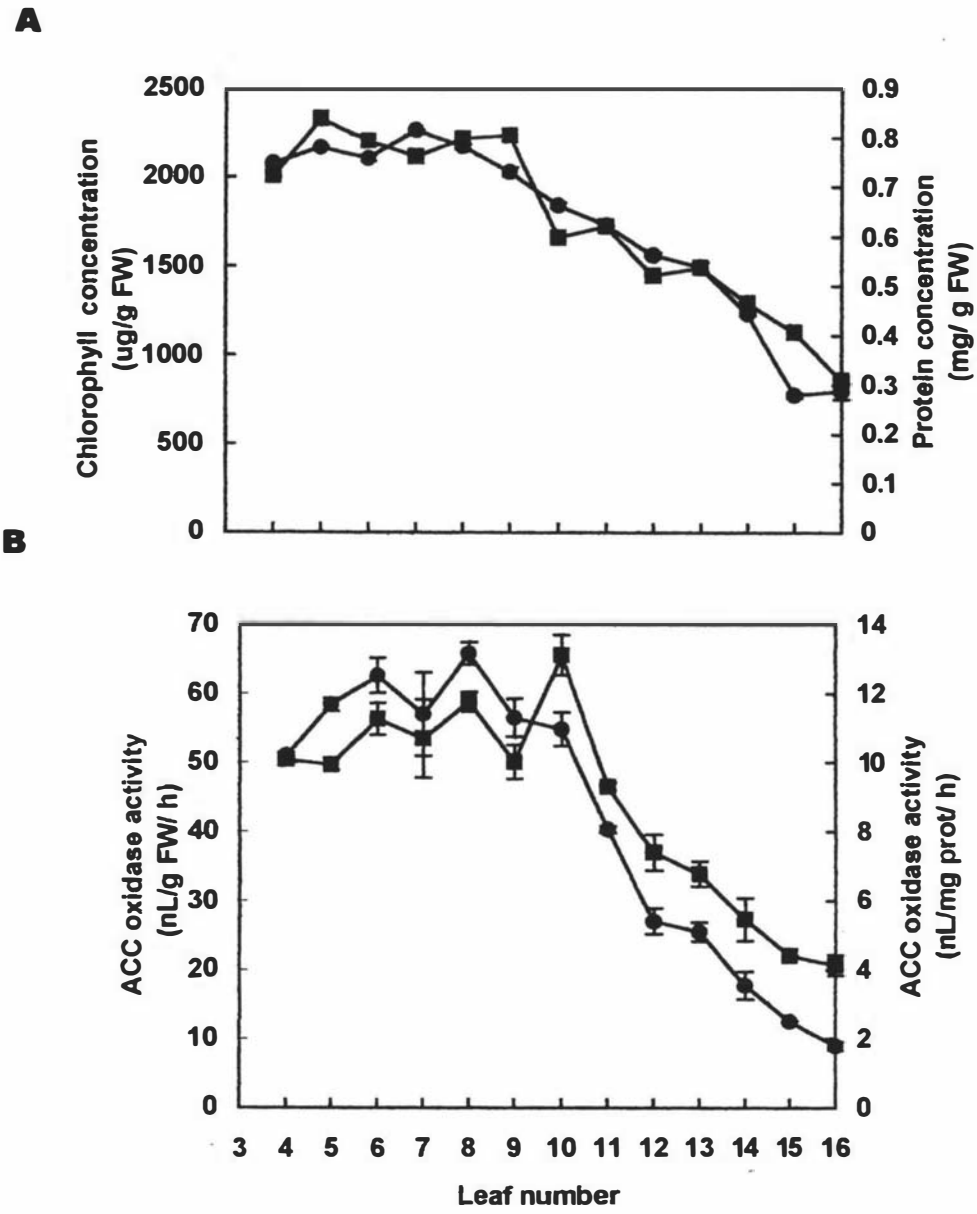

Figure 56. Chlorophyll concentration, protein concentration and ACC oxidase activity of mature and senescent leaves.

A. (—●--) Chlorophyll concentrations.
(--■--) Protein concentration.

B. (—●--) ACC oxidase activity *in vitro* expressed on a per unit fresh weight basis.
(--■--) ACC oxidase activity *in vitro* expressed on a per unit protein basis.

Where indicated the error bars are ± 1 sem for 3 internal replicates.

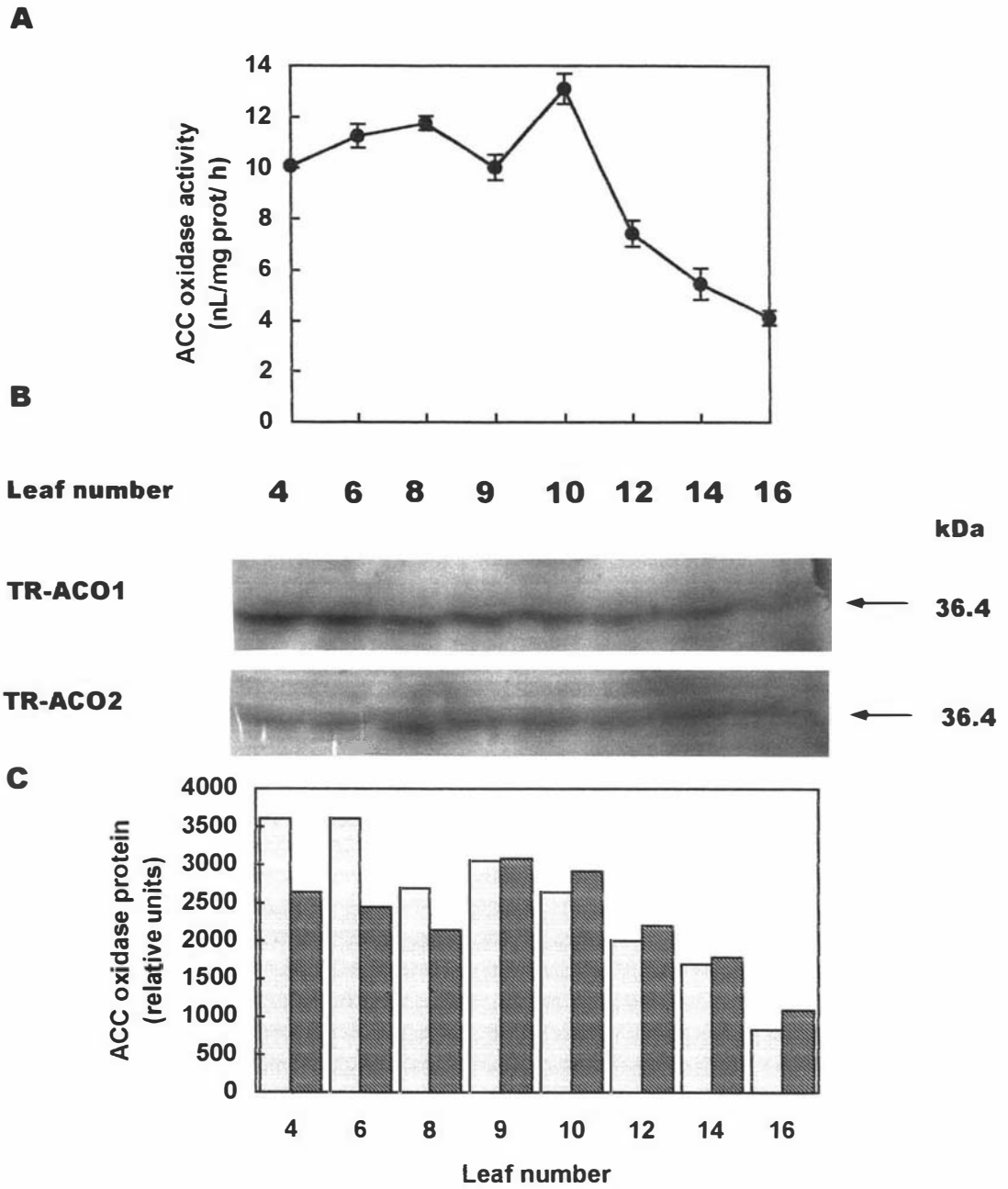

Figure 57. Changes in activity and protein accumulation of ACC oxidase during leaf maturation and senescence.

A. ACC oxidase activity *in vitro* of the leaf extracts used for western analysis.
B. Immunodetection of ACC oxidase with antibodies raised against TR-ACO1 and 2 His-tagged fusion proteins.
C. Quantitation of the levels of ACC oxidase detected by the polyclonal antibodies using image analysis.

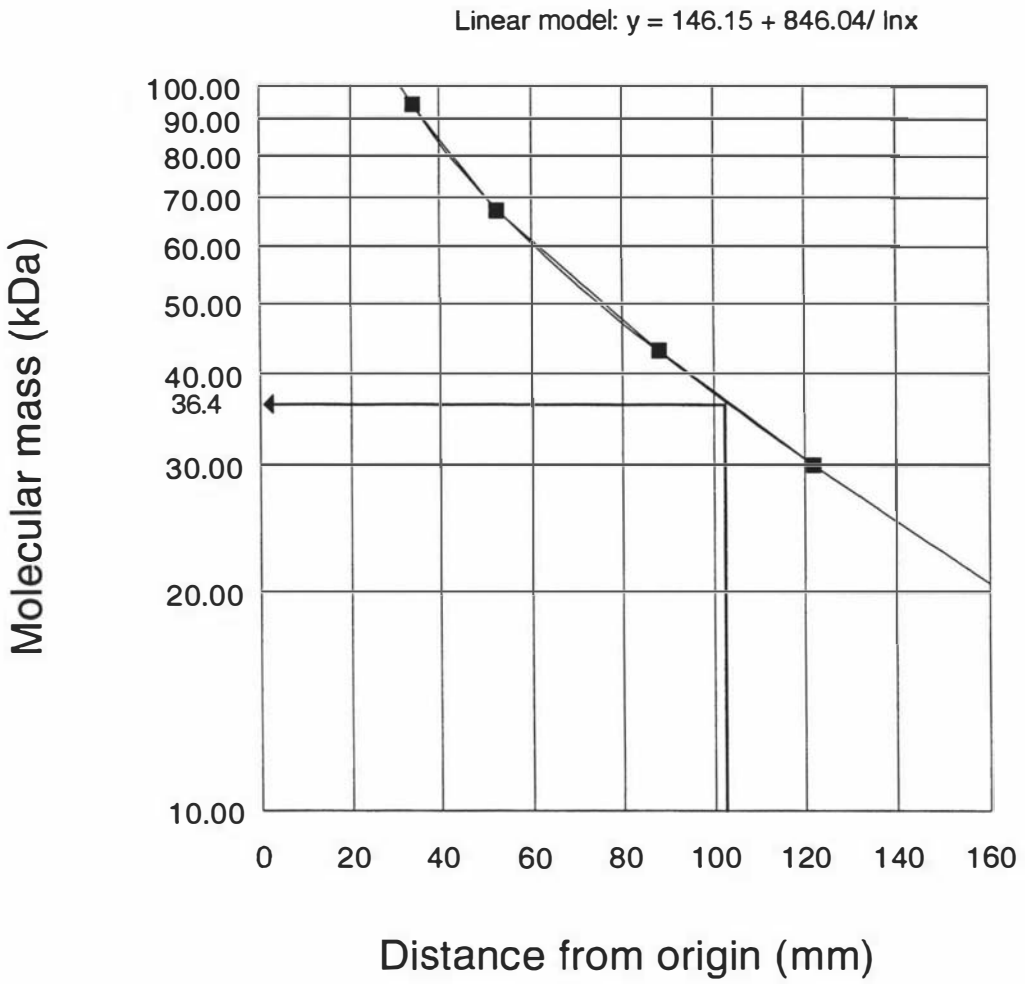

Figure 58. Calculation of the molecular weight of ACC oxidase protein.

The distance that the protein (recognised by the polyclonal antibodies raised against the TR-ACO1 protein) traveled was compared to the distance traveled by the molecular weight markers (Pharmacia). The graph was plotted with SlideWrite™ and the linear model of the programme together with the Function Evaluator used to estimate the size of the ACC oxidase protein.
The arrow denotes both the distance the ACC oxidase protein migrated in the gel and the estimation of its molecular weight.

Hitherto, this study has not been able to show, either by protein accumulation using antibodies or ACC oxidase activity *in vitro*, a pattern that matches with TR-ACO2 transcript accumulation in chlorotic tissues. Both accumulation of ACC oxidase protein and changes in ACC oxidase activity during leaf maturation and senescence (as judged by chlorosis) can be correlated only with the expression of the TR-ACO1 transcript.

More information on the influence of TR-ACO2 gene expression on ACC oxidase protein accumulation and activity may be gained by inducing and studying this gene transcript in non-chlorotic tissue. In tomato, a senescence (chlorotic) -associated ACC oxidase isoenzyme in leaf tissue was the isoform induced by mechanical wounding of mature green leaf tissue, and increased transcript accumulation was correlated both with increased protein accumulation and ACC oxidase activity *in vitro* (Barry *et al.*, 1996). Therefore, it may be possible to increase preferentially the expression of the senescence-associated isoform (TR-ACO2) in mature green tissue of white clover by mechanically wounding the tissue. Protein accumulation and activity of ACC oxidase may then be measured away from factors in the chlorotic tissue that may be interfering with the measurement of protein accumulation and activity of ACC oxidase.

The next section examines the effect of wounding (attached and detached) tissue on ethylene evolution, levels of transcript, and protein, and activity of ACC oxidase.

3.13 Exogenous control of ACC oxidase expression in leaf tissue of white clover

3.13.1 Ethylene evolution of detached wounded leaves

Mature green leaves that were detached, wounded (section 2.1.5) and incubated in the dark evolved *ca.* 1 nL g^{-1} FW h^{-1} ethylene for up to 1 h after wounding. The rate of ethylene production then increased to peak at 7 nL g^{-1} FW h^{-1} , 1.5 to 2 h after the initial wounding stimulus and then declined to be close to initial levels by 5.5 to 6 h (Figure 59A).

3.13.2 Changes in ACC oxidase gene expression in detached wounded leaves

Changes in TR-ACO1 and TR-ACO2 gene expression were examined over a six hour time period. Total RNA was isolated from leaves at 0, 0.5, 1, 2, 3, and 6 h after wounding, and

probed with [α-^{32}P]-dCTP labelled 3'-UTRs of TR-ACO1 and 2. Non hybridised label was removed by washing the blots at high stringency (0.1 X SSPE, 0.1 %SDS at 65 °C).

The 3'-UTR of TR-ACO1 hybridised faintly to a single RNA transcript (Figure 59B). The levels of this transcript remained similar up to 3 h after wounding, but by 6 h the transcript was no longer detectable. The 3'-UTR of TR-ACO2 also hybridised to a single RNA transcript (Figure 59C). No hybridisation could be detected before 2 h, but from 2 to 6 h the transcript accumulated greatly. Ethidium bromide staining of the RNA gels used for northern analysis confirmed that the increase in transcript accumulation of TR-ACO2 was not a result of the unequal loading of RNA (Figure 59D).

3.13.3 Changes in ACC oxidase activity in detached wounded leaves

ACC oxidase activity measured *in vitro* did not increase in the detached wounded leaves despite the large increase in the accumulation of the TR-ACO2 transcript (Figure 59A). There was a transient increase in enzyme activity 0.5 h after wounding (from *ca.* 32 to 47 nL mg^{1} prot. h^{-1}), but this occurred prior to the increase in the levels of the TR-ACO2 transcript. ACC oxidase activity was lowest when transcript levels of TR-ACO2 were highest (i.e. at 6 h after wounding). Activity at this time point appeared to correlate more closely with TR-ACO1 gene expression which was no longer detectable at this time.

3.13.4 Changes in ACC oxidase protein accumulation in detached wounded leaves

Changes in the accumulation of ACC oxidase protein were examined by immunodetection with antibodies raised to TR-ACO1 or TR-ACO2 fusion proteins.

The antibodies raised against the TR-ACO1 fusion protein recognised a protein on the western blots of *ca.* 36 kDa (Figure 59E). The levels of this protein remained similar throughout the 6 h time period. Similarly, the antibodies raised against the TR-ACO2 fusion protein recognised a protein of *ca.* 36 kDa (Figure 59F), but the recognition in contrast to TR-ACO1, was comparatively weak (as determined by the time required for detection by the GARAP reaction). The levels of this protein, like that recognised by the TR-ACO1 antibodies, also did not change significantly over the 6 h time period. The lack of change in levels of the 36.4 kDa protein over the 6 h time period was not an artifact caused by unequal protein loadings in the lanes as judged by the equivalence in staining of a duplicate protein gel (Figure 59G). It appears then, that the antibodies raised against the

TR-ACO2 protein are recognising the TR-ACO1 protein, and that there is little evidence that increased gene expression of TR-ACO2 either in chlorotic or wounded mature green extracts leads to either increased protein accumulation or activity of ACC oxidase.

Figure 59. Effect of wounding detached mature green leaves on ethylene evolution, ACC oxidase activity *in vitro*, TR-ACO1 and TR-ACO2 gene transcripts and ACC oxidase protein accumulation

A. (--■--) Ethylene evolution.
(--●--) ACC oxidase activity *in vitro* of detached wounded mature green leaves.
B. Transcript accumulation of TR-ACO1 in detached wounded mature green leaves. The size of the transcript is indicated.
C. Transcript accumulation of TR-ACO2 in detached wounded mature green leaves. The size of the transcript is indicated.
D. Visualisation of RNA on northern gel by ethidium bromide staining. Gels for TR-ACO1 and TR-ACO2 are as indicated.
E. Protein accumulation of ACC oxidase recognised by the polyclonal antibodies raised against the TR-ACO1 protein.
F. Protein accumulation of ACC oxidase recognised by the polyclonal antibodies raised against the TR-ACO2 protein.
G. Duplicate protein gel stained with CBB.

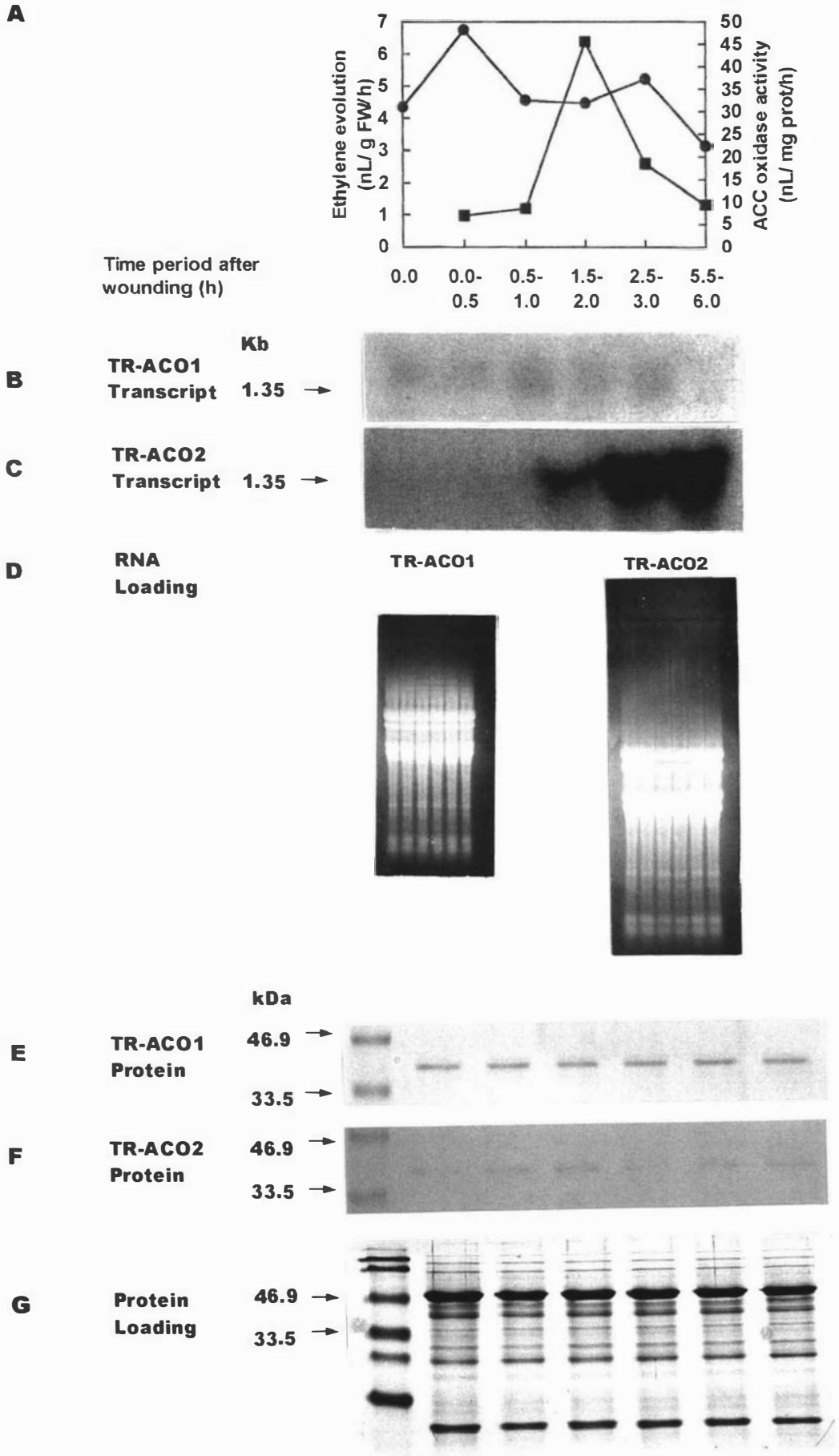
A
Ethylene evolution (nL/ g FW/h)
ACC oxidase activity (nL/ mg prot/h)
Time period after wounding (h)
0.0
0.0-0.5
0.5-1.0
1.5-2.0
2.5-3.0
5.5-6.0
B
TR-ACO1 Transcript
Kb
1.35
C
TR-ACO2 Transcript
1.35
D
RNA Loading
TR-ACO1
TR-ACO2
E
TR-ACO1 Protein
kDa
46.9
33.5
F
TR-ACO2 Protein
46.9
33.5
G
Protein Loading
46.9
33.5

3.13.5 Changes in ethylene evolution in non-wounded detached leaves

To act as a control, a set of detached non-wounded mature green leaves were subjected to the same analysis (Figure 60A). Unlike the wounded leaves, there was no peak in the rate of ethylene production after 1.5 to 2 h, but instead the rate of ethylene production increased gradually over 6 h time period to be highest at 6 h. However, the levels of ethylene evolution at this time were still not higher than the basal levels of ethylene production in the wounded leaves observed at 0.5 and 1 h after wounding (see Figure 59A).

3.13.6 Changes in ACC oxidase gene expression in non-wounded detached leaves

The pattern of gene expression in the non-wounded detached leaves was the same as that observed for the wounded leaves over the 6 h period (Figures 59B and C). The 3'-UTR of TR-ACO1 hybridised faintly to a single RNA transcript whose expression remained similar up to 3 h after leaf detachment, but by 6 h the transcript was no longer detectable (Figure 60B). The 3'-UTR of TR-ACO2 also hybridised to a single RNA transcript. Similar to the wounded leaves, no hybridisation of this transcript could be detected up to 2 h after detachment, but after 2 h there was a huge-fold increase in the levels of the transcript (Figure 60C). Again, ethidium bromide staining of the RNA gels used for northern analysis confirmed that the increase in transcript accumulation of TR-ACO2 was not a result of the unequal loading of RNA (Figure 60D).

3.13.7 Changes in ACC oxidase activity in non-wounded detached leaves

ACC oxidase activity in the detached non-wounded leaves remained around 32 nL mg^{-1} prot. h^{-1} throughout the 6 h, except at 2.5 to 3 h where it increased transiently to 43 nL mg^{-1} prot. h^{-1} (Figure 60A). However, by 6 h the activity had declined again, and therefore, did not correlate with the induction of the TR-ACO2 gene transcript.

3.13.8 Changes in ACC oxidase protein accumulation in non-wounded detached leaves

The antibodies raised against TR-ACO1 recognised a protein in non-wounded leaves similar to that recognised in wounded, and again the accumulation of this protein did not change significantly over 6 h time period (Figure 60F). Similarly, the antibodies raised against TR-ACO2 recognised a protein in non-wounded detached leaves similar to that

Figure 60. Effect of detachment of mature green leaves on ethylene evolution, ACC oxidase activity *in vitro*, TR-ACO1 and TR-ACO2 gene transcripts and ACC oxidase protein accumulation

A. (--■--) Ethylene evolution.
(--●--) ACC oxidase activity *in vitro* of detached mature green leaves.
B. Transcript accumulation of TR-ACO1 in detached mature green leaves. The size of the transcript is indicated.
C. Transcript accumulation of TR-ACO2 in detached mature green leaves. The size of the transcript is indicated.
D. Visualisation of RNA on northern gel by ethidium bromide staining. Gels for TR-ACO1 and TR-ACO2 are as indicated .
E. Protein accumulation of ACC oxidase recognised by the polyclonal antibodies raised against the TR-ACO1 protein.
F. Protein accumulation of ACC oxidase recognised by the polyclonal antibodies raised against the TR-ACO2 protein.
G. Duplicate protein gel stained with CBB.

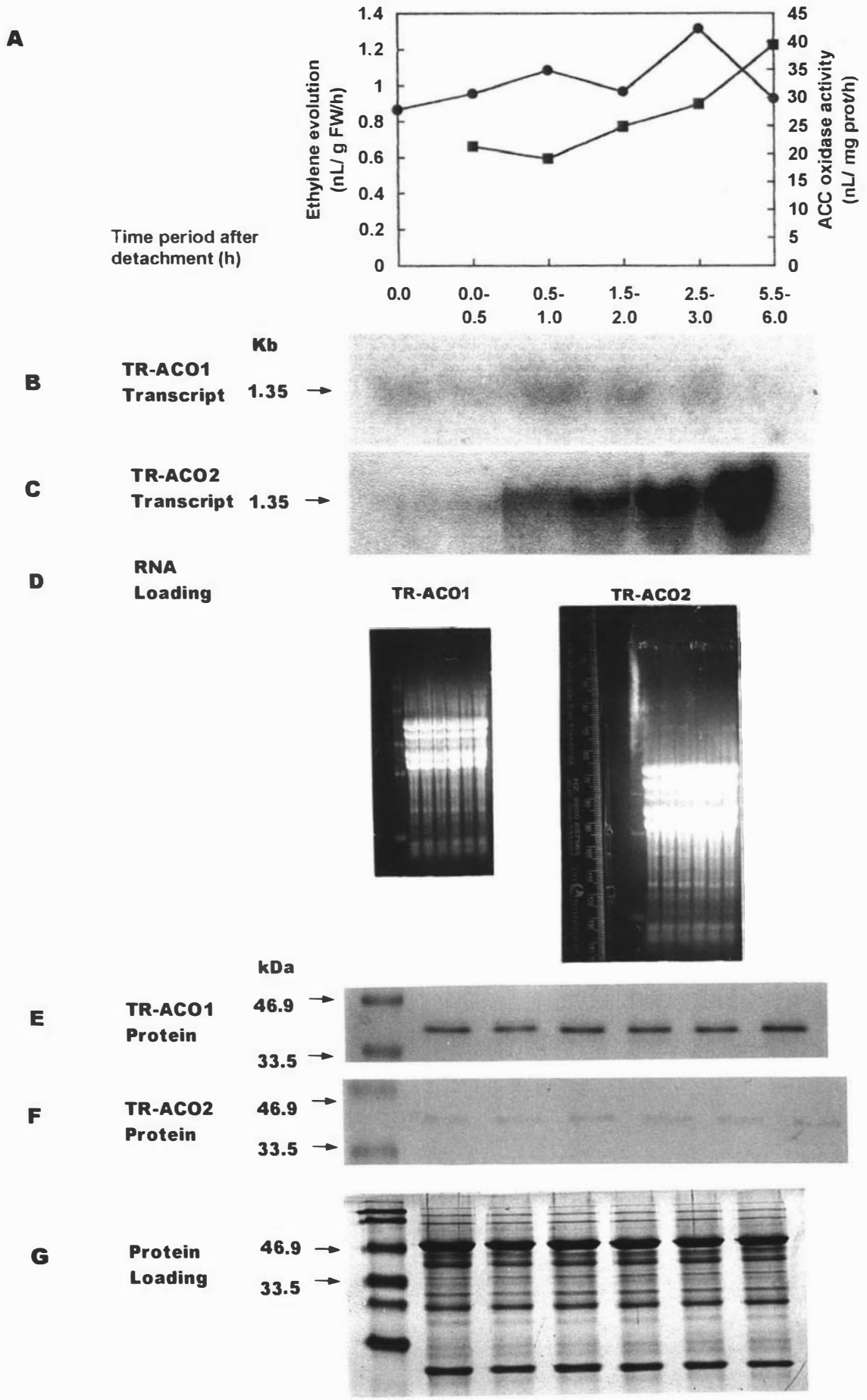
A
Ethylene evolution (nL/ g FW/h)
ACC oxidase activity (nL/ mg prot/h)
1.4
1.2
1
0.8
0.6
0.4
0.2
0
45
40
35
30
25
20
15
10
5
0
Time period after detachment (h)
0.0
0.0-0.5
0.5-1.0
1.5-2.0
2.5-3.0
5.5-6.0
Kb
B
TR-ACO1 Transcript
1.35
C
TR-ACO2 Transcript
1.35
D
RNA Loading
TR-ACO1
TR-ACO2
kDa
E
TR-ACO1 Protein
46.9
33.5
F
TR-ACO2 Protein
46.9
33.5
G
Protein Loading
46.9
33.5

recognised in wounded (Figure 60E). The levels again remained similar over the 6 h time period and did not correlate, therefore, with the induction of TR-ACO2 expression. The equivalence of protein loading was again confirmed with a duplicate protein gel (Figure 60G).

Taken together, the results from both detached wounded and detached non-wounded leaves suggest that the levels of the senescent-associated gene transcript, TR-ACO2, can be elevated in mature green leaves 2 h after leaf detachment. By contrast, the level of the TR-ACO1 transcript is not elevated in mature green leaves after detachment. However, no increase in protein accumulation or activity of ACC oxidase could be correlated with the increase in TR-ACO2 gene expression, despite the increase now being observed in mature green tissue (not chlorotic).

One of the findings of the above experiment was that the act of leaf detachment appeared to be sufficient to induce gene expression of the TR-ACO2 transcript, and that the induction may be independent of ethylene. To provide further evidence that the wounding stimulus acts independent of ethylene, the experiment was repeated, but with the inclusion of an ethylene adsorbing compound, Purafil.

3.13.9 The effect of an ethylene adsorbing compound on TR-ACO2 gene expression and ACC oxidase activity in detached mature green leaves.

The ability of Purafil to delay an ethylene-mediated process (chlorophyll loss) in leaves of white clover, genotype 10F, has been documented (Butcher, 1997). Therefore, it might be expected that Purafil could delay the wound-induced induction of TR-ACO2 gene expression if the induction is mediated by ethylene.

To examine this, the previous experiment was repeated except Purafil was included in two of the three treatments to adsorb ethylene.

1. Detached non-wounded leaves incubated in presence of Purafil.
2. Detached wounded leaves incubated in presence of Purafil.
3. Detached wounded leaves.

3.13.10 The effectiveness of Purafil in removing ethylene from around leaves

Inclusion of Purafil in the containers was completely effective in preventing the wound-induced 4.5-fold increase in ethylene production (from 1.9 to 9.2 nL g^{-1} FW h^{-1}) (Figure

61). However, it was not able to completely remove all traces of ethylene from around the tissue. A steady basal level of ethylene (1.8 nL g^{-1} FW h^{-1}) was observed for both non-wounded and wounded leaves incubated with Purafil over the 6 h time period.

In this experiment, unlike the previous one, leaves that were used for analysis of gene expression, and activity of ACC oxidase were not the leaves that were used for the measurement of ethylene evolution. Instead they were a duplicate set of leaves treated in parallel, except, as an added measure to minimise accumulation of ethylene, the leaves were never sealed in the containers.

3.13.11 The effect inclusion of Purafil had on TR-ACO2 gene expression in leaves

Inclusion of Purafil in the containers did not delay the increase in TR-ACO2 gene expression, despite being effective in preventing the peak in ethylene production in the air surrounding the leaves (Figure 62A). The TR-ACO2 gene transcript accumulated after 1.5 to 2 h in all three treatments, i.e. whether Purafil was present or not. Ethidium bromide staining of the RNA suggests that the loading was not completely equal in all lanes of this particular northern blot (Figure 62B). However, on closer inspection of the loadings, it is clear that both the increase in gene expression and the timing of the increase is not due to unequal loading.

3.13.12 The effect of Purafil on ACC oxidase activity in leaves

Wounded leaves incubated with Purafil, had consistently lower ACC oxidase activity (*ca.* 22 nL mg^{-1} prot h^{-1}) than either non-wounded leaves kept in containers with Purafil (*ca.* 50 nL mg^{-1} prot h^{-1}) or wounded leaves (*ca.* 50 nL mg^{-1} prot h^{-1}) over the 6 h time period following wounding. (Figure 62C). However, there was no increase in activity in the leaves treated with Purafil concomitant with the induction of the TR-ACO2 transcript.

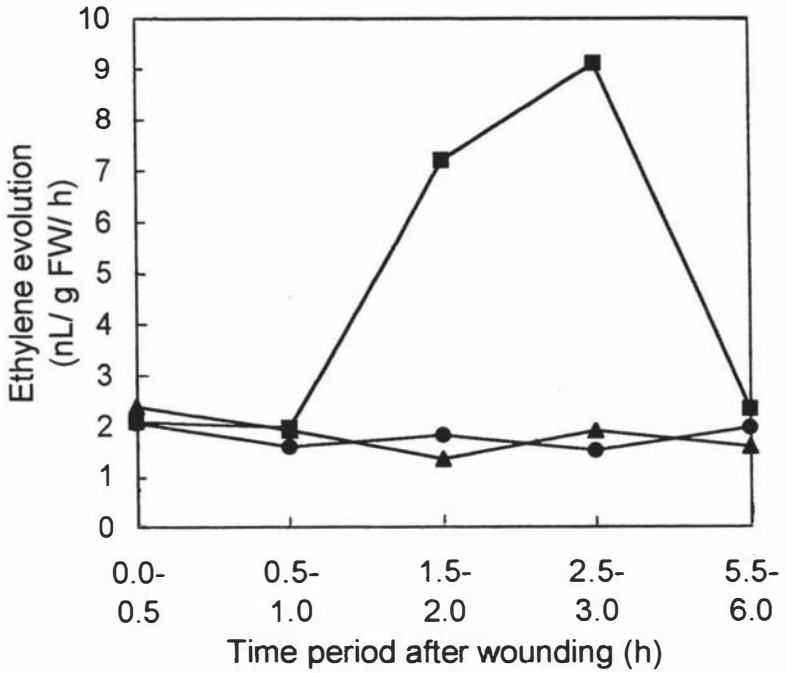

Figure 61. Ethylene evolution of detached wounded and non-wounded mature green leaves in the presence or absence of Purafil.

(--●--) Detached non-wounded leaves incubated in the presence of Purafil.
(--▲--) Detached wounded leaves incubated in the presence of Purafil.
(--■--) Detached wounded leaves.

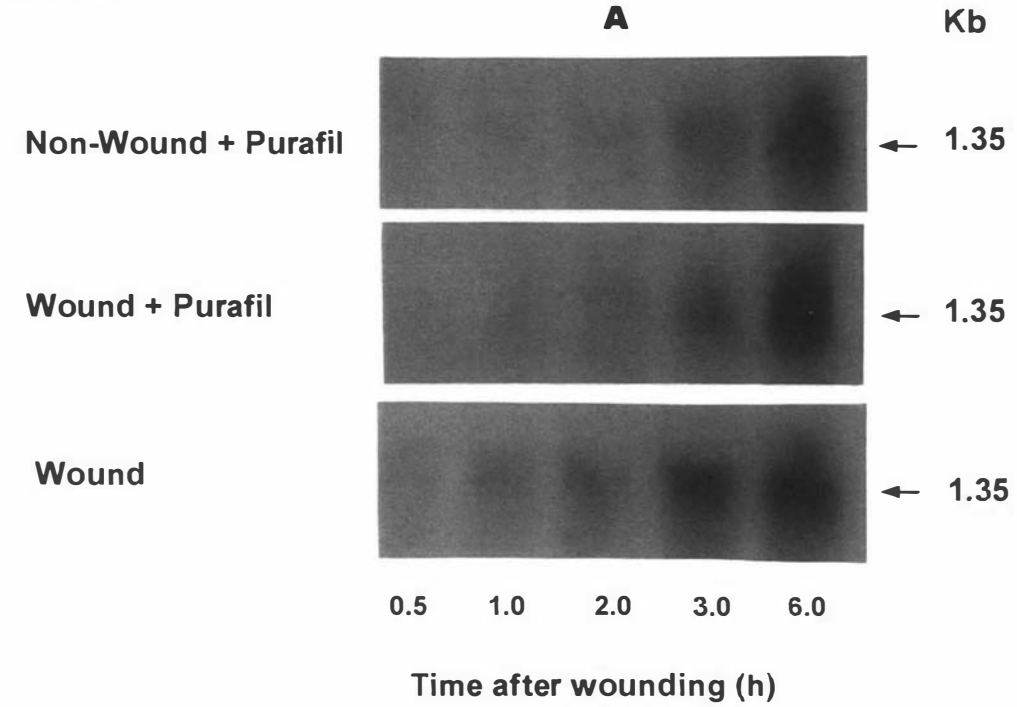

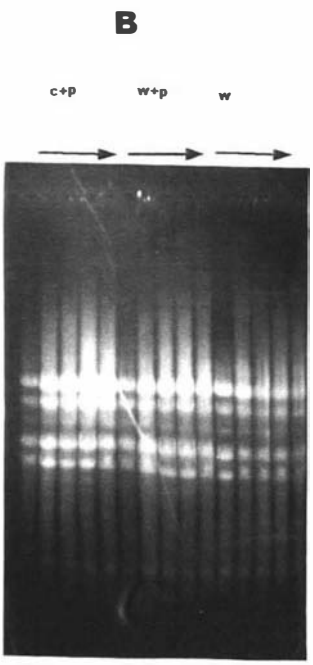

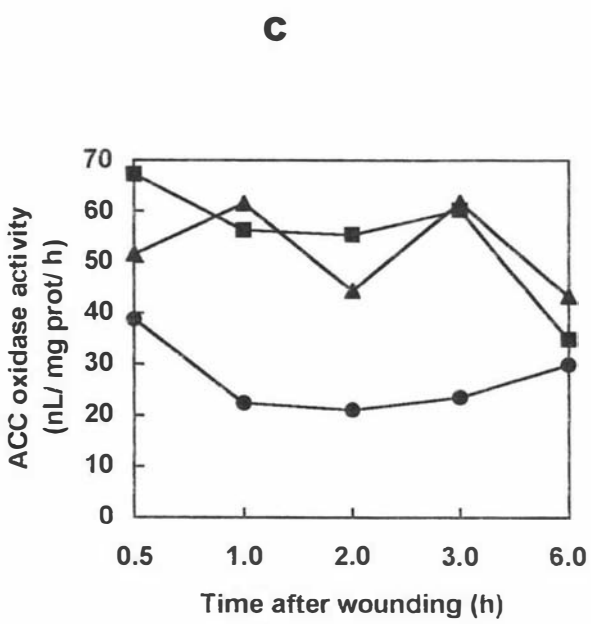

Figure 62. TR-ACO2 gene transcript accumulation and ACC oxidase activity *in vitro* in detached wounded and non-wounded mature green leaves incubated with or without Purafil.

A. Transcript accumulation of TR-ACO2. The size of the transcript is indicated to the right of the figure.
B. RNA stained by ethidium bromide.
C. ACC oxidase activity *in vitro* in the same tissue used for the northern analysis.
(--●--) Wounded leaves incubated with Purafil.
(--■--) Wounded leaves incubated without Purafil.
(--▲--) Detached non-wounded leaves incubated with Purafil.

The inability of Purafil to delay the increase in the TR-ACO2 gene transcript in detached mature green leaves suggests that the increase of this gene transcript may be independent of ethylene. However, Purafil was not able to remove completely all the ethylene from around the leaves. Furthermore, these experiments were performed on detached leaves incubated in the dark, and it has been shown with leaves from other species that these conditions (a common way of inducing chlorosis) can alter the pattern of gene expression of that observed *in planta* (Becker and Apel, 1993). Therefore, the next experiments were performed on mature green leaves still attached to the stolon and focus on the control of transcript expression under physiological conditions rather than the induction (by any means) of expression of TR-ACO2 in mature green leaves. In addition, Purafil was replaced by the ethylene action inhibitor 1-MCP to more closely investigate the effect of wound-induced ethylene production. Recently, 1-MCP has been used in melon leaves to show that the wound induced increase in ACO1 expression is independent of ethylene (Bouquin *et al.*, 1997), and so this compound was used to test further that wounding increases TR-ACO2 gene expression independently of ethylene.

3.13.13 Changes in TR-ACO1 and TR-ACO2 gene expression in attached wounded and non-wounded mature green leaves

The four treatments used in this experiment were:

1. Non-wound
2. Wound
3. 1-MCP (1 ppm) pretreatment for 30 min non-wound
4. 1-MCP (1 ppm) pretreatment for 30 min wound.

The concentration and time of exposure of the leaves to 1-MCP was based on the study of Bouquin *et al.*, (1997) who showed an exposure of 0.1 to 1 ppm for 10 min was sufficient to affect gene expression of CM-ACO1 in leaves of melon. The plants were kept under continuous illumination throughout the 24 h period. Leaves were harvested at 1, 2, 3, 6, and 24 h after the tissue in the wounding treatment were wounded.

Total RNA was isolated from leaves of all four treatments from all four time points and analysed by northern analysis. Duplicate blots were probed with either [α-^{32}P]-dATP labelled 3'-UTR of TR-ACO1 (Figure 63) or the 3'-UTR of TR-ACO2 (Figure 64) and the blots washed at high stringency (0.1 X SSPE, 0.1 %SDS at 65 °C).

The 3'-UTR of TR-ACO1 hybridised to an RNA transcript in non-wounded leaves that changed in abundance over the 24 hour time period suggesting a circadian type control of its expression (Figure 63). For instance, at 2:30 pm (afternoon) abundance of the TR-ACO1 transcript was comparatively high, by 3:30 pm (mid afternoon) the levels had decreased but were still comparatively high, at 4:30 pm (late afternoon) and 7:30 pm (night) the levels were low and by 24 h (1:30 next day; early afternoon) the level of the transcript had again become elevated.

Wounding the leaves changed the above pattern of gene expression of the TR-ACO1 transcript (Figure 63). As in the non-wounded leaves, gene expression of TR-ACO1 was highest initially. However, unlike the non-wounded leaves, the levels of the TR-ACO1 transcript continued to decline to be lowest 24 h after wounding.

Pre-treating non-wounded leaves with 1-MCP for 30 min prevented the putative circadian control of TR-ACO1 (Figure 63). The pattern of expression of TR-ACO1 in 1-MCP treated leaves was similar to that in wounded leaves, in that expression again declined to be lowest by 24 h.

TR-ACO1 expression in the wounded leaves pre-treated with 1-MCP was similar to the expression in non-wounded leaves pre-treated with MCP. However, the levels of the transcript remained higher for a longer period of time (up to 3 h after wounding compared with 2 h) before the levels declined to be very low by 24 h.

Ethidium bromide staining of the RNA indicated that equivalent amounts of RNA were loaded into each lane for each treatment used in the above northern studies (Figure 63). This suggests that the observed changes in TR-ACO1 gene expression in these treatments were not simply a result of unequal loadings of the RNA.

The senescence-associated gene transcript, TR-ACO2, was virtually undetectable in non-wounded mature green leaves over the 24 h time period which is what was predicted (Figure 64). Unlike expression of TR-ACO1, TR-ACO2 gene expression did not appear to be under circadian-type regulation.

Wounding induced gene expression of TR-ACO2 in attached leaves (Figure 64) with induction of TR-ACO2 gene expression being clearly evident in leaves 3 h after wounding. The level of the transcript then remained high throughout the remaining 24 h time period. This confirmed that dark incubation and leaf detachment were not necessary for induction of TR-ACO2, but could not rule out an involvement of wound-induced ethylene.

It was predicted that if wounding leaves induced TR-ACO2 expression independently of ethylene, then TR-ACO2 levels should be elevated in the presence of the ethylene action inhibitor, 1-MCP, and this is what was observed (Figure 64). Gene expression of TR-ACO2 was first detected at 2 h, was maximal at 6 h, and then declined to be virtually undetectable by 24 h.

However, pretreatment of leaves with 1-MCP in the absence of wounding also elevated expression of TR-ACO2 (Figure 64). Gene expression of TR-ACO2 was first detected at 2 h, was maximal at 3 h, and declined by 24 h to a level approximately that observed at 2 h. The finding that 1-MCP can itself, in the absence of wounding, elevate TR-ACO2 gene expression in leaves, means it still cannot be concluded whether wounding can induce TR-ACO2 gene expression independently of ethylene.

Ethidium bromide staining of the RNA used for analysis with the 3'-UTR of TR-ACO2 indicated that some of the lanes contained different quantities of RNA (Figure 64). However, the differences in loadings were concluded to be too small to explain the differences observed in the expression of TR-ACO2.

Finding that TR-ACO1 gene expression, but not TR-ACO2 gene expression, was under a circadian-type regulation, provided a further opportunity to examine whether the declining activity observed in the chlorotic extracts was due to the assay predominantly measuring the decline in the activity of the TR-ACO1 enzyme.

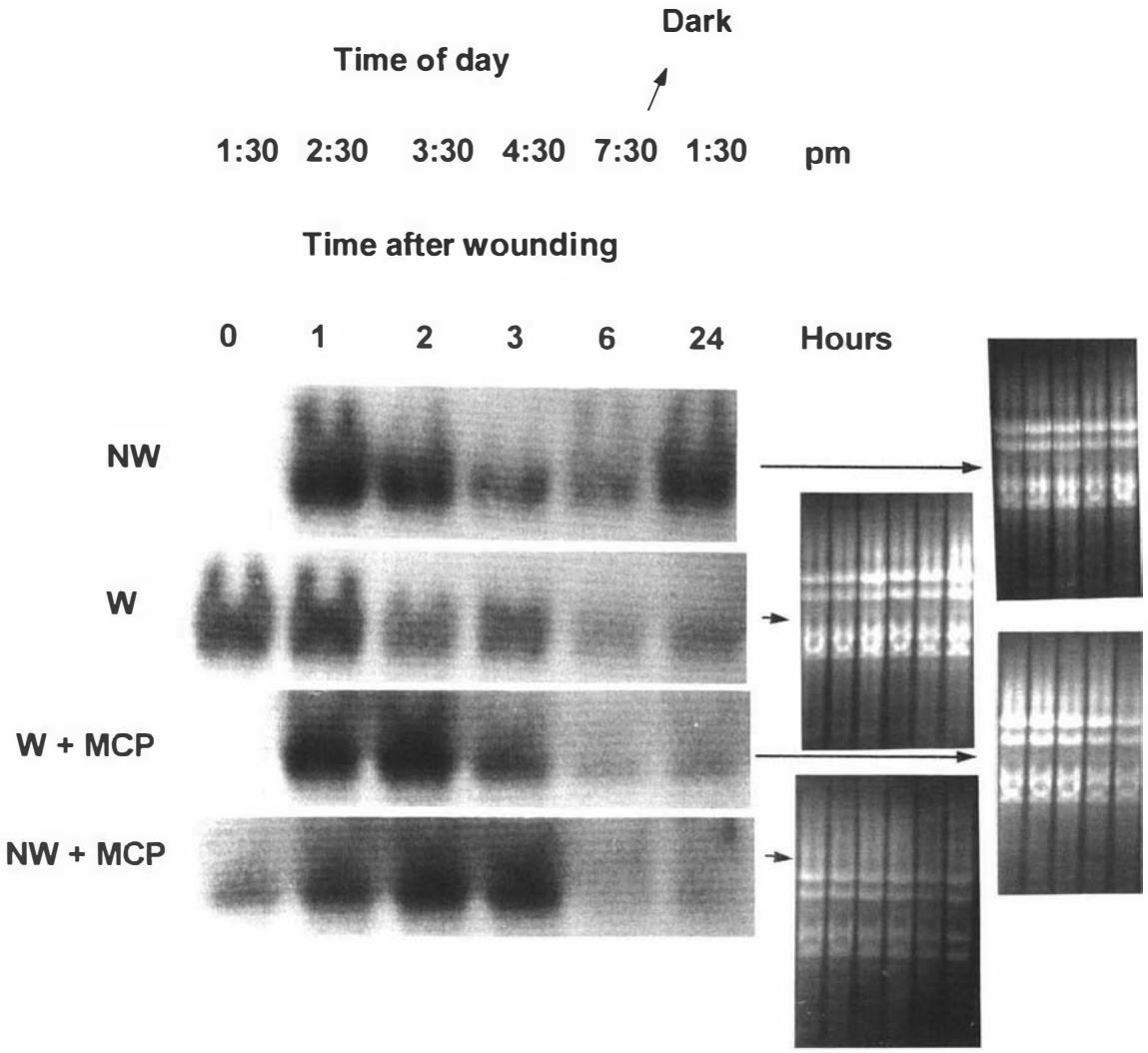

Figure 63. The effect of wounding attached leaves either with or without a 30 min pretreatment with 1-MCP on transcript expression of TR-ACO1.

Northern blots were probed with [α-^{32}P]-dATP labelled 3'-UTR of TR-ACO1. To the right of the northern blots are the corresponding RNA gels used for the blotting, stained with ethidium bromide to give an indication of the equivalence of loading of each lane.
As the time 0 point was the same for both wounded and non wounded only a single time 0 point was examined for the non 1-MCP treated plants and a single time 0 point for the 1-MCP treated plants.

NW	=non wound.
W	=wound.
W + MCP	=wound, 1-MCP pretreatment.
NW + MCP	=non wound,1-MCP pretreatment.

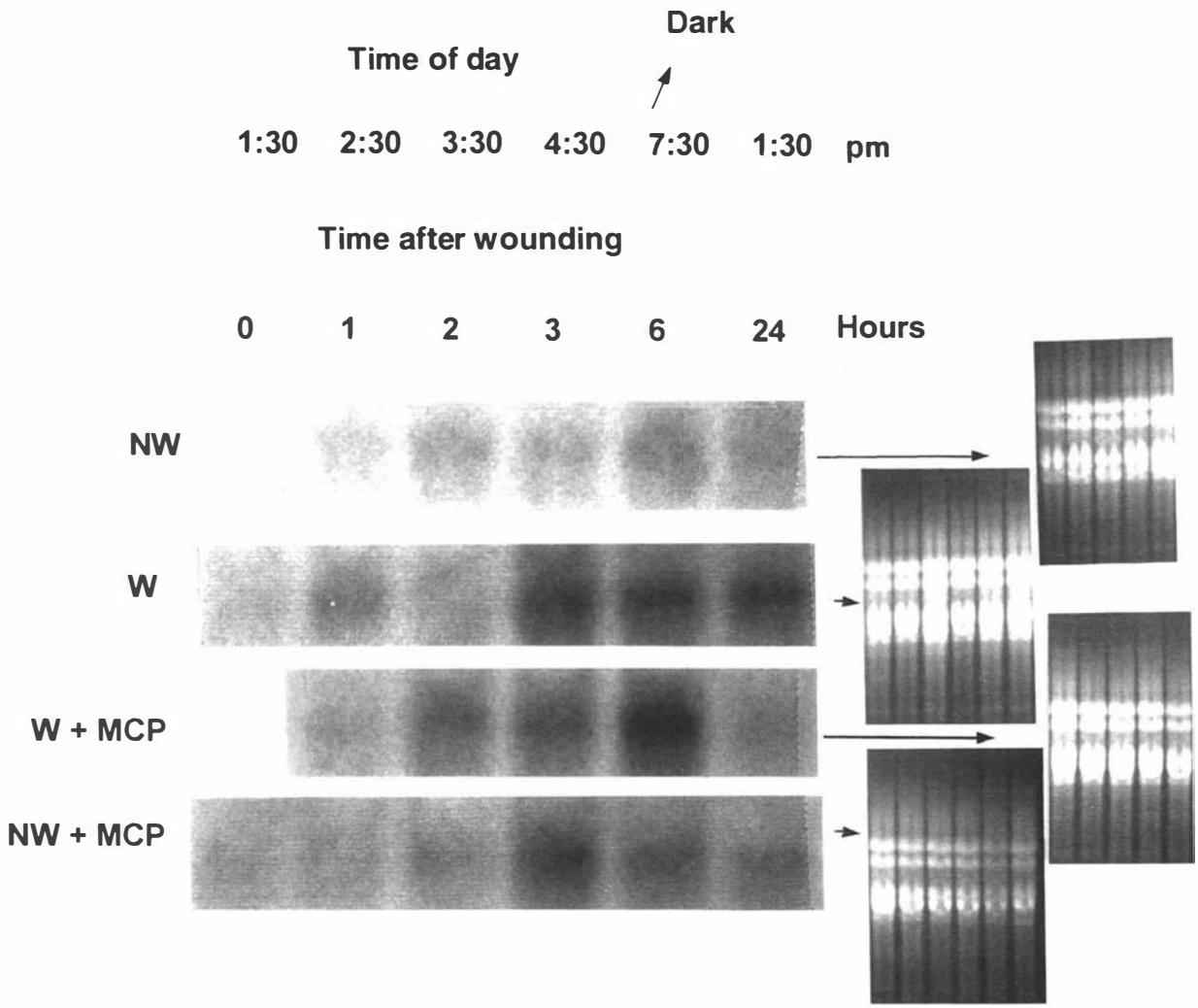

Figure 64. The effect of wounding attached leaves either with or without a 30 min pretreatment with 1-MCP on transcript expression of TR-ACO2.

Northern blots were probed with [α-^{32}P]-dATP labelled 3'-UTR of TR-ACO1. To the right of the northern blots are the corresponding RNA gels used for the blotting, stained with ethidium bromide to give an indication of the equivalence of loading of each lane.
As the time 0 point was the same for both wounded and non wounded only a single time 0 point was examined for the non 1-MCP treated plants and a single time 0 point for the 1-MCP treated plants.

NW	=non wound.
W	=wound.
W + MCP	=wound, 1-MCP pretreatment.
NW + MCP	=non wound,1-MCP pretreatment.

3.13.14 Changes in ACC oxidase activity *in vitro* in mature and senescing leaves over a 24 h time period

ACC oxidase activity was measured in mature green, onset of senescence, and senescent leaves harvested over a 24 h time period. ACC oxidase did appear to vary over the 24 h time period (Figure 65). Activity was highest at 11:30 am (light stage) and lowest at 9:00 pm (dark stage) in tissue extracts from all three developmental stages examined. This broadly matched transcript accumulation of the TR-ACO1 which was highest at 2:30 pm and lowest at 7:30 pm (Figure 63). This may suggest that since the chlorotic extract was showing a circadian-type rhythm in its ACC oxidase activity, it may be that it is the activity of the TR-ACO1-encoded enzyme in this extract which is predominantly being measured. However, the ACC oxidase activity *in vitro* did not in the tissue examined return at 24 h to the level of activity first observed at 0 h. Therefore, although there is tentative evidence for the activity being measured being under a circadian-type regulation, this phenomenon will need more detailed study before it can be concluded unequivocally.

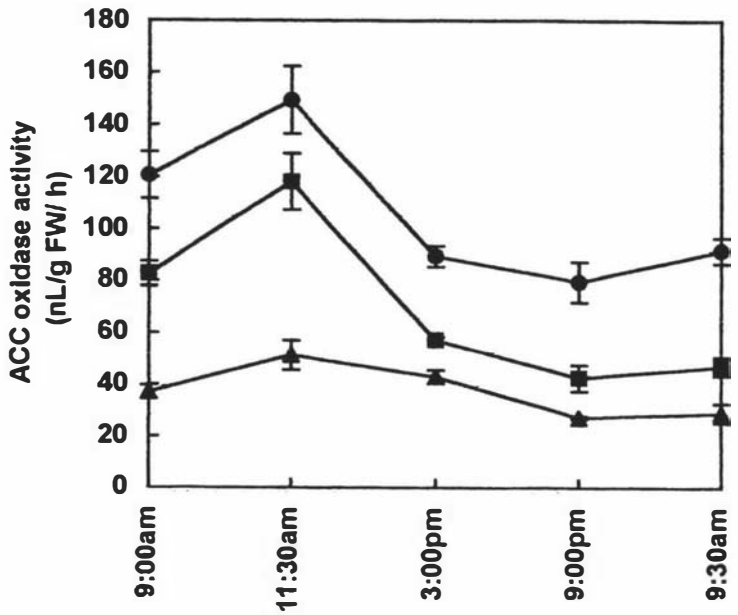

Figure 65. ACC oxidase activity measured *in vitro* in mature green, onset of senescence and senescent leaf tissue over a 24 h time period.

(--●--) Mature green leaf tissue.
(--■--) Onset of senescence leaf tissue.
(--▲--)Senescent leaf tissue.

Error bars = ± 1 sem for 3 internal replicates of single experiment.

4. Discussion

This thesis has extended the study of Butcher (1997) who first provided evidence for increased activity of the ACC-mediated ethylene biosynthetic pathway being the cause of the senescence-associated increase in ethylene production of leaf tissue in white clover.

In both the current study, and that of Butcher (1997), ethylene evolution was lowest in mature green leaves but increased as the leaves became progressively more chlorotic (Figure 15). This has been reported previously for leaves of other plants, whether the leaves have been detached and induced to senesce off the plant (for example, in oat, Gepstein and Thimann, 1981; pinto bean, tobacco and sugar beet leaves, Aharoni *et al.*, 1979), or have senesced naturally on the plant (tobacco, Alejar *et al.*, (1988) and cotton, Morgan *et al.*, (1992)). Leaf senescence, however, is not always characterised by elevated ethylene production. In *Phaseolus vulgaris,* ethylene evolution is highest (2 nL g^{-1} FW h^{-1}) during leaf expansion, then declines by 75 % as the tissue matures and remains constant at *ca.* 0.4 nL g^{-1} FW h^{-1} during senescence (yellowing) (Roberts and Osborne, 1981). In white clover, the rapid increase in ethylene production occurs in leaf tissue after chlorophyll levels have begun to decline and coincides with the period of most rapid chlorophyll loss (Figure 15). This is consistent with observations made with pinto bean, sugarbeet, tobacco (Aharoni *et al.*, 1979) and oat (Gepstein and Thimann, 1981) leaf tissue.

The quantities of ethylene evolved from attached leaf tissue of white clover during leaf maturation and senescence are slightly lower than that reported for leaves of other plants. In mature green leaves of white clover, ethylene evolution is between 0.25 and 0.3 nL g^{-1} FW h^{-1}, which is lower than the levels of ethylene evolved from oat (*ca.* 0.5 to 1 nL g^{-1} FW h^{-1}; Gepstein and Thimman, 1981) and tobacco leaf discs (1 nL g^{-1} FW h^{-1}; Aharoni *et al.*, 1979), and detached leaves of tomato (*ca.* 0.5 nL g^{-1} FW h^{-1}, John *et al.*, 1995). During leaf chlorosis in white clover, ethylene production increased *ca.* 8-fold to be 2 nL g^{-1} FW h^{-1} at leaf 16, while in oat, tobacco and tomato the levels increased 4-fold, 3-fold and 3-fold to 4, 3, and 1.8 nL g^{-1} FW h^{-1} respectively. The senescence-associated ethylene climacteric of leaves can be compared with that of flowers and fruits. In leaves, both the absolute levels and the fold increase in ethylene evolution during senescence are much lower than observed for senescing carnation flowers (1000-fold increase to 100 nL g^{-1} FW h^{-1}, Bufler, *et al.*, 1980) and ripening avocado fruit (115 nL g-1 fw h^{-1}, Hoffman and Yang, 1980).

Increased activity of the ACC-mediated ethylene biosynthetic pathway is considered to be primarily the cause of ethylene evolution of senescing leaves. Evidence for this originally came from experiments where:

1. Exogenous application of ACC to senescing (yellow) leaves was converted to ethylene (Osborne, 1991).
2. Exogenous application of ACC to leaves promoted the onset of leaf chlorosis in oat, while inhibitors of the pathway (AVG and Co^{2+}) delayed it (Gepstein and Thimann, 1981).
3. Downregulation of ACC oxidase, using antisense technology, severely reduced ethylene production in the senescent leaves of tomato (< 0.087 nL g^{-1} FW h^{-1} at the advanced stage of senescence) compared to non-transformed tomato leaf tissue (1.8 nL g^{-1} FW hr^{-1}; John *et al.*, 1995).

The increase in levels of endogenous ACC during leaf senescence of white clover (in both this study and that of Butcher (1997)) is further evidence for a role of the ACC-mediated pathway in senescence-associated ethylene production (Figure 16). An increase in levels of endogenous ACC in ageing tissue (associated with the ethylene climacteric) has previously only been reported for ripening fruit (for example, avocado, Hoffman and Yang, 1980) and senescing flowers (for example, carnation, Hanley *et al.*, 1989).

Although this study has confirmed that levels of endogenous ACC in leaves (as measured by the method of Lizada and Yang, 1979) increase during senescence, and that the increase precedes (or is coincident with) the increase in ethylene evolution, it also suggests that the Lizada and Yang method may be overestimating the senescence-associated increase in levels of endogenous ACC in this tissue. The method of Lizada and Yang relies on the chemical-based oxidation of ACC in a tissue extract to ethylene which is then measured with a gas chromatograph. However, if the crude extract of chlorotic leaves is partitioned by paper chromatography prior to chemical oxidation, it is found that substances at R_f 0.32 and R_f 0.49 are produced in leaf tissue during senescence that can be oxidised to ethylene (Figure 18). By comparison, authentic ACC (dissolved in water) in this system was found to have a relative mobility of 0.59, and only a very small amount of ethylene was produced at this region by the chlorotic extract. The substance(s) in the chlorotic leaf extracts are not considered to be a conjugated form of ACC as hydrolysis with 6 N HCl is necessary for release of ACC from conjugated forms prior to assay (Lizada and Yang, 1979). The

extraction of authentic ACC with the chlorotic leaf tissue resulted in a similar amount of ethylene produced by the substance at R_f 0.32, but an increase in the substance at R_f 0.49. This suggests that the compound at R_f 0.49 is ACC, and that its mobility in the chromatograph is hindered by association with endogenous compounds in the chlorotic leaf extract. It is possible that the substance(s) at R_f 0.32 could be an unsaturated fatty acid such as linolenic acid (18:3) as linolenic acid is known to increase during leaf senescence (Olsson, 1995), and linolenic acid can be oxidised in chemical systems to give rise to ethylene (Lieberman and Mapson, 1964).

Extracts of wounded mature green leaves were also analysed by paper chromatography in this study (Figure 18). This was carried out for two reasons. Firstly, it would indicate whether wounding elevates ACC levels in the leaf tissue, consistent with the effect of wounding on other tissue (for example, pericarp discs of both tomato and winter squash fruit, Hyodo, 1991). Secondly, any increased levels of endogenous ACC could then be used as an alternative indicator as to where endogenous ACC in the leaf extracts was resolving to on the chromatogram. Extracts of the wounded leaves produced increased levels of ethylene at two regions of the chromatogram. One region, at R_f 0.55, was very close to where authentic ACC (dissolved in water) resolved to. It was therefore concluded that wounding did elevate levels of ACC in mature green leaves of white clover, and that endogenous components in these leaf extracts retarded movement of ACC to a lesser extent than those in the chlorotic extracts. The second region of the chromatogram that produced ethylene was again at R_f 0.32. This was the same region that produced most of the ethylene in the chlorotic extracts and which was considered not to be ACC. This is interesting, as a substance(s) that is produced in increased amounts in senescent extracts also forms in detached mature green leaf tissue incubated in the dark. Detachment and dark incubation are accepted ways of inducing senescence (Gepstein and Thimann, 1981; Gan and Amasino, 1997). Furthermore, breakdown of phospholipids which leads to increases in free fatty acids has been reported to occur early during tissue senescence, for example, during petal senescence of *P. hybrida* (Borochov *et al.*, 1997). Therefore, as suggested for the chlorotic extract, the substance at R_f 0.32 in the mature green extract may be a fatty acid such as linolenate.

The Lizada and Yang method has still been used as the sole measure of ACC in some recent studies (for example, Banga *et al.*, 1996). However, the results with senescing leaf tissue of white clover suggests a need to use more powerful analytical tools to examine the

authenticity of ACC production in senescing tissue. ACC analysis by preparative HPLC combined with GC-MS has been described for roots of sunflower seedlings (Finlayson *et al.,* 1996) and hypocotyls of wounded Norway spruce (Ingemarsson and Bollmark, 1997). A less expensive, but equally high resolution alternative to GC-MS has been described by Hall *et al.,* (1993). This technique replaces the GC-MS procedure with a GC containing a nitrogen/ phosphorus detector.

Nevertheless, the chromatography approach broadly confirmed the Lizada and Yang assay which showed a positive correlation between endogenous ACC content and ethylene evolution during leaf senescence of white clover. This suggests that the ACC-mediated ethylene biosynthetic pathway is functional in chlorotic tissue. A more complete understanding of the role of this pathway in controlling ethylene production can be achieved by studying the regulation of ACC synthase and ACC oxidase. This thesis focused on gene expression, protein accumulation and activity of the second of these enzymes, ACC oxidase, during leaf maturation and senescence in white clover.

4.1 Biochemical characterisation of ACC oxidase

ACC oxidase activity in the crude leaf extracts of white clover could only be measured after passage of the extract through Sephadex G-25 (data not shown). This suggests that there are low molecular weight inhibitory substance(s) in the leaf extracts, as Sephadex G-25 is able to remove substances less than 5000 in molecular weight and is commonly used for desalting purposes. Obligate removal of putative low molecular weight inhibitors has also been reported for flavedo tissue of mandarin fruit (Dupille and Zacarias, 1996), but not for extracts from melon fruit (Ververidis and John, 1991), roots and leaves of sunflower and corn seedlings (Finlayson *et al.,* 1997), internodes of deepwater rice (Mekhedov and Kende, 1996), apple fruit cortical tissue (Fernandez-Maculet and Yang, 1992; Mizutani *et al.,* 1995), embryonic axes of chick pea seeds (Munoz De Rueda *et al.,* 1995), or senescing carnation petals (Nijenhuis-De Vries *et al.,* 1994). The nature of these inhibitory substances in white clover was not studied. However, there are chemicals and compounds found in some plant tissues that are known to inhibit ACC oxidase activity. These include cobalt (Ververidis and John, 1991) and tropalones (an iron chelator, Mr 117) (Mizutani *et al.,* 1998). The presence of an iron chelator could be tested for by examining whether the presence of higher amounts of iron in the assay enabled measurement of activity.

ACC oxidase has a pH optimum of 7.5 in a Tris-based assay (Figure 22). This optimum is similar to that of apple (pH 7.2 to 7.8, Kuai and Dilley), melon (pH 7.5, Smith *et al.*, 1992), avocado (pH 7.5 to 8.0, McGarvey and Christofferson 1992) and mandarin fruit (pH 7.5, Dupille and Zacarias, 1996). ACC oxidase of white clover has broad cofactor range (iron (20 to 80 mM) and bicarbonate (10 to 50 mM)) and cosubstrate requirements (ascorbate (30 to 150 mM)) (Figure 51) which is similar to the enzymes in banana (Moya-Leon and John, 1995); and cherimoya fruit (Escribano *et al.*, 1996), and also the enzyme in carnation petals (Nijenhuis-De Vries *et al.*, 1994).

The reaction catalysed by ACC oxidase assayed *in vitro* from mature green leaves was linear up to 20 min and then declined with a half-life of 22.5 min (Figure 19). This is very similar to the recombinant pTOM13 ACC oxidase protein expressed in *E. coli* and assayed *in vitro* (linear for 20 min, and activity then declining with a half life of 14 min, Smith *et al.*, 1994). Other studies have reported that ACC oxidase becomes non-linear after as little as 5 min for the enzyme in carnation petals (Nijenhuis-De Vries *et al.*, 1994) to as long as 50 min for the enzyme in pear fruit (Vioque and Castellano, 1998).

The non-linearity of the reaction is in part due to the interaction of the chemicals in the reaction mix, and can be independent of activity. For instance, in aerobic conditions, 0.1 mM Fe^{2+} has been shown to oxidise all the thiol groups of 2 mM DTT by 30 min at 30°C (Perry *et al.*, 1988). This in turn can compromise the ability of DTT to protect the cysteine sulphydryl groups of ACC oxidase from oxidation. The importance of maintaining the cysteine sulphydryl group(s) of ACC oxidase in the reduced form is evident by the finding that sulphydryl reagents such as trinitrobenzene sulphonate at a concentration of 1 mM or 5 mM inhibit the activity of ACC oxidase in mandarin fruit peel by 64 % (Dupille and Zacarias, 1996) and in melon fruit by 99.3 % (Smith *et al.*, 1992). There are three completely conserved cysteine residues in all ACC oxidases hitherto sequenced (including TR-ACO1 and TR-ACO2; Figures 27 and 28). Kadyrzhanova *et al.*, (1997) have proposed that the cysteine at position 28 (C^{28}) is the residue that must be retained in a reduced form, although this remains to be conclusively proven. Of the other two, C^{165} has been altered by site directed mutagenesis to alanine and shown not to be essential for activity, and C^{133} is considered to be part of a putative leucine zipper.

A second mechanism by which the reagents of the reaction mix may interact is through the interaction of Fe^{2+}, ascorbate and O_2 which is known as Udenfreind's reagent (Udenfreind

et al., 1954, cited in Barlow *et al.,* 1997). Udenfreind's reagent leads to the formation of H_2O_2, which in turn has been shown directly to inhibit activity of a recombinant pTOM13 ACC oxidase (Smith *et al.,* 1994). The target of H_2O_2 modification is thought to be thiol groups (Omkumar and Ramasarma, 1993), and in this regard DTT has been shown to be nearly as effective as catalase at preventing inactivation of the recombinant pTOM13 ACC oxidase (Smith *et al.,* 1994).

Although shaking is necessary for obtaining maximal enzyme activity, activity of ACC oxidase was inhibited by vortexing (Figure 20). It may be that vortexing increases the rate of oxidation or surface denaturation of ACC oxidase as vortexing can be detrimental to enzyme activity (Deutscher, 1990). Furthermore, ACC oxidase appears to undergo partial unfolding of the catalytically active conformation with time (Barlow *et al.,* 1997) and vortexing may hasten this process.

In terms of extraction requirements, the inclusion of DTT (2 mM) and ascorbate (30 mM) in the Tris-glycerol extraction buffer of Ververidis and John (1991) increased the recovery of ACC oxidase activity 4-fold *in vitro* (Figure 24). Increased recovery with ascorbate has also been documented for the cortical tissue of apple (Fernandez-Maculet and Yang, 1992; Kuai and Dilley, 1992) and flavedo tissue of mandarin fruit (Dupille and Zacarias, 1996), but not for the mesocarp of cherimoya fruit (Escribano *et al.,* 1996). Escribano *et al.,* (1996) found during partial purification of ACC oxidase from cherimoya fruit that activity *in vitro* was enhanced by inclusion of DTT and soluble PVP, but not ascorbate or Triton X-100. DTT has also been shown to increase recovery of ACC oxidase activity from flavedo tissue of mandarin fruit by 36 % (Dupille and Zacarias, 1996).

4.2 Molecular characterisation of ACC oxidase

RT-PCR with degenerate primers made to conserved domains among ACC oxidase sequences was successful in amplifying sequences that show high homology to ACC oxidases in the GenBank database. Amplified sequences were initially considered to be from the same gene if similarity in their sequences was greater than 94 %. On this basis, two distinct groups of sequences were identified, designated as TR-ACO1 and TR-ACO2 (Figures 27 and 28). These sequences showed 84 % homology in their nucleotide and 87 % identity in their amino acid sequences. In some studies, similarities in amino acid sequences have been used to indicate evolutionary relationships. For instance, ACC synthases that have IAA-inducible regulatory elements from different plants species appear

to be more similar in sequence than they are to other members of their own gene families. Because of this, it has been proposed that the IAA-inducible regulatory sequence co-evolved with a particular ACC synthase isoenzyme (Liang *et al.,* 1993). In this study, it was of interest to see whether TR-ACO2 was more closely related to other senescence-associated ACC oxidases than it was to TR-ACO1. If so, it may suggest that these isoenzymes have arisen from a common (senescence-associated) ancestor and/ or that the conditions associated with senescing tissue may select for an isoenzyme with particular sequence constraints. This was examined by aligning TR-ACO1 and TR-ACO2 sequences with randomly selected ACC oxidases and other 2-ODDs in the GenBank and determining their phylogenetic relationship using a tree building programme (Figure 32). The phylogenetic tree clearly clustered TR-ACO1 and TR-ACO2 within the ACC oxidase grouping, and also showed that TR-ACO2 had closer homology to the mature-green-associated TR-ACO1 than to the senescence-associated ACC oxidase of tomato (LE-ACO1, Barry *et al.,* 1996) and melon (CM-ACO1, Lassere *et al.,* 1997).

Both TR-ACO1 and TR-ACO2 sequences appear to encode functional enzymes, as their deduced amino acid sequences contain all the residues hitherto shown to be important (within the regions of TR-ACO1 and 2) for maximal activity of the enzyme (Zhang *et al.,* 1997; Charng *et al.,* 1997). More complete proof, however, will await either measurement of activity after heterologous expression of the complete cDNA sequences, or alternatively, after purification of the individual isoenzymes corresponding to each gene.

RT-PCR with degenerate primers made to conserved domains of ACC oxidase genes together with cloning and sequencing, was effective at identifying two members of the ACC oxidase gene family. However, all members of the gene family may not be readily identified by this method. Firstly, identification of gene sequences may be a function of the abundance of the transcript in tissue. That is, if the transcript is present in only low amounts in tissue it may not be readily amplified, and will therefore be cloned to a lesser extent. Consequently, the discovery of such gene transcripts may only be achieved by screening large numbers of clones. Secondly, interpretation error may be a factor. For instance, in this study as a starting point, cDNA sequences displaying greater than 94 % homology were considered to be encoded by the same gene. However, individual members of a gene family can display very high homology. For example, in tomato, LE-ACO1 and 3 show 94 % similarity in their nucleotide sequence (Barry *et al.,* 1996), which in this study would have been high enough initially, for them to have been considered to be encoded by

the same gene. Genomic Southern analysis has been used in other studies to indicate the number of members of particular gene families (Lasserre *et al.*, 1996). In this study, Southern analysis with the coding regions of TR-ACO1 and TR-ACO2 was able to confirm that the sequences were encoded by distinct genes, but it could not confirm that the sequences were specific to single genes, as multiple genomic fragments were recognised in each of the lanes (Figure 34).

The coding frame regions of TR-ACO1 and TR-ACO2 may have recognised multiple genomic fragments on the Southern blot because of:

1. restriction sites within, as yet unsequenced, regions of each gene
2. the presence of additional genes (or pseudogenes) similar in sequence, or
3. the allele for each gene is polymorphic.

To examine further the cause of the multiple hybridisation patterns, genomic DNA was re-probed with regions of the TR-ACO1 and TR-ACO2 cDNA sequences that were more divergent.

A characteristic of ACC oxidases is the sequence divergence at their 3'-UTR (Tang *et al.*, 1994; Kim and Yang, 1994; Barry *et al.*, 1996). For example, while LE-ACO1 and 3 of tomato share 94 % homology in their reading frame, the similarity in their 3'-UTR is only 47 %. Similarly, in *P. hybrida,* PH-ACO3 and 4 share 91 % similarity in their coding region but only 50 % at their 3'-UTR.

In this thesis, the 3'-UTRs of both TR-ACO1 and TR-ACO2 were successfully generated using 3'-RACE (Figures 41 and 42). In common with other ACC oxidases, the 3'-UTRs of TR-ACO1 and 2 were less similar in sequence (61 % homology) than their cognate coding regions (84 %). While this procedure generated only one 3'-UTR of TR-ACO1, it generated three 3'-UTRs of the TR-ACO2 sequence. Sequencing identified the two shorter sequences as truncated versions of the longest 3'-UTR. Truncated versions of ACC oxidase 3'-UTRs have also been observed in PH-ACO1 (*P. hybrida*, Tang *et al.*, 1993); and OS-ACO1 (rice, Mekhedov and Kende, 1996), while the presence of two polyadenylation signals in the 3'-UTR has been reported for VR-ACO1 (mungbean, Kim and Yang, 1994). In white clover, two putative polyadenylation sequences (each containing FUEs and NUEs, Rothnie, 1996) could be identified which may provide a basis for the three truncated versions of TR-ACO2 found.

The 3'-UTRs of TR-ACO1 and 2 were used as probes to reexamine the multiple hybridisation patterns obtained with the coding regions in genomic Southern analysis.

The 3'-UTR of TR-ACO1 hybridised to all the genomic fragments recognised by its cognate coding-frame region (Figure 47). This suggests that all the fragments recognised by the TR-ACO1 coding region also contain the 3'-UTR. It appears, therefore, that the multiple hybridisation pattern being recognised is not due to fragments produced by digestion within restriction sites of putative introns, because only one fragment (the one containing the 3'-UTR) would then be recognised. The high similarity in the 3'-UTR of the fragments do suggest that the fragments represent different alleles of a single gene (TR-ACO1), rather than very similar but distinct genes. In this regard, it should be noted that the genome of white clover is allotetraploid. That is, white clover contains two independently segregating genomes, so that there is potential for up to four polymorphic alleles for each gene. To confirm that the fragments recognised by the 3'-UTR of TR-ACO1 are polymorphic alleles requires segregation analysis using inbred lines of white clover.

Another possibility was that the TR-ACO1 gene had undergone a gene duplication event(s). For example, the PH-ACO1 gene of *P. hybrida* has been reported to have undergone a gene duplication event to give rise to PH-ACO2 which is a pseudogene (that is, it is not transcribed). Evidence for PH-ACO2 having resulted from a gene duplication of PH-ACO1 included its close proximity to PH-ACO1 (only 6 Kb downstream), the finding that it was a pseudogene, and of particular relevance to this study, that it showed very high sequence homology (93 %) in the 3'-UTR (which is atypical of ACC oxidase genes). Pseudogenes do occur in white clover. For example, four pseudogenes of alcohol dehydrogenase have been identified in white clover by screening a white clover genomic library (Nick Ellison, AgResearch, Palmerston North, NZ *pers. comm.*). In this thesis, the genomic Southern analysis using both coding-frame and 3'-UTRs of TR-ACO1 as probes could not distinguish between pseudogenes and other gene duplication events, or polymorphic alleles.

In contrast to the 3'-UTR of TR-ACO1, the 3'-UTR of TR-ACO2 hybridised to only a single genomic fragment in each lane of the Southern blot, and these fragments were a subset of that recognised by its cognate coding region (Figure 47). This suggested that the other non-recognised genomic fragments (in the coding region probed Southern), either did

not contain a 3'-UTR, or had a different 3'-UTR to TR-ACO2. If the fragments did not contain a 3'-UTR, then the fragments must have been excised away from the 3'-UTR by digestion within the putative, as yet undefined introns (that is, because the coding frame region recognised the fragments). This is considered unlikely, as the introns of the TR-ACO2 gene would need to have restriction sites for all three enzymes used in the digestion. The more likely explanation is that the non-recognised genomic fragments contained a 3'-UTR that is dissimilar to that of TR-ACO2. This suggests that there is an additional ACC oxidase in the genome of white clover that is similar in coding sequence to TR-ACO2, but has a divergent 3'-UTR. This has been reported for tomato where ACC oxidase gene transcripts of LE-ACO1 and 3 ACC share 94 % sequence similarity in their coding region, but only 47 % similarity in the 3'-UTR. The presence of additional genes could be confirmed by probing the Southern blot with the 5'-UTR of TR-ACO2. If the 5'-UTR recognised the same fragments as the 3'-UTR, then the complete coding portion of the gene must be within the fragment and so the other fragments would then be most likely representative of additional genes. Alternatively, the coding frame region of TR-ACO2 could be used to screen a genomic library.

In this thesis, further evidence was provided for the existence of an additional, as yet undefined, TR-ACO2 gene transcript using northern analysis. The coding region of TR-ACO2 hybridised to two RNA transcripts on the northern blot of *ca.* 1.17 Kb and 1.35 Kb (Figure 38). The size difference is similar to that between the largest and smallest version of the TR-ACO2 3'-UTR (Figure 42) and so, initially it was thought that the 1.17 Kb transcript was a truncated version of the 1.35 Kb transcript. However, this appears not to be true, as the largest 3'-UTR of TR-ACO2 did not recognise the 1.17 Kb transcript on the northern blot (Figure 48). It should have if the 1.17 Kb transcript was a truncated version of the 1.35 Kb transcript. Therefore, the 1.17 Kb transcript appears to have a distinct 3'-UTR to the 1.35 Kb transcript, which is consistent with the proposition that they are transcribed from different genes.

To offer support to this proposal, two distinct isoenzymes of ACC oxidase (SEI and SEII) have now been purified from chlorotic leaf tissue of white clover (Dr Deming Gong, Institute of Molecular BioSciences, Massey University, NZ *pers. comm*). Dr Gong has also identified a third isoenzyme in the mature green leaf tissue which is distinct from both SEI and SEII and is proposed to be the protein encoded by TR-ACO1.

4.3 Gene expression of TR-ACO1 and TR-ACO2 during leaf maturation and senescence

TR-ACO1 and TR-ACO2 transcripts were differentially expressed during leaf maturation and senescence of white clover (Figure 48). Levels of TR-ACO1 transcript were high in mature green leaves until the onset of senescence (as judged by chlorosis) at which time transcript accumulation declined to be lowest in the most senescent leaves examined. By contrast, gene expression of TR-ACO2 was very low in mature green leaves, but increased prior to the large decline in chlorophyll and climacteric rise in ethylene production. The differential expression of TR-ACO1 and TR-ACO2 during leaf senescence is consistent with what has now been found in tomato (Barry *et al.*, 1996) and melon (Lasserre *et al.*, 1997). In tomato, LE-ACO1 and LE-ACO3 gene transcripts accumulate during leaf senescence. However, LE-ACO3 only accumulates transiently, at the onset of senescence, and its levels are much lower than LE-ACO1. By contrast, levels of the LE-ACO1 transcript are high at all stages of senescence examined (onset, mid, and advanced, as judged by chlorophyll loss). In melon, gene expression of CM-ACO3 was highest in young leaves and declined to be lowest in the most chlorotic leaves examined (yellow-green adult), which is very similar to TR-ACO1 gene expression. Whereas, CM-ACO1 was lowest in young leaves, highest in pale-green adult leaves (representative of the onset of chlorosis) and slightly lower in yellow-green adult leaves. This pattern of expression more closely resembles that of TR-ACO2.

This study has extended the gene expression studies in melon and tomato leaf tissue by combining gene expression analysis during leaf maturation and senescence with data for both activity and protein accumulation of ACC oxidase.

4.4 Changes in ACC oxidase activity during leaf maturation and senescence

ACC oxidase activity, *in vitro*, was highest in mature green leaves and then declined as the leaves became chlorotic, such that activity was lowest in leaves evolving the highest amounts of ethylene (Figure 56). This was unexpected, as increased ethylene production during tissue ageing is typically accompanied with increased ACC oxidase activity *in vitro*, for example, in tomato (John *et al.*, 1995; Barry *et al.*, 1996), melon (Ververidis and John, 1991; Guis *et al.*, 1997), and apple fruit (Dong *et al.*, 1992; Reid, 1995), and in senescing carnation flowers (Nijenhuis-De Vries *et al.*, 1994; Woltering and Harren, 1989).

There are several possible reasons for the decline in activity, including genetic regulation, characteristics of the isoenzyme, or characteristics of the tissue environment. Each possibility is discussed below.

1. Genetic regulation.

i.) The decline in ACC oxidase activity *in vitro* may be due to reduced gene expression of ACC oxidase during leaf senescence, as studies have shown that ACC oxidase appears to be regulated at the level of gene transcription during tissue ageing. For example, increased ACC oxidase gene expression is accompanied with increased ACC oxidase activity *in vitro* during ripening of apple fruit (Dong *et al.*, 1992) and senescence of carnation petals (Nijenhuis-De Vries *et al.*, 1994).

The results from the gene expression studies of TR-ACO1 and TR-ACO2 show that gene expression of TR-ACO2 is enhanced during leaf senescence and so it might appear that activity should therefore be elevated. However, gene expression of TR-ACO1 may be much higher than gene expression of TR-ACO2 so that overall levels of activity follow the pattern of expression of TR-ACO1. This may be examined further by quantifying the expression of TR-ACO1 and TR-ACO2 using such techniques as RNase protection assay (Barry *et al.*, 1996) or quantitative RT-PCR with an internal standard (Scheuermann and Bauer, 1993).

ii.) The low ACC oxidase activity in senescent extracts may be explained by higher turnover of the transcript in this tissue. That is, the transcripts are degraded before they are able to be translated. For instance, the stability of transcripts in plant cells has been shown to be decreased by the presence of multiple AUUUA motifs (Ohme-Takagi *et al.*, 1993). A 60 bp sequence containing 11 copies of the AUUUA motif markedly destabilised a β-glucuronidase reporter transcript compared to another sequence with identical A+U content (Ohme-Takagi *et al.*, 1993). Three of these motifs have been found in TR-ACO2 but none in TR-ACO1 which may mean that the transcript of TR-ACO2 is less stable in the cell (Figure 42). However, it is doubtful whether the stability of the transcript is the reason for the lower activity. The senescence-associated increase in ACC oxidase activity in petunia flowers is associated with increased gene expression of PH-ACO1 and this transcript has two AUUUA pentamer motifs (Tang *et al.*, 1994)

2. Characteristics of the isoenzymes

i.) The declining ACC oxidase activity in the chlorotic extracts may be because the assay favours measurement of activity in the mature green extract. This might occur if the senescence-associated isoenzyme (presumably that encoded by TR-ACO2) has different assay requirements to that of the mature green associated isoenzyme (presumably that encoded by TR-ACO1). There is now evidence that different isoforms of ACC oxidase exist in tissues that have different assay requirements (Finlayson *et al.*, 1997). For example, ACC oxidase isoform(s) in the roots of corn and sunflower seedlings have different affinities for carbon dioxide, ascorbate, and a different response to pH than the isoform(s) in the leaves. However, in this study, the measurable activity in the chlorotic extracts had the same requirements for sodium bicarbonate, sodium ascorbate, iron sulphate, and pH as that measured in the mature green extracts (Figure 51).

It may be that increased gene expression of TR-ACO2 does not correlate with activity because the TR-ACO2-encoded isoenzyme in the chlorotic extract has a lower catalytic efficiency (K_{cat}/Km) than the isoenzyme in the mature green extract. This may have arisen because the isoenzyme in senescent leaves (presumably encoded by TR-ACO2) is exposed to much higher concentrations of ACC than the enzyme in the mature green leaves, and so has experienced less evolutionary selective pressure for it to function as efficiently. Evidence has recently arisen that supports the proposition that the small difference in deduced amino acid sequence identities between isoenzymes (for example, 13 % for TR-ACO1 and TR-ACO2), is enough to confer quite distinct kinetic properties. For instance, the translation products of three ACC oxidase cDNA sequences of tomato have been characterised after heterologous expression in yeast (Bidonde *et al.*, 1998). It was found that although LE-ACO3 and LE-ACO1 share 94 % identity in their amino acid sequence, the specific activity (*in vitro*) of LE-ACO3 is less than 50 % that of LE-ACO1 (65 % if measured *in vivo*). To establish whether the TR-ACO1- and TR-ACO2-encoded isoenzymes do have different kinetic characteristics will require measurement of their activity after either heterologous expression in *E. coli*, or yeast (like for the isoenzymes of tomato), or after purification of the isoenzymes from leaf tissue.

3. Characteristics of the tissue environment.

i.) The isoenzymes encoded by TR-ACO1 and 2 may be located in different subcellular locations and therefore require different extraction requirements. For instance, ACC

oxidases have now been localised by immunolocalisation techniques to both cytosolic, and apoplastic locations in suspension cultured cells of tomato and in ripening apple fruit respectively (Reinhardt *et al.,* 1994; Rombaldi *et al.,* 1994). Unlike the cytosolic enzyme which can be extracted from tissue in a simple Tris-glycerol buffer (for example, melon fruit, Ververidis and John, 1991), the apoplastic enzyme requires either PVPP or Triton X-100 to solubilise it from the cellular debris (for example, apple fruit, Dong *et al.,* 1992; Kuai and Dilley, 1992; Fernandez-Maculet and Yang, 1992). It is possible that the low activity observed *in vitro* is because TR-ACO2 (unlike TR-ACO1) is located in the apoplast. However, neither Triton X-100 or PVPP, when included in the extraction buffer, increased recovery of ACC oxidase in the chlorotic extracts (Figure 49).

ii.) The activity of TR-ACO2 may be lower in chlorotic leaves through being inhibited by activated oxygen species that are produced in greater quantities during senescence. For instance, in pea and oat, senescing leaves have increased levels of xanthine-oxidoreductase (which produces superoxide [$O_2^{\bullet}$]) and superoxide dismutase (that converts $O_2^{\bullet}$to H_2O_2) and decreased levels of catalase (Pastori and del Rio, 1994; Longa *et al.,* 1994). This results in the overproduction of H_2O_2, which is normally contained within peroxisomes (Pastori and del Rio, 1994), and which can be damaging to ACC oxidase (Smith *et al.,* 1994). Therefore, it may be that if H_2O_2 is over-produced during leaf senescence in white clover it causes a decline in ACC oxidase activity. However, against this is the measurement of increased ACC oxidase activity in senescing carnation petals (Nijenhuis-De Vries *et al.,* 1994) since in common with leaf senescence, petal senescence of carnation is also characterised by increased levels of superoxides (Mayak *et al.,* 1983) which may be converted to H_2O_2. Furthermore, the presence of DTT in the extraction buffer (which can protect the protein against H_2O_2 damage, Smith *et al.,* 1994) did not increase the percentage recovery of ACC oxidase activity in the senescent extracts. This might be expected if it was the damaging effects of H_2O_2 that was the cause of the decline. A more direct test will be to compare ACC oxidase activity obtained in the senescent tissue after extraction with and without catalase.

iii.) ACC oxidase activity may have been lower in senescent extracts due to degradation of the enzyme by the increased levels of proteases in these extracts. Proteases are proposed to increase during leaf senescence as they are needed for the recycling of leaf nitrogen back into the main body of the plant. Cysteine proteases have been reported to increase during leaf senescence of tomato (Drake *et al.,* 1996) and corn (Smart *et al.,* 1995). Cysteine

proteases are usually contained within vacuoles of cells, and so tissue homogenisation would release the proteases into the cell-free homogenate where potentially they can degrade ACC oxidase. However, if proteases are a major reason for the decline in activity, then performing the extraction over a very short time might be expected to result in much higher activity. This was not observed (Figure 53). Furthermore, carnation petal senescence is accompanied by increases in cysteine proteinases (Jones *et al.*, 1995) but increased activity of ACC oxidase measured *in vitro* during senescence can be detected (Nijenhuis-De Vries *et al.*, 1994).

iv.) The lower ACC oxidase activity in the chlorotic extracts may be due to the increased presence of proteinaceous inhibitors of the enzyme. For instance, the occurrence of proteinaceous inhibitors in plants that increase in abundance during leaf senescence has now been documented, such as a 17 kDa invertase inhibitor in tobacco leaves (Greiner *et al.*, 1998).

Proteinaceous inhibitors of ethylene production have also been reported, for example, in etiolated mungbean hypocotyls (Sakai and Imaseki, 1973). The presence of the inhibitor was first indicated by the ability of extracts of mungbean hypocotyls to inhibit ethylene production *in vivo* by intact hypocotyls. The inhibitor was subsequently purified and found to have a molecular weight of 112 kDa (Sakai and Imaseki, 1973). The inhibitor did not affect ACC synthase activity, but inhibited conversion of exogenously applied ACC to ethylene (Sakai and Maniwa, 1994). Importantly, the inhibitor has not been shown to affect ACC oxidase activity *in vitro* directly. The inhibitor has however been shown to exert an inhibitory action on various other metabolic processes including RNA, protein and lipid synthesis (Todaka *et al.*, 1978) and is thought to act through interaction with the cell membrane.

There are several ways to test whether factors in the senescent extract are the cause of reduced activity. Firstly, an assay *in vivo* may provide some information. The successful conversion of added ACC to ethylene by intact senescent tissue might suggest that homogenisation and extraction disrupts compartmentalisation and promotes the subsequent release of damaging substances which cause the loss in activity *in vitro*. Secondly, and with regard to the possible presence of proteinaceous inhibitors, the senescent extract (after column purification through Sephadex G-25 to remove low molecular weight substances) can be added to the mature green extract to observe whether the decline in activity was

greater than what would be expected by dilution alone. Thirdly, the enzyme can be completely purified. This approach should separate the enzyme away from any putative proteinaceous inhibitors.

These approaches were not pursued in this study. Instead, antibodies were raised to the translation products of TR-ACO1 and 2 expressed in *E. coli* and used to examine changes in protein accumulation of ACC oxidase during leaf maturation and senescence. As measurement of protein accumulation using antibodies can be independent of activity, this approach could provide information on whether post-transcriptional regulation controls activity of ACC oxidase during leaf maturation and senescence.

4.5 ACC oxidase protein accumulation during leaf maturation and senescence

Antibodies raised against the translation products of TR-ACO1 and TR-ACO2 both recognised a protein of *ca.*36.4 kDa on the western blot (Figure 57), which is similar to the reported sizes of ACC oxidase from other plants. The sizes reported for ACC oxidase include 41 kDa by gel filtration for melon (Smith *et al.,* 1992), 40 kDa by gel filtration or 36 kDa by SDS-PAGE for banana fruit (Moya-Leon and John, 1995), 66 kDa by native PAGE or 35 kDa by SDS-PAGE for cherimoya fruit (Escribano *et al.,* 1996), and in apple either 39 kDa by gel filtration (Dupille *et al.,* 1993), 35.3318 kDa by electrospray mass spectrometry (Pirrung *et al.,* 1993), and 39 kDa by SDS-PAGE (Dong *et al.,* 1992).

The pattern of protein accumulation recognised by both TR-ACO1 (raised in rabbits) and TR-ACO2 (raised in rats) antibodies was similar during leaf maturation and senescence. Levels of recognition were highest in mature green leaves (leaves 4 to 10) and declined to be lowest in the most chlorotic leaves examined (leaf 16). This broadly matched transcript accumulation of TR-ACO1, and activity (*in vitro*) of ACC oxidase, but clearly did not correlate with gene expression of TR-ACO2.

There are several possible explanations as to why western analysis showed ACC oxidase protein in leaves declining during senescence. It may be because the western analysis was not quantitative. For instance, the TR-ACO1 fusion protein may contain more antigenic determinants than does the TR-ACO2 fusion protein, so more antibodies bind to this isoenzyme on the western blot than do to the equivalent amount of TR-ACO2 isoenzyme. It may be also that the TR-ACO2 protein is unstable in extracts, or that there are post-

transcriptional control mechanisms which regulate translation of this gene transcript. This may explain why no differences were obtained in pH, ascorbate, iron and carbon dioxide requirements, as activity being measured in the chlorotic extract was predominantly the declining activity of the TR-ACO1 encoded isoenzyme.

To further understand whether the decline in activity and protein of ACC oxidase was due to the nature of the chlorotic extract, ACC oxidase protein and activity was measured in mature green leaves after induction of the senescence-associated TR-ACO2 transcript by wounding. The rationale was based on the finding in tomato, that the senescence-associated ACC oxidase transcript, LE-ACO1, could be induced by mechanical wounding in mature green leaves and be correlated with increased protein accumulation and activity (*in vitro*) of ACC oxidase (Barry *et al.*, 1996).

4.6 Gene expression, protein accumulation, and activity of ACC oxidase in wounded mature green leaves

In common with leaves of tomato (Barry *et al.*, 1996) and melon (Bouquin *et al.*, 1997), wounding preferentially increased gene expression of the senescence-associated transcript in mature green leaves of white clover (Figure 59). This enabled measurement of protein accumulation and activity of ACC oxidase away from the chlorotic tissue environment. However, unlike other plant species studied, the large increase in transcript after wounding did not result in increased ACC oxidase protein accumulation or activity. This suggests against factors specific to the chlorotic extracts causing the lower activity *in vitro*, and is further evidence for either post-transcriptional / translational control, or conditions in the assay (that in this study were not found) that are essential for measuring significant amounts of TR-ACO2 activity.

In the experiment described above, leaf tissue was detached, severely wounded, and incubated in the dark as the aim was solely to induce TR-ACO2 gene expression, so that activity and protein accumulation could be measured subsequently. However, on completion of the experiment other interesting aspects of TR-ACO2 gene regulation had arisen. For instance, it was found in control leaves that were not wounded, that the act of leaf detachment was sufficient for the induction of TR-ACO2 gene expression, despite there being no subsequent wound-induced peak in ethylene production (Figure 60). This suggested firstly, that increased gene expression was not in itself sufficient for the increased production of ethylene associated with wounding, and secondly, that the accumulation of

the gene transcript may be independent of wound-induced ethylene production. Wound-induced expression of the pVR-ACO1 gene transcript in etiolated mung bean hypocotyls has been previously reported to be mediated through ethylene effects as NBD (an ethylene action inhibitor) can suppress completely the induction. However, there is now a precedent for induction of ACC oxidase gene transcripts being independent of ethylene. For example, the CM-ACO1 transcript of melon was shown by RT-PCR to be induced in leaves after wounding independently of ethylene by using 1-MCP to inhibit ethylene action (Bouquin *et al.*, 1997). The authors subsequently showed using GUS-promoter fusion studies, that a separate wound response motif was present in the promoter region of CM-ACO1 that was independent of the ethylene-responsive-element also present.

In white clover, further evidence for induction of TR-ACO2 gene expression being independent of ethylene was provided by using the ethylene-adsorbing compound, Purafil. Purafil has been shown to be effective in delaying chlorophyll loss (considered an ethylene-mediated event) in leaves of white clover (Butcher, 1997). Therefore, incubation of leaves with Purafil may delay accumulation of the TR-ACO2 gene transcript if TR-ACO2 gene expression is being mediated by ethylene. It did not, which is consistent with the induction being independent of ethylene (Figure 62). However, a criticism of using Purafil to delay ethylene-mediated events is that the ethylene it removes has already passed through tissue and had the opportunity to interact with ethylene receptors. If detached leaves are to be used in future studies, then ethylene-action inhibitors such as silver thiosulphate (STS) or 1-MCP need to be used.

However, the discovery that wounding differentially regulates gene expression of TR-ACO1 and TR-ACO2 in detached leaves stimulated further interest on the regulation of these two transcripts. It was important from a physiological standpoint to confirm gene regulation of TR-ACO1 and 2 in leaves in wounded leaves that remained attached to the plant because of the potential for the wounding stimulus to be confounded with other stimuli that result from detachment and dark incubation. The study of Becker and Apel (1993) on barley leaves is of interest since they have shown that the commonly used method of reproducibly inducing senescence (as judged by chlorophyll loss) by leaf detachment and dark incubation increases expression of a number of genes not related to natural leaf senescence on the plant. Many of these were concluded to be stress-related. Therefore, it may not have been mechanical wounding *per se* that caused increased accumulation of TR-ACO2 in detached mature green tissue, but water deficit stress which

accompanies excision, or a response to accelerated ageing that is common to dark incubation.

TR-ACO1 and TR-ACO2 gene expression in wounded mature green leaves attached to the stolon confirmed the expression of TR-ACO1 and TR-ACO2 observed for detached (and wounded) leaves (Figures 62 and 63). Levels of the TR-ACO1 gene transcript were lowered after the leaves were wounded, while levels of the senescence-associated TR-ACO2 gene transcript were elevated. Therefore, it is apparent that TR-ACO1 gene expression is high in conditions where the leaf is not stressed (for example, non-wounded mature green) while TR-ACO2 gene expression is associated with stressed leaves (wounded mature green and senescent)

Wounding leaves that remained attached to the stolon showed that water stress and dark incubation (factors in the detached leaf experiment) were not required for induction of the TR-ACO2 gene transcript. However, this experiment could not confirm that TR-ACO2 gene induction occurred independently of ethylene. To address this, attached leaves were pretreated with 1-MCP (an inhibitor of ethylene action) for 30 min, and wounded. It was predicted that pretreatment of the leaves with 1-MCP would not prevent induction of the TR-ACO2 gene transcript, and therefore confirm that the induction by wounding was occurring independently of any ethylene-mediated effect. As predicted, the pretreatment with 1-MCP did not prevent induction of the TR-ACO2 gene transcript by wounding (Figure 64). However, the pretreatment of the leaves with 1-MCP (without a wounding stimulus) was enough to induce expression of the TR-ACO2 gene transcript, which therefore makes it difficult to conclude whether the induction was independent of ethylene.

The finding that 1-MCP influenced gene expression of both transcripts (TR-ACO1 gene expression was repressed) in non-wounded leaves, begs the question of how it is acting. In this study, the mode of action of 1-MCP was more consistent with it being a chemical that is acting to stress the plant rather than an inhibitor of ethylene action. There are several reasons for this. The first is that chlorophyll loss was not delayed in leaves exposed to 10 ppm ethylene after pretreatment with 1 ppm 1-MCP for 30 min compared with controls that were not given an 1-MCP pretreatment (data not shown). Furthermore, the leaves and petioles of plants pretreated with 300 ppb 1-MCP for 6 h wilted (data not shown) and wilting is considered to be mediated by ethylene. The following reasons are correlative and can be confirmed only after treating attached non-stressed leaves with ethylene, and

examining the effect on TR-ACO1 and TR-ACO2 gene expression. Treatment of non-wounded leaves with 1-MCP downregulated transcript accumulation of TR-ACO1 which means that expression should be high at times when ethylene production is high, for example, during senescence and wounding, and it is not.

It is clear that further work is needed to clarify whether induction of TR-ACO2 by wounding is independent of ethylene, and this should also involve treating intact plants with ethylene.

A further result that arose through the study of gene expression in wounded attached leaves was that TR-ACO1 (but not TR-ACO2) gene expression may be under a circadian-type control (Figure 65). TR-ACO1 gene expression was highest in the middle of the light phase (1:30 pm) and lowest in the dark (7:30 pm). This pattern of expression is consistent with what has been found for ACC oxidase mRNA in *S. longipes* (Kathiresan *et al.*, 1996). In *S. longipes*, ACC oxidase mRNA and activity reaches a maxima in the middle of the light phase and a minima by the middle of the dark phase, and the oscillations were found to be dampened under continuous illumination or darkness, indicating entrainment by phytochrome.

Of further interest was whether the circadian regulation of TR-ACO1 could be used to confirm that the ACC oxidase activity being measured by the *in vitro* assay was predominantly that of the TR-ACO1 encoded isoenzyme. If the lower activity measured in the chlorotic extracts was under circadian type regulation then it could be concluded that the activity being measured was the declining activity of the TR-ACO1 enzyme. This is what broadly was found, although the levels of enzyme activity after 24 h had not returned to the same levels that had been measured at 0 h as would be predicted. The levels of enzyme activity instead remained lower. A more detailed analysis, therefore, will be required in the future to show unequivocally whether such a rhythm of ACC oxidase activity does exist.

5. SUMMARY

Plants of white clover, genotype 10F, were propagated by the method of Butcher (1996) to produce individual stolons that contained leaf tissue representative of all stages of development, from leaf initiation, maturation through to senescence. The pattern of senescence was highly reproducible between harvests. The onset of chlorophyll loss (the

measure of senescence in this study) occurred in leaves between nodes nine to eleven. Comparatively low levels of ethylene were evolved from mature green leaves, whereas a large increase in ethylene evolution was measured from senescing leaf tissue. The increase in ethylene evolution occurred after chlorophyll levels had clearly started to decline. Coincident with the increase in ethylene evolution of the leaves was an increase in ACC, the enzymatic precursor of ethylene. This strongly implicates increased activity of the ethylene biosynthetic pathway as the cause of the increased ethylene production.

The regulation of ethylene biosynthesis during leaf maturation and senescence was further investigated by measuring the changes in ACC oxidase activity. ACC oxidase activity *in vitro* decreased as the leaves senesced. The decline in activity was coincident with the onset of chlorophyll loss and was more pronounced when activity was expressed on a per unit fresh weight basis (as compared with per unit protein basis).

A review of the literature suggests that this is the first study that has examined changes in ACC oxidase activity during ageing of leaf tissue. However, enzyme activity has been measured in other ageing tissues such as ripening fruit (Barry *et al.*, 1996) and senescing carnation petals (Nijenhuis-De Vries *et al.*, 1994). In these tissues, unlike the leaf tissue used in this study, enzyme activity was found to increase during ageing.

Gene transcripts encoding ACC oxidase were identified and gene expression studies undertaken in order to further understand the regulation of ACC oxidase activity during leaf maturation and senescence. The coding regions of putative ACC oxidase gene transcripts were generated using an RT-PCR approach. The sequences could be grouped (based on homology) into two distinct classes, designated TR-ACO1 and TR-ACO2. TR-ACO1 and TR-ACO2 showed 84 % similarity in nucleotide sequence and 87 % similarity in amino acid sequence. The TR-ACO1 and TR-ACO2 sequences were validated as encoding ACC oxidase by comparison with other ACC oxidases in the GenBank database.

Southern analysis using TR-ACO1 and TR-ACO2 sequences as probes indicated that both were encoded by distinct genes. However, the multiple genomic fragments recognised in each lane by each probe indicated that there may also be additional closely related genes.

Changes in gene expression of TR-ACO1 and TR-ACO2 during leaf maturation and senescence were examined using northern analysis. TR-ACO1 hybridised to a single RNA transcript of *ca.* 1.35 Kb on the northern blot that was highly expressed in mature green leaves, but declined in the leaves as they senesced. The pattern of TR-ACO1 gene

expression closely followed ACC oxidase activity measured *in vitro*. By contrast, TR-ACO2 hybridised to two RNA transcripts of *ca.* 1.17 Kb and 1.35 Kb on the northern blot. Expression of the 1.17 Kb and 1.35 Kb transcripts was low in mature green leaves, but increased prior to the onset of senescence to be highest in the senescent leaves. Therefore, the enhanced gene expression of the TR-ACO2 transcript did not correlate with the declining activity of ACC oxidase activity as measured *in vitro*.

The hybridisation of TR-ACO1 and TR-ACO2 to multiple genomic fragments on the Southern blot, together with the finding that TR-ACO2 also hybridised to two RNA transcripts on the northern blot, suggested that both TR-ACO1 and TR-ACO2 may not be specific for single genes. That is, they may be hybridising either to closely related, but distinct TR-ACO1-like genes or closely related but distinct TR-ACO2-like genes. Previous studies have shown that the 3'-UTR of ACC oxidase transcripts is the region that shows greatest sequence divergence. Therefore, the 3'-UTR of both TR-ACO1 and TR-ACO2 were generated and used to confirm the hybridisation patterns previously observed in the Southern and northern analyses.

The 3'-UTR of TR-ACO1 hybridised to all the genomic fragments recognised by its cognate coding frame. This suggests that all these fragments must contain a 3'-UTR. Since a characteristic of ACC oxidase gene transcripts is divergence in the 3'-UTR, the finding that they must contain, at the very least, similar 3'-UTRs suggests that the fragments are not representative of different genes, but are more likely to be either a result of gene duplication or due to the existence of polymorphic alleles (of which there can be up to four as white clover is allotetraploid - i.e. it contains two independently segregating genomes).

The 3'-UTR of TR-ACO2, in contrast to TR-ACO1, hybridised to only a subset of the fragments recognised by its cognate coding frame on the Southern blot. This suggests that the other genomic fragments do not contain the 3'-UTR. This may have arisen if there were sites for all three restriction enzymes in putative introns, or (and what is considered most likely) if the other genomic fragments contained a different 3'-UTR to that of TR-ACO2. This gene would therefore have a very similar coding region to TR-ACO2, but divergent 3'-UTR and thus be considered a distinct gene as opposed to a polymorphic allele of the same gene. The hybridisation of the 3'-UTR of TR-ACO2 to only the 1.35 Kb

transcript and not the 1.17 Kb transcript on the northern blot is further evidence for the existence of a second, as yet undefined, TR-ACO2-like gene sequence in the genome.

The cause of the apparent anomaly between high TR-ACO2 gene expression and low enzyme activity *in vitro* in the chlorotic extracts was further examined. Alteration of both the extraction and assay conditions used for measurement of enzyme activity *in vitro* did not provide evidence for activity in the mature green extract being preferentially measured compared with activity in the senescent extract (and so therefore could not explain the decline in activity). Analysis using antibodies was then undertaken to examine further the regulation of ACC oxidase during leaf maturation and senescence. This approach can be independent of activity as a functional enzyme is not required for recognition using antibodies. The antibodies raised against the translation products of TR-ACO1 and TR-ACO2 both recognised a protein of 36.4 kDa (the size expected from a consensus of published ACC oxidase sizes). The pattern of accumulation matched gene expression of TR-ACO1 and ACC oxidase activity *in vitro*. This suggests that either the TR-ACO2 protein is not being expressed, is rapidly turned over, or that the western analysis is not quantitative.

The lower enzyme activity in the chlorotic extracts may have been due to the greater instability of the enzyme in these extracts. Therefore, it was of interest to elevate gene expression of TR-ACO2 (the senescence-associated transcript) in mature green leaves (i.e. away from the chlorotic tissue environment) and observe whether ACC oxidase activity could then be correlated with levels of the TR-ACO2 transcript. Elevation of the TR-ACO2 transcript in mature green leaves was accomplished by incubating wounded detached leaf tissue in the dark. However, elevated gene expression of TR-ACO2 did not result in either increased accumulation of the 36.4 kDa protein or increased ACC oxidase activity *in vitro*. This again suggests that the protein encoded by the TR-ACO2 gene is either under some form of post-transcriptional regulation, is rapidly turned over, or is induced and active, but cannot be measured using both an activity assay and antibodies.

The above experiment raised the possibility that the wound-induced induction of TR-ACO2 was being mediated independently of ethylene. This was because the act of detachment followed by dark incubation (which did not significantly elevate ethylene production) was sufficient to elevate TR-ACO2 gene expression.

To examine further the cause of TR-ACO2 induction, leaves were detached and either wounded or not, and incubated in the presence of the ethylene adsorbing compound, Purafil. Purafil has previously been shown to be effective in delaying chlorophyll loss (an ethylene-mediated event) in leaf tissue of white clover (Butcher, 1997), and so Purafil may be expected to delay the increase in TR-ACO2 induction if the induction is mediated solely through ethylene. It did not, and was therefore consistent with the induction being independent of ethylene action. A criticism, however, of using Purafil is that the compound can only remove ethylene after it has passed through the tissue, and the ethylene therefore will have had the opportunity to interact with its receptor. Thus, it was considered appropriate to confirm the results obtained with Purafil using an inhibitor of ethylene action, (1-MCP).

Leaves were now wounded while still attached to the plant as the aim was also to examine gene expression under more physiological-type conditions. Wounding increased gene expression in attached leaves as it had done so in detached, confirming that the induction of TR-ACO2 occurs *in planta*. Pretreatment of the leaves with 1-MCP prior to wounding also did not prevent the increase in TR-ACO2 gene expression. This suggests that the increase may be independent of ethylene. However, because pretreatment of leaves with 1-MCP also elevated levels of the TR-ACO2 transcript in non-wounded leaves, it cannot be concluded that wounding induces the TR-ACO2 transcript independently of ethylene. 1-MCP treatment decreased expression of the TR-ACO1 gene transcript in non-wounded leaves. This appears to be inconsistent with 1-MCP acting as an ethylene action inhibitor, because it suggests that TR-ACO1 gene expression would be high when levels of ethylene are high, which it is not. TR-ACO1 gene expression is low in conditions where ethylene production has been shown to be elevated (i.e. wounding and senescence). It appears then, that 1-MCP, in this study has acted more as an elicitor of chemical stress, than as an inhibitor of ethylene action.

An additional difference that became apparent from studying gene expression of TR-ACO1 and TR-ACO2 in non-wounded attached leaves (not treated with 1-MCP) was that TR-ACO1 gene expression (but not TR-ACO2) appears to be under a circadian-type control. This in-turn may provide a further avenue from which to examine the cause of the declining ACC oxidase activity in senescing leaves. Preliminary evidence suggests that the lower activity of the chlorotic extract does vary with time of day, and since TR-ACO2 gene expression appears not to be under circadian regulation, this suggests that the assay is

measuring predominantly the declining activity of the TR-ACO1-encoded enzyme. However, further experiments will be needed to show this unequivocally.

5.1 Future Work

This study has uncovered many interesting avenues that can be pursued further. One, that may not be directly related to ethylene biosynthesis, is to examine further the origin of the substance(s) induced by wounding that give rise to the large amounts of non-ACC derived ethylene in the Lizada and Yang assay.

The discrepancy between TR-ACO2 gene expression and activity *in vitro* should be clarified. This should involve purification of the isoenzymes encoded by the TR-ACO1 and TR-ACO2 gene transcripts and detailed kinetic characterisation (including measurements of Km, and catalytic efficiencies). The gene expression studies have indicated that mature green leaves should be an excellent source of the enzyme encoded by the TR-ACO1 isoenzyme while senescing leaves will be an excellent source for the TR-ACO2 enzyme. Wounded mature green leaves (after a 24 h incubation) may be an alternative source of the TR-ACO2-encoded isoenzyme, as at this time TR-ACO1 gene expression is low, while that of TR-ACO2 is elevated. Purification and kinetic characterisation of TR-ACO1 and TR-ACO2 is already well underway by Dr Deming Gong.

The differential regulation of TR-ACO1 and TR-ACO2 is of further interest. If the *ca.* 1.17 Kb transcript recognised by the coding region of TR-ACO2 is, as predicted, encoded by a distinct gene to that of the 1.35 Kb recognised by the 3'-UTR of TR-ACO2, then the coding frame of TR-ACO2 should be used to reexamine whether the 1.17 Kb transcript is induced by wounding. It may not be.

Intact plants should be treated with ethylene to clarify whether TR-ACO1 and TR-ACO2 regulation can be mediated through ethylene, and further experiments should carried out with 1-MCP to confirm that the wound-induced induction of the TR-ACO2 gene transcript can be independent of ethylene. In this regard, other ethylene action inhibitors such as NBD or STS may be required, as 1-MCP application appeared to act more as a stressor of plant tissues than an inhibitor of ethylene action.

The promoter elements of TR-ACO1 and TR-ACO2 should be identified (for example, by inverse PCR or screening a genomic library) and response motifs (for example,

developmental, wound, ethylene, pathogenesis related) characterised (for example, by GUS-promoter fusion studies).

Nuclear factors that interact with the response motifs could be identified by gel shift assays and their genes cloned using a cDNA expression library. Gene expression of the DNA binding proteins themselves could then be examined.

This study on ACC oxidase provides only part of the answers to how ethylene production is controlled during leaf maturation and senescence. A more complete picture requires that ACC oxidase gene expression and activity be integrated with ACC synthase gene expression and activity, as both enzymes are equally committed (and important) for the production of ethylene in plants. Three distinct ACC synthases have now been isolated in leaves of white clover. Their expression during leaf maturation and senescence is currently being examined by Trish Murray at the Institute of Molecular BioSciences, Massey University, NZ.

6. BIBLIOGRAPHY

Abeles FB. 1973. *Ethylene in plant biology.* Abeles FB. Ed., Academic Press, New York.

Abeles FB, Morgan PW, Saltveit ME. 1992. *Ethylene in plant biology. 2nd ed.* Abeles FB, Morgan PW, Saltveit ME. Eds., Academic Press., California, 1992.

Acaster MA & Kende H. 1983. Properties and partial purification of 1-aminocyclopropane-1-synthase. *Plant Physiology* **72**, pp. 139-145

Adams DO & Yang SF. 1977. Methionine metabolism in apple tissue. Implication of *S*-adenosylmethionine as an intermediate in the conversion of methionine to ethylene. *Plant Physiology* **60**, pp. 892-896

Adams DO & Yang SF. 1979. Ethylene biosynthesis: Identification of 1-aminocyclopropane-1-carboxylic acid as an intermediate in the conversion of methionine to ethylene. *Proceedings of the National Academy of Science, USA* **76**(1), pp. 170-174

Aharoni N & Lieberman M. 1979. Ethylene as a regulator of senescence in tobacco leaf discs. *Plant Physiology* **64**, pp. 801-804

Alejar AA, De Visser R, Spencer MS. 1988. Ethylene production by attached leaves or intact shoots of tobacco cultivars differing in their speed of yellowing during curing. *Plant Physiology* **88**, pp. 329-332

Altschul SF, Gish W, Miller W, Myers EW, Lipman DJ. 1990. Basic local alignment search tool. *Journal of Molecular Biology* **215**, pp. 403-410

Amrhein N, Schneebeck D, Skorupka H, Tophof S, Stöckigt J. 1981. Identification of a major metabolite of the ethylene precursor 1-aminocyclopropane-1-carboxylic acid in higher plants. Naturwissenschaften **68,** pp. 619-620

Baker MJ & Williams WM. 1987. *White Clover.* Baker MJ & Williams WM. Eds., CAB International, Oxon, UK.

Balagué C, Watson CF, Turner AJ, Rougé P, Picton S, Pech JC, Grierson D. 1993. Isolation of a ripening wound-induced cDNA from *Cucumis melo* L. encoding a protein with homology to the ethylene-forming enzyme. *European Journal of Biochemistry* **212**, pp. 27-34

Banga M, Slaa EJ, Blom CWPM, Voesenek LACJ. 1996. Ethylene biosynthesis and accumulation under drained and submerged conditions. *Plant Physiology* **112**(1), pp. 229-237

Barendse GWM & Peeters TJM. 1995. Multiple hormonal control in plants. *Acta Botanica Neerlandica* **44**(1), pp. 3-17

Barlow JN, Zhang Z, John P, Baldwin JE, Schofield CJ. 1997. Inactivation of 1-aminocyclopropane-1-carboxylate oxidase involves oxidative modifications. *Biochemistry* **36**, pp. 3563-3569

Barry CS, Blume B, Bouzayen M, Cooper W, Hamilton AJ, Grierson D. 1996. Differential expression of the 1-aminocyclopropane-1-carboxylate oxidase gene family of tomato. *The Plant Journal* **9**(4), pp. 525-535

Baur AH & Yang SF. 1972. Methionine metabolism in apple tissue in relation to ethylene biosynthesis. *Phytochemistry* **11**, pp. 3207-3214

Becker W & Apel K. 1993. Differences in gene expression between natural and artificially induced leaf senescence. *Planta* **189**, pp. 74-79

Benichou M, Martinez-Reina G, Romojaro F, Pech J, Latche A. 1995. Partial purification and properties of a 36-kDa 1-aminocyclopropane-1-carboxylate-N-malonyltransferase from mung bean. *Physiologia Plantarum* **94**, pp. 629-634

Bidonde S, Ferrer MA, Zegzouti H, Ramarsamy S, Latche A, Peche JC, Hamilton AJ, Grierson D, Bouzayen M. 1998. Expression and characterisation of three tomato 1-aminocyclopropane-1-carboxylate oxidase cDNAs in yeast. *European Journal of Biochemistry* **253**(1), pp. 20-26

Bleecker AB, Estelle MA, Somerville C, Kende H. 1988. Insensitivity to ethylene conferred by a dominant mutation in *Arabidopsis thaliana*. *Science* **241**, pp. 1086-1089

Bleecker AB, Kenyon WH, Somerville SC, Kende H. 1986. Use of monoclonal antibodies in the purification and characterisation of 1-aminocyclopropane-1-carboxylate synthase, an enzyme in ethylene biosynthesis. *Proceedings of the National Academy of Sciences, USA* **83**, pp. 7755-7759

Bleecker AB & Patterson SE. 1997. Last exit: senescence, abscission, and meristem arrest in *Arabidopsis*. *The Plant Cell* **9**, pp. 1169-1179

Blume B & Grierson D. 1997. Expression of ACC oxidase promoter-GUS fusions in tomato and *Nicotiana plumbaginifolia* regulated by developmental and environmental stimuli. *The Plant Journal* **12**(4), pp. 731-746

Boerjan W, Bauw G, VAn Montagu M, Inze D. 1994. Distinct phenotypes generated by overexpression and suppression of *S*-adenosyl-L-methionine synthetase reveal developmental patterns of gene silencing in tobacco. *The Plant Cell* **6**, pp. 1401-1414

Boller T, Herner RC, Kende H. 1979. Assay for and enzymatic formation of an ethylene precursor, 1-aminocyclopropane-1-carboxylic acid. *Planta* **145**, pp. 293-303

Borochov A, Spiegelstein H, Philosoph-Hadas S. 1997. Ethylene and flower petal senescence: interrelationship with membrane lipid catabolism. *Physiologia Plantarum* **100**, pp. 606-612

Bouquin T, Lasserre E, Pradier J, Pech JC, Balague C. 1997. Wound and ethylene induction of the ACC oxidase melon gene CM-ACO1 occurs via two direct and independent transduction pathways. *Plant Molecular Biology* **35**, pp. 1029-1035

Bouzayen M, Cooper W, Barry C, Zegzouti H, Hamilton AJ, Grierson D. 1993. EFE multigene family in tomato plants: expression and characterization. **In** *Cellular and Molecular Aspects of the Plant Hormone Ethylene*. Pech JC, Latche A, Balague C. Eds., Kluwer Academic, Dordrecht, The Netherlands, pp. 76-81

Bouzayen M, Latche A, Pech JC, Marigo G. 1989. Carrier-mediated uptake of 1-(malonylamino)cyclopropane-1-carboxylic acid in vacuoles isolated from *Catharanthus roseus* cells. *Plant Physiology* **91**, pp. 1317-1322

Bradford MM. 1976. A rapid and sensitive method for the quantitation of microgram quantities of protein utilizing the principle of protein-dye binding. *Analytical Biochemistry* **72**, pp. 248-254

Britsch L & Grisebach H. 1986. Purification and characterisation of (2*S*)-flavanone 3-hydroxylase from *Petunia hybrida*. *European Journal of Biochemistry* **156**, pp. 569-577

Brock JL, Hay MJM, Thomas VJ, Sedcole JR. 1988. Morphology of white clover (*Trifolium repens* L.) plants in pastures under intensive sheep grazing. *Journal of Agricultural Science* **111**, pp. 273-283

Brougham RW, Ball PR, Williams WM, 1978. Ecology and management of white clover-based pastures. **In** *Plant Relations in Pastures.* Wilson JR. Ed.., CSIRO, Melbourne, pp. 309-324)

Buchanan-Wollaston V. 1997. The molecular biology of leaf senescence. *Journal of Experimental Botany* **48**, pp. 181-199

Bufler G & Mor Y. 1980. Some problems in the estimation of ACC (1-aminocyclopropane-1-carboxylic acid) from carnation flower tissue. *Acta Horticulturae* **113**, pp. 65-68

Bufler G, Mor Y, Reid MS, Yang SF. 1980. Changes in 1-aminocyclopropane-1-carboxylic-acid content of cut carnation flowers in relation to their senescence. *Planta* **150**, pp. 439-442

Burns JK & Evensen KB. 1986. Calcium effects on ethylene carbon dioxide and 1-aminocyclopropane-1-carboxylic-acid synthase activity. *Physiologia Plantarum* **66**(4), pp. 609-615

Butcher S. 1997. *Ethylene biosynthesis during leaf maturation and senescence in white clover.* Ph D Thesis, Department of Plant Biology and Biotechnology, Massey University, Palmerston North, NZ.

Butcher SM, Fountain D, McManus MT. 1996. Leaf senescence and clonal growth of white clover. *New Zealand Competitive Edge Joint Symposium,* Lincoln University, NZ, pp. 21-22

Callahan AM, Morgens PH, Wright P, Nichols KE. 1992. Comparison of Pch313 (pTOM13 Homolog) RNA accumulation during fruit softening and wounding of two phenotypically different peach cultivars. *Plant Physiology* **100**, pp. 482-488

Cameron AC, Fenton CAL, Yu Y, Adams DO, Yang SF. 1979. Increased production of ethylene plant tissues treated with 1-aminocyclopropane-1-carboxylic acid. *HortScience* **14**(2), pp. 178-180

Casas JL, Garcia-Canovas F, Tudela J, Acosta M. 1993. A kinetic study of simultaneous suicide inactivation and irreversible inhibition of an enzyme. application to 1-aminocyclopropane-1-carboxylate (ACC) synthase inactivation by its substrate *S*-adenosylmethionine. *Journal of Enzyme Inhibition* **7**, pp. 1-14

Chang C. 1996. The ethylene signal transduction pathway in *Arabidopsis*: an emerging paradigm? *Trends in Biochemical Science* **21**, pp. 129-133

Chang C, Kwok SF, Bleecker AB, Meyerowitz EM. 1993. *Arabidopsis* ethylene-response gene ETR1: similarity of product to two-component regulators. *Science* **262**, pp. 539-544

Chang C & Meyerowitz EM. 1995. The ethylene hormone response in *Arabidopsis*: a eukaryotic two-component signalling system. *Proceedings of the National Academy of Sciences, USA* **92**, pp. 4129-4133

Chapman DF & Robson MJ. 1992. The physiological role of old stolon material in white clover (*Trifolium repens* L.). *New Phytologist* **122**, pp. 53-62

Charng Y, Liu Y, Dong JG, Yang SF. 1997. On 1-aminocyclopropane-1-carboxylic acid (ACC) oxidase. **In** *Biology and Biotechnology of the Plant Hormone Ethylene,* Eds., Kanellis AK, Chang C, Kende H, Grierson D. Kluwer Academic, Dordrecht, The Netherlands, pp. 23-29

Chomczynski P. 1992. Solubilization in formamide protects RNA from degradation. *Nucleic Acids Research* **20**(14), p. 3791

Church GM & Gilbert W. 1984. Genomic sequencing. *Proceedings of the National Academy of Sciences, USA* **81**, pp. 1991-1995

Coleman LW & Hodges CF. 1991. Interference with the determination of 1-aminocyclopropane-1-carboxylic acid by various plant proteins. *Plant Physiology* **138**, pp. 7-11

Czerny T. 1996. High primer concentration improves PCR amplification from random pools. *Nucleic Acids Research* **24**(5), pp. 985-986

Destefano-Beltran LJC, Van Caeneghem W, Gielen J, Richard L, Van Montagu M, Van Der Straeten D. 1995. Characterization of three members of the ACC synthase gene family in *Solanum tuberosum* L. *Molecular & General Genetics* **246**(4), pp. 496-508

Deutscher MP. 1990. Maintaining protein stability. **In** *Methods in Enzymology.* Deutscher MP. Ed., Academic Press., San Diego, **182** [8]).

Dominguez M & Vendrell M. 1993. Ethylene biosynthesis in banana fruit: evolution of EFE activity and ACC levels in peel and pulp during ripening. *Journal of Horticultural Science* **68**(1), pp. 63-70

Dong JG, Fernandez-Maculet JC, Yang SF. 1992. Purification and characterization of 1-aminocyclopropane-1-carboxylate oxidase from apple fruit. *Proceedings of the National Academy of Science, USA* **89**, pp. 9789-9793

Dong Z & Dunstan D. 1996. A reliable method for extraction of RNA from various conifer tissues. *Plant Cell Reports* **15**, pp. 516-521

Drake R, John I, Farrell A, Cooper W, Schuch W, Grierson D. 1996. Isolation and analysis of cDNAs encoding tomato cysteine proteases expressed during leaf senescence. *Plant Molecular Biology* **30**, pp. 755-767

Dupille E, Rombaldi C, Lelievre JM, Cleyet-Marel JC, Pech JC, Latche A. 1993. Purification, properties and partial amino-acid sequence of 1-aminocyclopropane-1-carboxylic acid oxidase from apple fruits. *Planta* **190**(1), pp. 65-70

Dupille E & Zacarias L. 1996. Extraction and biochemical characterization of wound-induced ACC oxidase from citrus peel. *Plant Science* **114**, pp. 53-60

Emery RJN, Kathiresan A, Reid DM, Chinnappa CC. 1997. Ecotypic differences in rhythmicity of ethylene production in *Stellaria longipes*: the possible roles of ACC, MACC, and ACC oxidase. *Canadian Journal of Botany* **75**(7), pp. 1027-1033

English PJ, Lycett GW, Roberts JA, Jackson MB. 1995. Increased 1-aminocyclopropane-1-carboxylic acid oxidase activity in shoots of flooded tomato plants raises ethylene production to physiologically active levels. *Plant Physiology* **109**, pp. 1435-1440

Escribano MI, Merodio C, John P. 1996. Characterization of 1-aminocyclopropane-1-carboxylate oxidase partially purified from cherimoya fruit. *Journal of Agricultural and Food Chemistry* **44**(3), pp. 730-735

Espartero J, Pintor-Toro JA, Pardo JM. 1994. Differential accumulation of *S*-adenosylmethionine synthetase transcripts in response to salt stress. *Plant Molecular Biology* **25**, pp. 217-227

Ferguson DL, Al-Khatib K, Guikema JA, Paulsen GM. 1993. Degradation of proteins from thylakoid membranes in senescing wheat leaves at high temperature. *Plant, Cell and Environment* **16**, pp. 421-428

Fernandez-Maculet JC & Yang SF. 1992. Extraction and partial characterization of the ethylene-forming enzyme from apple fruit. *Plant Physiology* **99**, pp. 751-754

Ferrarese L, Trainotti L, Moretto P, De-Laureto PP, Rascio N, Casadoro G. 1995. Differential ethylene-inducible expression of cellulase in pepper plants. *Plant Molecular Biology* **29**, pp. 735-747

Finlayson SA, Liu JH, Reid DM. 1996. Localization of ethylene biosynthesis in roots of sunflower (*Helianthus annuus*) seedlings. *Physiologia Plantarum* **96**, pp. 36-42

Finlayson SA, Reid DM, Morgan PW. 1997. Root and leaf specific ACC oxidase activity in corn and sunflower seedlings. *Phytochemistry* **45**(5), pp. 869-877

Fluhr R & Mattoo AK. 1996. Ethylene-biosynthesis and perception. *Critical Reviews in Plant Sciences* **15**, pp. 479-523

Frohman MA, Dush MK, Martin GR. 1988. Rapid production of full-length cDNAs from rare transcripts: amplification using a single gene-specific oligonucleotide primer. *Proceedings of the National Academy of Sciences, USA* **85**, pp. 8998-9002

Fuhrer J. 1982. Ethylene biosynthesis and cadmium toxicity in leaf tissue of beans (*Phaseolus vulgaris* L.). *Plant Physiology* **70**(1), pp. 162-167

Gan S & Amasino RM. 1997. Making sense of senescence. *Plant Physiology* **113**, pp. 313-319

Gegenheimer P. 1990. Preparation of extracts from plants. **In** *Methods in Enzymology.*. Deutscher MP. Ed., Academic Press, San Diego **182** pp. 174-193

Gepstein S & Thimann KV. 1981. The role of ethylene in the senescence of oat leaves. *Plant Physiology* **68**, pp. 349-354

Gómez-Gómez L & Carrasco P. 1998. Differential expression of the *S*-adenosyl-L-methionine synthase genes during pea development. *Plant Physiology* **117**, pp. 397-405

Gowri G, Bugos R, Campbell W, Maxwell C, Dixon R. 1991. Stress responses in alfalfa (*Medicargo sativa*). *Plant Physiology* **97**, pp. 7-14

Grbic V & Bleecker AB. 1995. Ethylene regulates the timing of leaf senescence in *Arabidopsis. The Plant Journal* **8**, pp. 595-602

Greiner S, Krausgrill S, Rausch T. 1998. Cloning of a tobacco apoplastic invertase inhibitor. *Plant Physiology* **116**, pp. 733-742

Grierson D & Kader AA 1986. Fruit ripening and quality. **In** *The tomato crop: a scientific basis for improvement.* Atherton JG & Rudich J. Eds., Chapman and Hall, London, UK, pp. 241-280

Guis M, Bouquin T, Zegzouti H, Ayub R, Ben Amor M, Lasserre E, Botondi R, Raynal J, Latche A, BouzayenM, Balague C, Pech JC. 1997 Differential expression of ACC oxidase genes in melon and physiological characterisation of fruit expressing and antisense ACC oxidase gene. **In** *Biology and Biotechnology of the Plant Hormone Ethylene.* Kanellis AK, Chang C, Kende H, Grierson D. Eds., Kluwer Academic, Dordrecht, The Netherlands, pp. 327-337

Guo L, Arteca RN, Phillips AT, Liu Y. 1992. Purification and characterization of 1-aminocyclopropane-1-carboxylate N-malonyltransferase from etiolated mung bean hypocotyls. *Plant Physiology* **100**, pp. 2041-2045

Guy M & Kende H. 1984. Conversion of 1-aminocyclopropane-1-carboxylic acid to ethylene by isolated vacuoles of *Pisum sativum* L. *Planta* **160**, pp. 281-287

Hall KC, Else MA, Jackson MB. 1993. Determination of 1-aminocyclopropane-1-carboxylic acid (ACC) in leaf tissue and xylem sap using capillary column gas chromatography and a nitrogen/ phosphorus detector. *Plant Growth Regulation* **13**, pp. 225-230

Hamilton AJ, Bouzayen M, Grierson D. 1991. Identification of a tomato gene for the ethylene-forming enzyme by expression in yeast. *Proceedings of the National Academy of Sciences, USA* **88**, pp. 7434-7437

Hamilton AJ, Lycett GW, Grierson D. 1990. Antisense gene that inhibits synthesis of the hormone ethylene in transgenic plants. *Nature* **346**, pp. 284-287

Hanley KM, Meir S, Bramlage WJ. 1989. Activity of ageing carnation flower parts and the effects of 1-(Malonylamino)cyclopropane-1-carboxylic acid-induced ethylene. *Plant Physiology* **91**, pp. 1126-1130

Harpham NVJ, Berry AW, Knee EM, Roveda-Hoyos G, Raskin I, Sanders IO, Smith AR, Wood CK, Hall MA. 1991. The effect of ethylene on the growth and development of wild-type and mutant *Arabidopsis thaliana* (L.). *Annals of Botany* **68**, pp. 55-61

Harpster M, Howie W, Dunsmuir P. 1996. Characterization of a PCR fragment encoding 1-aminocyclopropane-1-carboxylate synthase in pepper (*Capsicum annuum*). *Journal of Plant Physiology* **147**(6), pp. 661-664

Hay MJM, Brock JL, Thomas VJ. 1989. Characteristics of individual white clover plants in grazed swards. *Proceedings XVI International Grasslands Congress,* Nice, France, pp. 1051-1052

He CJ, Drew MC, Morgan PW. 1994. Induction of enzymes associated with lysigenous aerenchyma formation in roots of *Zea mays* during hypoxia or nitrogen starvation. *Plant Physiology* **105**(3), pp. 861-865

He C, Morgan PW, Drew MC. 1996. Transduction of an ethylene signal is required for cell death and lysis in the root cortex of maize during aerenchyma formation induced by hypoxia. *Plant Physiology* **112**, pp. 463-472

Hoffman NE, Fu JR, Yang SF. 1983. Identification and metabolism of 1-(malonylamino)cyclopropane-1-carboxylic acid in germinating peanut seeds. *Plant Physiology* **71**, pp. 197-199

Hoffman NE & Yang SF. 1980. Changes of 1-aminocyclopropane-1-carboxylic acid content in ripening fruits in relation to their ethylene production rates. *Journal of the American Society for Horticultural Science* **105**(4), pp. 492-495

Hoffman NE, Yang SF, Ichihara A, Sakamura S. 1982B. Stereospecific conversion of 1-aminocyclopropane-1-carboxylic acid to ethylene by plant tissues. *Plant Physiology* **70**, pp. 195-199

Hoffman NE, Yang SF, McKeon T. 1982A. Identification of 1-(malonylamino)cyclopropane-1-carboxylic acid as a major conjugate of 1-aminocyclopropane-1-carboxylic acid, an ethylene precursor in higher plants. *Biochemical and Biophysical Research Communications* **104**(2), pp. 765-770

Hua J, Chang C, Sun Q, Meyerowitz EM. 1995. Ethylene insensitivity conferred by *Arabidopsis* ERS gene. *Science* **269**, pp. 1712-1714

Huang PL, Parks JE, Rottmann WH, Theologis A. 1991. Two genes encoding 1-amino cyclopropane-1-carboxylate synthase in zucchini (*Cucurbita pepo*) are clustered and similar but differentially regulated. *Proceedings of the National Academy of Sciences, USA* **88**(16), pp. 7021-7025

Hyodo H, 1991. Stress/wound ethylene. **In** *The Plant Hormone Ethylene*. Mattoo AK & Suttle JC Eds., CRC Press, Boca Raton, USA, pp. 43-63

Hyodo H, Hashimoto C, Morozumi S, Hu W, Tanaka K. 1993. Characterization and induction of the activity of 1-aminocyclopropane-1-carboxylate oxidase in the wounded mesocarp tissue of *Cucurbita maxima*. *Plant and Cell Physiology* **34**(5), pp. 667-671

Imaseki H, 1991. The biochemistry of ethylene biosynthesis. **In** *The Plant Hormone Ethylene*. Matto AK & Suttle JC Eds., CRC Press, Boca Raton, USA, pp. 1-20

Ingemarsson BSM & Bollmark M. 1997. Ethylene production and 1-aminocyclopropane-1-carboxylic acid turnover in *Picea abies* hypocotyls after wounding. *Journal of Plant Physiology* **151**, pp. 711-715

Inskeep WP & Bloom PR. 1985. Extinction coefficients of chlorophyll *a* and *b* in N,N-dimethylformamide and 80% acetone. *Plant Physiology* **77**, pp. 483-485

Ishige F, Yamazaki K, Mori H, Imaseki H. 1991. The effects of ethylene on the coordinated synthesis of multiple proteins: accumulation of an acidic chitinase and a basic glycoprotein induced by ethylene in leaves of azuki bean, *Vigna angularis*. *Plant and Cell Physiology* **32**(5), pp. 681-690

Jiao X, Philosoph-Hadas S, Su L, Yang SF. 1986. The conversion of 1-(malonylamino)cyclopropane-1-carboxylic acid to 1-aminocyclopropane-1-carboxylic acid in plant tissues. *Plant Physiology* **81**, pp. 637-641

John I, Drake R, Farrell A, Cooper W, Lee P, Horton P, Grierson D. 1995. Delayed leaf senescence in ethylene-deficient ACC-oxidase antisense tomato plants: molecular and physiological analysis. *The Plant Journal* **7**(3), pp. 483-490

John P. 1997. Ethylene biosynthesis: the role of 1-aminocyclopropane-1-carboxylate (ACC) oxidase, and its possible evolutionary origin. *Physiologia Plantarum* **100**(3), pp. 583-592

John P, Iturriagagoitia-Bueno T, Lay V, Thomas PG, Hedderson TAJ, Prescott AG, Gibson EJ, Schofield CJ. 1997. 1-aminocyclopropane-1-carboxylate oxidase: molecular structure and catalytic function. **In** *Biology and Biotechnology of the Plant Hormone Ethylene*. Kanellis AK, Chang C, Kende H, Grierson D. Eds., Kluwer Academic, Dordrecht, The Netherlands, pp. 15-22

Jones ML, Larsen PB, Woodson WR. 1995. Ethylene-regulated expression of a carnation cysteine proteinase during flower petal senescence. *Plant Molecular Biology* **28**(3), pp. 505-512

Junghans H & Metzlaff M. 1990. A simple and rapid method for the preparation of total plant DNA. *BioTechniques* **8**, p. 176

Kadyrzhanova DK, McCully TJ, Jaworski SA, Ververidis P, Vlachonasios KE, Murakami KG, Dilley DR. 1997. Structure-function analysis of ACC oxidase by site-directed mutagenesis. **In** *Biology and Biotechnology of the Plant Hormone Ethylene.* Kanellis AK, Chang C, Kende H, Grierson D. Eds., Kluwer Academic, Dordrecht, The Netherlands, pp. 5-13

Kathiresan A, Nagarathna KC, Moloney MM, Reid DM, Chinnappa CC. 1998. Differential regulation of 1-aminocyclopropane-1-carboxylate synthase gene family and its role in phenotypic plasticity in *Stellaria longipes. Plant Molecular Biology* **36**(2), pp. 265-274

Kathiresan A, Reid DM, Chinnappa CC. 1996. Light- and temperatue-entrained circadian regulation of activity and mRNA accumulation of 1-aminocyclopropane-1-carboxylic acid oxidase in *Stellaria longipes. Planta* **199**, pp. 329-335

Kawalleck P, Plesch G, Hahlbrock K, Somssich IE. 1992. Induction by fungal elicitor of S-adenosyl-L-methionine synthetase and *S*-adenosyl-L-homocysteine hydrolase mRNAs in cultured cells and leaves of *Petroselinum crispum. Proceedings of the National Academy of Sciences, USA* **89**, pp. 4713-4717

Kawase M. 1981. Effect of ethylene on aerenchyma development. *American Journal of Botany* **68**, pp. 651-658

Kende H. 1993. Ethylene biosynthesis. *Annual Review of Plant Physiology* **44**, pp. 283-307

Kepczynski J, Bihun M, Kepczynska E. 1997. Ethylene involvement in the dormancy of *Amaranthus* seeds. **In** *Biology and Biotechnology of the Plant Hormone Ethylene* (Kanelis AK, Chang C, Kende H, Grierson D. Eds., Kluwer Academic, London. UK, pp. 113-122

Kim CS, Kwak JM, Nam HG, Kim K, Cho BH. 1994. Isolation and characterisation of two cDNAs that are rapidly induced during the wound response of *Arabidopsis thaliana. Plant Cell Reports* **13**, pp. 340-343

Kim JH, Kim WT, Kang BG, Yang SF. 1997. Induction of 1-aminocyclopropane-1-carboxylate oxidase mRNA by ethylene in mung bean hypocotyls: involvement of both protein phosphorylation and dephosphorylation in ethylene signaling. *The Plant Journal* **11**(3), pp. 399-405

Kim WT, Campbell A, Moriguchi T, Yi HC, Yang SF. 1997. Auxin induces three genes encoding 1-aminocyclopropane-1-carboxylate synthase in mung bean hypocotyls. *Journal of Plant Physiology* **150**(1-2), pp. 77-84

Kim WT, Silverstone A, Yip WK, Dong JG, Yang SF. 1992. Induction of 1-aminocyclopropane-1-carboxylate synthase mRNA by auxin in mung bean hypocotyls and cultured apple shoots. *Plant Physiology* **98**, pp. 465-471

Kim WT & Yang SF. 1994. Structure and expression of cDNAs encoding 1-aminocyclopropane-1-carboxylate oxidase homologs isolated from excised mung bean hypocotyls. *Planta* **194**(2), pp. 223-229

Kim YS, Choi D, Lee MM, Lee SH, Kim WT. 1998. Biotic and abiotic stress-related expression of 1-aminocyclopropane-1-carboxylate oxidase gene family in *Nicotiana glutinosa* L. *Plant and Cell Physiology* **39**(6), pp. 565-573

Klee HJ. 1993. Ripening physiology of fruit from transgenic tomato (*Lycopersicon esculentum*) plants with reduced ethylene synthesis. *Plant Physiology* **102**(3), pp. 911-916

Knudsen F, Campa A, Stefani HA, Cilento G. 1994. Plant hormone ethylene is a Norrish type II product from enzymically generated triplet 1-butanal. *Proceedings of the National Academy of Science, USA* **91**, pp. 410-412

Kuai J & Dilley DR. 1992. Extraction, partial purification and characterization of 1-aminocyclopropane-1-carboxylic acid oxidase from apple fruit. *Postharvest Biology and Technology* **1**(3), pp. 203-211

Laemmli UK. 1970. Cleavage of structural proteins during the assembly of the of bacteriophage T4. *Nature* **227**, pp. 680-685

Lasserre E, Bouquin T, Hernandez JA, Bull J, Pech JC, Balague C. 1996. Structure and expression of three genes encoding ACC oxidase homologs from melon (*Cucumis melo* L.). *Molecular & General Genetics* **251**(1), pp. 81-90

Lasserre E, Godard F, Bouquin T, Hernandez JA, Pech JC, Roby D, Balague C. 1997. Differential activation of two ACC oxidase gene promoters from melon during plant development and in response to pathogen attack. *Molecular & General Genetics* **256**(3), pp. 211-222

Lay VJ, Prescott AG, Thomas PG, John P. 1996. Heterologous expression and site-directed mutagenesis of the 1-aminocyclopropane-1-carboxylate oxidase from kiwi fruit. *European Journal of Biochemistry* **242**(2), pp. 228-234

Lee MM, Lee SH, Park KY. 1997. Effects of spermine on ethylene biosynthesis in cut carnation (*Dianthus caryophyllus* L.) flowers during senescence. *Journal of Plant Physiology* **151**, pp. 68-73

Lelievre JM, Latche A, Jones B, Bouzayen M, Pech JC. 1997. Ethylene and fruit ripening. *Physiologia Plantarum* **101**(4), pp. 727-739

Lesham YY. 1992. Signal transduction, Ca^{2+}-triggered membrane glycerolipid turnover and growth/ senescence equilibria. **In** *Plant membranes: A biophysical approach to structure, development and senescence*. Lesham YY. Ed., Kluwer Academic, Dordrecht, The Netherlands, pp. 249-251

Li N & Mattoo K. 1994. Deletion of the carboxyl-terminal region of 1-aminocyclopropane-1-carboxylic acid synthase, a key protein in the biosynthesis of ethylene, results in catalytically hyperactive, monomeric enzyme. *The Journal of Biological Chemistry* **269**(9), pp. 6908-6917

Liang X, Abel S, Keller JA, Shen NF, Theologis A. 1992. The 1-aminocyclopropane-1-carboxylate synthase gene family of *Arabidopsis thaliana*. *Proceedings of the National Academy of Sciences, USA* **89**, pp. 11046-11050

Liang X, Shen NF, Theologis A. 1996. Li+-regulated 1-aminocyclopropane-1-carboxylate synthase gene expression in *Arabidopsis thaliana*. *The Plant Journal* **10**(6), pp. 1027-1036

Lieberman M. 1979. Biosynthesis and action of ethylene. *Annual Review of Plant Physiology* **30**, pp. 533-591

Lieberman M, Kunishi AT, Mapson LW, Wardale DA. 1965. Ethylene production from methionine. *Biochemical Journal* **97**, pp. 449-459

Lieberman M, Kunishi AT, Mapson LW, Wardale DA. 1966. Stimulation of ethylene production in apple tissue slices by methionine. *Plant Physiology* **41**, pp. 376-382

Lieberman M & Mapson LW. 1964. Genesis and biogenesis of ethylene. *Nature* **204**, pp. 343-345

Lincoln JE, Campbell AD, Oetiker J, Rottmann WH, Oeller PW, Shen NF, Theologis A. 1993. LE-ACS4, a fruit ripening and wound-induced 1-aminocyclopropane-1-carboxylate synthase gene of tomato (*Lycopersicon esculentum*). *The Journal of Biological Chemistry* **268**(26), pp. 19422-19430

Liu JH, Lee-Tamon SH, Reid DM. 1997. Differential and wound-inducible expression of 1-aminocyclopropane-1-carboxylate oxidase genes in sunflower seedlings. *Plant Molecular Biology* **34**, pp. 923-933

Liu JH, Mukherjee I, Reid DM. 1990. Adventitious rooting in hypocotyls of sunflower (*Helianthus annuus*) seedlings. III. the role of ethylene. *Physiologia Plantarum* **78**, pp. 268-276

Lohman KN, Gan S, Manorama JC, Amasino RM. 1994. Molecular analysis of natural leaf senescence in *Arabidopsis thaliana*. *Physiologia Plantarum* **92**, pp. 322-328

Longa MA, Del Rio LA, Palma JM. 1994. Superoxide dismutases of chestnut leaves, *Castanea sativa*: characterisation and study of their involvement in natural leaf senescence. *Physiologia Plantarum* **92**, pp. 227-232

Loomis WD. 1974. Overcoming problems of phenolics and quinones in the isolation of plant enzymes and organelles. **In** *Methods in Enzymology.* Fleischer S & Packer L. Eds., Academic Press, San Diego, **31** pp. 528-544

Lopez-Gomez R, Campbell A, Dong JG, Yang SF, Gomez-Lim MA. 1997. Ethylene biosynthesis in banana fruit: isolation of a genomic clone to ACC oxidase and expression studies. *Plant Science* **123**, pp. 123-131

Mapson LW, March JF, Rhodes MJC, Wooltorton LSC. 1970. A comparatative study of the ability of methionine or linolenic acid to act as precursors of ethylene in plant tissues. *Biochemical Journal* **117**, pp. 473-479

Martin MN, Cohen JD, Saftner RA. 1995. A new 1-aminocyclopropane-1-carboxylic acid-conjugating activity in tomato fruit. *Plant Physiology* **109**(3), pp. 917-926

Martin MN & Saftner RA. 1995. Purification and characterisation of 1-aminocyclopropane-1-carboxylic acid N-malonyltransferase from tomato fruit. *Plant Physiology* **108**, pp. 1241-1249

Mathooko FM, Inaba A, Nakamura R. 1998. Characterization of carbon dioxide stress-induced ethylene biosynthesis in cucumber (*Cucumis sativus* L.) fruit. *Plant and Cell Physiology* **39**(3), pp. 285-293

Maunders MJ, Holdsworth MJ, Slater A, Knapp JE, Bird CR, Schuch W, Grierson D. 1987. Ethylene stimulates the accumulation of ripening-related messenger-RNAs in tomatoes. *Plant, Cell and Environment* **10**(2), pp. 177-184

Maxson JM & Woodson WR. 1997. Transcriptional regulation of senescence-related genes in carnation flowers. **In** *Biology and Biotechnology of the Plant Hormone Ethylene*. Kanellis AK, Chang C, Kende H, Grierson D. Eds., Kluwer Academic, Dordrecht, The Netherlands pp. 155-162

Mayak S, Legge RL, Thompson JE. 1983. Superoxide radical production by microsomal membranes from senescing carnation flowers: an effect on membrane fluidity. *Phytochemistry* **22**(6), pp. 1375-1380

Mayne MB, Coleman JR, Blumwald E. 1996. Differential expression during drought conditioning of a specific *S*-adenosylmethionine synthetase from jack pine (*Pinus banksia* Lamb.) seedlings. *Plant, Cell and Environment* **19**, pp. 958-966

McGarvey DJ & Christoffersen RE. 1992. Characterization and kinetic parameters of ethylene-forming enzyme from avocado fruit. *The Journal of Biological Chemistry* **267**(9), pp. 5964-5967

McGarvey DJ, Yu H, Christoffersen RE. 1990. Nucleotide sequence of a ripening-related cDNA from avocado fruit. *Plant Molecular Biology* **15**, pp. 165-167

McKeon TA, Fernandez-Maculet JC, Yang SF. 1995. Biosynthesis and Metabolism of ethylene. **In** *Plant Hormones: Physiology, Biochemistry and Molecular Biology, 2nd.* Davies PJ. Ed., Kluwer Academic, Dordrecht, The Netherlands, pp 118-139

McKeon TA & Yang SF. 1984. A comparison of the conversion of 1-amino-2-ethylcyclopropane-1-carboxylic acid stereoisomers to 1-butene by pea epicotyls and by a cell-free system. *Planta* **160** pp. 84-87

Mekhedov SL & Kende H. 1996. Submergence enhances expression of a gene encoding 1-aminocyclopropane-1-carboxylate oxidase in deepwater rice. *Plant and Cell Physiology* **37**(4), pp. 531-537

Memelink J, Swords K M, Staehelin L A, Hoge JH. 1994. Southern, northern and western blot analysis. **In** *Plant Molecular Biology Manual, 2nd ed.* Gelvin SB & Schilperoot RA. Eds., Kluwer Academic, London, UK, pp. F-10

Michaels SD, John MC, Amasino RM. 1994. Removal of polysaccharides from plant DNA by ethanol precipitation. *BioTechniques* **17**(2), pp. 274-276

Mizutani F, Dong JG, Yang SF. 1995. Effect of pH on CO_2-activated 1-aminocyclopropane-1-carboxylate oxidase activity from apple fruit. *Phytochemistry* **39**(4), pp. 751-755

Mizutani F, Rabbany ABMG, Akiyoshi H. 1998. Inhibition of ethylene production and 1-aminocyclopropane-1-carboxylate oxidase activity by tropalones. *Phytochemistry* **48**(1), pp. 31-34

Moran R. 1982. Formulae for determination of chlorophyllous pigments extracted with N,N-dimethylformamide. *Plant Physiology* **69**, pp. 1376-1381

Morgan PW & Durham JI. 1980. Ethylene production and leaflet abscission in *Melia azedarach*. *Plant Physiology* **66**, pp. 88-92

Morgan PW, He C, Drew MC. 1992. Intact leaves exhibit a climacteric-like rise in ethylene production before abscission. *Plant Physiology* **100**, pp. 1587-1590

Moya-Leon MA & John P. 1994. Activity of 1-aminocyclopropane-1-carboxylate (ACC) oxidase (ethylene-forming enzyme) in the pulp and peel of ripening bananas. *Journal of Horticultural Science* **69**(2), pp. 243-250

Moya-Leon MA & John P. 1995. Purification and biochemical characterization of 1-aminocyclopropane-1-carboxylate oxidase from banana fruit. *Phytochemistry* **39**(1), pp. 15-20

Munoz De Rueda P, Gallardo M, Matilla AJ, Sanchez-Calle IM. 1995. Preliminary characterization of 1-aminocyclopropane-1-carboxylate oxidase properties from embryonic axes of chick-pea (*Cicer arietinum* L.) seeds. *Journal of Experimental Botany* **46**(287), pp. 695-700

Nakajima N & Imaseki H. 1986. Purification and properties of 1-aminocyclopropane-1-carboxylate synthase of mesocarp of *Cucurbita maxima* Duch. fruits. *Plant and Cell Physiology* **27**(6), pp. 969-980

Nakajima N, Mori H, Yamazaki K, Imaseki H. 1990. Molecular cloning and sequence of a complementary DNA encoding 1-aminocyclopropane-1-carboxylate synthase induced by tissue wounding. *Plant and Cell Physiology* **31**(7), pp. 1021-1029

Nakajima N, Nakagawa N, Imaseki H. 1988. Molecular size of wound-induced 1-aminocyclopropane-1-carboxylate synthase from *Cucurbita maxima* Duch. and change of translatable mRNA of the enzyme after wounding. *Plant and Cell Physiology* **29**(6), pp. 989-998

Nakatsuka A, Shiomi S, Kubo Y, Inaba A. 1997. Expression and internal feedback regulation of ACC synthase and ACC oxidase genes in ripening tomato fruit. *Plant and Cell Physiology* **38**(10), pp. 1103-1110

Neal MW & Florini JR. 1973. A rapid method for desalting small volumes of solution. *Analytical Biochemistry* **55**, pp. 328-330

Nieder M, Yip WK, Yang SF. 1986. Interferences and specificity of the 1-aminocyclopropane-1-carboxylic acid assay with the hypochlorite reagent. *Plant Physiology* **81**, pp. 156-160

Nijenhuis-De Vries MA, Woltering EJ, De Vrije T. 1994. Partial characterization of carnation petal 1-aminocyclopropane-1-carboxylate oxidase. *Plant Physiology* **144**, pp. 549-554

Oeller PW, Wong LM, Taylor LP, Pike DA, Theologis A. 1991. Reversible inhibition of tomato fruit senescence by antisense 1-aminocyclopropane-1-carboxylate synthase in tomato fruit. *Proceedings of the National Academy of Sciences, USA* **88**, pp. 5340-5344

Oerter KE, Munson PJ, McBride WO, Rodbard D. 1990. Computerised estimation of size of nucleic acid fragments using the four-parameter logistic model. *Analytical Biochemistry* **189**, pp. 235-243

Oetiker JH, Olson DC, Shiu OY, Yang SF. 1997. Differential induction of seven 1-aminocyclopropane-1-carboxylate synthase genes by elicitor in suspension cultures of tomato (*Lycopersicon esculentum*). *Plant Molecular Biology* **34**, pp. 275-286

Ohme-Takagi M & Shinshi H. 1995. Ethylene-inducible DNA binding proteins that interact with an ethylene-responsive element. *The Plant Cell* **7**(2), pp. 173-182

Olson DC, Oetiker JH, Yang SF. 1995. Analysis of LE-ACS3, a 1-aminocyclopropane-1-carboxylic acid synthase gene expressed during flooding in the roots of tomato plants. *The Journal of Biological Chemistry* **270**(23), pp. 14056-14061

Olson DC, White JA, Edelman L, Harkins RN, Kende H. 1991. Differential expression of two genes for 1-aminocyclopropane-1-carboxylate synthase in tomato fruits. *Proceedings of the National Academy of Sciences, USA* **88**(12), pp. 5340-5344

Olsson M. 1995. Alterations in lipid composition, lipid peroxidation and anti-oxidative protection during senescence in drought stressed plants and non-drought stressed plants of *Pisum sativum*. *Plant Physiology and Biochemistry* **33**(5), pp. 547-553

Omkumar RV & Ramasarma T. 1993. Irreversible inactivation of 3-hydroxy-3-methylglutaryl-CoA reductase by H_2O_2. *Biochimica et Biophysica Acta* **1156**, pp. 267-274

Osborne DJ. 1989. Abscission. *Critical Reviews in Plant Sciences* **8**, pp. 103-129

Osborne DJ. 1991. Ethylene in leaf ontogeny and abscission. **In** *The Plant Hormone Ethylene*. Mattoo AK & Suttle JC Eds., CRC Press, Boca Raton, Florida, USA, pp. 193-214

Osborne DJ, Walters J, Milborrow BV, Norville A, Stange MC. 1996. Evidence for a non-ACC ethylene biosynthesis pathway in lower plants. *Phytochemistry* **42**(1), pp. 51-60

Park KY, Drory A, Woodson WR. 1992. Molecular cloning of an 1-aminocyclopropane-1-carboxylate synthase from senescing carnation flower petals. *Plant Molecular Biology* **18**, pp. 377-386

Park SW & Chung WI. 1998. Molecular cloning and organ-specific expression of three isoforms of tomato ADP-glucose pyrophosphorylase gene. *Gene* **206**(2), pp. 215-221

Pastori GM & del Rio LA. 1994. An activated-oxygen-mediated role for peroxisomes in the mechanism of senescence of *Pisum sativum* L. leaves. *Planta* **193**, pp. 385-391

Payton S, Fray RG, Brown S, Grierson D. 1996. Ethylene receptor expression is regulated during fruit ripening, flower senescence and abscission. *Plant Molecular Biology* **31**, pp. 1227-1231

Pech JC, Latche A, Larrigaudiere C, Reid MS. 1987. Control of early ethylene synthesis in pollinated *Petunia* flowers. *Plant Physiology and Biochemistry, France* **25**(4), pp. 431-437

Peck SC & Kende H. 1995. Sequential induction of the ethylene biosynthetic enzyme by indole-3-acetic in etiolated peas. *Plant Molecular Biology* **28**, pp. 293-301

Peiser G & Yang SF. 1998. Evidence for 1-(malonylamino)cyclopropane-1-carboxylic acid being the major conjugate of aminocyclopropane-1-carboxylic acid in tomato fruit. *Plant Physiology* **116**(4), pp. 1527-1532

Peleman J, Saito K, Cottyn B, Engler G, Seurinck J, Van Montagu M, Inze D. 1989. Structure and expression analysis of the *S*-adenosylmethionine synthetase gene family in *Arabidopsis thaliana*. *Gene* **84**(2), pp. 359-369

Perry D, Abraham EP, Baldwin JE. 1988. Factors affecting the isopenicillin N synthetase reaction. *Biochemical Journal* **255**, pp. 345-351

Pirrung MC, Kaiser LM, Chen J. 1993. Purification and properties of the apple fruit ethylene-forming enzyme. *Biochemistry* **32**, pp. 7445-7450

Pogson BJ, Downs CG, Davies KM. 1995. Differential expression of two 1-aminocyclopropane-1-carboxylic acid oxidase genes in broccoli after harvest. *Plant Physiology* **108**, pp. 651-657

Pope B & Kent HM. 1996. High efficiency 5 min transformation of *Escherichia coli*. *Nucleic Acids Research* **24**(3), pp. 536-537

Polayes D & Hughs AJ. Efficient protein expression and simple purification using the pProEX™-1 system. *Focus* **16**(3), pp. 81-84

Porter AJR, Borlakoglu JT, John P. 1986. Activity of the ethylene-forming enzyme in relation to plant cell structure and organisation. *Journal of Plant Physiology* **125**, pp. 207-216

Prescott AG & John P. 1996. Dioxygenases: molecular structure and role in plant metabolism. *Annual Review of Plant Physiology* **47**, pp. 245-271

Raz V & Fluhr R. 1992. Calcium requirements for ethylene-dependent responses. *The Plant Cell* **4**, pp. 1123-1130

Reid MS. 1995. Ethylene in plant growth, development and senescence. **In** *Plant Hormones, Physiology, Biochemistry and Molecular Biology 2nd ed.* Davies PJ. Ed., Kluwer Academic, Dordrecht, The Netherlands, pp. 486-508

Reinhardt D, Kende H, Boller T. 1994. Subcellular localization of 1-aminocyclopropane-1-carboxylate oxidase in tomato cells. *Planta* **195**, pp. 142-146

Roach PL, Clifton IJ, Fülöp V, Harlos K, Barton GJ, Haijdu J, Andersson I, Schofield CJ, Baldwin JE. 1995. Crystal structure of isopenicillin-N-synthase is the first from a new structural family of enzymes. *Nature* **375**, pp. 700-704

Roberts JA & Osborne DJ. 1981. Auxin and the control of ethylene production during the development and senescence of leaves and fruits. *Journal of Experimental Botany* **32**, pp. 875-887

Roman G, Lubarsky B, Kieber JJ, Rothenberg M, Ecker JR. 1995. Genetic analysis of ethylene signal transduction in *Arabidopsis thaliana*: five novel mutant loci integrated into a stress response pathway. *Gene* **139**(3), pp. 1393-1409

Rombaldi C, Lelievre JM, Latche A, Petitprez M, Bouzayen M, Pech JC. 1994. Immunocytolocalization of 1-aminocyclopropane-1-carboxylic acid oxidase in tomato and apple fruit. *Planta* **192**(4), pp. 453-460

Rothnie HM. 1996. RNA as a target and an initiator of post-transcriptional gene silencing in transgenic plants. *Plant Molecular Biology* **32**, pp. 43-61

Rottmann WH, Peter GF, Oeller PW, Keller JA, Shen NF, Nagy BP, Taylor LP, Campbell AD, Theologis A. 1991. 1-aminocyclopropane-1-carboxylate synthase in tomato is encoded by a multigene family whose transcription is induced during fruit and floral senescence. *Journal of Molecular Biology* **222**(4), pp. 937-961

Rychlik W. 1993. Selection of Primers for Polymerase Chain Reaction. **In** *Methods in Molecular Biology : PCR Protocols: Current Methods and Applications.* White BA. Ed., Humana Press., Totowa, New Jersey, USA, **15** pp. 31-40

Sakai H, Hua J, Chen QHG, Chang CR, Medrano LJ, Bleecker AB, Meyerowitz EM. 1998. ETR2 is an ETR1-like gene involved in ethylene signalling in *Arabidopsis. Proceedings of the National Academy of Sciences, USA* **95**(10), pp. 5812-5817

Sakai S & Imaseki H. 1973. A proteinaceous inhibitor of ethylene biosynthesis by etiolated mung bean hypocotyl sections. *Planta* **113**, pp. 115-128

Sakai S & Maniwa Y. 1994. Inhibition of ethylene synthesis in mung bean hypocotyl segments by the proteinaceous inhibitors of ethylene synthesis. *Plant Physiology and Biochemistry Paris* **32**(3), pp. 385-389

Salisbury FB & Ross CW. 1985. Hormones and growth regulators. **In** *Plant Physiology, 3rd ed.* Carey JC. Ed., Wadsworth Publishing Company, Belmont, California, USA, pp 330-349

Sambrook J, Fritsch EF, Maniatis T. 1989. (Eds.) Molecular Cloning : A Laboratory Manual *2nd ed.,* Cold Spring Harbor Laboratory Press, New York, **1**

Sanders IO, Ishizawa K, Smith AR, Hall MA. 1990. Ethylene binding and action in rice seedlings. *Plant and Cell Physiology* **31**(8), pp. 1091-1099

Sanger F, Niklen S, Coulson AR. 1977. DNA sequencing with chain terminating inhibitors. *Proceedings of the National Academy of Sciences, USA* **74**, pp. 5436-5467

Sato T, Oeller PW, Theologis A. 1991. The 1-aminocyclopropane-1-carboxylate synthase of *Cucurbita*. *The Journal of Biological Chemistry* **266**(6), pp. 3752-3759

Sato T & Theologis A. 1989. Cloning the mRNA encoding 1-aminocyclopropane-1-carboxylate synthase, the key enzyme for ethylene biosynthesis in plants. *Proceedings of the National Academy of Sciences, USA* **86**(17), pp. 6621-6625

Satoh S & Esashi Y. 1984. Changes in ethylene production and in 1-aminocyclopropane-1-carboxylic acid (ACC) and malonyl-ACC contents of cocklebur seeds during their development. *Plant and Cell Physiology* **25**(7), pp. 1277-1283

Satoh S & Esashi Y. 1986. Inactivation of 1-aminocyclopropane-carboxylic acid synthase of etiolated mung bean hypocotyl segments by its substrate, *S*-adenosylmethionine. *Plant and Cell Physiology* **27**, pp. 285-291

Satoh T & Theologis A. 1989. Cloning the mRNA encoding aminocyclopropane-1-carboxylate synthase, the key enzyme for ethylene biosynthesis in plants. *Proceedings of the National Academy of Sciences, USA* **86**, pp. 6621-6625

Schaller GE & Bleecker A. 1995. Ethylene-binding sites generated in yeast expressing the *Arabidopsis* ETR1 gene. *Science* **270**, pp. 1809-1811

Scheuermann RH & Bauer SR. 1993. Polymerase chain reaction-based mRNA quantification using an internal standard: analysis of oncogene expression. **In** *Methods in Enzymology* **218**, pp. 446-473

Schröder G, Eichel J, Breinig S, Schröder J. 1997. Three differentially expressed *S*-adenosylmethionine synthetases from *Catharanthus roseus*: molecular and functional characterisation. *Plant Molecular Biology* **33**, pp. 211-222

Shinshi H, Usami S, Ohme-Takagi M. 1995. Identification of an ethylene-responsive region in the promoter of a tobacco class I chitinase gene. *Plant Molecular Biology* **27**, pp. 923-932

Sisler EC, Dupille E, Serek M. 1996. Effect of 1-methylcyclopropene and methylenecyclopropane on ethylene binding and action on cut carnations. *Plant Growth Regulation* **18**, pp. 79-86

Sisler EC & Serek M. 1997. Inhibitors of ethylene responses in plants at the receptor level: recent developments. *Physiologia Plantarum* **100**, pp. 577-582

Sitrit Y, Riov J, Blumenfeld A. 1988. Interference of phenolic compounds with the 1-aminocyclopropane-1-carboxylic acid assay. *Plant Physiology* **86**, pp. 13-15

Slater A, Maunders MJ, Edwards K, Schuch W, Grierson D. 1985. Isolation and characterisation of cDNA clones for tomato polygalacturonase and other ripening-related proteins. *Plant Molecular Biology* **5**, pp. 137-147

Smart CM, Hosken SE, Thomas H, Greaves JA, Blair BG, Schuch W. 1995. The timing of maize leaf senescence and characterisation of senescence-related cDNAs. *Physiologia Plantarum* **93**, pp. 673-682

Smith CJS, Slater A, Grierson D. 1986. Rapid appearance of an mRNA correlated with ethylene synthesis encoding a protein of molecular weight 35000. *Planta* **168**, pp. 94-100

Smith JJ, Ververidis P, John P. 1992. Characterization of the ethylene-forming enzyme partially purified from melon. *Phytochemistry* **31**(5), pp. 1485-1494

Smith JJ, Zhang ZH, Schofield CJ, John P, Baldwin JE. 1994. Inactivation of 1-aminocyclopropane-1-carboxylate (ACC) oxidase. *Journal of Experimental Botany* **45**, pp. 521-527

Somssich JE, Bollmann J, Hahlbrock L, Kombrink E, Schultz W. 1989. Differential early activation of defense-related genes in elicitor-treated parsley cells. *Plant Molecular Biology* **12**, pp. 227-234

Spanu P, Boller T, Kende H. 1993. Differential accumulation of transcripts of 1-aminocyclopropane-1-carboxylate synthase genes in tomato plants infected with *Phytophthora infestans* and in elicitor-treated tomato cell suspensions. *Journal of Plant Physiology* **141**(5), pp. 557-562

Stadtman ER & Oliver CN. 1991. Metal catalysed oxidation of proteins, physiological consequences. *The Journal of Biological Chemistry* **266**(4), pp. 2005-2008

Summers JE, Voesenek LACJ, Blom CWPM, Lewis MJ, Jackson MB. 1996. *Potamogeton pectinatus* is constitutively incapable of synthesizing ethylene and lacks 1-aminocyclopropane-1-carboxylic acid oxidase. *Plant Physiology* **111**, pp. 901-908

Tabor CW & Tabor H. 1984. Methionine adenosyltransferase (*S*-adenosylmethionine synthetase) and *S*-adenosylmethionine decarboxylase. *Advances in Enzymology* **56**, pp. 251-282

Tang X, Gomes AMTR, Bhatia A, Woodson WR. 1994. Pistil-specific and ethylene-regulated expression of 1-aminocyclopropane-1-carboxylic oxidase genes in *Petunia* flowers. *The Plant Cell* **6**, pp. 1227-1239

Tang XY, Wang H, Brandt AS, Woodson WR. 1993. Organization and structure of the 1-aminocyclopropane-1-carboxylate oxidase gene family from *Petunia hybrida*. *Plant Molecular Biology* **23**(6), pp. 1151-1164

Teare JM, Islam R, Flanagan R, Gallagher S, Davies MG, Grabau C. 1997. Measurement of nucleic acid concentrations using the DyNA Quant™ and the GeneQuant™. *BioTechniques* **22**(6), pp. 1170-1174

Ten Have A & Woltering EJ. 1997. Ethylene biosynthetic genes are differentially expressed during carnation (*Dianthus caryophyllus* L.) flower senescence. *Plant Molecular Biology* **34**, pp. 89-97

Theologis A, Zarembinski TI, Oeller PW, Liang X, Abel S. 1992. Modification of fruit ripening by suppressing gene expression. *Plant Physiology* **100**, pp. 549-551

Thomas H. 1990. Leaf development in *Lolium temulentum*: protein metabolism during development and senescence of attached and excised leaf tissue. *Journal of Plant Physiology* **136**, pp. 45-50

Thomas H, Ougham HJ, Emyr Davies TG. 1992. Leaf senescence in a non-yellowing mutant of *festuca pratensis*, transcripts and translation Products. *Journal of Plant Physiology* **139**, pp. 403-412

Thomas H & Stoddart. 1980. Leaf senescence. *Annual Review of Plant Physiology* **31**, pp. 83-111

Thompson JD, Higgins DG, Gibson TJ. 1994. Clustal W: improving the sensitivity of progressive multiple sequence alignment through sequence weighting, positions-specific gap penalties and weight matrix choice. *Nucleic Acids Research* **22**, pp. 4673-4680

Todaka I, Watanabe A, Imaseki H. 1978. Multiple effects of the inhibitory protein of ethylene production on cellular metabolism. *Plant and Cell Physiology* **19**(4), pp. 561-571

Trebitsh T, Staub JE, O'Neil SD. 1997. Identification of a 1-aminocyclopropane-1-carboxylic acid synthase gene linked to the female (F) locus that enhances female sex expression in cucumber. *Plant Physiology* **113**, pp. 987-995

Tsai DS, Arteca RN, Bachman JM, Phillips AT. 1988. Purification and characterization of 1-aminocyclopropane-1-carboxylate synthase from etiolated mungbean hypocotyls. *Archives of Biochemistry and Biophysics* **264** pp. 632-640

Tsai DS, Arteca RN, Arteca JM, Phillips AJ. 1991. Characterization of 1-aminocyclopropane-1-carboxylate synthase purified from mung bean hypocotyls. *Journal of Plant Physiology* **137**(3), pp. 301-306

Van Der Straeten D, Van Wiemeersch L, Van Damme J, Goodman H, Van Montagu M. 1989. Purification and amino acid sequence analysis of 1-aminocyclopropane-1-carboxylic acid synthase from tomato pericarp. **In** *Biochemical and Physiological Aspects of Ethylene Production in Lower and Higher Plants*. Clijsters H, De Proft M, Marcelle R, Van Poucke M. Eds., Kluwer Academic, Dordrecht, The Netherlands, pp. 93-100

Van Slogteren CMS, Hoge JHC, Hooykaas PJJ, Schilperoot RA. 1983. Clonal analysis of heterogeneous crown gall turmour tissues induced by wild type and shooter mutant strains of *Agrobacterium tumefaciens* - expression of T-DNA genes. *Plant Molecular Biology* **2**, pp. 321-333

Venis MA. 1984. Cell-free ethylene-forming systems lack stereochemical fidelity. *Planta* **162**, pp. 85-88

Ververidis P & John P. 1991. Complete recovery in vitro of ethylene-forming enzyme activity. *Phytochemistry* **30**, pp. 725-727

Vioque B & Castellano JM. 1998. *In vivo* and *in vitro* 1-aminocyclopropane-1-carboxylic acid oxidase activity in pear fruit: role of ascorbate and inactivation during catalysis. *Journal of Agricultural and Food Chemistry* **46**, pp. 1706-1711

Vogel JP, Schuerman P, Woeste K, Brandstatter I, Kieber JJ. 1998. Isolation and characterisation of *Arabidopsis* mutants defective in the induction of ethylene biosynthesis by cytokinin. *Genetics* **149**(1), pp. 417-427

White MF, Vasquez J, Yang SF, Kirsch JF. 1994. Expression of apple 1-aminocyclopropane-1-carboxylate synthase in *Escherichia coli*: kinetic characterisation of wild-type and active-site mutant forms. *Proceedings of the National Academy of Sciences, USA* **91**, pp. 12428-12432

Whittaker DJ, Smith GS, Gardner RC. 1997. Expression of ethylene biosynthetic genes in *Actinidia chinensis* fruit. *Plant Molecular Biology* **34**, pp. 45-55

Woltering EJ & De Vrije T. 1995. Ethylene: a tiny molecule with great potential. *BioEssays* **17**(4), pp. 287-290

Woltering EJ & Harren F.1989. Early changes in ethylene production during senescence of carnation and *Phalaenopsis* flowers measured by laser photoacoustic detection. **In** *Biochemical and Physiological Aspects of Ethylene Production in Lower and Higher Plants* Clijsters H, De Proft M, Marcelle R, Van Poucke M. Eds., Kluwer Academic, Dordrecht, The Netherlands, pp. 263-270

Yang C, Wessler A, Wild A. 1993. Studies on the diurnal courses of the contents of abscisic acid, 1-aminocyclopropane carboxylic acid and its malonyl conjugate in needles of damaged and undamaged spruce trees. *Journal of Plant Physiology* **141**, pp. 624-626

Yang SF & Dong JG. 1993. Recent progress in research of ethylene biosynthesis. *Botanical Bulletin of Academia Sinica* **34**(2), pp. 89-101

Yang SF & Hoffman NE. 1984. Ethylene biosynthesis and its regulation in higher plants. *Annual Review of Plant Physiology* **35**, pp. 155-189

Yip WK, Dong JG, Yang SF. 1991. Purification and characterisation of 1-aminocyclopropane-1-carboxylate synthase from apple fruits. *Plant Physiology* **95**(1), pp. 251-257

Yoshiyama M, Yajima H, Atsumi T, Esashi Y. 1996. Mechanism of action of ethylene in promoting the germination of cocklebur seeds, 2. the role of C_2H_2 in the enhancement of priming effects. *Australian Journal of Plant Physiology* **23**(2), pp. 133-139

Yu SJ, Kim S, Lee JS, Lee DH. 1998. Differential accumulation of transcripts for ACC synthase and ACC oxidase homologs in etiolated mung bean hypocotyls in response to various stimuli. *Molecules and Cells* **8**(3), pp. 350-358

Yu YB, Adams DO, Yang SF. 1979. Regulation of auxin-induced ethylene production in mung bean hypocotyls, role of 1-aminocyclopropane-1-carboxylic acid. *Plant Physiology* **63**, pp. 589-590

Zhang Z, Barlow JN, Baldwin JE, Schofield CJ. 1997. Metal catalyzed oxidation and mutagenesis studies on the iron (II) binding site of 1-aminocyclopropane-1-carboxylate oxidase. *Biochemistry* **36**, pp. 15999-16007

Zhou D, Kalaitzis P, Mattoo AK, Tucker ML. 1996. The mRNA for an ETR1 homologue in tomato is constitutively expressed in vegetative and reproductive tissue. *Plant Molecular Biology* **30**, pp. 1331-1338